Advanced Diesel Combustion Strategies for Ultra-Low Emissions

Olivier Laguitton

October 2005

A thesis submitted in partial fulfilment of the requirements of
the University of Brighton for the degree of
Doctor of Philosophy

School of Engineering, University of Brighton
in collaboration with
Ricardo UK

ABSTRACT

The programme of work described in this thesis represents an exploration of the fundamentals of diesel combustion to achieve ultra-low engine-out emissions. The objectives were firstly to establish operating conditions and configuration that offer the potential to meet future emissions legislation, and secondly to develop an improved understanding of these requirements on combustion characteristics. The initial part of the programme demonstrated the validity of conducting investigations on a single-cylinder engine and formed a solid baseline for following studies. The second part examined the effects of reducing compression ratio and modifying the cylinder head flow capabilities at part load and full load conditions, whilst maintaining all the other operating conditions fixed. The main findings were that soot and NO_x emissions reduced, the latter reductions diminishing as injection timing was retarded. It was concluded that lower pressure and temperature during the injection event promoted mixing, which suppressed diffusion combustion at the most retarded injection timings. Combined with the leaner charge, the resulting combustion rates were reduced, with the conclusion that NO_x formation in premixed combustion was less sensitive to pressure and temperature. In addition, compression ratio offered increased load capabilities by further advancing the injection timing. The third part investigated the impact of injection timing and lowering global oxygen concentration, which led to large NO_x reductions. The main effects of lowering oxygen concentration were to increase the heat capacity and to delay auto-ignition. The injection timing also influenced auto-ignition and mixing: early injections yielded homogeneous-charge combustion while late injections resulted in premixed-charge combustion. Extreme timings enabled the mixture to lean out before auto-ignition, however, early injection was not possible at high loads, as premature combustion occurred due to rich regions in the charge. Premixed-charge combustion operation was applied to higher speeds and loads to demonstrate NO_x and soot emissions benefits but also the trade-off with fuel consumption and unburned hydrocarbon emissions. Finally, a NO_x formation concept is suggested for premixed combustion. The approach demonstrates that local in-cylinder parameters can be assumed from global elements, such as oxygen concentration and maximum rate of pressure change. It is proposed that the relationship can be utilised as feedback parameters for closed-loop control strategies.

ACKNOWLEDGEMENTS

I wish to express my deepest gratitude to my wife, sons and family in general, who have encouraged me every day in my undertakings.

I wish to thank Dr Martin Gold for his support during this part of my professional life and my other supervisors who have also played an important role in this, Prof. Morgan Heikal and Dr Cyril Crua.

I also wish to thank Nick Owen and Neville Jackson for enabling and supporting such a career development full of learning experiences at the University of Brighton and at Ricardo UK - STC.

I also wish to thank Ralph Wood, Tim Cowell, Bill Whitney, Ken Maris at the School of Engineering at the University of Brighton and Nigel Fox, Chris Rowe, Jackie Crump, Chris Lenartowicz at Ricardo UK - STC and many others, for their valuable support, guidance, skills and technical knowledge.

I wish to thank the members of the Commission for the Exhibition of 1851 for giving me the opportunity of such a professional and academic experience

DECLARATION

I declare that the research contained in this thesis, unless otherwise formally indicated within the text, is the original work of the author. The thesis has not been previously submitted to this or any other university for a degree, and does not incorporate any material already submitted for a degree.

Signed: Dated:

DISCLAIMER

As the contents of this thesis are my own work, they reflect my views and not necessarily those of the collaborators.

COPYRIGHT

TABLE OF CONTENTS

LIST OF TABLES

LIST OF FIGURES

NOMENCLATURE

UNITS

BSN, BSU: Bosch Smoke Number, Bosch Smoke Unit
dB A: decibel (with filtering method A)
°CA: degree crankangle
FSN: Filter Smoke Number
ppm: part per million
rev, r: revolution
Rs: Ricardo swirl

ABREVIATIONS AND ACRONYMS

AFR: Air-Fuel Ratio
BMEP, GIMEP, NMEP, PMEP: Brake, Gross, Net, Pumping Mean Effective Pressure
ATDC or BTDC: After or Before Top Dead Centre
CN: Cetane Number
CO: Carbon monoxide
CO_2: Carbon Dioxide
CR: Compression Ratio
DCCS: Dilution Controlled Combustion Strategy
DI, IDI: Direct Injection or Indirect Injection
dP/dt: rate of pressure change
ECE: Economic Commission for Europe
EEC: European Economic Community
EGR: Exhaust Gas Recirculation
FC: Fuel Consumption
G_{xx}: Emissions xx mass flow rates
H: Intake Humidity Ratio
H_2: Hydrogen
HC: Hydrocarbon
HCCI: Homogeneous Charge Compression Ignition
H/C: Hydrogen-over-Carbon ratio

HCLI: Homogeneous Charge Late Injection

HPLI: Highly Premixed Late Injection

HR, ROHR: Heat Release or Rate Of Heat Release

HSDI: High Speed Direct Injection

ICP: In-Cylinder Pressure

IP: Injection Pressure

IS: Indicated Specific

IT: Injection Timing

kw_{RCE2}: Emissions wet to dry conversion factor

max: maximum

N/A: Not Applicable

NO: Nitrogen Oxide

NO_x: Nitrous Oxides

NO_2: Nitrogen Dioxide

O_2: Oxygen

O_3: Ozone

$[O_2]_{cylinder}$: In-cylinder oxygen concentration

PCCI: Premixed Charge Compression Ignition

PFI: Port-Fuel Injected

PM: Particulate Matter

P_{vap}: Barometric Vapour Pressure

qm_{Exhdry}: Dry molar exhaust flow

RON: Research Octane Number

SOC or SOR: Start Of Combustion or Reaction

SOI or EOI: Start or End Of Injection

Tot Ems: Total Emissions

1 INTRODUCTION

1.1 Background and present objectives

Great challenges lie ahead for the diesel passenger-car engine if it is to maintain its present and successful course. One of the most critical is to meet future emissions regulations whilst improving performance and fuel economy at a minimal cost penalty. The current and emerging after-treatment technologies are definite enablers giving encouraging results in terms of meeting the emissions targets. Unfortunately, their cost and complexity threaten the competitiveness of the diesel engine package. Conversely, research work carried out over the past few years, aiming to tackle the emissions at their source, has highlighted an alternative approach for significant Nitrous Oxide (NO_x) and Particulate Matter (PM) emissions reductions. The principle relies on the optimisation of the combustion phasing relative to the injection predominantly through the use of increased rates of Exhaust Gas Recirculation (EGR), combined with novel injection systems and strategies and combustion chamber designs (piston-bowl shape and Compression Ratio, CR). This approach leads to the next generation in diesel combustion, and offers potentially, not only more robust and simpler solutions, but also more cost effective methods of meeting future regulations.

The programme of work described in this thesis represents an exploration of the fundamentals of diesel combustion to achieve low engine-out emissions. The initial study examined the impact of reduced compression ratio while the second part of the programme examined the emissions reduction at source approach with investigations of combustion phasing, relative to the injection event and TDC, and charge oxygen concentration. The first objective was to establish the operating conditions and configuration necessary to achieve NO_x emissions legislation, such as Tier 2 Bin 5 in the United States and possible Euro 6 requirements, with only evolutionary changes in the combustion system configuration. The second objective was to develop an improved understanding of the relationship between the operating conditions on the combustion characteristics. The purpose of these analyses was to provide a better fundamental understanding of the in-cylinder processes and subsequently to facilitate their implementation and control in future applications. A conceptual model of the

relationships was identified to form the foundation for future closed-loop control strategies.

1.2 Approach of the investigations

In order to allow as wide an exploration as possible, a single-cylinder diesel research engine was employed with a configuration based on that of a current production 2.0 litre, 4-cylinder automotive engine. The test cell was developed so that inlet-air pressure and temperature, exhaust backpressure, EGR temperature as well as injection pressure could be set independently rather than be limited by hardware characteristics such as those of an engine mounted high pressure fuel pump or turbocharger. The engine and test cell presented levels of flexibility and control beyond those currently available on multi-cylinder engines. Some of the main advantages are outlined as follows:

- Flexibility of engine: the operating conditions' ranges, such as the inlet air and EGR temperatures, or inlet-manifold and fuel injection pressures, were all easily extendable as opposed to the numerous constraints limiting the conventional multi-cylinder engine operation
- Isolation of different parameters: the impact of specific parameters on the in-cylinder and combustion characteristics could be isolated by undertaking single variable responses, facilitated by the flexibility
- Isolation of the cylinder: cylinder-to-cylinder variations and result averaging were avoided making the emissions and fuel consumption directly representative of the measured in-cylinder and combustion characteristics, which is representative of future control requirements for accuracy: cylinder-to-cylinder control.

1.3 Structure of the thesis

The thesis is structured into five parts:

- Chapter 2: the passenger-car emissions legislation evolution in Europe and its predicted future steps are presented, including reasons for diesel engines maintaining a strong position in the passenger car market. An overview is presented of current diesel-engine operation, in terms of combustion and emissions processes, as well as the main diesel-engine developments over the past decade. A review is given of the two approaches to advanced combustion operation as proposed in the literature, focusing on the operating conditions and the impact on combustion and emissions. These approaches aim to control NO_x and PM emissions in the cylinder and rely on the optimisation of the combustion phasing relative to the injection
- Chapters 3 and 4: the single-cylinder engine and associated systems have been described and a demonstration of the validity of conducting investigations on a single-cylinder engine given. A total of eight part load and three full load conditions were chosen to characterise the engine, which was closely representative of the 4-cylinder engine and identified as Build #1. Prior to transferring operating conditions, the gas exchange processes of the 4-cylinder engine were matched for each load condition. Exhaust backpressure valves settings were established and an orifice plate defined that allowed an accurate reproduction of the turbocharger and after-treatment on engine Build #1. For each condition, minor changes to the injection timing (IT) and swirl control were identified that offered the best matched to NO_x and soot (used to represent PM) emissions from the 4-cylinder engine. This data formed a solid reference for the research programme
- Chapter 5: analysis of reduced compression ratio and of increased inlet-port flow capabilities. Compression ratio was reduced from 18.4 to 16.0:1 by changing the piston bowl volume, with only a slight modification to the combustion chamber geometry. In addition, the inlet port flow was increased, which consequently reduced the minimum level of swirl of the cylinder head. These revisions were identified as Build #2. The effects of these changes are assessed by repeating measurements at three of the part load conditions and one full load condition, whilst fixing all the other

operating conditions. In order to explain the results, consideration was given to the detail of the in-cylinder and combustion characteristics

- Chapter 6: analysis of combustion phasing and lowering global in-cylinder oxygen concentration, considered as the major enablers for ultra-low NO_x and soot emissions. This experimental study was the major portion of the analysis and was conducted on Build #2 engine. A light and medium load condition were chosen as key test points since they were representative of loads where the advanced combustion operation had been tested but not always successfully. Detailed investigations included large ranging injection-timing responses at different oxygen concentrations and loads, with all the other operating conditions fixed. Results showed early injections yielded Homogeneous Charge Compression Ignition (HCCI) combustion while the late injections yielded Premixed Charge Compression Ignition (PCCI) combustion. Both extremes enabled the mixture to lean out before the combustion, however, early injections were not possible at high loads as premature combustion occurred due to rich regions in the charge. Premixed charge combustion operation was applied to higher speeds and loads to demonstrate NO_x and soot emissions benefits but also to demonstrate the trade-off with fuel consumption and unburned hydrocarbon (HC) and Carbon Monoxide (CO) emissions
- Chapter 7: as a result of the better understanding of the combustion, a NO_x formation concept was suggested for low NO_x and soot emissions combustion operation. It is demonstrated how NO_x emissions are predominantly determined by oxygen concentration and rate of pressure change in the cylinder. This simplification is made possible in fully-premixed-charge combustion, where local in-cylinder parameters can be assumed from global parameters. It is proposed that this concept could form the foundations of closed-loop control strategies for managing ultra-low engine-out NO_x emissions.

2 DIESEL ENGINE COMBUSTION – AN OVERVIEW

2.1 Future emissions directives for diesel passenger cars

Authorities around the world including from the United States, the European Union, Japan and Korea are imposing ever more stringent emissions legislation for type approval, which car manufacturers must respect to ensure the saleability of their vehicles. In Europe, the United Nations Economic Commission for Europe (ECE), based in Geneva, and the European Economic Community (EEC), based in Brussels, have been establishing emissions legislation since 1970. These gasoline and diesel passenger car and light-duty vehicle regulations were controlled using a 'big bag' approach, collecting emissions over the ECE 15 drive-cycle. This was replaced by a constant volume sampling approach in 1983. In 1988, a swept-volume based legislation was created and standards for diesel particulates were introduced. From 1992, more rigorous test procedures were implemented: gasoline and diesel applications were separated, the testing drive-cycle was extended, light-commercial and off-road vehicles were included. Regulations were also added such as average tailpipe emissions, CO emissions at idle and durability of anti-pollution devices, as described in the Mira web page (2003). The latest directives have included on board diagnostic systems and low ambient temperature tests. The emissions regulations from Euro 3 to the proposed consultation level Euro 5 (Society of Motor Manufacturers and Traders web page, 2005) are shown in Table 2-1. It gives both gasoline and diesel (Indirect and Direct Injection, IDI, DI) limits in mass per kilometre of CO, HC, NO_x and PM emissions for passenger cars. It is evident that the major challenges raised by these directives are for NO_x and PM emissions since their maximum limits for diesel applications are expected to reduce by 60 and 90 % respectively from Euro 3 to proposed Euro 5. These trends are common to all industrialised countries with the main difference being the dates from which the directives become effective. Similar limits common to both gasoline and diesel are being enforced even earlier in the United States with the California emission standards leading the way. For example, Tier 2 Bin 5 emissions regulation effective from 2007 has lower NO_x emissions limits than the proposed Euro 5 and can be referred to as a possible Euro 6 level.

Level	Effective for type approval[1]	Application	CO (g/km)	HC (g/km)	NO_x (g/km)	$HC+NO_x$ (g/km)	PM (g/km)
Euro 3[2&3]	01/2000-12/2004	Gasoline	2.30[4]	0.200	0.15	N/A	N/A
	01/2000-12/2004	Diesel	0.64	N/A	0.50	0.56	0.050
Euro 4[2]	01/2005->2008	Gasoline	1.00	0.100	0.08	N/A	N/A
	01/2005->2008	Diesel	0.50	N/A	0.25	0.30	0.025
'Euro 5'[5]	Beyond 2008	Gasoline	1.00	0.075	0.06	N/A	0.005
	Beyond 2008	Diesel	0.05	N/A	0.20	0.25	0.005

(1): For production, directives effective 12 months later.
(2): For vehicles above 2500 kg, directives effective 12 months later.
(3): For vehicles above 2000 kg designed to carry more than 6 passengers, directives effective from 01/2003.
(4): Increase due to extra urban drive-cycle added to drive-cycle in 2000.
(5): Dates and values given as consultation levels detailed in Society of Motor Manufacturers and Traders web page (2005).

Table 2-1: Emissions legislations from Euro 3 to proposed Euro 5.

In addition to this emissions legislation, a carbon dioxide (CO_2) average fleet emissions for new cars has been introduced by the Association des Contructeurs Européens d'Automobiles, which has voluntarily committed to achieving 140 g/km CO_2 fleet average by 2008 and envisages self-imposing 120 g/km by 2012, as detailed in the Official Journal of the European Communities by Bjerregaard (1999). The task is challenging when considering the fleet average emissions in Europe in 2000 and 2001 were 169 g/km and 164 g/km CO_2 respectively. Both the Japanese Automobile Manufacturers Association and the Korean Automobile Manufacturers Association have also adopted this commitment in principle. This highlights the challenges faced by the engine and vehicle developers which is made all the more difficult by market demand for ever more power with comparable or better fuel economy.

There are various options available to the car manufacturers in order to enable them to comply with these emissions regulations. Electric, fuel-cell and solar vehicles are all contenders to substitute the internal combustion engine as a means of getting round the emissions legislation. These are currently onerous routes (see the Department for

Transport web page, 2003), with existing constraints in terms of infrastructure, range, performance and comfort. Alternate fuel solutions such as compressed natural gas, liquid petroleum gas, hydrogen (H_2), emulsified, bio or wide-cut fuels have been implemented in dual-fuel engine vehicles (with diesel or gasoline) but are faced with a scarcely developed infrastructure, storage and high-cost of fuel issues, and above all, do not offer the same level of benefits as the alternate powertrain solutions, as identified by Armstrong (2002). Therefore, this limits their application to contained fleets such as public-transport, airport or agricultural vehicles, which already benefit from their own fuelling stations. Another concept is found in the hybrid vehicles powered by an electric motor combined with an internal combustion engine. They offer potentially more powerful powertrains, with fuel economy and emissions benefits from the electrical motor. The engine can be operated where it is most efficient with the electric motor in generate or motor mode depending on the engine output relative to the driver requirements. The electric motor also gives the possibility to cut the engine temporarily leading to a 'zero emissions' mode. The present limitation of such vehicles resides in the high cost and large weight and size of the required battery system. An intermediate concept can be found with the mild-hybrid vehicle powered by a smaller electric motor linked with an internal combustion engine. This seems the most viable short-term approach and does not rely so much on large battery systems. Despite the fact that this last solution provides fuel economy and emissions benefits without the cost implications and other limitations of the alternate solutions (see Laguitton et al., 2002), it still relies heavily on the characteristics of the internal combustion engine to fulfil high levels of fuel economy and meet the emissions targets.

From Table 2-1, it is unclear why the internal combustion engine of a mild-hybrid vehicle should be anything other than gasoline due to the relatively lower cost of such engines. However, when considering fleet average CO_2 emissions commitments, the current high-efficiency of the diesel engine gives it an advantage over gasoline, as long as the tailpipe emissions can be improved. In light of the improvements made to diesel-engine emissions and efficiency over the past decade, certainly inconceivable by diesel-engine developers a decade ago, it is expected that the diesel engine will be able to make equally impressive improvements in the next decade. It is with that in mind that developers continue their efforts to comply with the regulations.

2.2 Conventional diesel combustion

2.2.1 Description of conventional diesel combustion

Combustion products are inevitable during the fuel and air transformation to power. These and the efficiency of the process are strongly dependent upon, firstly, the charge-air, its temperature, pressure, motion and contents, secondly, the combustible fuel, its type, injection, atomisation, evaporation, and thirdly, their states and interaction, leading to the auto-ignition and combustion of the charge. In 1995, Monaghan (1995) suggested a series of essential requirements for future High Speed Direct Injection (HSDI) diesel passenger-car engines in order to provide the best results. These included turbo-charging, after-cooling, modulated EGR, four valves, levels of swirl up to 2.5 Rs, optimised, deep and re-entrant bowls, central and vertical injectors, high-pressure electronically-controlled injection systems offering the highest mean effective fuel injection pressures and finally, oxidation catalysts. In the event, the naturally aspirated two-valve engine has given way to a turbocharged and after-cooled four-valve engine with variable rates of cooled EGR and with variable geometry turbines starting to appear. The pre-chamber IDI engine with an injection system capable of delivering 200 bar has given way to an efficient DI engine with a highly flexible injection system capable of delivering up to 1600 bar, whether using a common rail or unit injectors. In the meantime, after-treatment such as close-coupled diesel oxidation catalysts and diesel particulate filters has become widespread. The improved fuel and air management have enabled diesel passenger-car engines to increase their efficiency and performance considerably, whilst reducing emissions to meet present emissions legislation.

In these modern DI diesel engines, combustion is usually composed of a premixed-combustion phase, followed by a diffusion-combustion phase (Heywood, a, 1988). During premixed combustion, the levels of mixing are high and the local Air-Fuel Ratios (AFR) of the mixture range from above 14.5:1, being stoichiometric, to beyond the limit of flammability in the outer boundary of the spray. This globally lean mixture is characterised by low temperature combustion. Once the premixed-combustion flame has propagated to the newly forming fuel-air mixture, this leads to the diffusion-combustion phase, as can be seen in high-speed video during

combustion in a rapid compression machine (Crua, 2002). The flame stabilises in a mixture zone where appropriate conditions in terms of AFR, temperature and pressure are met to allow combustion, which is why the diffusion-combustion phase is also known as the mixing-controlled combustion. During this phase, the in-cylinder temperatures are high, as a result of the premixed combustion, and the burning mixtures are characterised by close-to-stoichiometric AFRs. This phase continues until the injection is ended. A schematic of the fuel spray and the AFR distribution in the spray is proposed in Figure 2-1 based on these facts. The temperature profile in the case of combined premixed and diffusion combustion is based on data collected by Tadakazu et al. (1998) using the two-colour method and on results given by Flynn et al. (2000).

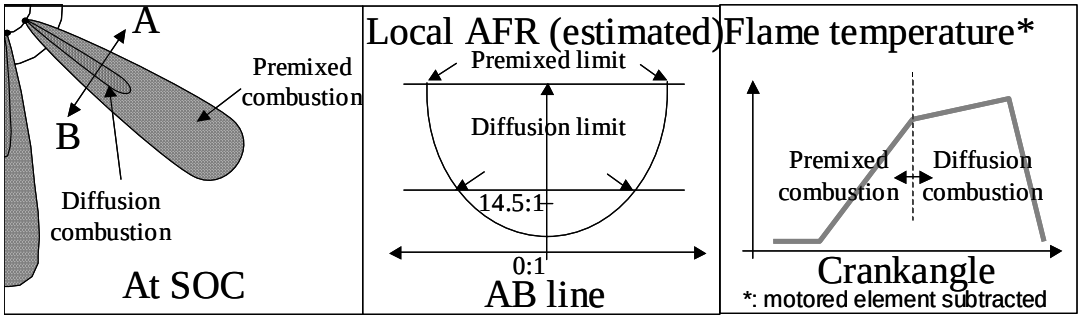

Figure 2-1: Conventional diesel mixing and combustion characteristics.

Premixed combustion is characterised by a high Rate Of Heat Release (ROHR) or pressure change, which is a consequence of the combustion of the fuel injected during the auto-ignition delay. Figure 2-2 represents a schematic of the in-cylinder pressure obtained during conventional diesel combustion and the derived rate of pressure change, which tracks the rate of heat release. This illustrates the presence of the two phases during the combustion. A light load case is also depicted to illustrate the profile of the rate of pressure change when the totality of the fuel is injected, evaporated and mixed with the air before auto-ignition, leading to a fully-premixed-charge combustion. The representation does not make clear the difficulties in determining whether there is diffusion combustion or not based on the rate of pressure change. Equally, even when all the fuel has been injected before auto-ignition occurs, it does not guarantee that the combustion is of a fully-premixed nature. Once the fuel is injected, all of it needs to evaporate and mix with the air to ensure there will be no diffusion combustion.

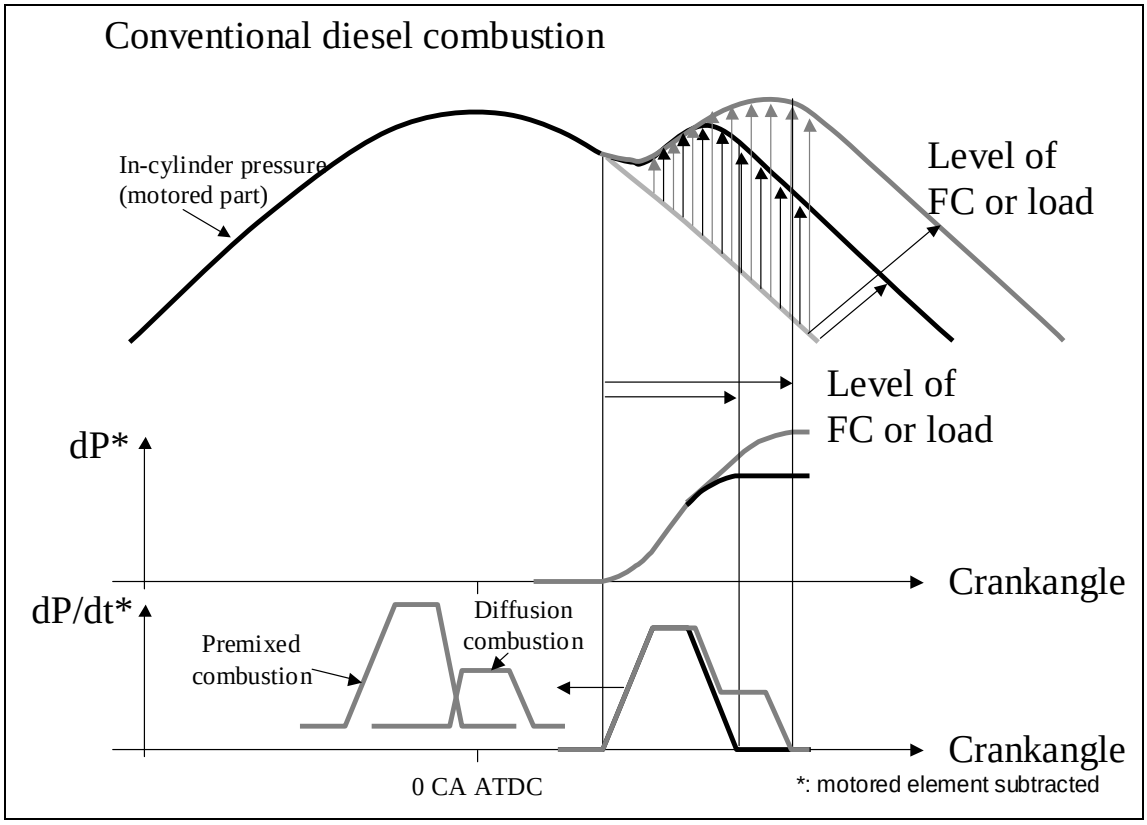

Figure 2-2: Summary of conventional diesel combustion.

2.2.2 Description of conventional diesel emissions

HC, CO, NO_x and PM emissions shown in Table 2-1 represent the regulated emissions. The main mechanisms for their formation are described by Heywood (b) (1988) and are related to the mixing and flame temperature characteristics described in Figure 2-1. HC emissions are formed in two possible ways in a conventional diesel engine. The first is when the local fuel-air mixture is too lean to ignite or to support a propagating flame (over-leaning) and the second is when the fuel-air mixture is too rich to ignite or support a flame (under-mixing). In gasoline engines where homogeneous mixtures are prevalent, HC emissions have several additional sources, ranging from colder temperatures near the cylinder walls quenching the flame, to crevices trapping the mixture, oil absorbing and desorbing the mixture during the compression and expansion strokes. This explains the higher HC emissions observed with more recent developments of diesel combustion, detailed in Section 2.3. CO emissions are formed in areas of the combustion where the AFR is close to stoichiometric or below, reflecting a lack of oxygen. This has rarely been an issue

with conventional diesel engines since even in the worst cases, the flame is stabilised at a mixture with an AFR above stoichiometric.

PM emissions are formed in the fuel-rich regions in the liquid core of the diesel fuel spray, within the flame region at temperatures between 1000 and 2800 K. The pyrolysis of fuel by surrounding hot burned gases forms PM. A large portion of the PM is then burned with oxygen giving a yellow colour to the flame, however, a smaller portion grows and agglomerates to form PM emissions, which exit the cylinder as visible smoke. The diffusion-combustion phase is the main contributor to PM emissions since premixed combustion is characterised by high levels of mixing making it too lean to form PM. However, if the diffusion-combustion phase temperature is high enough, it will promote PM oxidation and reduce the total emissions. In the following sections, PM emissions will also be referred to as soot or smoke emissions, which are both expressions commonly used to describe them. These are estimated from the filter paper opacity method described in a later section.

NO_x emissions, grouping both nitrogen dioxide and nitric oxide, the latter being predominant, are formed during the combustion when high temperatures are reached. These conditions are achieved during the combustion of a close-to-stoichiometric mixture in a high pressure and temperature environment. A direct correlation has been established between the NO_x formation rates and the flame temperatures in the combustion above 700 K. These conditions are realised during diffusion combustion, once the flame temperatures have been raised by the premixed-combustion phase and when the flame is stabilised in a fuel-air mixture zone just lean of stoichiometric. Premixed combustion will not contribute much to NO_x emissions since the temperatures are too low and the mixture is well mixed. The extended Zeldovich mechanism, described by Heywood (b) (1988), is widely used in computational fluid dynamics to model NO_x emissions. Nakayama et al. (2003) used it to illustrate the impact of oxygen concentration on the calculation of adiabatic flame temperature and the associated calculated NO_x emissions, as shown in Figure 2-3. It highlighted the strong dependence between NO_x emissions and flame temperature.

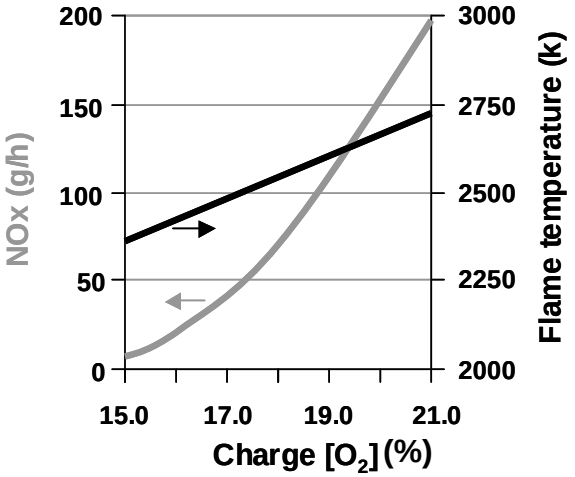

Figure 2-3: Temperature effect on NO_x emissions using the Zeldovich mechanism.

To date, there are two approaches to tackling tailpipe NO_x and PM emissions, one using after-treatment for NO_x, and the other using particulate filters for PM, as described by Knecht (2000), Lejeune et al. (2002), Wuensche et al. (2003) or Henein et al. (2003). The approach is determined by the potential for a particular engine to be optimised for low PM or low NO_x in conjunction with the appropriate after-treatment capabilities, taking into consideration cost, technology development and also durability. Figure 2-4 illustrates the two options for meeting Euro 4 based on a typical PM versus NO_x emissions trade-off curve of an engine meeting Euro 3 emissions regulations. Euro 5 and Tier 2 Bin 5 emissions targets are also indicated in the figure.

The NO_x after-treatment approach minimises PM emissions, treating NO_x engine-out emissions with a lean NO_x trap or a selective catalytic reduction system. One method of minimising PM emissions is to advance the injection timing to obtain a large portion of diffusion combustion. Despite representing ideal conditions for PM formation, these remain in a hot in-cylinder environment, promoting their oxidation. Another method consists of increasing the injection pressure to increase the mixing. The drawback in both cases is an increase in NO_x formation. This approach is fuel efficient since advancing injection timing or increasing injection pressure both contribute to a more rapid combustion, however, NO_x after-treatment is still in its infancy. The diesel particulate filter approach minimises NO_x emissions by retarding the injection timing to reduce combustion flame temperatures, as detailed by Gill et al. (2002) or Kidoguchi et al (2002). These authors also obtained reductions in NO_x emissions using EGR, which acts as a heat sink, which limits the temperature increase

during the combustion. Engine-out PM emissions are increased due to the lower in-cylinder temperatures limiting the oxidation process during and after the combustion process. A diesel particulate filter is inserted in the exhaust line to trap and burn PM emissions. With the current state of development and production, the diesel particulate filters are an efficient means of reducing PM emissions.

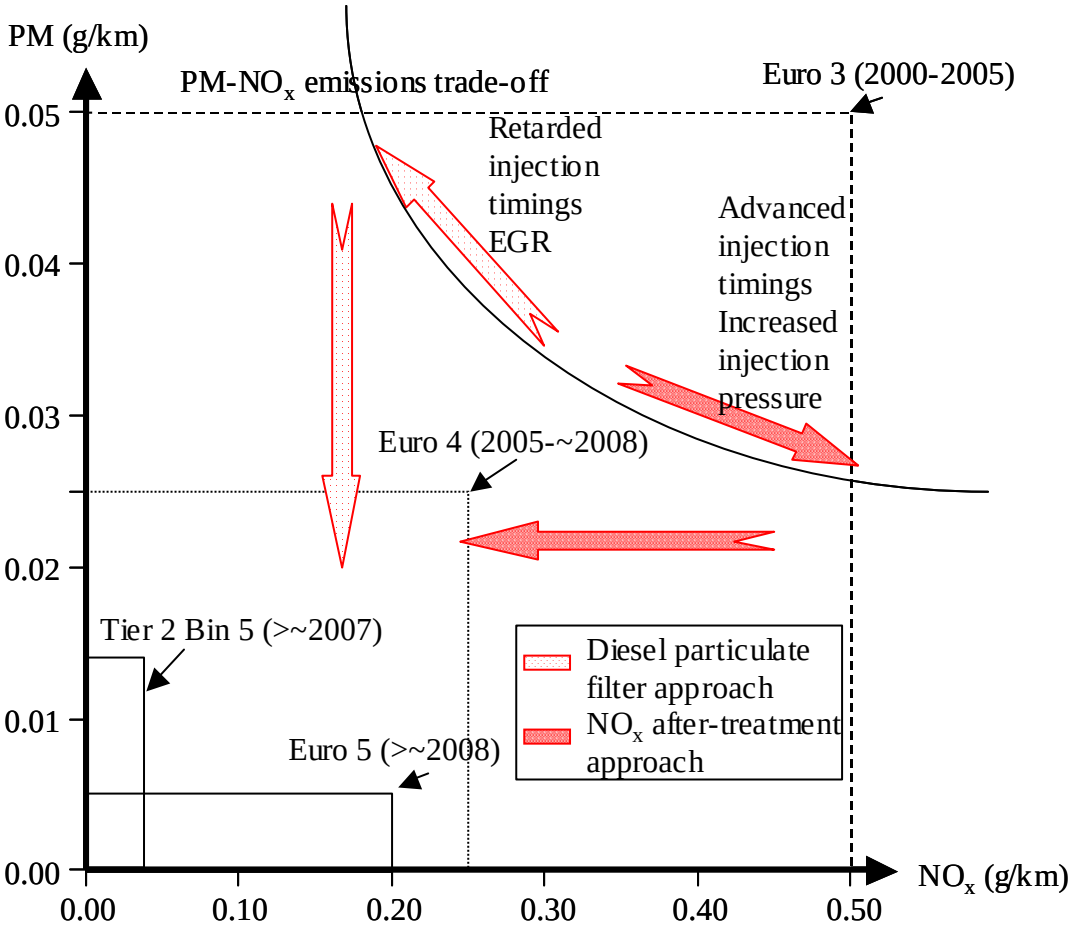

Figure 2-4: Approaches for achieving PM and NO_x emissions targets.

As can be seen in Figure 2-4, additional engine-out emissions reductions and after-treatment are required to meet future emissions targets, even in the case where mild-hybrid powertrain applications start making their appearance. Reducing engine-out NO_x and PM emissions has become the priority for diesel-engine and after-treatment developers, and especially the priority of the diesel-engine developers in order to alleviate the cost of after-treatment and keep the diesel powertrain cost competitive.

2.2.3 Major influencing parameters on the combustion and emissions

Since Monaghan's 1995 future light-duty diesel engine specification, the key developments to increase the efficiency, reduce emissions and further increase power have been in terms of compression ratio reductions permitted by the development of cold start technology, EGR rate increases and level of swirl reductions, both permitted by injection system strategies developed using the flexibility and capability of modern injection systems and engine controllers. Care must be taken when comparing results from different investigations since the starting points may vary. For example, in many cases, varying a parameter to understand its impact in the combustion process requires a re-optimisation of another: when investigating the impact of injection pressure on emissions, the bowl shape and main-injection timing should be optimised for each injection pressure. Therefore, a study carried out with an optimised piston bowl and injection timing for 1600 bar injection pressure will not give the same results as a study carried out with an optimised set-up for a 600 bar injection pressure. Trends will always be valuable but may not always be comparable.

- Compression ratio reduction:

A recent trend for diesel engines is the reduction of compression ratio, which is achieved by modifying the piston bowl shape and volume. Despite lower compression ratios leading to lower combustion efficiencies, the fact that compression is one of the largest contributors to friction necessitates a compromise between thermal efficiency and friction, Heywood (c & d) (1988). For the same maximum admissible In-Cylinder Pressure (ICP), i.e. structural strength, a compression ratio change from 20 to 14:1 only gives a small drop in efficiency, whereas the lower ratio considerably reduces engine friction, leakage and torque requirement for starting, as described by Taylor (1984). Jackson (2000) proposed a compression ratio of 15:1 as being the right balance between the two factors whilst pointing out that the current HSDI ratios of 18 to 20:1 are necessary to provide sufficient pressures and temperatures for cold starts. If compression ratio is reduced and the inlet-manifold pressure and temperature are maintained constant, the in-cylinder pressure and temperature at TDC decrease, thereby increasing auto-ignition delay, as described by Laguitton et al. (2002). With a current application, if compression ratio is reduced below 18:1, the auto-ignition delay

becomes such that it does not ignite during the compression or expansion stroke and the engine fails to start. The cold-start condition is currently the limiting factor in reducing compression ratio further. Glow plugs are common in diesel engines to assist in cold starts by heating the air before the compression stroke and this technology is improving to allow further ratio reductions. In addition, further reductions may be possible when considering flywheel mounted starter generators, capable of adjusting engine cranking speeds, or electrically assisted boost systems, capable of increasing the inlet-manifold pressure without relying on the turbine, or even variable valve timing, enabling a high compression ratio build to be used for starting and then capable of decreasing the effective compression ratio. An additional benefit from lowering the compression ratio highlighted by Jackson (2000) is that higher specific ratings are achievable for the same maximum in-cylinder pressure (P_{max}). At full load, higher levels of inlet-manifold pressure are possible for the same injection timing or more advanced injection timings are possible, both extending the full load torque capabilities. Reduction in compression ratio has been a key parameter for reducing engine friction, however, its reduction is now considered more and more for emissions purposes. Lower compression ratios lead to lower in-cylinder pressures and temperatures during the injection and combustion, which increase the auto-ignition delay and reduce the rates of combustion, as shown by Kawano et al. (2005), who reduced the effective compression ratio by retarding the intake valve opening. Based on studies by Kennaird et al. (2002), the penetration of the fuel spray is also extended with lower in-cylinder pressures, and combined with the increased auto-ignition delay, these effects lead to improved fuel-air mixing. This is expected to reduce PM emissions and also peak combustion pressures and temperatures, and hence NO_x formation as shown by Araki et al. (2005).

- EGR and associated inlet-manifold pressure increases:

A clear trend for diesel engines is the use of increasing EGR rates in order to control NO_x formation in the combustion chamber. EGR is mainly used at speeds and loads at which the engine operates during an emissions drive cycle. It acts in two ways on the combustion. Firstly, it increases the auto-ignition delay, as visible in the results shown by Henein et al. (2001), which increases the premixed-combustion phase relative to the diffusion combustion. This limits the amount of close-to-stoichiometric, hot

combustion. Secondly, EGR acts as a heat sink, thereby reducing the peak burned-gas temperatures, and hence NO_x formation, Heywood (e) (1988). The drawback of EGR is its effect on soot emissions since at equal inlet-manifold pressure, it substitutes itself for part of the air. This is compensated for by developments in turbo-charging and injection systems as illustrated by Jackson (2000) and Payri et al. (2003) who operated engines at higher inlet-manifold pressures and higher injection pressures. In order to operate the engine at high EGR rates without increasing the inlet-manifold pressure requirements, it is necessary to cool the recirculating gases to increase their density and to introduce larger masses for the same volume, but care must be taken to avoid issues with HC emissions and water condensation in the EGR for durability reasons (Gatellier and Walter, 2002). The requirements for higher EGR rates, as well as for increased specific power outputs, have encouraged technology development in the field of turbo-charging. The aim has been to increase the inlet-manifold pressure in order to maintain AFR targets despite greatly increasing the EGR rate and to increase the air mass flow at higher loads, thereby reducing smoke emissions by supplying more oxygen, and increasing the load capabilities. This offers realistic engine downsizing opportunities which aim to maintain the same full load torque (Laguitton et al., 2002), whilst reducing fuel consumption at part load due to reduced engine weight, pumping losses and friction as well as operating more efficiently at higher loads at similar speeds. The bigger turbochargers provide higher inlet-manifold pressures and full load torque capabilities, but the vehicle driveability then becomes a concern since the bigger turbines suffer from longer transient response times and poor low speed performance. Supercharging does not have this drawback since it is disconnected from the exhaust system but its impact on efficiency is negative. Turbo-charging can increase fuel consumption at lower loads even when used with a waste gate since it increases the backpressure, thus pumping losses, as detailed by Chi et al. (2002). They describe the benefits of technologies such as variable geometry turbines or variable nozzle turbines in terms of higher levels of inlet-manifold pressure achievable and lower pumping losses at lower loads. Other appealing solutions making their first appearance in vehicles or in development are twin turbocharger applications and electrically driven compressors. These reduce or eliminate the negative effects of the turbine.

- Levels of swirl reduction:

Swirl increases the fuel-air interactions and results in reduced PM emissions. For applications with variable levels of swirl, a high level is used at low loads and engine speeds, where the benefits of swirl are greater than the impact of throttling the engine and depriving it of air, whereas a lower level is used for higher loads to obtain the highest air mass flow possible, as described by Kawashima et al. (1998). The main effect of swirl is to increase the gaseous fuel and air interactions, as described by Browne et al. (1986), increasing the portion of fuel burned in the premixed-combustion, without affecting the auto-ignition delay. Unfortunately, current engines have different levels of swirl requirements during their operation, yet they rarely have variable swirl capabilities. The current practise is to define a level of swirl giving the best compromise between full load and part load soot emissions. At full load, the highest volumetric efficiency must be achieved for maximum 'breathing' of the engine, whereas at part load, the fuel-air mixing must be increased through air motion since the use of EGR causes higher soot emissions. The drawback of increasing swirl is that it degrades the volumetric efficiency and increases the pumping losses, and hence fuel consumption. Different mechanisms of swirl generation are used, from inlet-port configuration, helical or tangential (Kawashima et al., 1998), to port deactivation by throttling (Henein et al., 2001), or various levels of valve lift or flow guiding blades (Shenghua et al., 1999). The requirements for increased levels of swirl become less with conventional diesel combustion strategies as the injection systems take a larger role in the mixing process, as demonstrated by Whelan (2001).

- Injection system development, control and strategies:

The injection-system improvements represent perhaps the most significant step in diesel engine evolution and have taken place on several levels. The driving force behind these improvements is that a better injection in terms of atomisation, evaporation and fuel-air mixing, leads to a more controlled combustion, reducing emissions and fuel consumption. In an attempt to increase the fuel-air interactions, the injector-nozzle hole diameters have been steadily reduced, following the manufacturing and durability limitations, as smaller holes are known to generate

smaller droplets, which tend to evaporate and mix faster. In order to compensate for the flow restriction imposed by the diameter reduction, the number of holes has increased leading to a compromise between hole size and number of holes. Injection pressure is also in constant increase since it acts in three ways. The first compensates for the smaller holes to maintain the fuel-injection rates. The second increases the level of fuelling before auto-ignition so fuel-air interactions are maximised leading to low soot emissions (NO_x emissions increase but in a much smaller proportion than the soot emissions reduction, Chi et al., 2002). The third leads to much higher air entrainment and hence mixing, which reduces soot emissions. To counter the potential cavitation in injector nozzles associated with the higher injection pressures, conical-hole profiles with rounded inlets are used, as described by Mahr (2002) and illustrated by Blessing et al. (2002). These trends can be seen when comparing injector nozzles used by Bae and Kang (2000) in research work conducted before 2000 and injector nozzles used by the same team a few years later. Bae and Kang (2000) were investigating five-hole injector nozzles with hole diameters of 0.142 mm, whereas two years later they were studying six-hole injector nozzles with hole diameters down to 0.126 mm and with various conical hole profiles (Bae et al., 2002). Other emissions and fuel consumption reductions are to be expected with the appearance of faster responding injectors such as fast-acting solenoids, high-pressure unit injectors, piezo-electric injectors as illustrated by Takeuchi and Toyao (2002). These developments increase the ability to control the injection and allow the use of multiple injections to control the combustion. During one cycle, several combinations are now possible: pilot, early-pilot, main, split-main, post and far-post injections or simply several identical successive injections.

In order to control the fuel injection system and other engine systems, such as the EGR and variable nozzle turbine mentioned earlier, the control systems and their capabilities have been in constant progress. Most control systems are open loop, which means that the various systems around the engine are set based on predefined models, as functions of different requirements. Currently, some advanced controllers are closed-loop controlled, which means that the operating conditions are set and varied based on the response to the setting. Nakayama et al. (2003) focused their work on the control of oxygen concentration, and used it to control NO_x emissions during engine transient responses. Olsson et al. (2001) used closed-loop control of the angle

of 50 % burn of combustion as a means of controlling fuel consumption. More recently, Neunteufl et al. (2004) established a control strategy based on both the angle of 50 % burn and the maximum rate of pressure change. The application example focused on the phasing of the combustion relative to TDC, however, no reasons were given for the selection of the maximum rate of pressure change. Gartner et al. (2002) based a control strategy concept on the angle of 50 % burn and a representation of oxygen contents in the cylinder based on the air mass flow. The angle of 50 % burn was chosen as it is widely accepted as a measure of combustion efficiency and which offered a good correlation with NO_x emissions. The progress in injection system control has also enabled more complex strategies to be used as described below.

Pilot injections are used to reduce combustion noise, however, they can lead to increased soot emissions, as described by Lejeune et al. (2000). Noise is suppressed by injecting a small amount of fuel during the compression stroke, which burns before the main-injection, thereby increasing the in-cylinder pressure and temperature. This reduces the auto-ignition delay, and hence the premixed combustion. By burning the main-injection fuel as it enters the combustion chamber limits the rapid increase in rate of pressure change, hence noise. Apart from an increase in soot emissions, the pilot injection has limited adverse effects due to the small quantity of fuel it represents. Chi et al. (2002) observed an increase in HC emissions due to the over-leaning of the pilot injection but that this increase could be minimised by optimising the pilot-injection timing. Trueba et al. (2002) described how the correct timing of the pilot and main injections were essential in creating the appropriate conditions for the main combustion. If the main injection occurs when the pilot-injection fuel has started burning or has fully burned, the higher in-cylinder temperature and pressure lead to an instantaneous combustion of the fuel during the main injection. This suppresses the rapid pressure increase during premixed combustion and consequently reduces noise and NO_x formation. If the pilot injection occurs too early, it becomes too lean to burn and results in an increase in fuel consumption and HC emissions. The unburned fuel also increases the premixed-combustion phase and increases NO_x emissions. Badami et al. (2002) investigated the impact of two pilot injections, which usually resulted in similar trends but more pronouncedly. The second pilot injection assisted in the combustion of the earlier first pilot injection.

Post injections, occurring after the main injection, are used to reduce PM emissions, whilst having limited effects on NO_x emissions, as detailed by Badami et al. (2002), Beatrice et al. (2002) and Lejeune et al. (2000). The main role of these late injections is to re-activate the combustion which proves beneficial for further oxidation of PM and for improved fuel consumption.

Concerning the main injection, Gill et al. (2002) showed that if its timing was retarded, NO_x emissions and noise decreased whereas fuel consumption, PM and HC emissions increased. The lower in-cylinder pressure and temperature obtained with retarded injections reduce NO_x emissions, but limit the post-combustion PM oxidation processes. The increased premixed-combustion phase due to the lower in-cylinder pressure and temperature conditions also results in over-leaning of the outer-boundary of the fuel spray and an associated increase in HC emissions. The reduced PM emissions associated with the increased premixed combustion were not sufficient to offset the reduced oxidation processes, therefore resulting in an overall increase. The increase in fuel consumption is related to the increased lost energy at exhaust valve opening. Beatrice et al. (2002) compared a combined pilot injection and main injection with a combined pilot injection and split-main injection. The split injection approach showed benefits in terms of NO_x and PM emissions for no apparent increase in fuel consumption. The split injection was thought to enhance the utilisation of air and delay part of the combustion acting in the same way as post injection, promoting soot oxidation. The separation between injections, referred to as dwell, was varied and showed that increased dwell led to increased soot and reduced NO_x emissions. The larger dwell led to a more retarded second part of the main injection, which resulted in lower combustion temperatures hence reduced oxidation of PM. However, Brooks et al. (2004) found that a pilot injection and a split-main injection led to potential NO_x and soot emissions reductions but that these were accompanied by fuel consumption increases linked with the longer aspect of the injection and the later phasing relative to TDC of both the injection and the combustion. The flame temperature of split-injection combustion studied by Chmela and Riediger (2000) showed higher average temperatures than for normal injection, which explained the increased soot oxidation.

A summary of the effects of different strategies, i.e. pilot and main, pre injection (close pilot) and main, two pre injections and main, two pre injections, main and post

injections has been given by Ricaud and Lavoisier (2002). The last strategy resulted in a slight reduction in noise and fuel consumption and a reduction of more than 50 % in soot, HC and CO emissions for fixed NO_x emissions. Groenendijk and Müller (2002) published the first multiple-injection results, using successive identical injections to achieve homogeneous charge combustion. The reasons for investigating multiple injections were to increase the fuel-air interactions and to reduce the wall wetting. This illustrates the new approach to diesel engine combustion made possible by accurate control of the injection.

2.3 Stepping away from conventional diesel combustion

2.3.1 Background and concept

Research in diesel combustion over the past decade, by Takeda et al. (1996), Aoyama et al. (1996), Yanagihara (1997), Suzuki et al. (1997), Yokota et al. (1997), Kawashima et al. (1998), Iwabuchi et al. (1999), or Gatellier and Walter (2002), can be considered as a revolutionary step towards a new diesel-cycle engine. It represents a just-as-fundamental a switch as that from homogeneous to stratified mode in a gasoline engine, except that it is going in the opposite direction: the conventional stratified diesel compression-ignition combustion gives way to homogeneous charge combustion. It demonstrates the capability of reducing NO_x and PM emissions simultaneously, thus potentially offering an extended use of diesel engines without (or with greatly reduced) after-treatment requirements. This is all the more appealing since the technologies required for this step are already proven. The concept was initially investigated for gasoline applications in order to increase combustion stability (Onishi et al., 1979), to reduce the rapidity of the energy release (Najt and Foster, 1983), and later to suppress throttling at light and medium loads to increase efficiency (Thring, 1989). Thermodynamically, homogeneous charge combustion is closest to that ideal, i.e. the most efficient, constant-volume Otto cycle, as observed by Beatrice (2002). This is achieved by a very rapid combustion since in theory it is supposed to be global with no propagation. Hultqvist et al. (2001) agreed with this but found its application limited to the highly diluted mixtures to limit the maximum pressure rise and Heat Release (HR) during the bulk combustion.

The application of homogeneous charge combustion is based on a combination of gasoline and diesel engine operating characteristics. In gasoline applications, early injection with no throttling to limit pumping losses provided a lean, homogeneous mixture. Oakley et al. (2001) operated controlled auto-ignition or homogeneous charge combustion with gasoline for AFRs reaching 80:1. The high level of mixing guaranteed the homogeneity, hence the very low soot emissions, and the high AFRs guaranteed a diluted charge, far from stoichiometry, which resulted in low combustion temperatures, hence low NO_x emissions. The premixed charge was not spark-ignited but ignition was triggered by compression as with diesel engines and resulted in a global combustion of the charge with minimal flame propagation. This auto-ignition was facilitated either with elevated inlet-manifold temperatures of 320 °C or with specific valve timing to increase the amount of hot residuals or to increase the compression ratio. In diesel applications, the lean, homogeneous mixture was also the main objective to guarantee low NO_x and soot emissions.

Homogeneous charge combustion operation has long been considered as an appropriate operating mode for gasoline or natural gas applications due to the lower boiling points and higher critical compression ratios of gasoline or natural gas. These characteristics make more possible the formation of a homogeneous mixture with fewer knock and wall-wetting issues, as detailed by Heywood (f) (1988). The long-chain nature of diesel fuel and its boiling point, circa 100 °C higher than gasoline, make it more difficult to evaporate but more susceptible to premature combustion. Many studies have been undertaken to identify the most appropriate fuel for homogeneous charge combustion, from Thring (1989) to more recently Ryan III (2000), Ryan III and Matheaus (2002) and Shudo and Ono (2002). The general conclusions were that the most appropriate fuels are those with high Research Octane Numbers (RON) and low Cetane Numbers (CN), high Hydrogen-over-Carbon (H/C) ratios (including hydrogen added to fuel), low boiling temperatures and high elevated pressure auto-ignition temperatures. The only mention of diesel concerns the engines in which the research was carried out, since they offered the required high compression ratios, as illustrated by Olsson et al. (2001), Morimoto et al. (2001) and Kong et al. (2001). Diesel fuel has only recently been considered. Ryan III tested blends of diesel and gasoline, which was of particular interest since these fuels are widely available. The advantages of these blends are that the gasoline part increases

the fuel's resistance to knock, retarding auto-ignition and increasing the mixing and evaporation processes, whereas the diesel part facilitates auto-ignition. This cancels the need for higher compression ratios and inlet-manifold temperatures generally used to trigger homogeneous charge combustion with gasoline.

Diesel-fuelled homogeneous charge combustion regained researchers' interest due to the ever more stringent emissions legislation and the various steps made in diesel-engine technology. These steps were such as the use of high rates of cooled EGR, flexible, high-pressure capable injection systems, variable levels of swirl and cold-start technology permitting lower compression ratios. These steps are key to solving the initial problems encountered with diesel fuel, associated with poor evaporation and premature auto-ignition, and thus to the application of homogeneous charge combustion in diesel-fuelled engines. There are two possible approaches to the achievement of ultra-low combustion emissions, both aiming to obtain a lean and highly mixed charge. The first relies on early injections to achieve the mixture characteristics prior to ignition, best described as HCCI combustion. The second relies on late injections and the charge-air characteristics to enhance the fuel-air mixing to a level of fully-premixed state before the auto-ignition, best described as PCCI combustion. Weissback et al. (2003) described these two potential approaches to enable HSDI diesel engines to meet future emissions regulations, in terms of their local excess air and flame temperature, as can be seen in Figure 2-5.

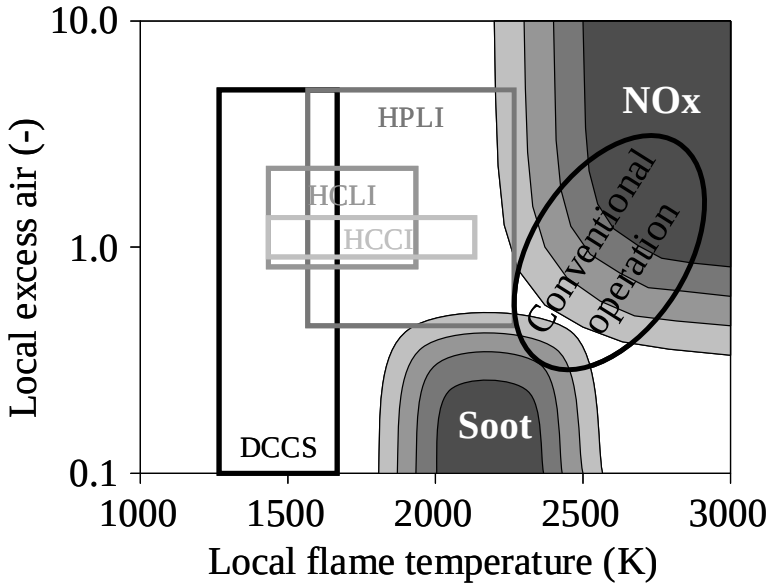

Figure 2-5: Combustion types for ultra-low NO_x and soot emissions.

Dilution Controlled Combustion Strategy (DCCS) is applied with high EGR rates (80 %) but results in very poor combustion efficiencies and is therefore not a viable option. PCCI combustion incorporates what Weissback has named Homogeneous Charge Late Injection (HCLI) and Highly Premixed Late Injection (HPLI), differentiating the levels of homogeneity of the premixed charge, which is dependant on the load.

2.3.2 HCCI operation

2.3.2.1 Description and challenges

The HCCI combustion was the first type of homogeneous charge combustion to appear in diesel engines and is a direct transfer of HCCI operation in gasoline engines. It relies on a chemically and physically homogeneous mixture and ignition is triggered by compression. There is no diffusion combustion but a global near-instantaneous combustion, offering the same ultra-low NO_x and soot emissions characteristics as for the gasoline application. The lean nature of the mixture results in negligible soot emissions and ultra-low NO_x emissions due to the low flame temperatures. Whilst this type of combustion offers clearly the best results in terms of NO_x and soot emissions, it also has drawbacks in terms of HC and CO emissions. The injection timing and the AFR become limited to very narrow operating ranges, especially as the load increases. A fuel-rich limit is set to avoid knock (excessive stress for the cylinder-head group) and increased NO_x emissions (when stoichiometric) whereas a lean limit is set to avoid misfire. Typically, two distinct stages are present in the combustion with the HCCI operation, as described by Hultqvist et al. (2001), Kong et al. (2001), Groenendijk and Müller (2002). The first stage is associated with the initial rupture of the long chains, often referred to as a cool combustion or low temperature oxidation (Simescu et al., 2003), which consists of a low temperature kinetics process. This initiates the active radicals, which trigger the main combustion, also referred to as the high temperature oxidation. The cool combustion does not occur with iso-octane fuel but is present under certain conditions with gasoline, (Kaneko et al., 2001), reinforcing the long chain theory. For high AFRs, it seems the cool combustion serves to increase the in-cylinder temperature in order to trigger the main combustion, i.e. the second distinct peak of the heat release,

and avoids misfire. EGR is used to reduce the oxygen concentration and to control the rate of combustion, especially for the higher loads where closer-to-stoichiometric mixtures are present.

There are two main difficulties associated with HCCI operation. The first is the control of start of combustion. In a conventional diesel engine, Start Of Combustion or Reaction (SOC or SOR) is generally a function of the in-cylinder temperature and pressure and local AFR (Heywood, g, 1988) and closely coupled with the injection. The mixture varies from infinitely rich to infinitely lean from the centre to the periphery of a stratified-diesel fuel spray, thus providing systematically at least one zone with the appropriate AFR for auto-ignition. On the other hand, the homogeneity in HCCI combustion means that there is theoretically only a single value of AFR throughout the combustion chamber and this is usually very lean, 45:1 (see Groenendijk and Müller, 2002, Yanagihara, 2002, Ryan and Matheaus, 2002), and even 55:1 (see Takeda et al., 1996). This occurs because HCCI operation is limited to lean mixtures to avoid high temperature combustion. Any in-homogeneities of the charge would trigger premature combustion, since some local zones would have lower fuel concentration and others higher, the latter more favourable to ignition, as explained by Heywood (g) (1988) and as can be seen in simulation results such as those obtained by Noda and Foster (2001). Shimazaki et al. (1999) found that any in-homogeneities in the mixture resulting from early injection of gaseous fuel have a large impact on the ignition timing and the rate of combustion. Premature combustion is accompanied by negative work during compression and additional mechanical stress. Equally, the increased fuel concentration leads to hotter combustion which offsets any NO_x reduction. For these reasons, accurate control of local and hence global AFR is required since it determines the start of combustion. Sufficient time must be allowed to ensure the homogeneity of the mixture at auto-ignition, thus requiring very early injection timing, which has the effect of decoupling the injection and the combustion.

The second main challenge for HCCI operation is the potential increase in noise, HC and CO emissions. The early injection causes over-leaning of the fuel-air mixture as well as flame quenching due to the proximity of the combustion to the colder cylinder walls, which can also lead to oil dilution. These effects are sources of HC emissions

traditionally found in gasoline applications, where the charge occupies the entire combustion chamber. The rapid reaction rate of HCCI operation has thermodynamic benefits but also has highly undesirable effects such as increased noise. This is especially problematic as HCCI operation is limited to light load operating conditions when high levels of fuel dilution are possible.

2.3.2.2 Examples of HCCI combustion application

PREDIC:

Takeda et al. (1996) have applied HCCI combustion to a diesel-fuelled single-cylinder engine with a swept volume of 2004 cc, a compression ratio of 16.5:1 and a level of swirl 0.5 Rs. They examined the impact of injection timing, CN and AFR on emissions, fuel consumption and heat release for different injector set-ups, including one with two diametrically opposed injectors capable of 1500 bar injection pressure (twice 2 holes of 0.17 mm in diameter). The double injectors were positioned so that the fuel sprays would collide in the middle of the chamber to limit wall-wetting with very early injection. Results obtained with different CN fuels indicated that with an injection timing of -140 °CA ATDC, higher CN values led to two-stage combustion as can be seen in Figure 2-6, taken from Takeda et al. (1996). This was not the case with lower CN fuels. Earlier injection timings were possible with the higher CN fuel and resulted in further NO_x and smoke emissions reductions. However, this was accompanied by a rapid increase in fuel consumption. An examination of the instantaneous heat release curves indicated that the lower NO_x emissions were achieved when the gradient of the curves was reduced, reflecting reduced rates of combustion. Photographs showed a luminous combustion flame obtained with an injection timing of 3 °CA ATDC, whereas the flame was non-luminous in the case of an injection timing of -140 °CA ATDC. This non-luminous flame characterises the combustion of a lean mixture, representative of HCCI combustion and indicative of low PM formation and oxidation.

Most testing was done with CN 19 fuel not requiring high EGR rates or low compression ratios to retard the start of combustion. Tests showed that as load

increased, the operating window for the injection timing reduced, constrained by knock and misfiring limits, as can be seen in Figure 2-7, also taken from Takeda et al. (1996). The lower loads resulted in more diluted mixtures, which benefited from a wider injection-timing window whilst still able to achieve very low NO_x emissions. It is thought that the higher levels of fuel dilution retarded the auto-ignition. Significant increases in HC and CO emissions (respectively up to 4000 and 5000 ppm) were attributed to the over-leaning of the mixture. Some tests were carried out using a 30-hole central injector leading to slightly lower fuel consumption and smoke, HC and CO emissions compared with the conventional injector, which may be associated with the finer atomisation and more localised mixture due to the reduced penetration of the fuel spray.

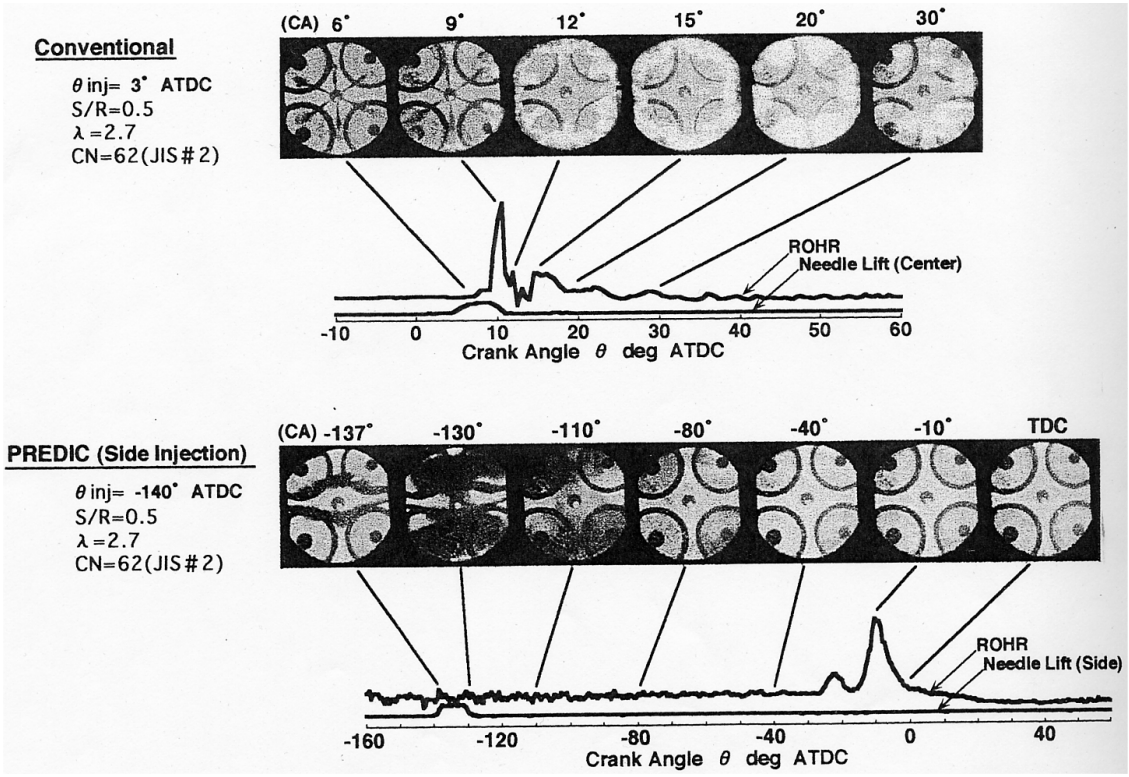

Figure 2-6: Instantaneous heat release and photographs of HCCI operation.

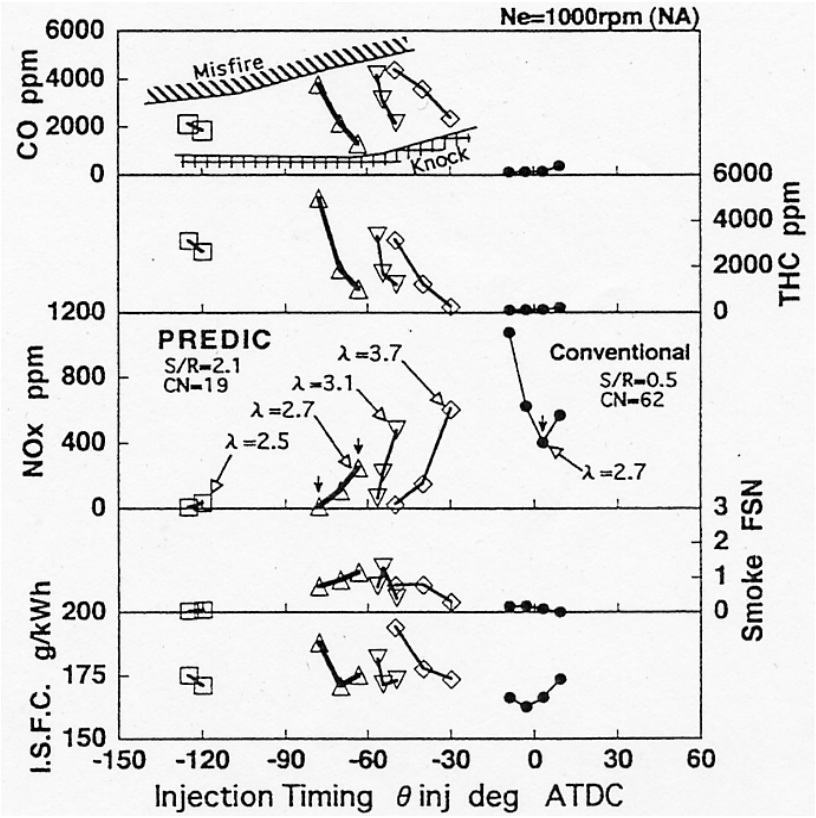

Figure 2-7: Example of effect of injection timing and load on HCCI operation.

Reprinted with permission from SAE 961163 © 1996 SAE International.

In an attempt to solve the problem of high HC and CO emissions during HCCI operation, Akagawa et al. (1999) investigated the effects of EGR rate and oxygenated fuels on fuel consumption and the effects of the top-land crevice volume on HC and CO emissions and on adhesion of fuel on the walls. They also investigated double injections, the first early injection to form a homogeneous and lean mixture and the second later one for conventional combustion. Much higher loads were found possible whilst achieving low NO_x emissions but this was accompanied by an increase in fuel consumption. Multiple injections were also investigated by Morita et al. (2000) and further developed by Nishijima et al. (2002), investigating the effects of split injections and water injection. Split injections reduced HC and CO emissions but unfortunately increased NO_x emissions.

UNIBUS:

Yanagihara et al. (1997) has also applied HCCI combustion with diesel fuel. They transferred the experience gained by Aoyama et al. (1996) on gasoline HCCI

operation to a diesel fuelled application. The results showed NO_x emissions halved in a 915 cc single-cylinder engine as well as in a 2000 cc engine both with 18:1 compression ratio. Yanagihara (2001) used piezo-actuator injectors with pintle-type injector nozzles to reduce the spray penetration in an attempt to limit the over-leaning of the charge. The investigations examined the impact of the injection timing, level of fuelling, EGR rate and double injections on emissions, torque, instantaneous heat release and load. These results were compared to conventional diesel combustion with the same injector. The engine was operated at 1000 rev/min with an injection pressure of 400 bar. Low levels of fuelling and low injection pressures were thought to be most appropriate to limit wall wetting and knock with this particular injector nozzle. For an injection timing of 60 °CA BTDC, low temperature oxidation occurred at 23 °CA BTDC and high temperature oxidation at 10 °CA BTDC. A luminous flame was not observed due to the negligible PM available for oxidation, confirmed by low PM emissions.

The effect of advancing the injection timing with a fixed level of fuelling (15 mm^3) from TDC to 150 °CA BTDC is presented in Figure 2-8, taken from Yanagihara (2001). From TDC to 30 °CA BTDC, NO_x emissions increased up to 1500 ppm, as a result of increased rates of combustion and flame temperatures. The latter also increased soot oxidation, reducing soot emissions and limited HC formation and emissions. For a fixed level of fuelling, the load increased from 1.5 to 2.5 bar Indicated Mean Effective Pressure (IMEP) indicating a much better combustion efficiency and phasing relative to TDC. From 30 to 60 °CA BTDC, NO_x emissions were returned to their initial low level and soot emissions also reached very low levels whereas HC emissions started increasing, due to over-leaning. These trends highlight the effect the increased levels of mixing have on reducing the flame temperature, and hence the NO_x emissions. It is expected that the negligible soot emissions are no longer due to high levels of oxidation but to low levels of formation. Load decreased to 2 bar and is probably a result of negative work. Earlier injection timings confirm the trends with low NO_x and soot emissions and high HC emissions as a result of HCCI combustion. Unfortunately, the load dropped to 0.5 bar which is unacceptable. Double injections were then used and EGR rate increased to the maximum level achievable. This doubled the load whilst NO_x emissions remained ultra-low (10 ppm) but highlighted a very high fuel consumption penalty. Further studies were then

carried out looking at the possibility of using a second injection closer to TDC to trigger the combustion (Hasegawa and Yanagihara, 2003), which reduced the NO_x benefits but also the fuel consumption penalty.

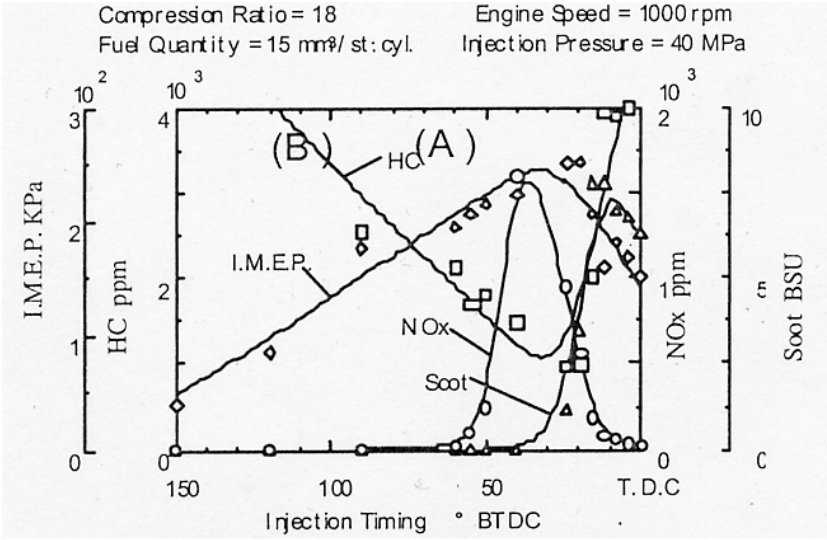

Figure 2-8: Example of effect of injection timing on HCCI operation.

Reprinted with permission from the author.

2.3.3 PCCI operation

2.3.3.1 Description and challenges

The PCCI operation aims to achieve the same lean and homogeneous mixture as that obtained with HCCI operation and the associated NO_x and soot emissions reductions. The main difference with HCCI operation is in the way the mixture is prepared. Late injections, rather than early, combined with high EGR rates enable the start of combustion to be delayed thereby allowing all the fuel to be injected before auto-ignition. The increased fuel-air interactions form a fully-premixed charge prior to combustion rather than the combined premixed and diffusion combustion, as can be seen by the rate of pressure change in Figure 2-2. The reduction in NO_x and soot emissions is a function of the level of premix at the time of combustion, which is itself a function of the delay between the end of injection and start of combustion. This type of combustion is also more flexible in operating AFR ranges and does not require precise control of the local AFR to control start of combustion since this is mainly achieved through injection timing. Typically, a single-stage combustion process

occurs with PCCI combustion, which resembles more the conventional diesel premixed combustion, compared with the low and high temperature oxidation phases seen with HCCI combustion (Kimura et al., 1999).

The PCCI combustion does not offer the same levels of emissions reduction nor does it have the same challenges. It is an approach generally more adapted to diesel-fuelled applications as it does not rely on early injection timings and is therefore less prone to wall wetting and high increases in HC and CO emissions. Furthermore, the combustion is not fully decoupled from the injection as in HCCI operation due to the late injections used, making the control of the start of combustion easier. PCCI operation can be used as a target across the engine speed and load, not meeting the target does not result in excessive cylinder head stresses and ultimately engine failure as would be the case with HCCI operation, but it results in higher NO_x and soot emissions. EGR is used to delay the start of combustion, as detailed by Kimura et al. (1999). This reduces the constant-volume Otto cycle aspect but serves to give even further reductions in NO_x emissions.

2.3.3.2 Example of PCCI combustion application

MK:

Kawashima et al. (1998) were one of the first teams to present an application of PCCI operation, which was achieved by employing high levels of swirl. The levels of swirl investigated were between 3.5 and 10 Rs, much higher than in conventional DI diesel engines. Kimura et al. (1999) conducted more detailed investigations on a single-cylinder engine with a swept volume of 488 cc and a compression ratio of 18:1, with EGR capabilities at light load and injection pressures up to 700 bar. This approach relies on the combustion phasing relative to the injection. Its essence is the completion of injection before auto-ignition. This increases the air entrainment in the spray before combustion and thereby reduces the amount of stoichiometric mixture and also suppresses diffusion combustion. In contrast with HCCI operation, the injection is retarded as much as possible past TDC to inject into lower in-cylinder pressures and temperatures in order to delay auto-ignition and increase fuel-air interactions. The

typical instantaneous heat release shows a single phase. Kimura et al. (1999) demonstrated low PM emissions backed-up by an indiscernible flame in an optical set-up and a tenfold reduction in NO_x emissions at 2000 rev/min 5 bar Brake Mean Effective Pressure (BMEP). This may seem like a standard engine calibration process, but in reality it is a step towards a new type of combustion. Furthermore, the authors explained the underlying processes, which prove very useful in understanding the engine optimisation requirements.

The impact of the three measures used to suppress diffusion combustion are shown in Figure 2-9, (taken from Kimura et al., 2001). Lowering the oxygen concentration from 21 to 15 % was the first, which had as effect a drastic reduction in NO_x emissions. This measure increased the auto-ignition delay and limited the hot and close-to-stoichiometric diffusion combustion, and hence NO_x emissions. This also led to the over-leaning of the fuel-air mixture in the outer boundary of the spray, thereby increasing HC emissions. The lower oxygen concentration limited the PM oxidation processes and led to incomplete combustion, another source of HC emissions. The thermal efficiency was slightly improved from 40 to 41 %, which was close to the measurement accuracy, but may result from a faster combustion despite being retarded. Retarding the injection timing from 3 to -7 °CA ATDC was the second measure, which led to a further decrease in NO_x emissions due to a further reduction, and maybe total suppression, of diffusion combustion. The increased fuel-air interactions, resulting from the lower in-cylinder pressures and temperatures during the injection and combustion, as well as the increased delay in auto-ignition, were also beneficial for PM emissions. A further over-leaning of the fuel-air mixture increased HC emissions. Despite the faster combustion, the impact of retarding the combustion relative to TDC reduced thermal efficiency. Finally, the third measure was an increase in level of swirl. This limited the over-leaning of the fuel spray by limiting radial penetration in favour of tangential motion. It also reduced smoke emissions by increasing the air entrainment. This was accompanied by an increase in the rate of combustion as demonstrated by the increases of both NO_x emissions and thermal efficiency.

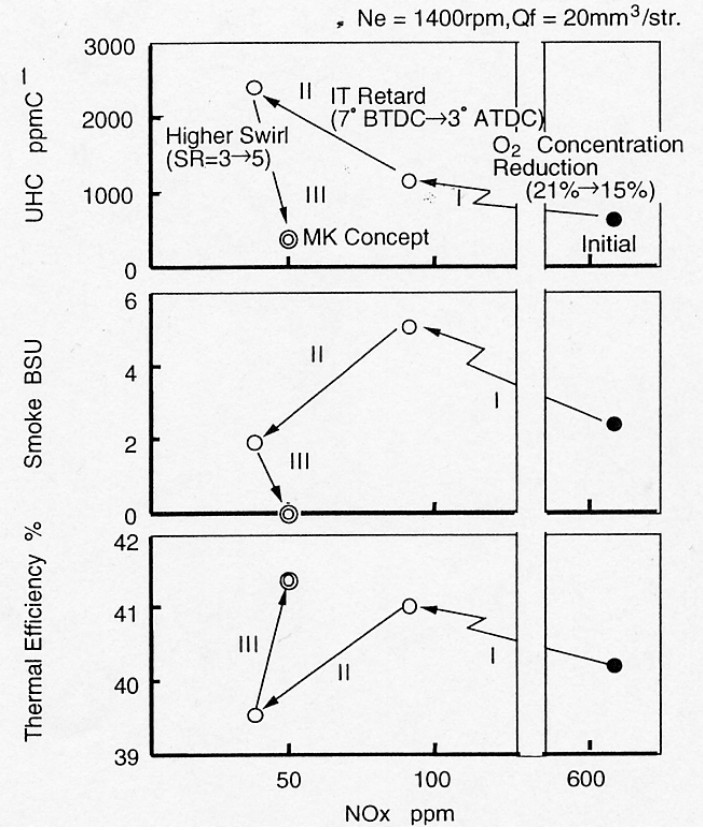

Figure 2-9: Example of requirements for PCCI operation and their impact.

Reprinted with permission from SAE 2001-01-0200 © 2001 SAE International.

Further work (Kimura et al., 2001) was carried out on a four-cylinder engine with a swept volume of 2488 cc, mainly extending the range of PCCI operation. Injection pressure was increased to shorten the injection duration and the compression ratio was reduced to 16:1 in order to reduce the pressure and temperature in the cylinder during the compression, thereby delaying auto-ignition further. EGR used in the first instance was cooled in order to increase the rates achievable, thus retarding the auto-ignition further and serving as a thermal capacitance. More recent work by Kawamoto et al. (2004) proposed the use of higher CN fuel, which went against other HCCI operating requirements, but was recommended to reduce HC emissions under cold-start conditions. The major advantage of PCCI combustion is illustrated here by its ease of implementation since it does not require additional or different hardware. Equally, its operation with conventional hardware did not affect the engine specific power output negatively.

2.3.4 Other related investigations

The research carried out to date has investigated means of realising the full benefits of HCCI and PCCI combustion. There are many comparison elements amongst different operating conditions, including the heat release or instantaneous heat release, BMEP, IMEP and Gross IMEP (GIMEP), combustion efficiency, EGR rate, AFR, Brake Specific Fuel Consumption (BSFC), auto-ignition delay and emissions characteristics. These are directly monitored or calculated from the inlet-manifold, exhaust and in-cylinder pressures and temperatures, torque, emissions (HC, NO_x, PM, CO, CO_2), air and fuel flows… These have been investigated for many operating conditions and a wide range of hardware, in order to understand their impact on combustion and to provide an understanding of the requirements to control the mixture, the start of combustion or start of reaction and the rate of reaction during HCCI or PCCI combustion. The main operating conditions varied to assess their impact are listed below:

- Engine hardware: piston-bowl geometry, compression ratio, port geometries
- Engine operation: speed and load range, valve timing
- Fuel: pump, bio, single-component fuel, pure or blends or with additives
- Injection system: injector and nozzle characteristics
- Injection operation: timing, pressure, number of injections, quantity
- Inlet: temperature, pressure, EGR rate
- Mixture: motion, turbulence, AFR.

Table 2-2 lists key diesel-fuelled research and shows the main parameters investigated and the results. Only recently has the research using diesel fuel taken off, which explains the increase in the number of publications in the last five years.

Authors, affiliation & year of publication	Areas studied and results
Ryan III, 2000, Southwest Research Institute	• Investigating: impact of fuel characteristics on compression ignition in a single-cylinder engine and six multi-cylinder prototype engines. • Varying: CN from 42 to 53, density from 830 to 869 kg/m^3, mono-aromatics from 10 to 25 %, poly-aromatics from 2.5 to 10 %, looking at the impact on weighted NO_x emissions and on the impact of EGR. • Conclusions: NO_x emissions increased with fuel density and aromatic content, remained constant for varying CN and decreased for higher hydrogen contents. Fuel type did not affect the impact of EGR.
Kong et al., 2001, Engine Research Center, University of Wisconsin-Madison and Division of Combustion Engines, Lund Institute of Technology	• Investigating: impact of operating conditions on HCCI operation using experimental and modelling results in a diesel, 2440 cc, CR 16.1:1, single-cylinder engine (caterpillar 3400 series SCOTE). • Varying: injector type, IP form 500 to 900 bar, single or split injection, AFR from 50 to 60:1, IT from 131 to 44 °CA BTDC, speed from 700 to 1500 rev/min, looking at the impact on ICP, ROHR, combustion duration, ignition delay. • Conclusions: not all variables reported. ROHR showed two phases. Little impact was obtained from engine speed on combustion duration and ignition delay.
Yokota et al., 1997, Hino Motors	• Investigating: impact of multiple injections on compression ignition in a diesel, CR 18:1, 2147 cc, single-cylinder engine equipped with 900 bar IP capable injection system. • Varying: number of holes from 6 to 30, cone angle from 55 to 155 °, IT from 5 to -20 °CA BTDC with different strategies, looking at the impact on NO_x and HC emissions, Bosch Smoke Unit (BSU), BSFC, ROHR and combustion flame. • Conclusions: multiple injections (Homogeneous Charge Intelligent Multiple Injection Combustion System) were worse than pilot and main injections with traditional IT. Multiple injections were better for NO_x emissions, FC, BSU with worse HC and CO emissions at retarded ITs. Early multiple injections led to lower ROHR and benefited from the 30-hole injector nozzle.

Authors, affiliation & year of publication	Areas studied and results
Iwabuchi et al., 1999, Mitsubishi Motors Corporation	• Investigating: impact of injector-nozzle hole configuration on spray and combustion characteristics for Premixed Compression Ignition in a 4-valve, diesel, CR 12:1, 2000 cc, single-cylinder engine equipped with 800 bar IP-capable injection system, 80 ° cone angle, level of swirl 2.2 Rs. • Varying: EGR/AFR of 0 % / 59:1 to 58 % / 20:1, IT from 80 °CA BTDC to 10 °CA ATDC, injector-nozzle type and hole configuration, looking at BSFC, ROHR and NO_x, HC and smoke emissions, flame luminescence, spray penetration and angle, simulated cone angle effect and adhered fuel to wall. • Conclusions: Premixed Compression Ignition results with conventional injector nozzle worsened in most cases. An optimised injector nozzle reducing penetration and enhancing the mixing gave a tenfold reduction in NO_x and smoke emissions below conventional levels. HC emissions improved but remained elevated for a BSFC penalty of circa 10 %. Impinged spray injector nozzle linked with lower CR led to lower ROHR. Combustion occurring earlier than TDC decreased the efficiency. If EGR increased, SOR retarded and ROHR decreased in amplitude and duration leading to an increase in efficiency.
Ryan III and Matheaus, 2002, Southwest Research Institute	• Investigating: impact of fuel type on compression ignition in a combustion bomb and in a 702 cc, Port-Fuel Injected (PFI), single-cylinder engine with CR from 14 to 16:1. • Varying: fuel from Fisher Tropsch Naphtha to diesel with up to 80 % gasoline content, inlet-manifold temperature from 110 to 170 °C, CN from 20 to 100, RON from -600 to 100, looking at the impact on Bosch Smoke Number (BSN), SOR, HR, ICP, elevated pressure auto-ignition temperatures and ignition delay. • Conclusions: for inlet-manifold temperatures up to 150 °C, both the lower temperatures and gasoline contents led to higher BSN. Higher CRs advanced SOR. Higher gasoline contents required higher inlet-manifold temperatures to react and led to higher ICPs and cumulative heat released. Higher CNs lowered the elevated pressure auto-ignition temperatures and the opposite was seen with higher RONs.

Authors, affiliation & year of publication	Areas studied and results
Shimazaki et al., 2003, Isuzu Advanced Engineering Center	• Investigating: impact of near-TDC injection for premixed diesel combustion using a 125 ° cone angle with a large bowl in a 4-valve, diesel, CR 16.5:1, 1298 cc, single-cylinder engine equipped with 1200 bar IP-capable injection system, level of swirl 1.1 Rs. • Varying: IP from 30 to 1200 bar, IT from 40 to -5 °CA BTDC, CN from 19 to 61 looking at ROHR, ICP, BMEP, BSCO, BSFC, $BSNO_x$, BSHC and smoke. • Conclusions: with CN 19, $BSNO_x$, BSCO, BSHC and smoke emissions were lowest at 25 °CA BTDC. Earlier ITs led to a general increase in emissions for the same BSFC. When IP was varied from 900 to 1200 bar, emissions decreased for a stable IMEP but friction losses from pump resulted in increased BSFC. With 60 % EGR and AFR of 58:1, CN 61 gave lower NO_x emissions than with CN 19 but higher smoke emissions for ITs near TDC. Late injections at 4 °CA ATDC showed benefits for smoke and NO_x emissions but large penalties in terms of BSFC.
Su et al., 2003, State Key Lab of Engines, Tianjin University	• Investigating: impact of multiple injections and bump combustion chamber on premixed and lean diffusion combustion in a 2-valve, diesel, CR 15:1, 1620 cc single-cylinder engine equipped with 800 bar IP-capable injection system, level of swirl 1.8 Rs. • Varying: piston bowl with or without inner ring, AFRs from 20 to 30:1 by increasing inlet-manifold pressure, number of injections from 1 to 4 early injections plus one main injection, level of fuelling, IT from 150 to -3 °CA BTDC, looking at ICP, ROHR, PM, NO_x and HC emissions. • Conclusions: Early injections led to a two-phase heat release, the peak typically towards 20 °CA BTDC, and the second nearer TDC. The earlier the injections, the later the second phase of HR. Earlier injections led to lower NO_x, higher HC and smoke emissions whereas when adding a main injection, NO_x and smoke emissions trends inversed. The bump impact seemed to be beneficial also in conventional mode for smoke emissions by avoiding bowl impingement. When using 4+1 pulses, the first four seemed to work against the engine as the combustion occurred before TDC.

Authors, affiliation & year of publication	Areas studied and results
Simescu et al., 2003, Southwest Research Institute	• Investigating: impact of simultaneous PFI and DI strategies on PCCI operation and emissions in a diesel, CR 16.6:1, 14.6 L, 6-cylinder engine equipped with electronic unit injectors. • Varying: for a fixed load, fuel injected in port from 0 to 70 %, IT of PFI from 310 to 370 °CA ATDC, main IT from 10 to -5 °CA BTDC, looking at ROHR, ICP, BSFC, mass fraction burned and NO_x, CO and smoke emissions. • Conclusions: Varying PFI timing did not affect the combustion. With the main IT unchanged, the higher portions of PFI led to lower ROHR in main combustion, but higher ICPs at low load. At low loads, PFI seemed beneficial for NO_x emissions whereas at higher loads, DI seemed more appropriate. HC emissions and BSFC both increased with increasing portion of PFI. With main injection at TDC or later, a low and a high temperature oxidation occurred and finished before the main injection started. This cancelled the increase in CO emissions previously obtained with the increases in BSFC and smoke emissions reduced. NO_x emissions were reduced by up to 35 %. Large cylinder-to-cylinder variations were observed.
Gatellier and Walter, 2002, Ranini et al, 2004, Institut Français du Pétrole	• Investigating: Narrow nozzle cone angle and adapted piston geometry operating conditions in a diesel, 416 cc, single-cylinder engine equipped with 1350 bar IP capable injection system and multiple injections and 100 ° cone angle • Varying: CR 18.0 to 14.0:1, speed 1500 and 2500 rev/min, load from 2 to 8 bar IMEP, looking at PM, NO_x, CO, HC emissions, BSFC. • Conclusions: Typical two-stage HCCI combustion occurred. EGR was not cooled below 90 °C to avoid condensation issues. At 1500 rev/min, high CR with advanced ITs led to penalty in BSFC due to premature ignition, hence negative work. Lower EGR rates were required to delay the combustion with lower CR. Lower CR led to lower NO_x and PM emissions but also lower HC and CO emissions. Results at 2500 rev/min showed that the increased speed was beneficial for early injection timings because time to TDC was shorter reduced the auto-ignition delay in crankangle terms. The trends for HC and CO emissions were clearer. Concerns for diesel oxidation catalysts were raised due to the reduced exhaust temperatures. Electrically assisted boost, multiple injections, variable valve actuation were seen as extremely valuable for HCCI operation.

Table 2-2: Key research in diesel-fuelled HCCI and PCCI operation.

Table 2-3 lists the main actors in the diesel-like n-heptane fuelled fundamental HCCI and PCCI combustion research work and shows the main parameters investigated and the results. This type of fuel is clearly much more attractive and has been extensively used since it offers the same auto-ignition properties as diesel fuel but has a much lower boiling temperature of circa 100 °C (similar to gasoline). The main advantage is that it permits easy evaporation with very early injection timing, especially in HCCI combustion, without the usual wall-wetting issues. Its lower molecular weight, density and its higher calorific value must be kept in mind when making comparisons with diesel-fuel results. This allows an improved understanding of the mixing requirements, without needing to address the poor evaporation problems. It seems to be an acceptable approach when considering the great leaps forward being made in injection systems technology. Indeed, engine developers are now able to rely on multiple-injection capable injection systems with micro-hole injector nozzles and high injection pressures, thus leading to extremely rapid injection and evaporation, which explains the value of the diesel-like n-heptane based research.

Authors, affiliation & year of publication	Areas studied and results
Tanaka et al., 2001, Mitsubishi Heavy Industries and Mitsubishi Motors Corporation	• Investigating: impact of in-cylinder conditions on HCCI combustion characteristics in a rapid compression machine with similarities to a small diesel engine at 1100 rev/min, n-heptane, 900 bar IP-capable injection system. (Concept also demonstrated on diesel fuelled, CR 15:1, 4249 cc, 4-cylinder engine). • Varying: AFRs from 8 to 60:1, oxygen concentration from 15 to 21 %, CR from 6 to 8:1, looking at ICP, ROHR, flame luminosity, ignition delay, PM and NO_x emissions concentrations. • Conclusions: despite injecting 5 minutes before the compression, results indicate that higher CRs and oxygen concentrations led to earlier ignition, faster combustion and higher pressures. The ignition delay increased slightly for increased AFRs.

Authors, affiliation & year of publication	Areas studied and results
Suzuki et al., 1997, Traffic Safety and Nuisance Research Institute	• Investigating: impact of <u>in-cylinder conditions</u> on HCCI diesel combustion characteristics in a 4-valve, PFI and DI, CR 20.4:1, 522 cc, single-cylinder engine equipped with 1800 bar IP-capable injection system and with iso-octane and n-heptane for PFI-premixed and light oil for DI, running at 1500 rev/min and IT of 15 °CA BTDC. • Varying: port injected to total injected ratio from 0 to 1 (1 being all PFI), EGR from 0 to 30 %, RON from 50 to 100, AFRs from 30 to 80:1, load from low to maximum acceptable in conventional mode (smoke limited), looking at ICP, ROHR, ignition delay, mass fraction burned, Indicated Specific Fuel Consumption (ISFC), maximum load, NO_x, CO, HC and smoke emissions • Conclusions: Varying premixed ratio had little impact on ISFC. NO_x and smoke emissions decreased with increased ratios whereas HC and CO emissions increased. For loads between 50 and 75 % full load and RONs between 75 and 100, NO_x emissions with the increased ratios reached the level of the lower loads and RONs tested. This was achieved with little impact on smoke emissions. Increasing EGR reduced NO_x emissions to the detriment of smoke emissions.
Groenendijk and Müller, 2002, Institute for Internal Combustion Engines, Technical University of Braunschweig	• Investigating: impact of <u>homogeneity</u> on compression ignition via simulation and experimental results using n-heptane (same CN as diesel), in a CR 14.7:1, 3+1-valve, 1800 cc, single-cylinder engine. • Varying: IT from 11 to 95 °CA BTDC, 8 injections of 5 mg or one injection of 40 mg of fuel, EGR/AFR of 0 % / 45:1 to 50 % / 28:1, IPs from 800 to 1400 bar, looking at the impact on NO_x and CO emissions, Filter Smoke Number (FSN), BSFC and combustion flame. • Conclusions: higher EGR rates retarded auto-ignition and lowered HR and NO_x emissions while increasing CO emissions. Advancing IT delayed auto-ignition, lowered HR, NO_x, CO and smoke emissions and BSFC.

Authors, affiliation & year of publication	Areas studied and results
Christensen and Johansson, 2002, Division of Combustion Engines, Lund Institute of Technology	• Investigating: impact of swirl and turbulence on combustion characteristics in a 2-valve, PFI, 50 % iso-octane, 50 % n-heptane (RON 50), CR 11.1:1, 1600 cc single-cylinder engine (Volvo TD100 HDD). • Varying: level of swirl from 2 to 2.8 Rs, combustion chamber from disc to square bowl, looking at the impact on turbulence, ROHR and its peak timing, ICP, combustion duration, HC, CO, NO_x emissions, mean temperature, combustion efficiency. • Conclusions: square combustion chamber geometry required lower inlet-manifold temperatures since it got hotter. It also increased combustion duration and lowered ROHR. Swirl did not influence the combustion duration.
Peng et al., 2003, Department of Mechanical Engineering, Brunel University	• Investigating: impact of AFR and EGR rate on HCCI operation in an n-heptane, PFI, CR 18:1, 500 cc, single-cylinder engine with an inlet-manifold temperature of 30 °C. • Varying: lambda from 1.5 to 15, EGR from 0 to 70 % by mass, avoiding the misfiring and knock areas and looking at IMEP, level of fuelling, coefficient of variation of IMEP, start and duration of low temperature reaction, length of the negative temperature coefficient, start and duration of the main combustion, NO_x, HC and CO emissions and BSFC and the maximum combustion temperatures. • Conclusions: maximum IMEP was achieved for the lowest lambdas, where the coefficient of variation of IMEP, main combustion delay and duration, and CO emissions were most sensitive to EGR, and the NO_x and HC emissions were highest. The low temperature reaction was controlled by EGR whereas the AFR controlled the duration. The start and duration of the main combustion were controlled by lambda and EGR for the higher loads.

Table 2-3: Key research in n-heptane-fuelled HCCI and PCCI operation.

2.4 Objectives for present work

As illustrated by the above described research work, low NO_x and PM emissions have been demonstrated on research and production engines and have given some indications as to how these types of combustion can be obtained. It is clear that PCCI combustion does not offer the same low NO_x emissions as HCCI combustion,

however, it is characterised by much lower HC and CO emissions. This can be seen by comparing results shown in Figure 2-7 with those in Figure 2-9, despite the fact that they are taken at different speeds and loads and on different engines. Although injection is complete before auto-ignition, the PCCI combustion mixture is not as lean as in HCCI combustion and therefore results in higher NO_x emissions. An advantage PCCI operation has over HCCI operation is its ease of implementation as well as its simpler control requirements.

The present work proposes to extend investigation further to ultra-low NO_x and soot emissions using PCCI operation by further increasing mixing and reducing flame temperatures with the objective of meeting Tier 2 Bin 5 and possible Euro 6 NO_x emissions targets. It is believed that by achieving ultra-low NO_x emissions using PCCI operation and by extending its operating limits will reduce the need for HCCI operation and limit the associated increase in HC and CO emissions. Beyond aiming for these NO_x emissions targets, the programme focuses on developing understanding of the impact that evolutionary hardware and advanced combustion operation have on the combustion characteristics, notably on the maximum rate of in-cylinder pressure change. This is in order to improve control of the operation and hence combustion, and in time, can offer further emissions reductions with the potential to improve fuel economy.

It is necessary to rely on available fuels, such as pump grade diesel fuel. Its poor evaporation and good auto-ignition characteristics make it a relatively difficult and challenging fuel to use. Gasoline blends in diesel could be envisaged as possible candidates in the longer term, as these provide a better evaporation process remaining resistant to auto-ignition. A blending injector could be used, as described by Takasaki et al. (2002), injecting diesel or water through the same injector nozzle. A similar approach has been tested and reported by Olsson et al. (2001), using one injector to deliver the charge and another to trigger its combustion. These options would provide considerable benefit, giving the possibility to run on diesel or gasoline or a mixture of both. However, despite this appealing and challenging operating mode, the present work will focus on the use of one injector and diesel fuel.

In addition to the previous consideration, PCCI operation is investigated in an evolutionary but conventional combustion system, with current technology as the starting point of the work but moving on to include variants based on the expected near term hardware developments. This allows the limits of PCCI operation in a conventional engine to be identified. The technologies and features considered include multiple-injection systems, lower compression ratios, variable levels of swirl, higher and highly-cooled EGR rates. As a result, modifications or improvements on the single-cylinder engine used for the investigations can include:

- Lower compression ratios to reduce in-cylinder pressures and temperatures
- Injection system capable of multiple injections per engine cycle
- Injection system capable of high pressures from low to high engine speeds
- Air system capable of advanced turbo-charging system inlet pressures
- EGR system capable of high rates and levels of cooling.

3 EXPERIMENTAL APPARATUS

3.1 Description of test cell and associated systems

3.1.1 Choice of experimental set-up

There are many ways of characterising operating conditions and their influence on combustion. Pressurised and heated air could be delivered into a test chamber to investigate combustion related phenomena, such as the impact of injection pressure on soot emissions, and would present invaluable information for fundamental understanding. However, this approach would not be suitable to investigate real world requirements like fuel injection timing and associated mixing effects. In the present case, where the effect of air management and injection strategies needed to be investigated, the hesitation was between conducting the programme in a 'real' multi-cylinder engine or in a 'research' single-cylinder engine. Since the focus was on combustion development, the single-cylinder engine was selected for its increased operating flexibility. This enabled the analyses to concentrate on the events in one cylinder rather than the average of four cylinders, which will be beneficial when working near the combustion limits. A view of the single-cylinder engine and facility is shown in Figure 3-1. Novel functionalities in terms of control were added to increase the flexibility of operations.

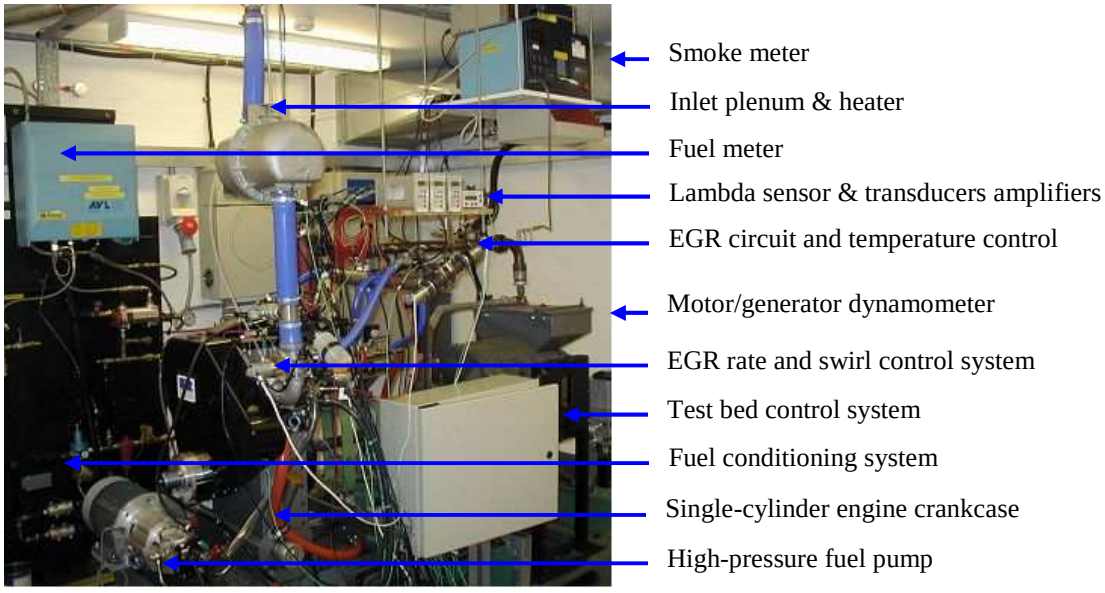

Figure 3-1: General view of test cell, engine and equipment.

3.1.2 Schematics of test cell and instrumentation

The test cell can be divided into several systems such as for air handling, fuel control or general thermal management. Some systems common to engine test cells were carried over from previous programmes, such as the oil and coolant, the fuel conditioning and part of the instrumentation, while others needed upgrading, such as the inlet conditioning and dynamometer, since their capabilities would not meet the testing requirements. Finally, systems were added to complete the installation and control of the diesel engine, such as the EGR circuit. Much effort went into its specification and design to provide advanced and novel functionalities especially in terms of flexibility and range of control. The general layout is shown in the schematic in Figure 3-2. The emissions lines and analysers, the high-speed data acquisition unit, the injection system and control computers are not represented within this diagram.

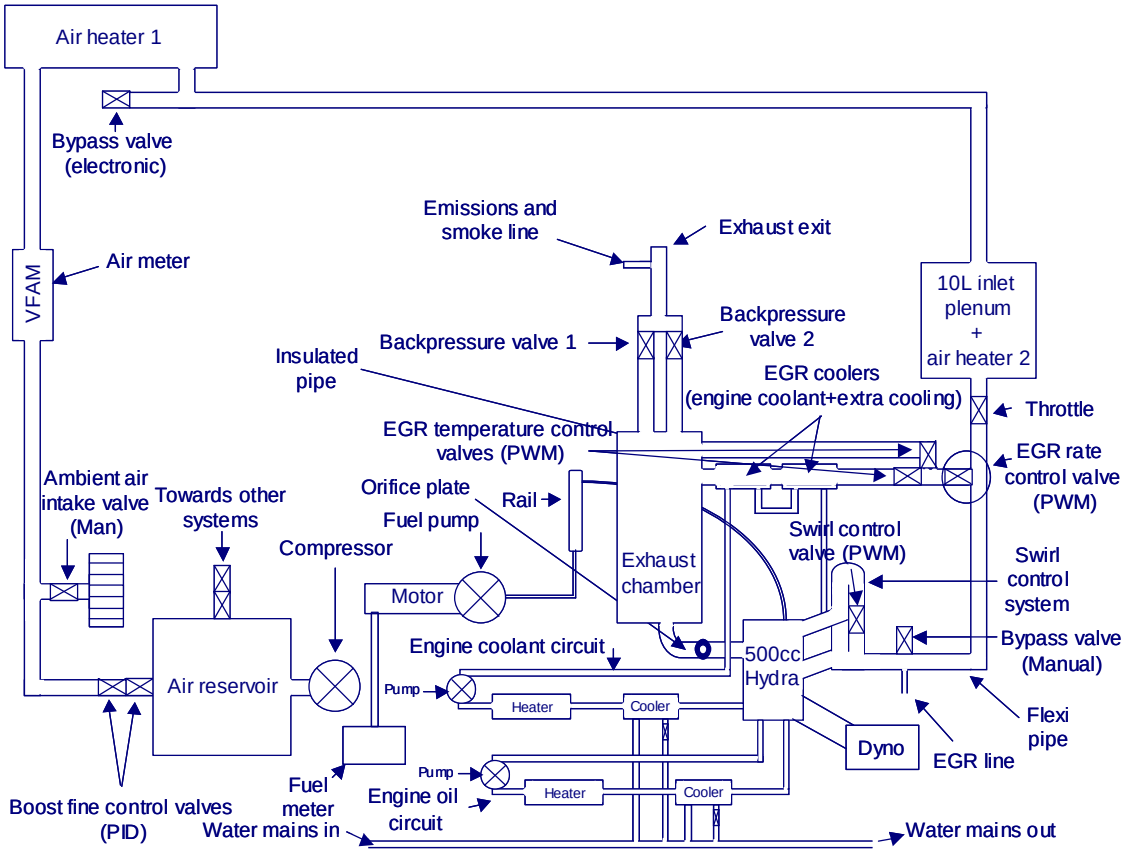

Figure 3-2: Schematic of layout of test-cell systems.

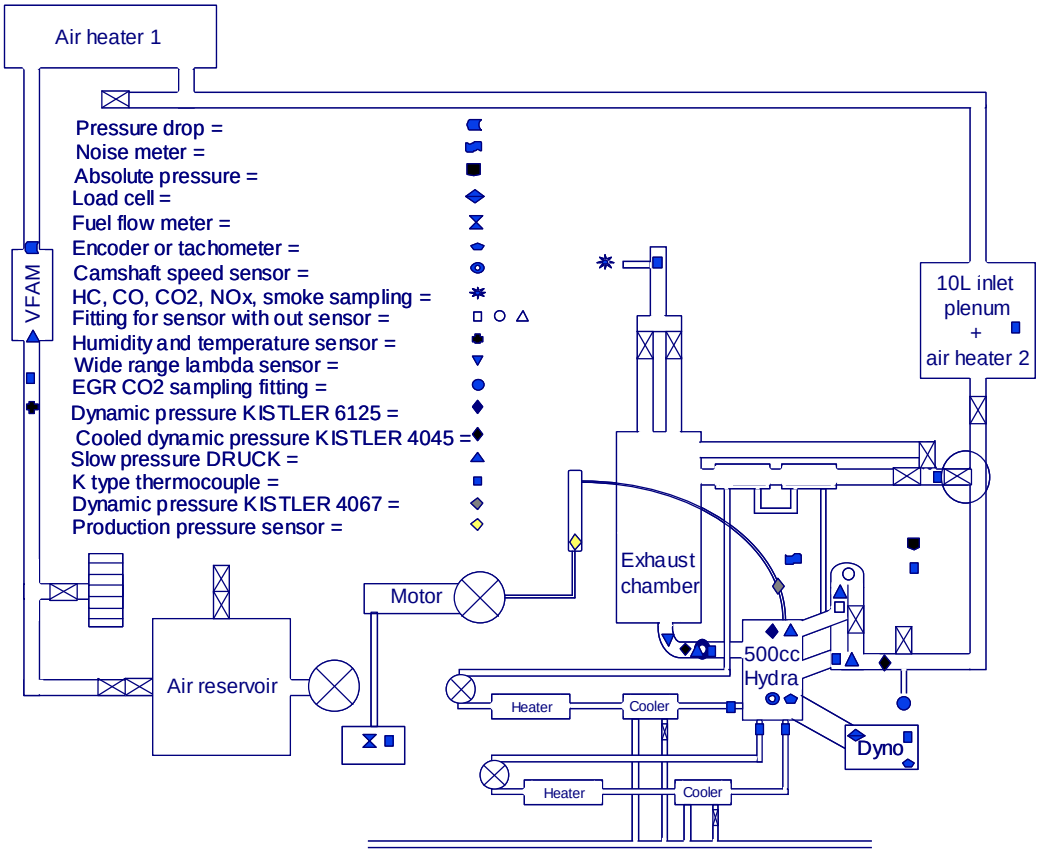

Figure 3-3: Schematic of layout of test-cell instrumentation.

Figure 3-3 shows the different sensors and their positions on and around the engine. They served two purposes: one being for the control and monitoring of engine operation and the other being for test data acquisition. A flush-mounted in-cylinder pressure transducer was selected for its ability to provide suitable data for heat release calculations, which were considered as the key characteristics for the analysis of the combustion. The general instrumentation was calibrated at six monthly intervals, to maintain quality assurance, while the in-cylinder pressure sensor was calibrated every 100 hours of engine operation.

3.1.3 Detailed description of test-cell systems

DYNAMOMETER:

The dynamometer was replaced with a Lawrence Scott LA38 unit as its specifications were considered appropriate to contain future engine power and torque targeted for

this programme. It was capable of generating 50 kW at 4000 rev/min and absorbing in excess of 100 Nm from 1000 to 4000 rev/min. Dynamometer temperature was monitored (type K thermocouple) and maintained below 50 °C in order to maximise its life and hence minimise potential test-cell downtime. A tachometer gave the dynamometer speed, which was compared with the engine speed to check the drive-shaft integrity, while a load cell was used to measure the engine torque. This was zeroed and checked on a daily basis by applying a calibrated weight equivalent to 24 Nm torque to verify the stability and accuracy of the torque measurement.

OIL AND COOLANT SYSTEMS:

The oil and coolant systems were carried over from previous programmes. Both oil and coolant engine-in temperatures were set at 90 °C with flows kept constant, including the flow passing through the EGR coolers. The coolant engine-out temperature was also measured (type K thermocouple). At the early stages of the engine-commissioning phase, the coolant flow was adjusted to obtain a temperature increase of 7 °C across the cylinder head similar to value obtained on the 4-cylinder engine when operating at 4000 rev/min full load. This limited the thermal stress across the cylinder head. The flow was then fixed throughout the investigations. This approach offers a constant through the research programme, but could lead to excessive cooling at lower engine speeds when compared to a multi-cylinder engine, since the flow would be proportional to engine speed on the latter engine.

INLET SYSTEM:

In terms of inlet-manifold pressure, a closed-loop control system was used with the feedback pressure measured in the inlet manifold (DRUCK, 0-5 bar gauge). An additional fast-response pressure transducer (cooled dynamic KISTLER 4045A5, 0-5 bar absolute) was used to measure the dynamic pressure. Two air compressors supplied pressurised air up to 9 bar in a large reservoir and a series of valves controlled the pressure to the required level. A new inlet-manifold pressure control valve was necessary to control the pressure up to 2.0 bar gauge required for this programme. In terms of inlet-manifold temperature, a closed-loop control system was also used with feedback temperature measured in the inlet manifold (type K

thermocouple). Trials with only air heater 1 (see Figure 3-2) resulted in overheating before the target temperature was achieved due to the distance from in the inlet manifold and the inevitable very slow response. For these reasons, air heater 2 was added in the inlet plenum, which helped to decrease the response time during the heating or cooling phase and increased testing efficiency. Air heater 2 was significantly smaller than the air heater 1 but sufficed thanks its proximity and to the increase in temperature that the EGR system could provide, detailed later. The inlet plenum containing the air heater 2 also acted as a damping volume in order to reduce the impact of pulsating EGR on the engine operation. This was not an issue on the 4-cylinder engine since the EGR flowed much more continuously from all cylinders. In addition, the inlet system comprised of a viscous flow air meter, a slow-response pressure transducer (DRUCK, 0-2 bar gauge), a type K thermocouple and a 0-100 % hygrometer to allow air mass flow and other correction factor calculations.

EXHAUST AND EGR SYSTEMS:

The exhaust and EGR systems were complex since they had the difficult task of replicating the 4-cylinder engine systems by providing the same functionalities as well as characteristics. Beyond its primary role, the exhaust system was designed to provide a stable gas supply for the EGR. In an effort to reduce the effect of pulsating gas flows previously mentioned, an exhaust chamber was inserted upstream from the EGR supply point. The drawback of this was that by virtue of the increased volume the EGR path was extended, therefore increasing the heat exchange area. For very light load cases, this would result in excessive cooling of the EGR. In order to resolve this issue, an EGR temperature control was developed. This consisted of two routes, one insulated supplying hot EGR and one equipped with two coolers supplying colder EGR. This allowed EGR temperature to range from current Euro 4 operation levels to much colder levels. The routes were both equipped with electrically actuated valves at the inlet-manifold junction, as can be seen in Figure 3-2, to control the mix of gases to obtain the targeted temperature monitored using a type K thermocouple. For the single to 4-cylinder engine matching, the target temperature would be the one measured on the 4-cylinder engine. Another issue raised by the complexity of this flexible EGR system was that the path for the EGR was more restrictive. By inserting backpressure valves 1 and 2 at the exit of the exhaust chamber, the exhaust gas flow restriction

could be varied thus forcing EGR to the inlet manifold. The valves had some effect on the pumping losses and combined with an orifice plate played a major role in the simulation of the impact of after-treatment and turbine on the pumping losses of the engine. The valves enabled the accuracy of the pumping loop effect to be extended to all speeds and loads. This made the impact of the pumping loop on the gas exchange processes more realistic and will be discussed in more detail in the following chapter. The exhaust and EGR systems clearly underline the efforts made to create a set-up comparable with the 4-cylinder engine. Although the overall size of the EGR circuit has been increased on the single-cylinder engine, the two heat exchangers, the bypass, the two temperature control valves and the rate valve have the advantage of providing a level of functionality rare in present engine applications. Equally, although the configuration of the installation is not considered viable for future production, it will direct the requirements for future multi-cylinder engine EGR systems.

A fast-response pressure transducer (cooled dynamic KISTLER 4045A5, 0-5 bar absolute), a slow-response pressure transducer (DRUCK, 0-2 bar gauge) and a type K thermocouple were placed in the exhaust manifold. The temperature measurement is critical since it should not exceed 760 °C, which is deemed a safe operating limit on the 4-cylinder engine. A lambda sensor (wide range ETAS lambda sensor) was also added as a comparative check with the lambda calculation from the emissions analyser. This verification of the emissions analyser behaviour was preferred to the usual check with lambda derived from the fuel and air mass flow meters since the viscous flow air meter proved to be unreliable for very low air mass flows and could only serve as an indicator. The emissions sampling are described separately.

EMISSIONS SYSTEM:

The emissions system comprised of a smoke meter and an exhaust gas analyser, with the sample point located far enough from the exhaust manifold to ensure the measurement was representative of the entire flow. The smoke meter was of the type AVL 415 Variable Sampling Smoke Meter, which works on the principle of filtering. The darkness of the filter paper is analysed by using a reflective photometer, which translates to outputs in FSN (filter smoke number). This number is then converted into soot or PM emissions produced. An average of two measurements was acquired for

accuracy and reliability. If the exhaust gas did not mark the paper then the number was 0.0 FSN while 3.0 FSN would be on the upper limit of acceptability for production passenger-car engines. The accuracy was of +/- 0.2 FSN.

The exhaust gas analyser was initially a HORIBA MEXA 9100DEGR analyser used for the investigations in Chapter 4 and then a HORIBA MEXA 7100DEGR analyser. A back-to-back test was performed and showed no differences in the measurements. Both systems used the same measurement principles with an accuracy of 3 % over a maximum of 8 hours and a linearity of the signals of +/- 1 %. They could provide concentrations of five types of emissions in the exhaust: total hydrocarbon, oxygen, carbon dioxide (exhaust and inlet for the EGR), carbon monoxide and nitrous oxides:

- The HC emissions analyser is based on the flame ionisation detection method. The gas to be analysed is introduced into a hydrogen flame passing between two electrodes. The constant voltage applied creates an ion flow, which is proportional to the number of carbon atoms
- The oxygen (O_2) emissions analyser is based on the magneto-pneumatic condenser microphone detection method. By applying an uneven magnetic field to a gas by exciting an electromagnet, it will draw gases with paramagnetic susceptibility towards the strongest part of the field, thus increasing the pressure at that location. By exciting alternately two electromagnets, the pressure oscillations can be converted to electrical signals via a condenser microphone. This output increases linearly with O_2 concentration
- Both the CO_2 and CO emissions analysers are based on the non-dispersive infrared absorptiometry detection method. A molecule formed of different atoms will absorb infrared energy at a specific wavelength and at a degree proportional to its concentration. The difference in infrared intensities between an infrared beam passing through a reference gas and passing through the gas to be analysed is measured. Two metallic membrane detectors output electrical signals for each gas molecule concentration to be measured. The signals are then converted to the concentrations of CO_2 and CO in the gas to be analysed
- The NO_x emissions analyser is based on the chemiluminescent detection method. A Silicon photo-diode adjacent to the reaction chamber senses the

chemiluminescent emitting photons. Once the nitrogen dioxide (NO_2) fraction of the gas to be analysed is dissociated to form nitric oxide (NO), the gas is mixed with ozone (O_3) thus resulting in light emitting reactions proportional to the concentration of NO, which encompasses the concentration of NO and of NO_2 emissions.

In terms of layout, there were four main emissions lines: one transporting the exhaust gas to the HC emissions analysers, which was heated at 191 °C since these were measured wet; another transporting the exhaust gas to all the other analysers, which did not need heating since they were measured dry; a further line from the inlet manifold to a separate additional CO_2 emissions analyser for the calculation of the EGR rate; finally, a line connecting some known concentration gases to the sampling point in order to check for leaks. A daily test for leaks was carried out to check for inconsistencies, which consisted of sending the gases with known concentrations directly to the sampling point while the gas analysers were in measurement. A daily zero and span check of the analysers were carried out. This was done by sending pure nitrogen gas and then gases with known fractions (within the expected measurement range) of $HC/O_2/CO_2/CO/NO_x$ to the different analysers. An oven was added to the set-up to control the gas temperature at 191 °C prior to entering the heated line. This was to protect for the test conditions with very low exhaust-gas temperatures and high levels of unburned fuel. These conditions would result in absorption and desorbtion phenomena of HC emissions in the first part of the heated line, where the temperature of the gas would be lower than 191 °C, which would offsetting the results and leading to erroneous conclusions.

FUEL SYSTEM:

The fuel system was divided into two parts. The low-pressure side consisted of a fuel tank, low-pressure pumps, a filter, a temperature conditioning system and a fuel meter. The conditioning consisted of cooling and controlling the fuel temperature to 40 °C once it had been through the high-pressure side and before it returned to the high-pressure pump again. The fuel meter was of the type AVL 733 Dynamic Fuel Meter, which determines fuel consumption by gravimetric balance method. The fuel was weighed over one minute and the accuracy was of +/- 1.0 %.

The high-pressure side was controlled by a prototype Delphi injection control consisting of a Delphi production high-pressure pump driven by an electrical motor at a constant speed of 1500 rev/min and a single injector. The pump speed was equivalent to an engine speed of 3000 rev/min where it can deliver injection pressures over the range of 300 to 1600 bar. Running the high-pressure fuel pump separately made the injection-pressure range as wide as the pump could deliver and independent of engine speed. This increased the capabilities of the injection system relative to a conventional multi-cylinder engine mounting, allowing the investigations to define future injection-pressure requirements. In production, the injection pressure is controlled via an inlet-metering valve allowing just the required amount of fuel to be pressurised. The pressure would be adjusted by actuating spill valves in the injectors themselves using a high-frequency signal. This requires a 16-bit controller and sufficient spill flow, neither of which were available, therefore the fuel pressure was controlled using an additional high-pressure valve fitted on the rail. A production injection-pressure sensor was fitted on the rail allowing the control and monitoring of fuel pressure. A fast-response pressure transducer (dynamic KISTLER 4067A2000, 0-2000 bar absolute) was also mounted in the fuel line between the rail and the injector to provide high-time-resolution pressure data. The injection hardware is mentioned in the engine description. The fuel used throughout the investigations was ultra-low sulphur diesel BP Ford reference fuel, the main properties are shown in Appendix A.

CONTROLLERS AND DATA-ACQUISITION SYSTEMS:

An operations, injection-system and high-speed-data acquisition computers were used to control the operations and log the data. The operations-control computer and systems were initially developed for previous programmes. A series of modifications were made on the initial version to accommodate the additional test-cell systems, such as the EGR and its numerous valves, and to increase the results analysis efficiency, by displaying real time calculations of emissions mass flows. The operations-control computer managed the activation of pumps (engine and fuel coolant, oil and low and high-pressure fuel pumps), the activation of the dynamometer and the injection system power supply, the setting of inlet-manifold pressures and temperatures, engine speed, rate and temperature of EGR, level of swirl and also served to trigger the data storage, including the smoke emissions and fuel consumption measurements.

The operations-control computer also served to monitor the various temperatures and pressures mentioned earlier as well as several emissions-related calculations (AFR, EGR rate, mass flows and total emissions). These data formed the first group of low-time-resolution data recorded for each test point. An average taken over a 30 s acquisition period formed the stored value. The parameters stored are listed below:

- Temperatures (°C): coolant engine-in and engine-out, oil engine-in and out, ambient, fuel high-pressure-pump-in and out, dynamometer air-out, viscous flow air meter -in, inlet plenum and manifold, EGR in and out, EGR coolant in and out, exhaust manifold and sampling point
- Absolute and relative pressures (mbar): ambient, viscous flow air meter in and out, inlet manifold, throttled inlet manifold (swirl system), exhaust manifold
- Emissions (ppm or % or g/h) and fuel consumption (kg/h): HC, CO, CO_2, O_2, NO_x, Inlet CO_2, smoke (FSN), FC, Lambda and emissions analyser ranges
- Other: dynamometer and engine speeds (rev/min), valve settings and swirl throttle position feedback (%), humidity (%), torque (Nm), inputted load (bar GIMEP), net load (bar NIMEP) and pumping losses (bar PMEP).

The injection-system control computer and systems were developed by Delphi. They had the same injector current driver as in the 4-cylinder engine's injection system control but allowed multiple injections with much greater flexibility in terms of the injection timing. This system controlled the number of injections, which could be as many as 8, the fuel injection pressure, start angle and duration of the injection drive current. A comparison of the drive current from a production unit and from the one used in this programme is shown in Figure 3-4. Slight differences were visible during the initial peak-current phase but were considered as insignificant in this programme since these would only be likely to affect the needle-opening phase during cold starts. For each test point, the injection pressure averaged over 10 s, the start of injection angles and durations were recorded, forming the second group of low-time-resolution data recorded for each test point, which served primarily as reference data.

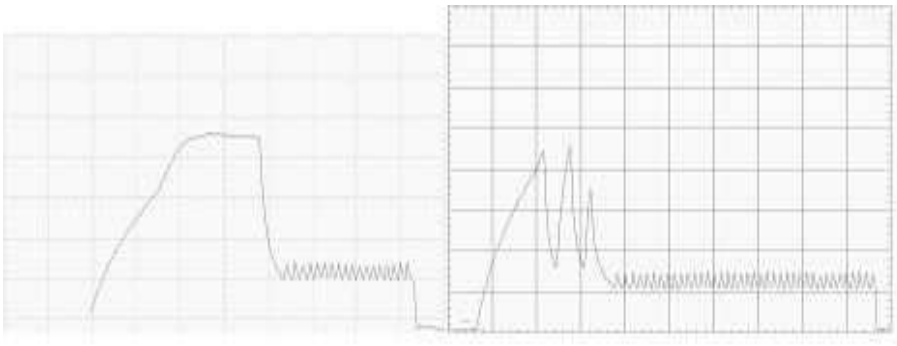

Figure 3-4: Injection drive currents from single and 4-cylinder engines.

Left: with 4-cylinder engine, right: with single-cylinder engine injection system control. Vertical scale: 5 A/division, horizontal scale: 100 µs/division.

The high-speed-data acquisition-control system and 'Adapt-CAS' software were developed by MTS. The CAS computer could record 100 engine cycles of up to 16 inputs at the shaft encoder resolution of 0.5 °CA, i.e. 720 times per engine revolution. Average traces of the 100 cycles could be obtained for most traces. In addition, raw and calculated data were displayed, which were useful for setting the engine operating conditions. This formed a third group of high-time-resolution data recorded for each test point. This acquisition system was ideal for fast-response sensors but also proved useful for slow-response sensors. Eight channels were used for this programme, which were as follows:

- Fast-response in-cylinder pressure transducer
- Fast-response inlet-manifold pressure transducer
- Fast-response exhaust pressure transducer
- Fast-response injector fuel-line pressure transducer
- Fast-response injector driver current
- Fast-response injector pulses
- Slow-response combustion noise meter (AVL 450 Combustion Noise Meter)
- Slow-response inlet-manifold pressure transducer.

The in-cylinder pressure was the most important acquisition since the gross, net and pumping loads, as well as the maximum in-cylinder pressure and location were derived from it, and were essential for controlling the test points and for monitoring the engine performance. Pressure variation and combustion information, such as the instantaneous heat release and the angles of 5, 50, 95 % fuel mass fraction burned

were derived from the pressure traces using the CAS software. In addition, this system served to monitor injection pressure, start and end of the injection drive current and the coefficient of variation of the IMEP.

In terms of combustion analysis, the gasoline origins of the CAS software led to concerns as to the suitability of the heat release calculations for diesel engines compared to that of more diesel-oriented heat release calculations software. However, comparisons were undertaken in order to identify differences. These showed that calculations led to a very close match in terms of profile, which was closely linked to the pressure variation during the engine cycle. The only discrepancy between calculations was in the amplitude. It is believed that the fewer inputs used by CAS, such as the fuel calorific value and the surfaces for heat exchange, lead to an offset in the results. An additional observation highlighted the need to use representative single-cycle pressure traces as a base for the calculation whenever the pressure variability on a cycle-by-cycle basis was high. Ensemble averaging of the pressure traces was shown to lead to non-representative and ultimately misleading results. In those cases, single pressure traces would be more representative despite leading to more irregular traces due to measurement noise. For these reasons, it was found that CAS instantaneous heat release calculations or simply the rate of pressure change of single cycles would provide a sound basis for all the analyses.

3.2 Key acquired data and associated post-processing calculations

At part load, the investigations mainly focus on fuel consumption, noise and emissions for particular operating conditions at a particular speed and load. At full load, the focus is more on peak in-cylinder pressure, exhaust temperature and smoke emissions. In order to understand why such air, EGR and fuel-injection strategies offer the best compromise between fuel consumption and emissions or AFR and smoke, an in-depth analysis of the combustion characteristics is required. The main data were acquired from two separate sources (operations-control and CAS computers). They provided data for two separate groups of calculations. The first included the emissions levels and the associated calculations: these were recorded over 30 s, averaged and expressed in percent volume or parts per million in the

exhaust flow. In order to compare results, these were transformed into emissions flow rates in grams per hour or per kilowatt-hour, AFRs and EGR rates using the emissions equations described below. The second included the in-cylinder pressure data and the associated calculations: 100 engine-cycles of different pressures, drive current and signals were recorded and averaged. The combustion equations were used in order to compare these results. The data were expressed in terms of average in-cylinder pressure traces, combustion characteristics, indicated values and cycle-to-cycle variability. The calculations are described by the following equations:

EMISSIONS EQUATIONS:

The intake humidity ratio was used in the calculations of the wet to dry conversion factor. Its calculation is shown in Equation 3-1. It is calculated using the barometric pressure, the relative humidity of the air, the water to air molar mass ratio and a calculation of the barometric vapour pressure at the humidity measurement point shown in Equation 3-2:

$$H = H_{ratio} \cdot \frac{P_{vap}}{\left(P_{baro} - P_{vap}\right)} \tag{3-1}$$

$$P_{vap} = RH \cdot 10^{\left(2.78571 + \frac{(7.502 \cdot T_{amb})}{(237.3 + T_{amb})}\right)} \tag{3-2}$$

Where P_{vap} is the barometric vapour pressure at the humidity measurement point (Pa),

RH is the ambient (intake) air relative humidity (%),

T_{amb} is the ambient (intake) air temperature (°C),

P_{baro} is the barometric pressure at the humidity measurement point (Pa),

H_{ratio} is the water to air molar mass ratio (-).

The emissions wet to dry conversion factor was used to convert wet to dry volumetric concentrations for exhaust gas components. It is one of the first calculations presented since it was used directly or indirectly in all the following calculations and is shown in Equation 3-3. It is calculated using volumetric concentrations of molecules containing oxygen, the humidity ratio and the fuel H/C ratio:

$$kw_{RCE2} = \frac{1}{1 + \frac{n \cdot ([CO_2]+[CO]) + \left(([CO_2]+[CO]) \cdot \left(1+\frac{n}{2}\right) + ([CO_2]+2\cdot[O_2]) \right) \cdot \frac{H \cdot M_{air}}{[O_2]_{air} \cdot M_{H_2O}}}{2 + \left(1 + \frac{1}{2} \cdot \frac{H}{[O_2]_{air}} \cdot \frac{M_{air}}{M_{H_2O}}\right) \cdot \frac{2}{K} \cdot \frac{[CO]}{[CO_2]}}} \qquad (3\text{-}3)$$

Where M_{xx} is the molar mass of xx (kg/mol),

$[O_2]_{air}$ is the dry volumetric concentration of oxygen in air (-),

K is the water-gas reaction equilibrium constant (-),

n is the fuel H/C ratio (-),

$[xx]$ is the dry volumetric concentration of the xx species (-),

H is the intake humidity ratio (-).

The total emissions check was the first main calculation. It was used to check the analysers were functioning correctly and that subsequent calculations based on the emissions analysers were correct and is shown in Equation 3-4. It is calculated using the dry volumetric concentrations of seven components and should equal unity:

$$Tot\ Ems = [CO_2]+[CO]+[O_2]+[H_2]+[HC]+[NO_x]+[N_2] \qquad (3\text{-}4)$$

Where $[xx]$ is the dry volumetric concentration of the xx species (-),

$[H_2]$ and $[N_2]$ are calculated using the chemical reaction, fuel H/C ratio, water-gas reaction equilibrium equation and wet to dry conversion factor.

The dry AFR Spindt was the first of two calculations, which were used to characterise the operating conditions. It was preferred to the AFR calculated from the air mass flow and fuel mass flow measurements since the air mass flow can be difficult to measure on a single-cylinder engines, due to pulsating and low overall air mass flow. The AFR was compared with the Lambda sensor to check the emissions analysers were functioning correctly. It is reverse calculated from the emissions measurements, when based on dry emissions; it is referred to as dry AFR. The calculation is shown in Equation 3-5. It is calculated using the dry volumetric concentrations and the fuel H/C ratio and gives the air to fuel mass ratio:

$$AFR = F_b \cdot \frac{1}{[O_2]_{air}} \cdot \frac{M_{air}}{M_{fuel}} \left(\left(\frac{1+\frac{R}{2}+Q}{1+R} \right) + \frac{n}{4} \cdot \frac{K}{(K+R)} \right) \qquad (3\text{-}5)$$

Where $F_b = \frac{[CO_2]+[CO]}{[CO_2]+[CO]+[HC]}$,

$R = \frac{[CO]}{[CO_2]}$ and $Q = \frac{[O_2]}{[CO_2]}$,

M_{xx} is the molar mass of xx (kg/mol),

$[O_2]_{air}$ is the dry volumetric concentration of oxygen in air (-),

K is the water-gas reaction equilibrium constant (-).

The EGR rate was the second of two calculations, which were used to characterise the operating conditions. When based on dry emissions measurements, it is referred to as dry EGR and is shown in Equation 3-6. It is calculated using the ambient, exhaust and inlet-manifold dry volumetric concentrations of CO_2 and is given in percent (%):

$$EGR = \frac{[CO_2]_{inlet} - [CO_2]_{ambient}}{[CO_2]_{exhaust} - [CO_2]_{ambient}} \quad (3\text{-}6)$$

Where $[CO_2]_{xx}$ is the dry volumetric concentration of CO_2 in locations xx (-).

The dry molar exhaust flow was used to convert volume fractions in the exhaust in emissions mass flows. It is shown in Equation 3-7, where it is calculated using the dry AFR Spindt, the fuel meter measurement, the molar mass of air and the wet to dry conversion factor and is given in mol/s:

$$qm_{Exh_{dry}} = qm_{Fuel} \cdot \frac{(1+AFR)}{M_{air}} \quad (3\text{-}7)$$

Where M_{air} is the molar mass of air (kg/mol),

qm_{Fuel} is the measured fuel mass flow (kg/s),

AFR is the dry AFR Spindt (-).

The soot emissions concentration in kg/m^3 was used to estimate soot emissions mass flow and shown in Equation 3-8. It is calculated using the filter smoke number:

$$Soot_{AVL} = \frac{4.95}{0.405} \cdot \frac{1}{10^6} \cdot FSN \cdot e^{(0.38 \cdot FSN)} \quad (3\text{-}8)$$

Where FSN is the filter smoke number (FSN).

The emissions mass flows in kg/s were used for comparing the impact of operating conditions on emissions. Their calculations are shown in Equations 3-9 to 3-15, based on the dry volumetric (molar) concentrations and molar rate of dry exhaust:

$$G_{CO_2} = M_{CO_2} \cdot [CO_2] \cdot qm_{Exh_{dry}} \quad (3\text{-}9)$$

$$G_{CO} = M_{CO} \cdot [CO] \cdot qm_{Exh_{dry}} \quad (3\text{-}10)$$

$$G_{HC} = M_{HC} \cdot [HC] \cdot qm_{Exh_{dry}} \quad (3\text{-}11)$$

$$G_{NO_x} = M_{NO_2} \cdot [NO_x] \cdot qm_{Exh_{dry}} \quad (3\text{-}12)$$

$$G_{NO_x\,corr} = K_{NO_x} \cdot G_{NO_x} \quad (3\text{-}13)$$

$$G_{NO} = M_{NO} \cdot [NO] \cdot qm_{Exh_{dry}} \quad (3\text{-}14)$$

$$G_{NO\ corr} = K_{NO_x} \cdot G_{NO} \quad (3\text{-}15)$$

Where $qm_{Exh_{dry}}$ is the dry molar exhaust flow (mol/s),

$[xx]$ is the dry volumetric concentration of the xx species (-),

M_{xx} is the molar mass of the xx species (kg/mol),

K_{NO_x} is a humidity correction (-) calculated using the humidity ratio, the intake-air temperature and the dry AFR Spindt.

COMBUSTION EQUATIONS:

Start and End Of Injection (SOI and EOI) were measurements defined by the injection drive current trace. The start of injection was the angle at which the current trace raised above 1 A and the end of injection was the angle at which the current decreased below 1 A once the start of injection had been recorded. These values are generally given in °CA ATDC.

PMEP represented the work produced during the pumping strokes of the engine and GIMEP represented the work produced during the compression and expansion strokes only, enabled the comparison of different operating conditions to focus on the combustion, subtracting the effects of engine friction and pumping losses. NIMEP is the sum of GIMEP and PMEP. The calculations for GIMEP and PMEP in Pa are shown in Equations 3-16 and 3-17, based on the in-cylinder volume and the corresponding pressures, with 0 °CA ATDC referenced to the firing TDC:

$$GIMEP = \frac{\int_{-180}^{180} PdV}{V_{di}} \quad (3\text{-}16)$$

$$PMEP = \frac{\int_{180}^{540} PdV}{V_{di}} \quad (3\text{-}17)$$

Where V is the in-cylinder volume (m^3),

P is the in-cylinder pressure (Pa),

V_{di} is the displacement volume (m^3).

The heat release and the instantaneous heat release calculations were used to characterise the pressure variations during the combustion. Their calculations are shown in Equations 3-18 and 3-19. They are calculated using the polytropic exponent derived for each cycle, the in-cylinder pressures and volumes at the current and previous crankangle and are given in Joules (J) and Joules per second (J/s) respectively:

$$HR_i = \frac{\left(\lambda \cdot P_i \cdot \left(V_i - V_{i-1}\right)\right) + \left(V_i \cdot \left(P_i - P_{i-1}\right)\right)}{\lambda - 1} \quad (3\text{-}18)$$

$$ROHR_i = \frac{dHR}{dt} \quad (3\text{-}19)$$

Where λ is the polytropic exponent at crankangle i (-),

P_i is the in-cylinder pressure at crankangle i (Pa),

V_i is the in-cylinder volume at crankangle i (m^3).

The different angles of percent burn were based on the heat release calculations. When 5 % of the integrated instantaneous heat release had occurred, the angle was identified and recorded. Angles of 5, 50, 95 % mass fraction burned are available and give and idea of the rapidity of the combustion.

3.3 Ensemble averaged or single-cycle measurements and calculations

The investigations focused on building correlations between emissions and fuel consumption and the actual in-cylinder pressure variations during the engine cycle as

well as related calculations such as the instantaneous heat release or the rate of pressure change. Both qualitative and quantitative information were sought as means of analysing and explaining the various effects observed on the combustion during the investigations. The qualitative data were the rate of pressure change and the instantaneous heat release, focusing on their profile during the initial part of the combustion, the portion of the premixed combustion, defined by a peak shape, and diffusion combustion, defined by a lower rate of heat release or pressure variation. The quantitative data were the start and end of combustion, the maximum rate of pressure change and the phasing of the heat release or pressure variation relative to TDC.

Early in the course of the investigations, it was found that single-cycle profiles of rates of pressure change or instantaneous heat release offered the most representative data, as described earlier. This was due to the fact that, despite an apparent stability in the operation of the engine, as indicated by a coefficient of variation of 2.1 % of gross load and of 3.7 % for the angle of 5 % burn at 1500 rev/min 6.6 bar GIMEP, the variations in start of combustion would lead to a series of in-cylinder pressure profiles. In such a case, if ensemble averaging was used to process the hundred cycles of pressure data acquired, it would lead to a smoothed, unrepresentative profile of the instantaneous heat release and rate of pressure change, with longer duration and lower rates as depicted in Figure 3-5. As a consequence, before the analysis could progress, a single, representative engine cycle was selected for each test point from the hundred cycles of pressure data. The selection was based on it offering a good representation of the combustion, in terms of start of combustion and angle of 50 % burn. In the illustration shown in Figure 3-5, the selection of the pressure trace 2 would have been made. A remark can be added concerning the maximum rate of pressure change. Although the timing of the combustion showed some variations, the maximum rate of pressure change was stable, indicated by a coefficient of variation of 2.7 %. Therefore, all cycle derived results shown in the next chapters are based on single-cycle values.

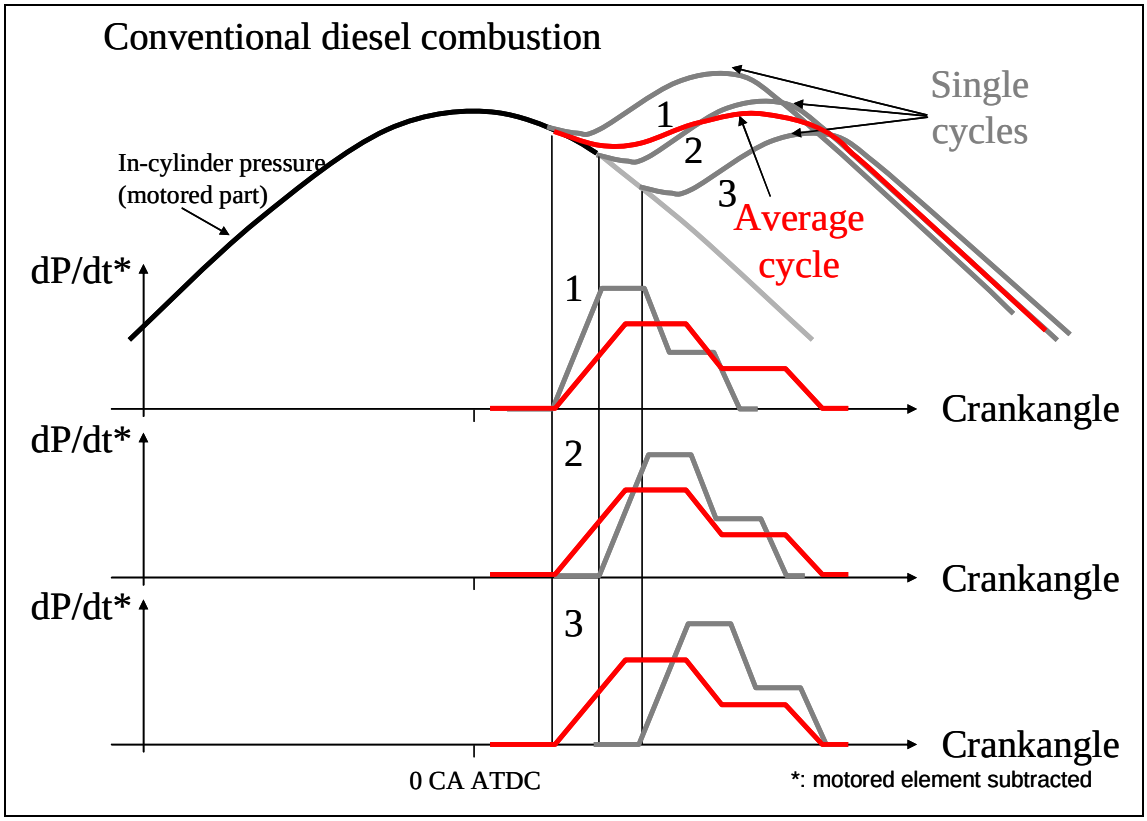

Figure 3-5: Effect of ensemble averaging on combustion characteristics.

3.4 Accuracy of measurements and calculations

The accuracies of the pressure, emissions, fuel consumption and smoke measurements have already been detailed. These were considered as accurate and repeatable, offering little variability from one measurement to another, as monitored through daily check points. However, caution must be taken when comparing HC emissions due to possible absorption and desorbtion processes, despite all the precautions taken. Error bars were not added to the emissions or fuel consumption values for clarity.

All the in-cylinder data is known with a crankangle resolution of 0.5 °CA leading to an accuracy of +/- 0.5 °CA on angles of portions of fuel burned. The error on duration calculations such as the angle from 5 to 95 % burn is therefore +/- 1.0 °CA.

3.5 Description of the diesel single-cylinder research engine

The single-cylinder research engine was built to represent one cylinder of an HSDI diesel engine with a 2.0 L swept volume. This swept volume was chosen as being representative of the most important share of the diesel passenger-car engine market in Europe in the foreseeable future. In terms of build, it comprised a crankcase and crankshaft which were common to both gasoline and diesel research engine applications, with the flywheel, piston and conrod being the only distinctions. The cylinder head, valves and camshafts were from a production 4-cylinder engine. The head was mounted on the cylinder barrel, which also provided support, coolant and oil flow, and sealed the unused ports, valves and cooling passages. Figure 3-6 shows the single-cylinder engine before its installation in the test cell.

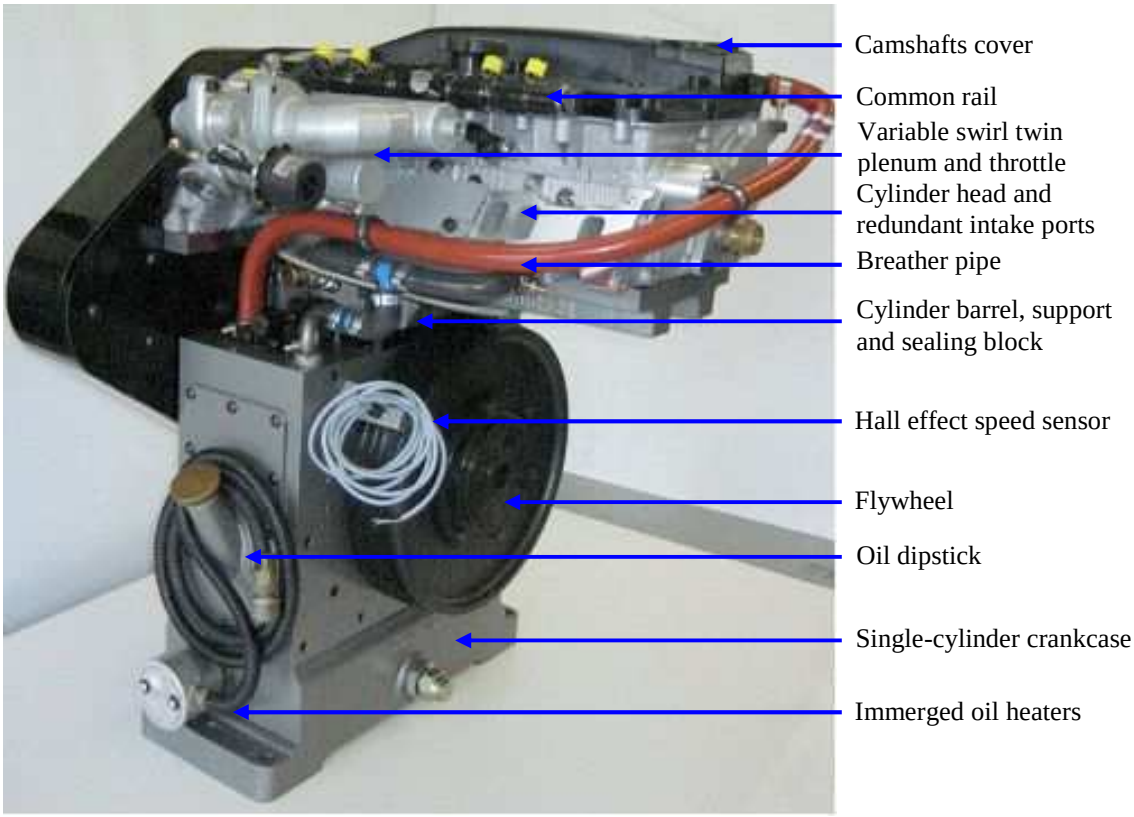

Figure 3-6: View of single-cylinder engine before installation.

Two builds were available. Build #1 was the directly comparable single-cylinder version of the 4-cylinder engine, which was used to define appropriate and realistic settings based on existing multi-cylinder engine test data. Build #2 was the build

configuration to be used through the advanced combustion investigations. The hardware came from two sources: it was either in production (Build #1 piston, conrod, injection system, cylinder head, Build #2 conrod and injection system) or approaching production (Build #2 cylinder head, piston). A 2.0 L 16-valve FORD production cylinder head with a production piston and connecting rod were used for the testing during the single to 4-cylinder engine matching. The compression ratio was initially of 18.4:1 and then reduced to 16.0:1 in Build #2 engine, once the matching phase was complete (Chapter 4). In order to achieve this reduction whilst maintaining the necessary squish volume (the volume comprised between the top of the piston and the cylinder head at TDC, which is important for fuel-air mixing), the piston bowl volume was increased, resulting in a deeper bowl shape with a reduced pip. Cross-sections of both pistons are shown in Figure 3-7. The cylinder head had a tangential or directional port and a helical port. Combined with a variable swirl system, which consisted of a twin plenum with a throttle on the helical port plenum, the levels of swirl could be varied from 1.5 to 4.5 Rs. The maximum level of swirl was obtained when the helical port was completely shut. In Build #2 engine, the port geometry was optimised for higher flow capabilities. The level of swirl range was slightly lowered to 1.0 to 3.5 Rs, with a complimentary reduction in gulp factor. This increased the volumetric efficiency reflecting the trends of reducing levels of swirl as the injection system takes a larger role in the fuel and air interactions. Figure 3-8 shows the level of swirl and gulp factor for different levels of port de-activation using the variable swirl throttle on both the multi and the single-cylinder engines.

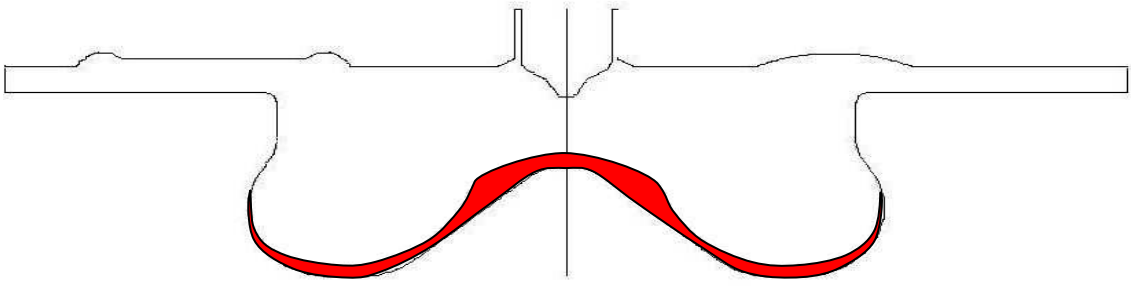

Figure 3-7: Build #1 and #2 engine piston-bowl cross-sections (red: increased volume).

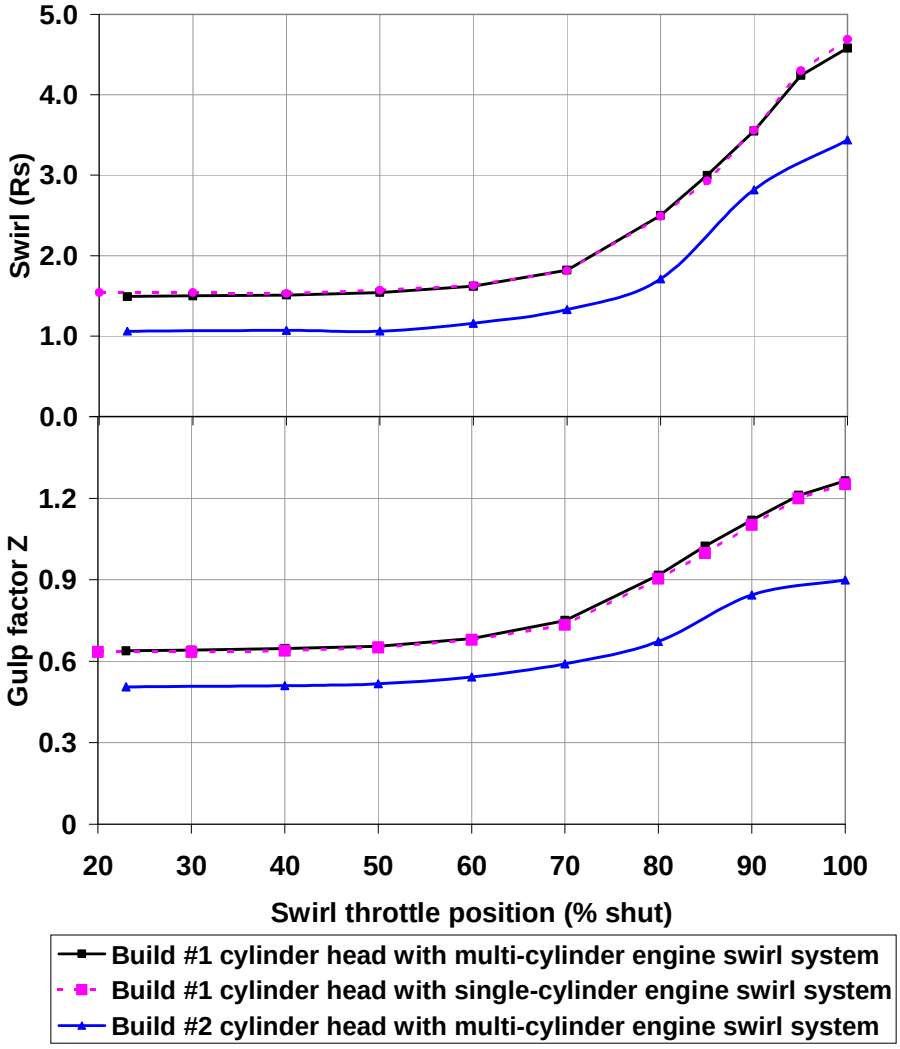

Figure 3-8: Build #1 and Build #2 cylinder heads gulp and swirl characteristic.

The injection system was production equipment developed by Delphi. The injector and injector nozzle used for the matching phase were an NPO DFI 1.3 injector with a 7-hole, 154 ° cone angle, 680 cc/min flow injector nozzle. The injector nozzles are characterised by the number of holes, the angle between the holes axis of two diametrically opposed holes, referred to as the cone angle, and the flow of the injector when a fuel pressure of 100 bar is applied and the needle in its high position. The hole size can be part of the specification but this is usually determined from the coefficient of discharge, which was of 0.76 for all injector nozzles used in this programme. The protrusion of the injector nozzle in the combustion chamber was initially kept constant and was defined from the production engine using a 1.6 mm copper washer. Beyond its injector-nozzle-positioning role, this washer provides the sealing of the injector body on the bottom of the injector pocket in the cylinder head. The engine

specifications of the baseline Build #1 and of the Build #2 and the injector nozzles used are summarised in Table 3-1. A fast-response in-cylinder pressure transducer (KISTLER 6125, 0-250 bar absolute) was positioned near the injector to measure the in-cylinder pressure. Since there were no requirements for cold-start investigations, it was positioned in the cylinder head where the glow plug was fitted. An adaptor was made to obtain a flush-mounted face therefore improving the quality of the pressure trace for post-processing and heat release calculations.

		Build #1	Build #2
Engine	Swept volume	500 cc	
	Bore x stroke	86 mm x 86 mm	
	Inlet valves arrangement	One tangential and one helical valve	
	Speed range	750 to 4500 rev/min	
	Maximum in-cylinder pressure	1000 rev/min: 110 bar - 1250 rev/min: 130 bar 1500 rev/min and higher: 150 bar	
	Maximum exhaust temperature	760 °C	
	Compression ratio	18.4:1	16.0:1
	Piston bowl volume	22.0 cc	26.3 cc
	Level of swirl range	1.5 to 4.5 Rs	1.0 to 3.5 Rs
Injection system	Fuel type	Diesel BP FORD reference fuel	
	High-pressure pump	Delphi DFP 1.2	
	Fuel pressure range	300 to 1600 bar	
	Injector	Delphi NPO DFI 1.3	
	Injector nozzle	7-hole, 680 cc/min, 154 °, 0.76 coefficient of discharge	7-hole, 680 cc/min + 8-hole, 777 cc/min, 154 °, 0.76 coefficient of discharge

Table 3-1: Specification summary of Build #1 and Build #2 engines.

4 SINGLE TO 4-CYLINDER ENGINE MATCHING

4.1 Introduction

There were two main purposes for the work presented in this chapter. The first was to demonstrate the transferability of multi-cylinder engine operating conditions and characteristics to a research single-cylinder engine thereby making any research on the single-cylinder engine meaningful. The second was to recreate the 4-cylinder baseline operating characteristics on the single-cylinder engine in terms of noise, emissions and fuel consumption or combustion efficiency, to serve as reference for the future planned investigations.

The operating conditions and characteristics used as matching targets were based on data available from the 4-cylinder version of the engine. In the original 4-cylinder engine, calibration tests had been conducted to minimise NO_x emissions (one of the operating characteristics) as much as possible whilst maintaining acceptable fuel economy. The main 4-cylinder engine operating conditions were the swirl throttle position, AFR, EGR rate and its temperature, injection timing and pressure. As has been seen in work by Henein et al (2001) or Gill et al. (2002), the optimisation led to a retarded injection timing approach and high rates of cooled EGR since these would lower the combustion temperatures, and hence NO_x emissions. Increased injection pressure and high levels of swirl were employed to improve the mixing and limit soot emissions. The higher injection pressure increased fuel conversion efficiency and helped maintain fuel consumption within 10 % of the initial Euro 4 measured values. This resulted in NO_x emissions close to the Euro 5 targets.

The task of successfully transferring operating conditions from one engine to the other was complicated by the fact that many of the engine sub-systems were different, as described in Chapter 3. The present chapter covers how this was done for a series of key operating points by making the inlet and exhaust systems behave as much as possible like those of a multi-cylinder engine. It goes on to present the resulting characteristics of the transfer of the 4-cylinder engine operating conditions onto the Build #1 single-cylinder engine. The operating conditions together with the measured values of emissions, load and fuel consumption served as a baseline for all subsequent

phases of the programme. Detailed examinations of in-cylinder pressure and instantaneous heat release traces were also conducted at some key operating points in order to illustrate the impact of injection timing for different testing approaches.

4.2 Matching process

In order to confirm that the single-cylinder research engine offered a robust experimental set-up for the planned investigations, a good match between it and the 4-cylinder engine was needed. A number of key operating points to represent the engine behaviour across its speed and load operating ranges was chosen. Before attempting a transfer of the operating conditions and characteristics, the 4-cylinder exhaust and intake strokes were analysed at each key point in order to identify how best to replicate them. The pumping loop was identified and once it was matched at each point by selecting the appropriate orifice plate and adjusting the backpressure valves settings, the 4-cylinder engine operating conditions were transferred. Most operating conditions and characteristics during the 4-cylinder engine test programme were known and could be set just as accurately on the single-cylinder engine, such as the injection pressure or the EGR rate. However, the injection timing and the level of swirl were operating conditions not directly transferable due to differences in the system. To transfer these, injection-timing and swirl responses were conducted in order to redefine their settings and ensure a good match.

4.3 Selection of key operating points

Ideally, in order to optimise engine-operating conditions for a particular vehicle (weight and transmission) over a particular emissions drive-cycle, the calibration at each point of the drive cycle should be optimised. However, a more efficient approach is to use a simulation model or data from a similar vehicle over the drive cycle to identify a series of representative operating speeds and loads. These become the key points and permit more focused testing. By attributing appropriate weighting factors to each point, drive-cycle emissions and fuel consumption predictions can be obtained based on actual test results. An appropriate compromise between accuracy and testing

time determines the number of test points considered. In the present work, a drive-cycle simulation was not carried out but a selection of key points was made to cover the 'regulated' operating zone, as shown in Figure 4-1. This region plays an important role in the emissions and fuel consumption of a typical 2.0 L diesel passenger-car. 4-cylinder engine operating data were available at these points enabling comparisons to be made with the single-cylinder engine. These part load points were divided into two groups. The primary group comprised five points which were used throughout the investigations, noted Primary 1 to 5 (P1 to P5) and three points made up the secondary group, noted Secondary 1 to 3 (S1 to S3), which covered the part load testing area from idle to 2000 rev/min at very light loads. Three full load points, noted Full 1 to 3 (F1 to F3), were added to represent the full load torque curve from 1000 rev/min to maximum torque at 2000 rev/min to rated power at 4000 rev/min.

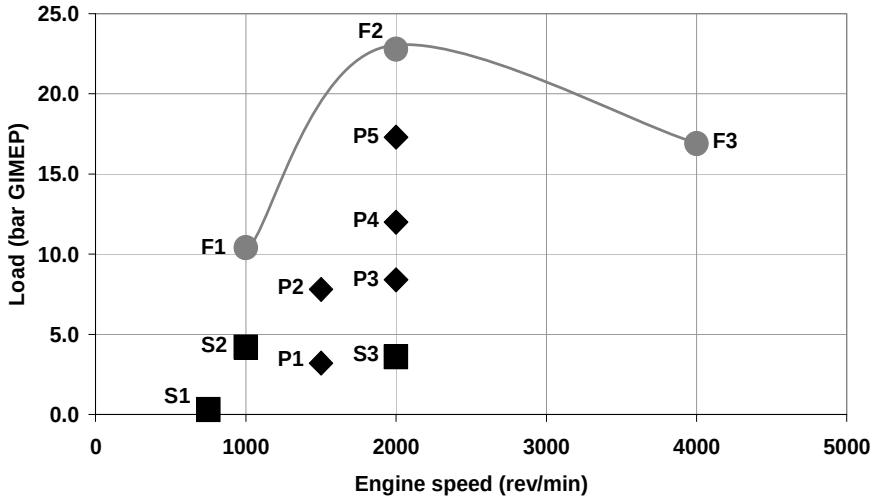

Figure 4-1: Part load and full load key operating points selected.

4.4 Gas exchange processes matching

The single-cylinder engine was identical to the 4-cylinder in terms of build characteristics but the associated inlet and exhaust systems were very different, as described in Chapter 3. Not only did the 4-cylinder engine have higher charge-air and EGR flows, it also had a turbine driving the compressor and after-treatment systems opposing the natural exhaust flow, all affecting the gas dynamics in the combustion chamber. Whilst these details of the gas behaviour could not be reproduced on the single-cylinder engine, the pumping losses were used to characterise the behaviour on

the 4-cylinder engine and served as target in the single-cylinder engine. This allowed more realistic intake and exhaust events to be obtained. The result was comparable volumetric efficiencies, in-cylinder pressures and temperatures during the intake and exhaust strokes, hence similar trapped residuals and initial conditions during the compression stroke and the combustion. A combination of backpressure valves and an orifice plate was used to achieve this. The plate was inserted at a similar distance to that from the exhaust port to the turbine inlet on the 4-cylinder engine. The aim was to maintain an appropriate level of backpressure in the cylinder when the exhaust valves opened. Additional backpressure valves (1 and 2), inserted in parallel beyond the exhaust chamber, allowed a fine control on the average level of backpressure to improve the pumping loop match. These valves were also useful to provide some flexibility in the level of backpressure at the other speeds and loads, rather than relying on a unique setting. This resulted in a good match of the pumping losses. The backpressure valve 2 was fully open for the rated power key point and fully shut for all the other key operating points.

The orifice plate sizing took place at 4000 rev/min full load. The rated power condition is used to size the orifice plate since it offers the highest level of backpressure linked to the highest gas flow. The 4-cylinder engine data showed that the backpressure in the exhaust was dominantly linked to the flow and not to the turbine work. This was confirmed by the observation that exhaust pressures increased with speeds above the rated torque point despite the inlet-manifold pressures decreasing and the turbine recuperating less work. To establish the orifice diameter, a series of tests was conducted with different orifice diameters and backpressure valves settings at 4000 rev/min full load. The pumping losses and the in-cylinder pressure data were compared with those from the 4-cylinder engine. The influence of parameters such as injection timing had a minimal effect on the pumping losses compared with those of inlet-manifold and exhaust-manifold pressures. The resulting in-cylinder pressure traces and pumping losses of the tests carried out with backpressure valve 1 20 half turns shut (out of 25) and valve 2 fully open are shown in Figure 4-2. The impact of increasing the orifice diameters from 24 to 27 mm was less visible. However, not imposing any additional flow restrictions other than those of a straight pipe 50 mm in diameter resulted in lower in-cylinder pressures during the exhaust stroke, as can be seen in Figure 4-3. An orifice plate of 27 mm in diameter

and backpressure valve 1 20 half turns shut and valve 2 fully open were selected as they provided a good match in terms of pumping losses and would therefore result in comparable combustion chamber filling and emptying events. Figure 4-3 also shows the different in-cylinder pressure traces from the single and 4-cylinder engines at 4000 rev/min, the single-cylinder engine results are with and without a 27 mm in diameter orifice plate, at the same backpressure valves settings. The 4-cylinder engine pumping losses of -1.20 bar PMEP were closely matched by the optimised settings which resulted in losses of -1.18 bar PMEP for the single-cylinder engine. For the same valves settings but without the orifice plate, the pumping losses were -0.41 bar PMEP, which was much lower than the 4-cylinder engine and would have resulted in very little residual gas and unrealistic combustion chamber filling and emptying events. Some differences were visible in in-cylinder pressures between the single and 4-cylinder engines during the intake and exhaust strokes but these were considered as negligible.

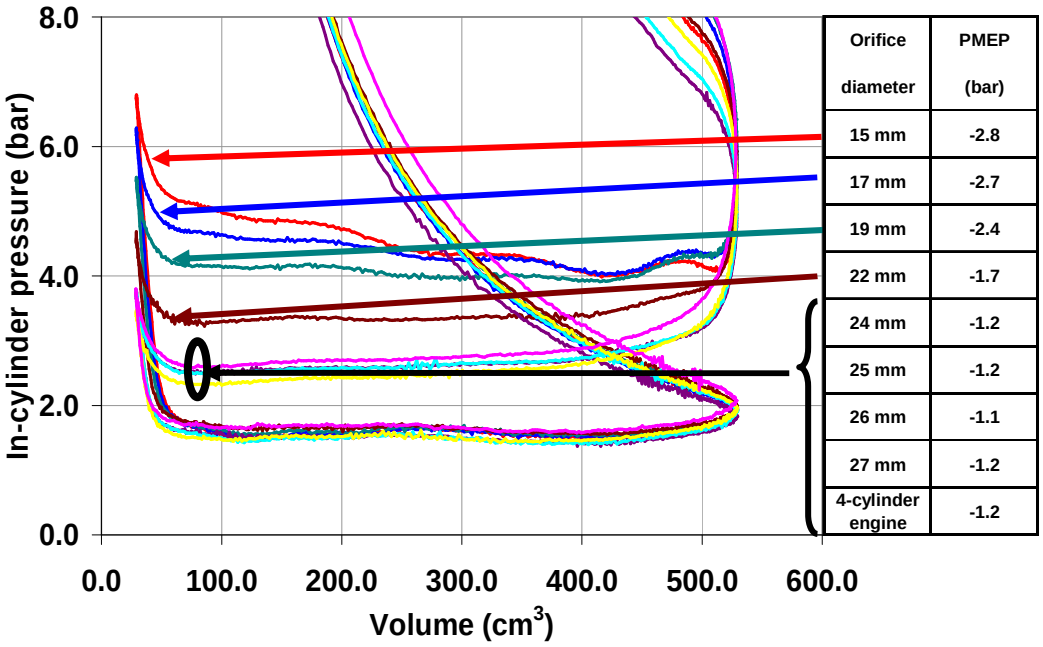

Figure 4-2: Impact of orifice plate on in-cylinder intake and exhaust pressures.

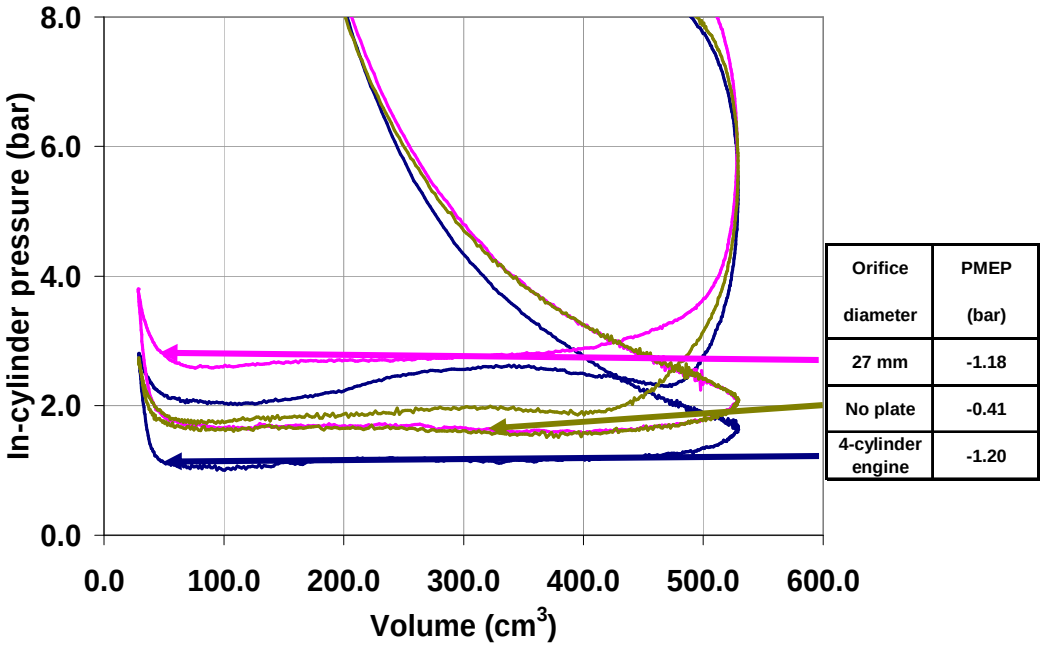

Figure 4-3: Single and 4-cylinder engines in-cylinder intake and exhaust pressures.

Code	Type	Speed / load	Backpressure valves settings
F1	Full load	1000 / Full load	1: 23.5 half turns shut & 2: shut
F2	Full load	2000 / Full load	1: 19.5 half turns shut & 2: shut
F3	Full load	4000 / Full load	1: 20 half turns & 2: open
P1	Primary	1500 / 2 bar BMEP	1: 24 half turns shut & 2: shut
P2	Primary	1500 / 5 bar BMEP	1: 24 half turns shut & 2: shut
P3	Primary	2000 / 6 bar BMEP	1: 23.5 half turns shut & 2: shut
P4	Primary	2000 / 10 bar BMEP	1: 23 half turns shut & 2: shut
P5	Primary	2000 / 16 bar BMEP	1: 22.5 half turns shut & 2: shut
S1	Secondary	750 / idle	1: 24.5 half turns shut & 2: shut
S2	Secondary	1000 / 3 bar BMEP	1: 24.5 half turns shut & 2: shut
S3	Secondary	2000 / 2 bar BMEP	1: 24 half turns shut & 2: shut

Table 4-1: Exhaust backpressure valves settings for key operating points.

Once the orifice plate size was fixed, the backpressure valves were adjusted to match the 4-cylinder engine pumping losses at each key point. This was achieved by operating the engine at each key point with the targeted inlet-manifold temperature, swirl throttle position, AFR, EGR rate and injection pressure, and an injection timing and duration, hence fuelling and load, similar to the 4-cylinder engine and adjusting the backpressure valves settings to obtain comparable pumping losses. Good matches were achieved as shown in the comparative tables in Section 4.5. One exception was at P5, where the valves needed shutting more to force the required EGR back to the inlet, thereby increasing pumping losses above the levels found with the 4-cylinder engine. The resulting settings of the backpressure valves, in multiples of half turns,

are summarised in Table 4-1 for all the key points, grouped by type in order of speed and load.

4.5 Matching of the 4-cylinder engine

4.5.1 Transfer of operating conditions and characteristics

Once representative intake and exhaust strokes were achieved at each key point, the 4-cylinder engine operating conditions were applied to the Build #1 single-cylinder engine in order to characterise it at the different key points and compare the results with those from the 4-cylinder engine. Figure 4-4 represents a schematic of the engine with the operating conditions on one side and the operating characteristics on the other. The approach consisted firstly in matching the operating conditions, which were believed to be directly transferable to the single-cylinder engine, such as EGR rate, AFR, inlet-manifold temperature and injection pressure, shown in blue in Figure 4-4. In green are shown the operating conditions needing redefining. The backpressure valves settings were one of these conditions, discussed earlier to match the pumping losses, the pilot-injection timing and separation were the other operating conditions, for the key points S1 to S3 and P1 to P3 with pilot injections. The pilot and main injection settings of the 4-cylinder engine formed a starting point, from which the pilot-injection quantity was adjusted to obtain similar level of noise as on the 4-cylinder engine, and the separation readjusted to minimise HC, NO_x and soot emissions. This was done to verify similar pilot-injection settings could be used on the single-cylinder engine. Finally, two operating conditions shown in red Figure 4-4 were varied in an aim to investigate their impact and redefine their settings. The main injection timing was investigated in order to illustrate that comparable NO_x and soot emissions to the 4-cylinder engine could be achieved on the single-cylinder engine. The injection-timing responses went from the most retarded injection timing possible before the engine misfired to advanced injection timings making sure the 4-cylinder engine injection timing was included. At the injection timing where a good match was obtained, swirl investigations were carried out for those points at which the swirl throttle had been used to modify the levels of swirl on the 4-cylinder engine. This was done since the swirl system was unlikely to operate exactly as on the 4-cylinder

engine for the same reasons the exhaust system needed adapting. This redefined the setting and gave a clear understanding of its impact on smoke or soot emissions.

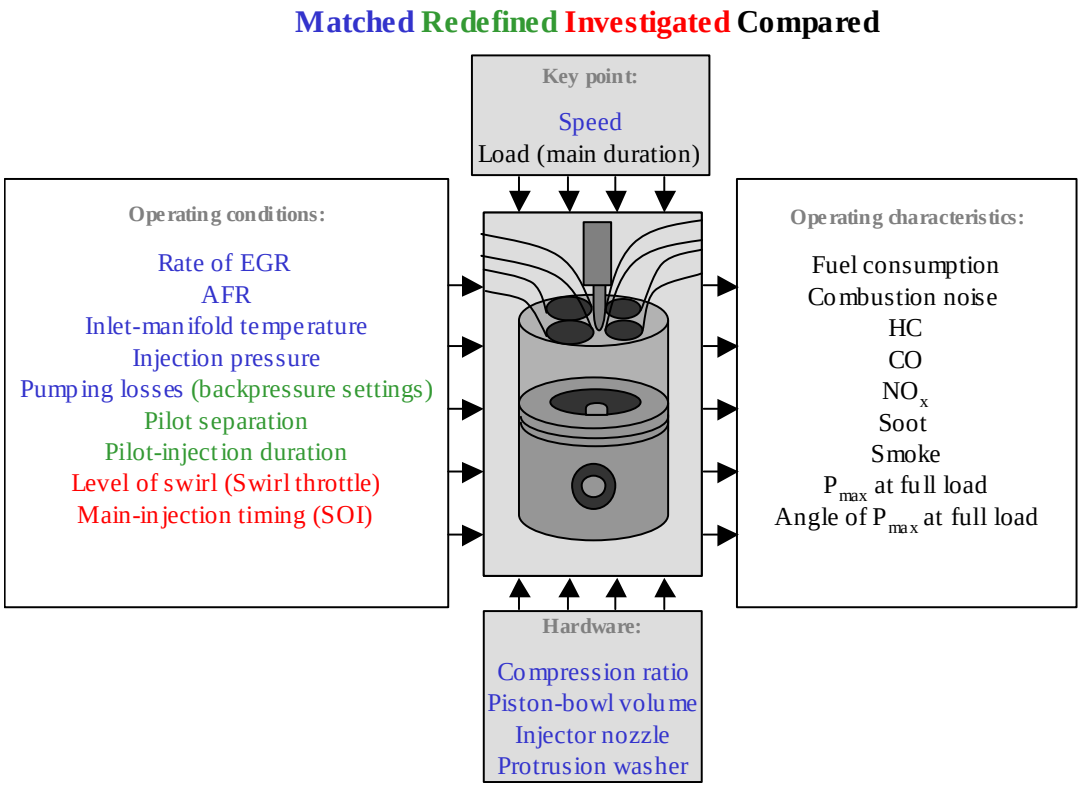

Figure 4-4: Major operating conditions used during matching phase.

As the brake torque on a single-cylinder engine is not comparable to that of the 4-cylinder engine due to the different friction losses, the load needed redefining on the single-cylinder engine. There are several potential ways of doing so but two were chosen in the present investigations. The first one was to fix the fuel consumption to the value recorded on the 4-cylinder engine and to vary the injection timing. Each injection timing would result in a particular gross load. The second approach was to match the level of fuelling at the centre point, being a similar injection timing to the 4-cylinder engine, to identify the gross load and to vary the injection timing whilst maintaining the load constant. During both approaches, the injection timing resulting in comparable NO_x and soot emissions would be selected, thus creating a new reference in operating conditions, gross load, fuel consumption and emissions. At part load, the first approach was used for the light load conditions at key points S1 to S3 and P1, but it was found difficult to apply due to drift in injections with time, which meant fixing fuel consumption was not a simple task. The second approach turned out

to be more practical since the load was calculated in real time by the data acquisition system and was therefore easier to use as a target. This approach was therefore applied to the medium and higher load key points P2 to P5. At full load, the AFR and fuel consumption were matched and the injection timing was adjusted to achieve the same maximum in-cylinder pressure. A possible alternative approach consisted in matching the gross load and AFR of the 4-cylinder engine by adjusting the level of fuelling and the inlet-manifold pressure. However, the variability in the gross load from one cylinder to another in the 4-cylinder engine and the fact that a 1 °CA TDC offset results in a 10 % change in load meant that this approach was questionable.

4.5.2 Part load key point matching

The following tables present a comparison between the Euro 5 4-cylinder engine operating characteristics and those achieved on the single-cylinder engine for the part load key points. Table 4-2 shows key points S1 to S3, which were three very light load secondary key points. Table 4-3 shows key points P1 and P2, which were light and medium load primary key points at 1500 rev/min. Finally, Table 4-4 shows key points P3 to P5, which were medium to high load primary key points at 2000 rev/min. In each case the graphs present NO_x and soot emissions, fuel consumption and gross load during the injection-timing response. The swirl investigations are also presented where relevant with green arrows indicating increasing levels of swirl. The red squares represent the equivalent result for the 4-cylinder engine (or 25 % of the total values for emissions and fuel consumption) and the larger points on the response curves present the selected reference point for each key point on the single-cylinder engine. The emissions are shown in g/h, which can be converted to g/km by a weighting factor if the time spent at each key point is known, making comparisons with the legislative values possible. In each case, the comparison tables detail the operating conditions and characteristics for the 4-cylinder engine and the finally selected conditions and characteristics on the single-cylinder engine. Table 4-2 shows the secondary key point results obtained during injection-timing investigations conducted with fixed swirl throttle position, AFR and EGR rate, pilot-injection separation and quantity. These responses were carried out with a fixed level of fuelling.

S1: 750 rev/min idle		Part load	Single	Multi
Fixed fuel consumption		Fuel consumption (kg/h)	0.09	0.09
		Wet EGR rate (%)	52.9	52.3
		Dry AFR (-)	59.9	56.2
		Inlet temperature (°C)	58	51
	Matched	Pump. losses (bar PMEP)	-0.1	-
		Injection pressure (bar)	311	317
		Swirl throttle (% shut)	70	N/A
		Pilot separation (°CA)	19.0	19.0
	Redefined	SOI (°CA ATDC)	2.0	2.1
		Pilot duration (µs)	300	~300
		Load (bar GIMEP)	0.4	0.4
		Combustion noise (dB A)	74.0	72.9
		HC (g/h)	1.67	0.30
		CO (g/h)	6.1	3.16
	Compared	NO_x (g/h)	0.58	0.79
		Soot (g/h)	0.00	0.01
		Smoke (FSN)	0.00	0.61
		Inlet pressure (bar)	1.009	0.996
	Monitored	Exhaust temperature (°C)	116	112
		Exhaust pressure (bar)	1.081	1.104
S2: 1000 rev/min 3 bar BMEP		Part load	Single	Multi
Fixed fuel consumption		Fuel consumption (kg/h)	0.31	0.33
		Wet EGR rate (%)	45.0	44.5
		Dry AFR (-)	23.8	24.1
		Inlet temperature (°C)	72	69
	Matched	Pump. losses (bar PMEP)	-0.1	-0.2
		Injection pressure (bar)	475	482
		Swirl throttle (% shut)	74	74
		Pilot separation (°CA)	20.0	14.0
	Redefined	SOI (°CA ATDC)	-3.0	-2.3
		Pilot duration (µs)	300	~300
		Load (bar GIMEP)	3.5	4.2
		Combustion noise (dB A)	83.4	79.5
		HC (g/h)	N/A	0.40
		CO (g/h)	8.83	4.65
	Compared	NO_x (g/h)	0.46	0.75
		Soot (g/h)	0.45	0.44
		Smoke (FSN)	2.35	2.07
		Inlet pressure (bar)	1.125	1.025
	Monitored	Exhaust temperature (°C)	230	240
		Exhaust pressure (bar)	1.178	1.178
S3: 2000 rev/min 2 bar BMEP		Part load	Single	Multi
Fixed fuel consumption		Fuel consumption (kg/h)	0.56	0.58
		Wet EGR rate (%)	41.7	41.2
		Dry AFR (-)	32.7	32.5
		Inlet temperature (°C)	92	92
	Matched	Pump. losses (bar PMEP)	-0.6	-0.4
		Injection pressure (bar)	801	810
		Swirl throttle (% shut)	59	60
		Pilot separation (°CA)	28.0	26.0
	Redefined	SOI (°CA ATDC)	3.0	0.8
		Pilot duration (µs)	270	~270
		Load (bar GIMEP)	3.2	3.6
		Combustion noise (dB A)	86.7	86.5
		HC (g/h)	N/A	1.70
		CO (g/h)	18.92	22.63
	Compared	NO_x (g/h)	1.71	1.50
		Soot (g/h)	0.06	0.11
		Smoke (FSN)	0.26	0.45
		Inlet pressure (bar)	1.234	1.162
	Monitored	Exhaust temperature (°C)	288	290
		Exhaust pressure (bar)	1.604	1.473

Table 4-2: Secondary part load key point results.

Soot emissions had profiles that reflected characteristics observed on the 4-cylinder engine and also trends observed by Chi et al. (2002). From advanced injection timings, retardation usually results in decreased NO_x emissions while soot emissions increase as described by Gill et al. (2002). This usually explains why a diesel particulate filter is used in the exhaust line in conjunction with a low NO_x emissions strategy. However, further retardation led to a reversal in soot emission trends in all these light load conditions thereby offering simultaneous low NO_x and soot emissions. It is conjectured that the explanation for this has two components. The first is that retarding the injection timing beyond TDC led to an injection occurring in a reduced in-cylinder pressure environment, enhancing the fuel spray penetration and distribution. The second factor was linked to the fact that the auto-ignition delay was increased, also due to the lower in-cylinder pressure and temperature during the injection, which gave more time for the fuel to penetrate and mix with air. Both factors are expected to reduce soot emissions. It is believed that these areas were not exploited a few years ago due to the lower injection pressures available with the result that the fuel could not be injected fast enough to give sufficient time for the fuel and air to mix. Retarded injection timings would therefore have lead to misfire or unacceptable levels of fuel consumption. In terms of NO_x emissions, in all cases, the more advanced the injection timing, the higher the emissions. The combustion associated with earlier injection timings resulted in higher pressures and flame temperatures, which explain the higher NO_x emissions. While these investigations were carried out with fixed fuel consumption, the gross loads did not vary during the injection timing responses and were all lower than the values recorded on the 4-cylinder engine. The rapid combustion associated with these light load conditions and occurring near TDC means that timing has little impact on the energy loss when the exhaust valves open, in comparison with higher loads where the tail end of the combustion affects the in-cylinder pressures just before exhaust valves opening.

The final reference points were selected to match the 4-cylinder engine soot emissions. They corresponded to similar injection timings as recorded on the 4-cylinder engine. NO_x emissions were lower compared with the 4-cylinder engine apart from key point S3 but these deviations were small compared with the possible orders of magnitude changes over the speed and load ranges, as visible in the NO_x versus soot emissions summary in Figure 4-11.

Table 4-3 shows the 1500 rev/min primary key point P1 and P2 results obtained during injection-timing investigations conducted with fixed swirl throttle position, AFR and EGR rate, pilot-injection separation and quantity. These responses were carried out with a fixed level of fuelling for key point P1 and with fixed load for key point P2. Once reference points were determined, swirl investigations were conducted at those injection timings.

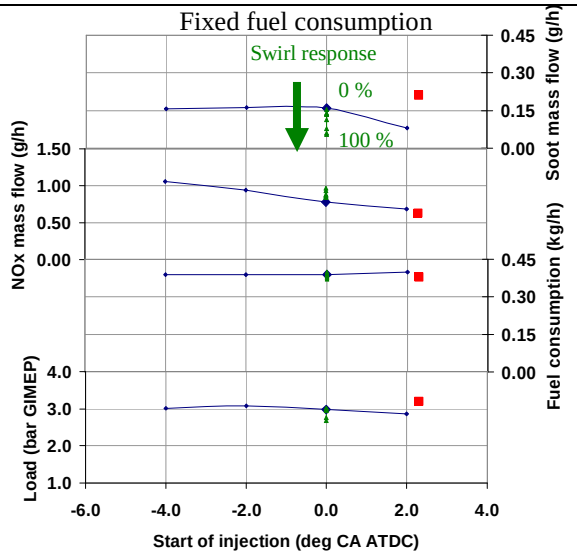

P1: 1500 rev/min 2 bar BMEP		Part load	Single	Multi
	Matched	Fuel consumption (kg/h)	0.39	0.38
		Wet EGR rate (%)	45.4	45.8
		Dry AFR (-)	29.3	30.2
		Inlet temperature (°C)	88	89
		Pump. losses (bar PMEP)	-0.2	-0.2
		Injection pressure (bar)	545	550
	Redefined	Swirl throttle (% shut)	46	48
		Pilot separation (°CA)	26.0	26.0
		SOI (°CA ATDC)	0.0	2.3
		Pilot duration (µs)	300	~300
		Load (bar GIMEP)	3.0	3.2
	Compared	Combustion noise (dB A)	84.3	83.6
		HC (g/h)	1.57	1.38
		CO (g/h)	16.81	14.33
		NO_x (g/h)	0.78	0.63
		Soot (g/h)	0.16	0.21
		Smoke (FSN)	0.91	1.04
	Monitored	Inlet pressure (bar)	1.153	1.049
		Exhaust temperature (°C)	245	250
		Exhaust pressure (bar)	1.236	1.207

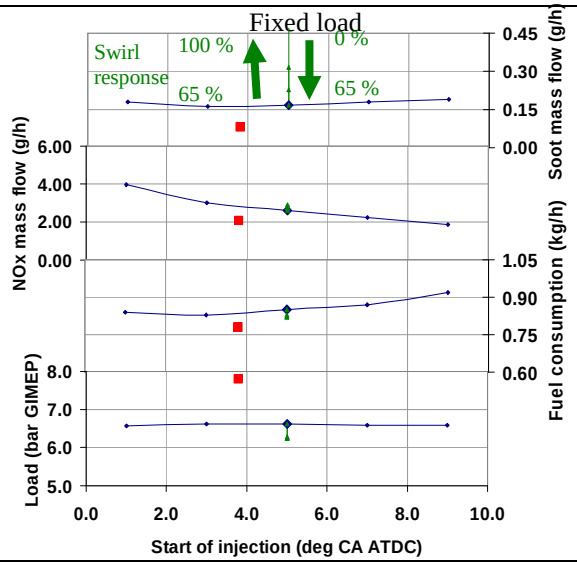

P2: 1500 rev/min 5 bar BMEP		Part load	Single	Multi
	Matched	Wet EGR rate (%)	28.1	27.3
		Dry AFR (-)	22.0	22.8
		Inlet temperature (°C)	53	54
		Pump. losses (bar PMEP)	-0.7	-0.5
		Injection pressure (bar)	900	907
	Redefined	Fuel consumption (kg/h)	0.85	0.78
		Swirl throttle (% shut)	65	68
		Pilot separation (°CA)	26.0	25.0
		SOI (°CA ATDC)	5.0	3.8
		Pilot duration (µs)	260	~260
		Load (bar GIMEP)	6.6	7.8
	Compared	Combustion noise (dB A)	88.2	87.3
		HC (g/h)	N/A	0.75
		CO (g/h)	10.33	9.83
		NO_x (g/h)	2.61	2.06
		Soot (g/h)	0.17	0.08
		Smoke (FSN)	0.64	0.34
	Monitored	Inlet pressure (bar)	1.255	1.202
		Exhaust temperature (°C)	429	370
		Exhaust pressure (bar)	1.754	1.528

Table 4-3: Primary part load key point results at 1500 rev/min.

Soot emissions at key point P1 had the same profile as observed at the secondary key points S1 to S3, and the same remarks could be made to explain the results. Concerning the soot emission profile at key point P2, it showed a similar pattern as

the profile described by Gill et al. (2002). Soot emission increased as the injection timings were retarded, which was opposite to the trend observed at key point P1 or at the secondary key points. It is believed that the increased level of fuelling to maintain the load and the higher in-cylinder pressures from increasing the inlet-manifold pressure to maintain the AFR caused this. Concerning NO_x emissions, a typical response was obtained, with reducing emissions as the injection timing is retarded. In terms of gross load, the values obtained at key point P1 were all within 10 % of the 4-cylinder engine value for a similar fuel consumption. However, at key point P2, despite a higher fuel consumption value, the gross load was significantly lower than on the 4-cylinder engine.

At key point P1, the reference point was selected because it matched the 4-cylinder engine soot emissions and offered a close match in terms of gross load. There was a difference in NO_x emissions but this was small relative to the range of possible values, which is visible in the summary in Figure 4-11. At key point P2, where the load was fixed rather than the fuel consumption, higher soot emissions were observed across the injection-timing response. An injection timing of 5 °CA ATDC was selected despite a better NO_x emissions match being possible with more retarded injection timings. This was to limit fuel consumption, which was noticeably higher than the level recorded on the 4-cylinder engine whilst resulting in a lower gross load. It was unclear why the single-cylinder engine produced more NO_x emissions than the 4-cylinder engine. Despite a more retarded injection timing, slightly lower AFR and higher EGR rate, emissions were higher.

The results of the swirl investigation carried out at key point P1 showed that soot emissions were constant for positions of the throttle valve between fully open and 60 % shut and that they rapidly decreased from that position to fully shut, when the level of swirl went from 1.6 to 4.5 Rs. This indicated that the additional air motion was beneficial to the mixing thereby reducing soot emissions. However, at key point P2, soot emissions decreased for closing swirl throttle positions between fully open and 65 % shut and then started increasing again until the swirl throttle was fully shut. It is supposed that at this higher load and hence longer injection period, gaseous fuel plume-to-plume interactions reduce the level of mixing with air. During the investigations, the impact on NO_x emissions, fuel consumption and load was

negligible. For the reference points, swirl throttle positions were similar to those recorded on the 4-cylinder engine. However, the use of the swirl throttle is expected to have a negative impact on the pumping losses thereby requiring a higher gross load to compensate the net load, hence higher fuel consumption. Since these two key points formed the starting point of the next phase of the programme, a more detailed analysis of the in-cylinder pressure traces combined with the instantaneous heat release was undertaken.

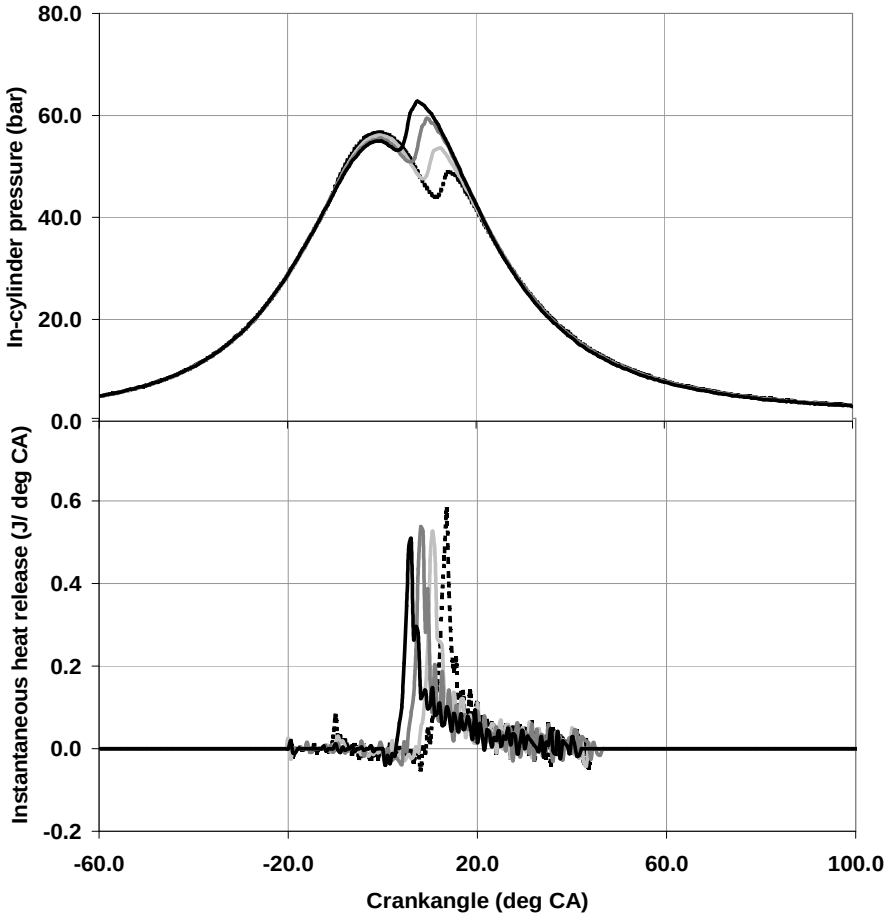

Figure 4-5: Key point P1 instantaneous heat release and pressure traces.

Figure 4-5 illustrates the results in terms of in-cylinder pressure and instantaneous heat release of an injection-timing response for the key point P1. The instantaneous heat release is plotted as the heat release per degree crankangle and integration over the complete curve amounts to the total heat released. Its profile follows closely that of the rate of in-cylinder pressure change. The fact that the injection-timing response was carried out with a fixed level of fuelling was visible in the instantaneous heat release traces since the area beneath the traces was approximately constant for all

injection timings, indicating a fixed level of energy released associated with the fixed level of fuel injected. On the other hand the integration of the area beneath the in-cylinder pressure traces would reveal a decreasing level of gross load as the injection timing was retarded. However, the small differences recorded in gross load make this difficult to visualise.

Figure 4-6 follows the same pattern as key point P1 for P2 during the injection-timing response. Only the instantaneous heat release traces for the most advanced and retarded injection timings tested are shown. The difference in the approach taken to carry out the injection-timing response was expected to be visible: an integration of the area beneath the instantaneous heat release traces should reveal an increased level of heat released as more fuel was injected to maintain the load when the injection timing was retarded, however, the accuracy of this method would make small differences in fuel consumption difficult to detect. Equally, an integration of the area beneath the in-cylinder pressure traces should reveal a constant level of gross load, also difficult to detect. In terms of instantaneous heat release, for the most advanced injection timing, evidence of a premixed-combustion phase followed by a diffusion-combustion phase was visible. This could explain why soot emissions increased slightly when the injection timing was advanced from 3 to 1 °CA ATDC. The reason for this is that as the fuel is injected earlier and therefore into a hotter and higher-pressure environment, it results in earlier auto-ignition, occurring before the injection and mixing process are finished. The resulting diffusion-combustion phase forms more PM and the emissions reflect an equilibrium between the formed and oxidised PM. At the most retarded injection timing, the instantaneous heat release trace gives evidence that the nature of the combustion has gone from a combined premixed and diffusion combustion to a fully-premixed-charge combustion. It is interesting to note that the maximum level of the instantaneous heat release increased as the injection timing was retarded, which would correspond with the increased extent of the premixed-combustion phase proportional to the increased level of fuelling. However this did not lead to higher NO_x emissions. It is believed that NO_x emissions are more dependant on the initial and maximum gradients of the rates of heat release or pressure gradient, which reduce as the injection timing is retarded, as shown in more detail in Figure 4-7.

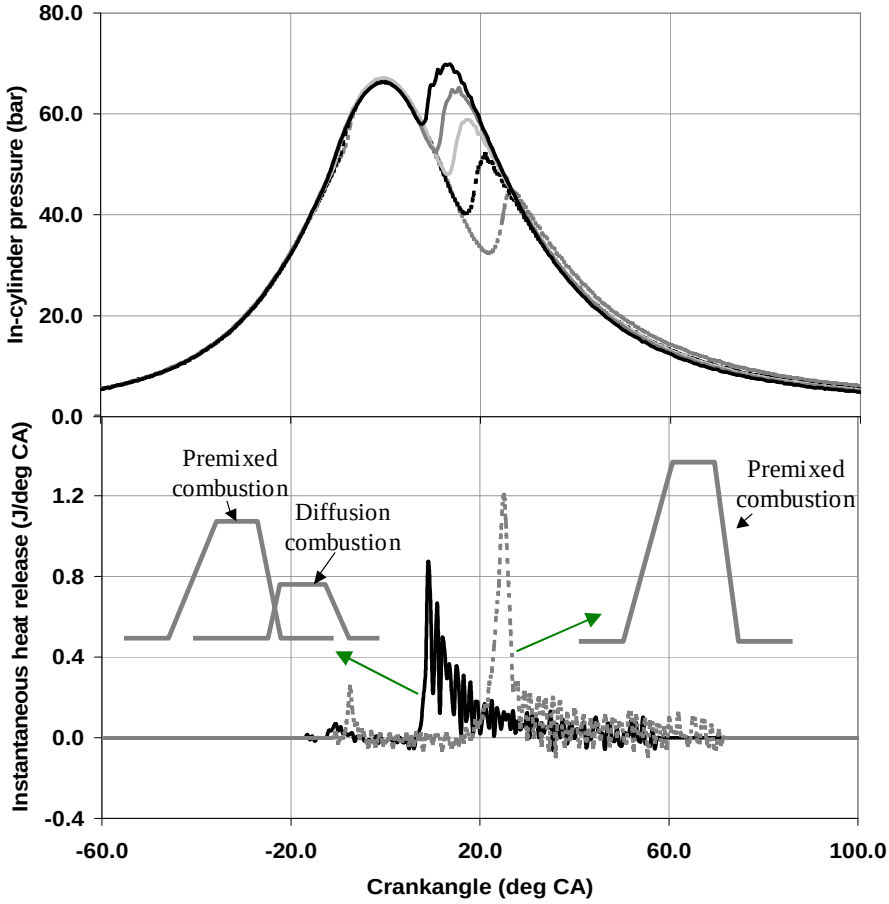

Figure 4-6: Key point P2 instantaneous heat release and pressure traces.

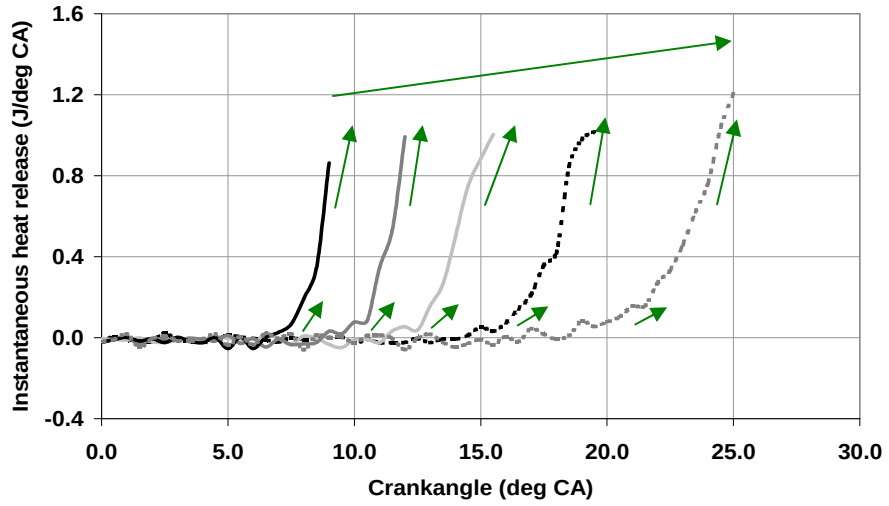

Figure 4-7: Key point P2 initial rates of instantaneous heat release traces.

Table 4-4 shows the 2000 rev/min primary key point results. An injection-timing investigation was conducted at these key points with fixed swirl throttle position and pilot-injection separation and quantity, where appropriate, EGR rate, AFR and load, being the second approach discussed in Section 4.5.1, and as used for key point P2. A

swirl investigation was conducted at key point P3 at the selected reference injection timing but not at key points P4 and P5 where the swirl throttle position was fully open on the 4-cylinder engine. Soot and NO_x emissions and fuel consumption at these key points had the same profile as observed in the earlier primary key point P2 investigated at fixed load and in line with the observations by Gill et al. (2002). The same remarks can be made to explain the results. Operating the engine at a similar fuel consumption and start of main injection as on the 4-cylinder engine determined the load, which was then used as a target during the investigations. The load values were lower than on those recorded on the 4-cylinder engine at key points P3 and P4, but comparable at key point P5.

At key point P3, soot emissions were all close to the level of the 4-cylinder engine reference point. The selection of the single-cylinder engine reference point was based on a compromise between NO_x emissions and fuel consumption. Selecting a more retarded injection timing would have improved NO_x emissions match but would have increased the difference in fuel consumption between the engines. Furthermore, the difference in fuel consumption was small relative to the spread of values seen over the speed and load ranges, as can be seen in the summary Figure 4-11. At key point P4, a good match was achieved for NO_x and soot emissions and fuel consumption with an injection timing of 2.2 °CA later than for the 4-cylinder engine. Concerning key point P5, the chosen point was selected because it provided the best match in terms of NO_x emissions, fuel consumption and load. Much higher soot emissions were observed across the injection-timing response. Since similar operating conditions had been used as on the 4-cylinder engine, the actual engine build was questioned, especially as AFR was of 18.3:1 compared with 17.9:1 for the 4-cylinder engine. Poorer air utilisation was a possible cause and this was blamed on the injector position relative to the piston bowl which resulted in a poorly optimised combustion chamber. The protrusion of the injector into the combustion bowl was believed to be incorrect in the single-cylinder engine. The exact injector location has a big impact on the spray path, and hence on its interaction with the bowl and consequently, on the resulting air utilisation. The effects of this are especially important at high loads. NO_x emissions were also higher when compared with those of the 4-cylinder engine, which was a possible effect of the higher AFR compared with the 4-cylinder engine.

P3: 2000 rev/min 6 bar BMEP		Part load	Single	Multi
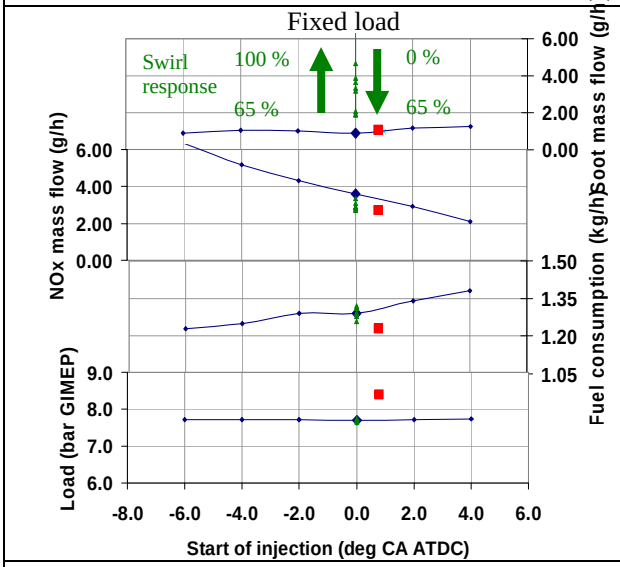	Matched	Wet EGR rate (%)	31.3	30.8
		Dry AFR (-)	21.6	21.4
		Inlet temperature (°C)	68	66
		Pump. losses (bar PMEP)	-0.7	-0.5
		Injection pressure (bar)	1070	1075
	Redefined	Fuel consumption (kg/h)	1.29	1.23
		Swirl throttle (% shut)	64	62
		Pilot separation (°CA)	33.0	33.0
		SOI (°CA ATDC)	0.0	0.8
		Pilot duration (µs)	210	~210
		Load (bar GIMEP)	7.7	8.4
	Compared	Combustion noise (dB A)	87.9	86.3
		HC (g/h)	1.88	0.65
		CO (g/h)	14.46	13.28
		NO_x (g/h)	3.62	2.69
		Soot (g/h)	0.92	1.04
		Smoke (FSN)	1.62	1.75
	Monitored	Inlet pressure (bar)	1.423	1.443
		Exhaust temperature (°C)	450	442
		Exhaust pressure (bar)	1.928	1.916
P4: 2000 rev/min 10 bar BMEP		Part load	Single	Multi
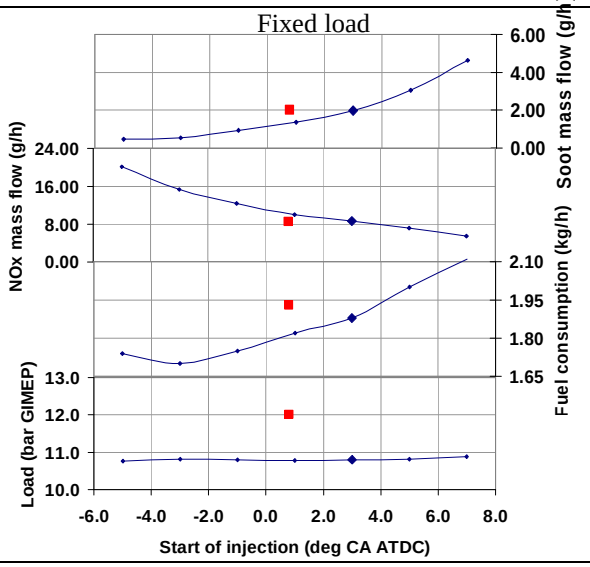	Matched	Wet EGR rate (%)	21.3	21.5
		Dry AFR (-)	21.1	21.0
		Inlet temperature (°C)	58	62
		Pump. losses (bar PMEP)	-0.7	-0.6
		Injection pressure (bar)	1190	1199
	Redefined	Fuel consumption (kg/h)	1.88	1.93
		Swirl throttle (% shut)	0	0
		Pilot separation (°CA)	N/A	N/A
		SOI (°CA ATDC)	3.0	0.8
		Pilot duration (µs)	N/A	N/A
		Load (bar GIMEP)	10.8	12.0
	Compared	Combustion noise (dB A)	88.4	86.2
		HC (g/h)	1.60	0.65
		CO (g/h)	15.99	11.95
		NO_x (g/h)	8.65	8.48
		Soot (g/h)	1.98	2.00
		Smoke (FSN)	2.07	2.08
	Monitored	Inlet pressure (bar)	1.740	1.886
		Exhaust temperature (°C)	508	537
		Exhaust pressure (bar)	2.144	2.403
P5: 2000 rev/min 16 bar BMEP		Part load	Single	Multi
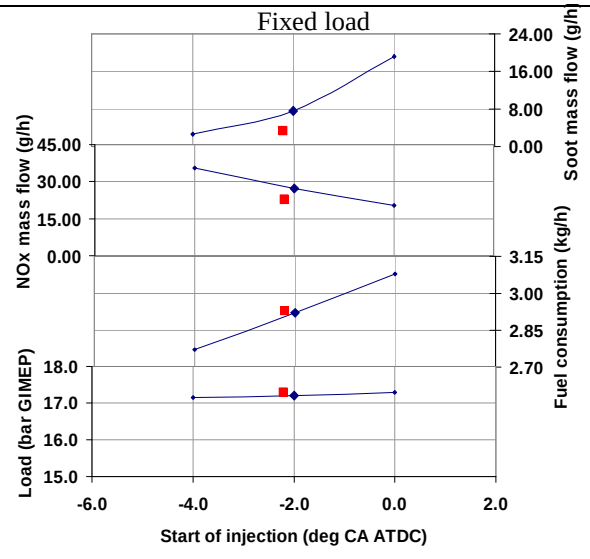	Matched	Wet EGR rate (%)	14.0	14.0
		Dry AFR (-)	18.3	17.9
		Inlet temperature (°C)	59	58
		Pump. losses (bar PMEP)	-0.7	-0.2
		Injection pressure (bar)	1197	1200
	Redefined	Fuel consumption (kg/h)	2.92	2.93
		Swirl throttle (% shut)	0	0
		Pilot separation (°CA)	N/A	N/A
		SOI (°CA ATDC)	-2.0	-2.2
		Pilot duration (µs)	N/A	N/A
		Load (bar GIMEP)	17.2	17.3
	Compared	Combustion noise (dB A)	83.8	83.7
		HC (g/h)	1.79	0.38
		CO (g/h)	26.86	16.75
		NO_x (g/h)	27.32	22.68
		Soot (g/h)	7.60	3.25
		Smoke (FSN)	3.46	2.32
	Monitored	Inlet pressure (bar)	2.149	2.197
		Exhaust temperature (°C)	588	642
		Exhaust pressure (bar)	2.504	2.409

Table 4-4: Primary part load key point results at 2000 rev/min.

The results of the swirl investigation carried out at key point P3 showed that soot emissions decreased slightly for positions of the throttle valve between fully open and 65 % shut. However, for throttle valve positions beyond 65 %, soot emissions increased rapidly. This indicated that an optimum level of swirl of 1.7 Rs was required. It also seemed to indicate that there was a maximum level of swirl, which was a compromise between the utilisation of air by increased air motion and gaseous fuel plume-to-plume interaction. It is believed that the longer gaseous plumes obtained during the higher loads and therefore injection durations led to the dramatic increases in soot emissions when the gaseous plumes would interact and overlap.

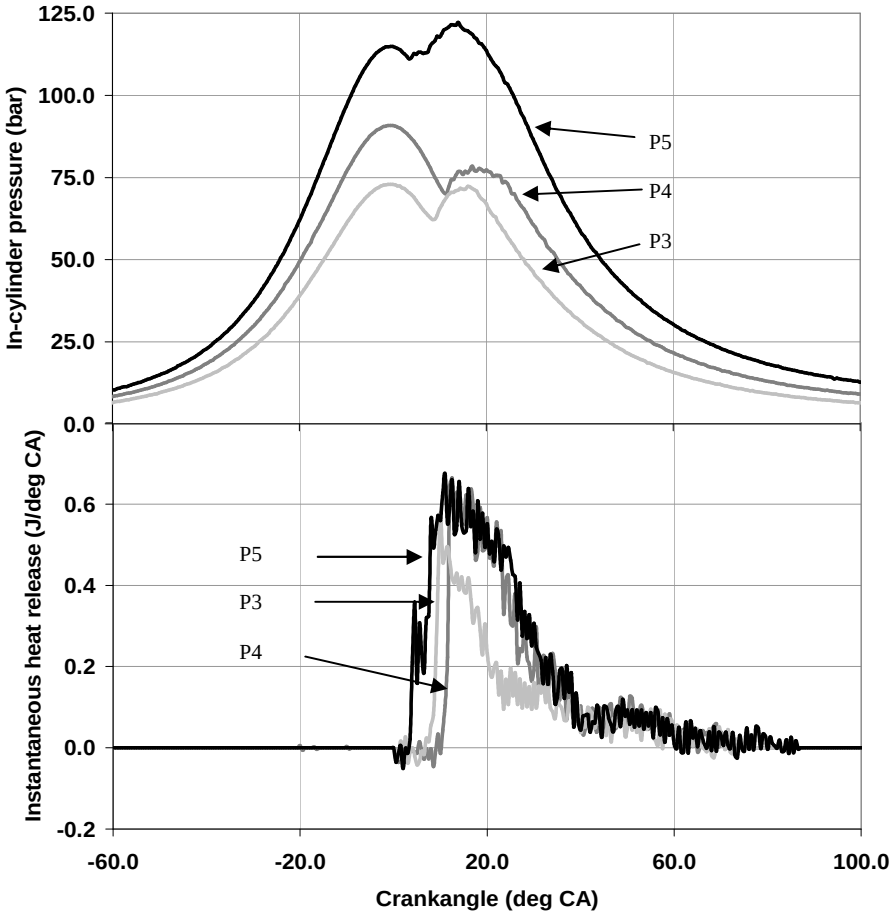

Figure 4-8: Key points P3 to P5 instantaneous heat release and pressure traces.

Figure 4-8 shows the curves of the in-cylinder pressure and instantaneous heat release at the different loads at 2000 rev/min. At fixed engine speed, increased load led to increased in-cylinder pressures due to the inlet-manifold pressure increasing almost proportionally to the fuel increase. From medium to high loads, the premixed-combustion phase represents a diminishing proportion of the fuel mass burned

compared to the diffusion-combustion phase. All load conditions in the figure show long diffusion-combustion phases, which result in high NO_x and soot emissions, the latter especially if the utilisation of air is poor, which was the case at key point P5. The initial instantaneous heat release traces are out of sequence and may be due to the design of experiment approach used to optimise the key points on the 4-cylinder engine. This makes it difficult to find clear trends in the operating conditions from one load to another as their optimisation takes many parameters into account.

4.5.3 Full load key point matching

Table 4-5 represents a comparison between the multi and the single-cylinder engines results for the full load key points. It shows key points F1 to F3, which form a representation of the full load curve, passing from the lowest speed point to the rated torque point and finally to the rated power point. In each case the graphs present smoke emissions, maximum in-cylinder pressure, fuel consumption and gross load during the injection-timing response. The red squares represent the equivalent result for the 4-cylinder engine (or 25 % of the total values for emissions and fuel consumption) and the larger points on the response curves represent the selected reference point for each key point on the single-cylinder engine. In each case, the comparison tables detail the operating conditions and characteristics for the 4-cylinder engine and the finally selected conditions and characteristics on the single-cylinder engine. Although these points are not represented in the regulation test procedures, they are important because they characterise the maximum performance capabilities of the engine and smoke and maximum in-cylinder pressure are often limiting factors in calibration for maximum load. These responses were carried out by matching the AFR and fuel consumption along with inlet-manifold temperature, injection pressure, swirl throttle position and pumping losses. Pilot-injection separation and quantity were fixed during the injection-timing response at key point F1. The injection-timing responses went from the most advanced injection timing possible before reaching the maximum in-cylinder pressure limit to a more retarded injection timing making sure the 4-cylinder injection timing was included. Some additional AFR investigations were carried out to understand the impact of AFR on smoke emissions. Green arrows indicate the impact of increasing AFR where relevant.

F1: 1000 rev/min Full Load		Full load	Single	Multi
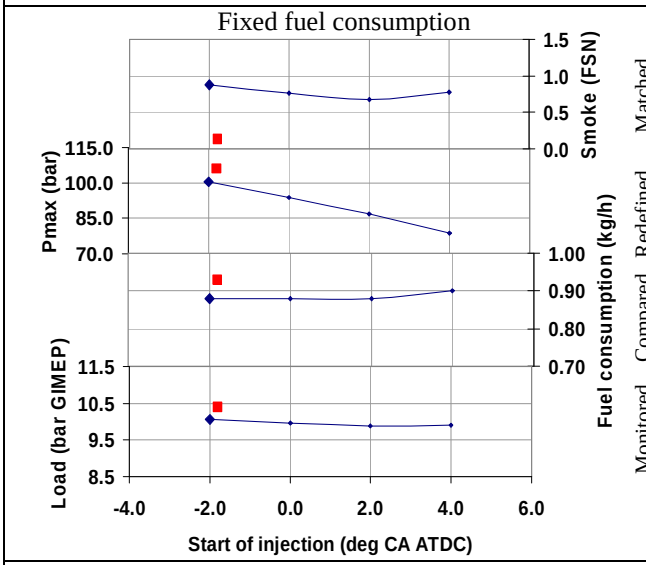	Matched	Fuel consumption (kg/h)	0.88	0.93
		Dry AFR (-)	18.8	18.4
		Inlet temperature (°C)	31	29
		Pump. losses (bar PMEP)	-0.2	-0.3
		Injection pressure (bar)	851	854
		Swirl throttle (% shut)	0	0
	Redefined	Pilot separation (°CA)	32.0	28.0
		SOI (°CA ATDC)	-2.0	-1.8
		Pilot duration (µs)	240	~240
	Compared	Load (bar GIMEP)	10.0	10.4
		Combustion noise (dB A)	85.5	81.7
		Smoke (FSN)	0.88	0.13
		P_{max} (bar)	100.6	106.0
	Monitored	Angle P_{max} (°CA ATDC)	9.1	9.1
		Inlet pressure (bar)	1.145	1.225
		Exhaust temperature (°C)	434	422
		Exhaust pressure (bar)	1.231	1.486
F2: 2000 rev/min Full Load		Full load	Single	Multi
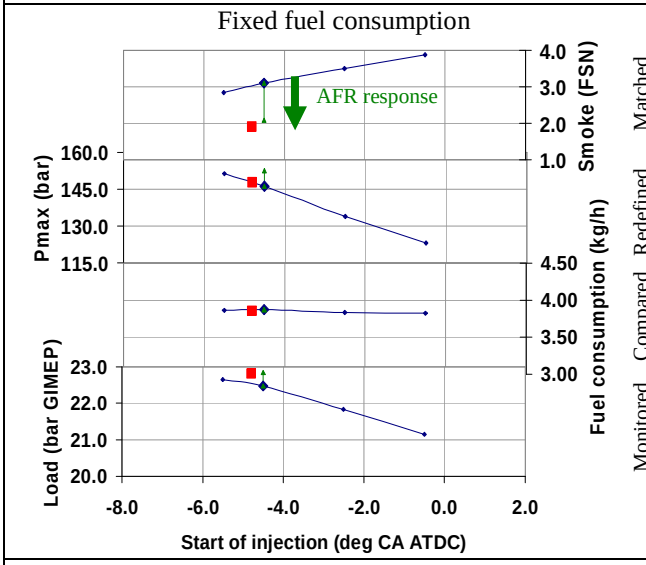	Matched	Fuel consumption (kg/h)	3.87	3.85
		Dry AFR (-)	17.5	17.5
		Inlet temperature (°C)	50	50
		Pump. losses (bar PMEP)	-0.1	0.0
		Injection pressure (bar)	1205	1200
		Swirl throttle (% shut)	0	0
	Redefined	Pilot separation (°CA)	N/A	N/A
		SOI (°CA ATDC)	-4.5	-4.8
		Pilot duration (µs)	N/A	N/A
	Compared	Load (bar GIMEP)	22.5	22.8
		Combustion noise (dB A)	83.8	82.7
		Smoke (FSN)	3.10	1.90
		P_{max} (bar)	146.1	147.6
	Monitored	Angle P_{max} (°CA ATDC)	11.4	12.7
		Inlet pressure (bar)	2.303	2.384
		Exhaust temperature (°C)	631	679
		Exhaust pressure (bar)	1.911	2.304
F3: 4000 rev/min Full Load		Full load	Single	Multi
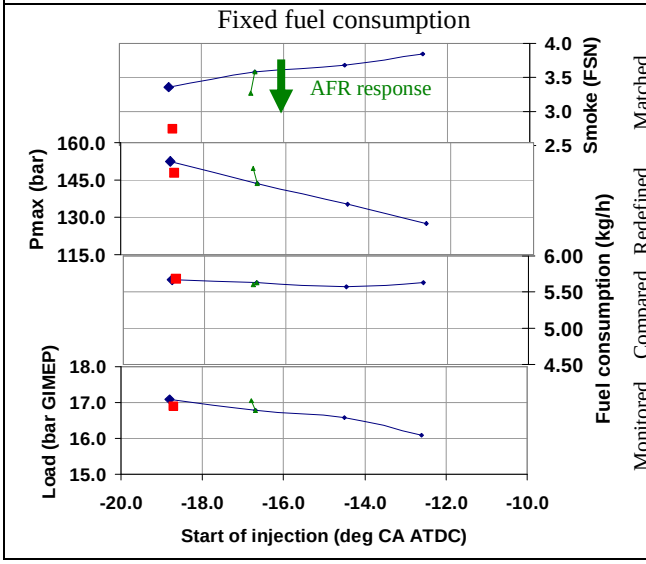	Matched	Fuel consumption (kg/h)	5.67	5.68
		Dry AFR (-)	20.1	20.1
		Inlet temperature (°C)	57	56
		Pump. losses (bar PMEP)	-1.2	-1.2
		Injection pressure (bar)	1567	1599
		Swirl throttle (% shut)	0	0
	Redefined	Pilot separation (°CA)	N/A	N/A
		SOI (°CA ATDC)	-19.0	-18.7
		Pilot duration (µs)	N/A	N/A
	Compared	Load (bar GIMEP)	17.1	16.9
		Combustion noise (dB A)	95.3	94.4
		Smoke (FSN)	3.36	2.74
		P_{max} (bar)	152.6	147.7
	Monitored	Angle P_{max} (°CA ATDC)	5.4	6.3
		Inlet pressure (bar)	2.240	2.094
		Exhaust temperature (°C)	673	748
		Exhaust pressure (bar)	1.863	2.853

Table 4-5: Full load key point results.

The smoke emissions obtained at key point F1 were particularly low throughout the injection-timing response and only comparable with the measurement accuracy. The smoke emissions recorded on the 4-cylinder engine were particularly low. At key points F2 and F3, the response was in line with what was expected since advancing the injection timing reduced smoke emissions. It is thought that the advanced injection timings led to better fuel, air and piston interactions and also longer residence times of PM formed in high temperature environments. This promotes PM oxidation as described by Morgan et al. (2003) and resulted in lower engine-out smoke emissions. It is worth noting that smoke emissions at key points F2 and F3 were much higher throughout the injection-timing responses than the levels recorded on the 4-cylinder engine.

In terms of maximum in-cylinder pressure, its behaviour was as expected as the maximum pressure increased as the injection timing advanced and became a limiting factor at key points F2 and F3 as to how advanced the injection timing could be since the engine design was not capable of more than 150 bar. As the tests were carried out with fixed fuel consumption, advancing the injection timing clearly increased the load at key points F2 and F3. For the full load key points, the results for the same injection timings were selected as the reference points. They resulted in higher smoke emissions but similar maximum in-cylinder pressures. The poor match in terms of smoke emissions led to the additional investigation of the impact of AFR at key points F2 and F3 at injection timings where there was scope for the in-cylinder pressure to increase, i.e. at injection timings retarded from the most advanced timings tested. An increase in AFR from 17.5:1 to 18.5:1 at key point F2 and from 20.1:1 to 21.3:1 at key point F3 reduced smoke emissions but they remained higher than for the 4-cylinder engine. This seemed to indicate that for the same amount of air and fuel in the cylinder, confirmed by similar AFR and fuel consumption as on the 4-cylinder engine, the utilisation of air was poorer leading to increased smoke emissions. This could again suggest that the different injector position relative to the piston bowl was therefore not optimised, as mentioned in the part load section. The poor match in smoke emissions required further investigations to understand the reasons behind the step change. This will be described in the next section.

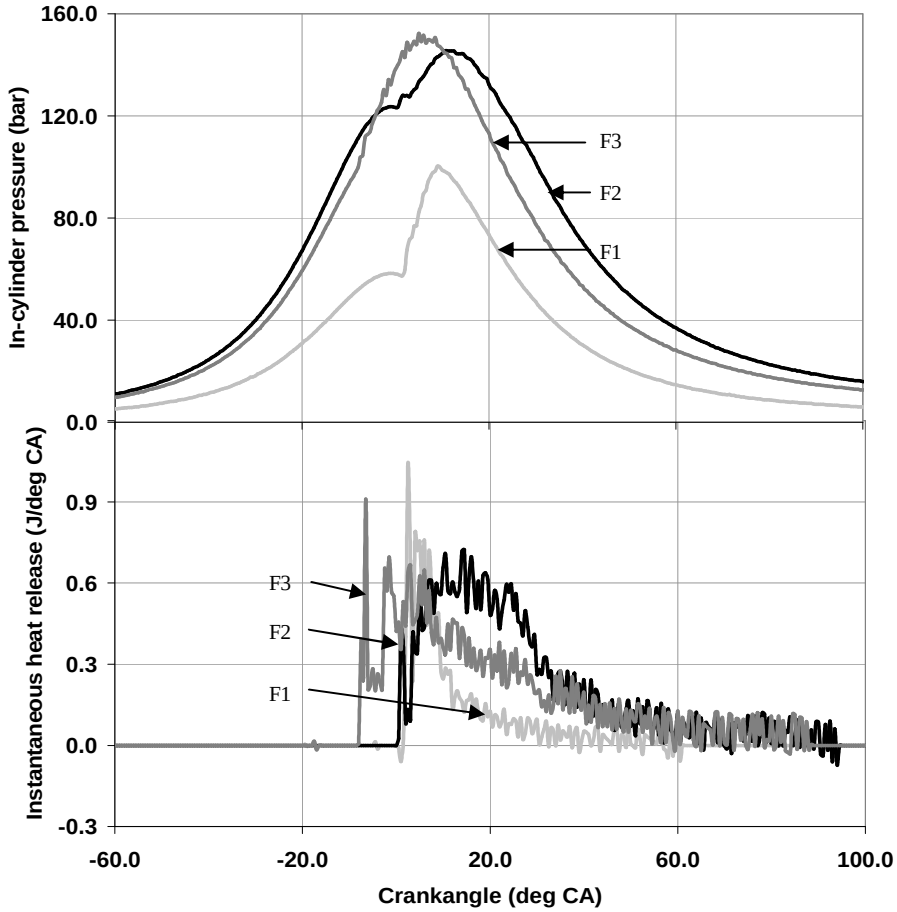

Figure 4-9: Full load instantaneous heat release and pressure traces.

Figure 4-9 shows the in-cylinder pressure and instantaneous heat release at full load at the three different speeds and helps explain the notions of rated torque and rated power. The instantaneous heat release is plotted per degree crankangle and integration over the complete curve amounts to the total heat released, which is proportional to the mass of fuel injected. The load corresponds to the integration of the area beneath the in-cylinder pressure trace and is proportional to the gross load. The rated torque case corresponds to the maximum level of fuelling per engine cycle and this was achieved at 2000 rev/min, which resulted in the highest total heat release. At higher engine speeds, the same quantity of fuel would not have sufficient time to burn due to the reduced cycle time. The load or torque is also higher as visible from the in-cylinder pressure trace, however, the maximum power is achieved for a reduced level of fuelling and load per cycle but at the higher speed of 4000 rev/min. Both these cases show high proportions of diffusion combustion. The 1000 rev/min full load trace reflects both the lower maximum in-cylinder pressure admissible and the lower loads also possible at that speed. It also shows a shorter combustion where both

premixed and diffusion combustion are present. It is possible that high levels of PM are formed during the diffusion-combustion phase but that the residence time in the hot in-cylinder environment lead to high levels of PM oxidation, which explains the low smoke emissions recorded at key point F1.

4.5.4 Testing with modified injector location

Since the results at full load conditions represented such a step change in smoke emissions and the injector position relative to the piston bowl was suspected to be the major cause, a different injector-nozzle protrusion was tested. The injector was placed 0.6 mm deeper in the piston bowl by replacing the 1.6 mm washer situated at the injector sealing face by a 1.0 mm washer. The aim was for a larger portion of the fuel spray to penetrate into the bowl rather than over it, thereby increasing the utilisation of air. For similar full load settings, smoke emissions were all less and the differences with the 4-cylinder engine values were reduced and lay within 0.3 FSN as shown in Figure 4-10. Smoke emissions decreased from 0.88 to 0.24 FSN at 1000 rev/min, from 3.10 to 2.21 FSN at 2000 rev/min and from 3.36 to 2.91 FSN at 4000 rev/min. As already stated, the main reason for these decreases was thought to be a better utilisation of air in the combustion chamber. These tests highlighted the importance in combustion chamber design of the protrusion, and indirectly of the injector-nozzle cone angle, and also demonstrated the high sensitivity of the engine operating characteristics to this feature.

Investigations with this deeper protrusion were also conducted at some part load conditions and was also found to present soot emissions benefits. The impact of increasing the protrusion resulted in smoke or soot emissions values all below the 4-cylinder engine values. The main improvement was at key point P5 where smoke emissions went from 3.46 to 2.39 FSN, offering a close match with the 2.32 FSN value recorded on the 4-cylinder engine. The impact of the protrusion change on NO_x emissions was an increase of less than 5 % at key point P5. This reflects the better fuel-air interactions decreasing soot emissions but increasing the quality of the combustion, thereby leading to higher temperatures and associated NO_x emissions. The fuel consumption was unchanged.

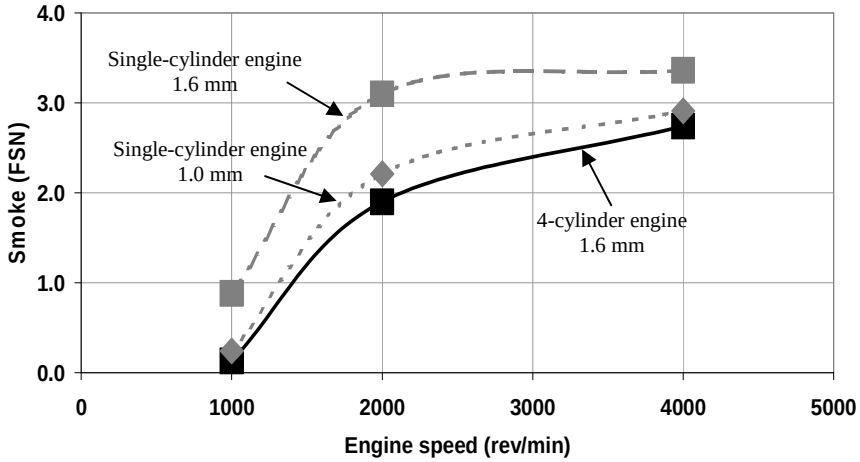

Figure 4-10: Impact of injector protrusion on smoke emissions at full load.

4.5.5 Discussion

This section presents an evaluation of the two sets of data and identifies and evaluates the most significant differences. HC emissions were generally higher for the single-cylinder engine than for the 4-cylinder engine. This increase seemed to be linked to the fact that the engine was running cooler than the 4-cylinder engine at all but the rated power condition. There were two main reasons for this. The coolant flow was set for the 4000 rev/min full load condition in order to limit the maximum temperature difference across the cylinder head. This flow was then fixed for all engine speeds whereas the cooling flow on the 4-cylinder engine would have decreased with the engine speed since the pump was engine driven. It is expected that excessive levels of cooling were present at lower engine speeds on the single-cylinder engine. The cooling flow was fixed rather than adding another variable to the investigations, which would have added to the complexity of the experiments. The other possible cause for the increase in HC emissions was that the general engine and exhaust-manifold temperatures were lower due to the larger proportion of heat losses with the single cylinder. The late oxidation of HC emissions would have been quenched in the cylinder and exhaust system. Some HC emissions readings from the emissions analyser were not shown in the tables since the different sampling point set-up led to high levels of HC emissions hang-up in the heated line, which caused a measurement offset. These values were therefore unusable for the engine-matching phase. However, since the subsequent test phases of the programme were likely to result in a hundredfold increase in HC emissions, as shown by Takeda et al. (1996), the offset in

HC emissions was considered negligible. Modifications were made to the sampling system after the single to 4-cylinder engine matching. An oven was inserted at the sampling point to maintain the exhaust-gas temperature above 190 °C in the sampling line thereby avoiding condensation of HC emissions.

A summary of the comparison between the part load key point results on the single and 4-cylinder engines is given in Figure 4-11 in terms of NO_x versus soot emissions. In general, the match achieved between engines exceeded expectations. As described, the key points P2 and P5 represented the worse matches for both NO_x and soot emissions. The discrepancies in NO_x emissions were small relative to the impact of load and at key point P5 were linked with the AFR being higher and the EGR rate being lower than on the 4-cylinder engine. However at key point P2, they were mainly due to a compromise between NO_x emissions and fuel consumption, as a more retarded injection timing would have improved the NO_x emissions match but worsened the fuel consumption agreement. The increased soot emissions at key point P5 seemed to be linked to the poor utilisation of air, however this was improved by optimising the injector-nozzle position relative to the piston bowl.

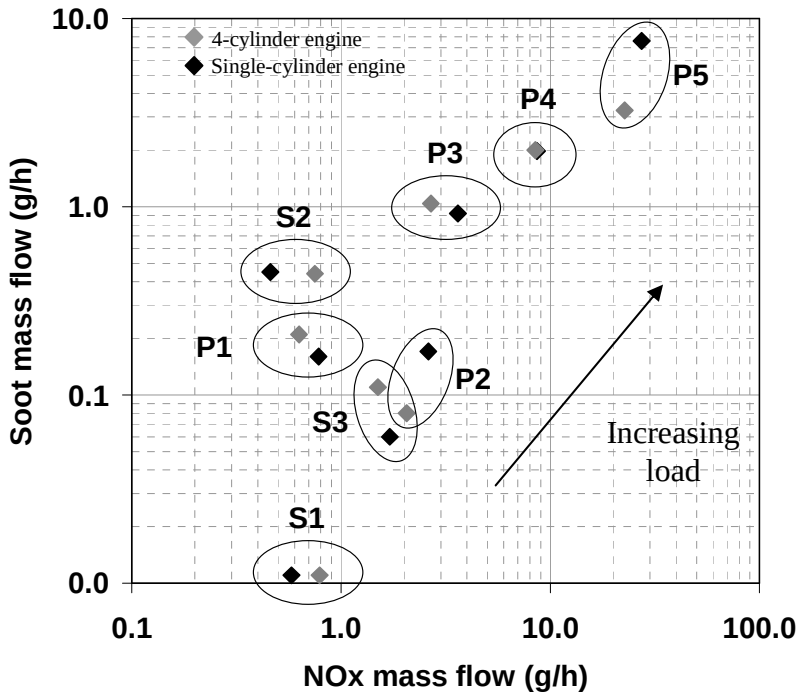

Figure 4-11: Part load NO_x and soot emissions comparison summary.

A summary of the comparison between the part load key point results on the single and 4-cylinder engines in terms of fuel consumption versus load is given in Figure 4-12. In general, the match achieved between engines was also good but not so surprising since fuel consumption was one of the parameters matched in most of the investigations. The single-cylinder engine load seemed to be consistently lower than on the 4-cylinder engine. Only key point P2 presented a large deviation. It is believed that the imprecision of the gross load measurement from the 4-cylinder engine may be a cause for this. Equally, the reference point selected was 1.2 °CA later than for the 4-cylinder engine, which is expected to increase the fuel consumption and explain the variation in fuel consumption.

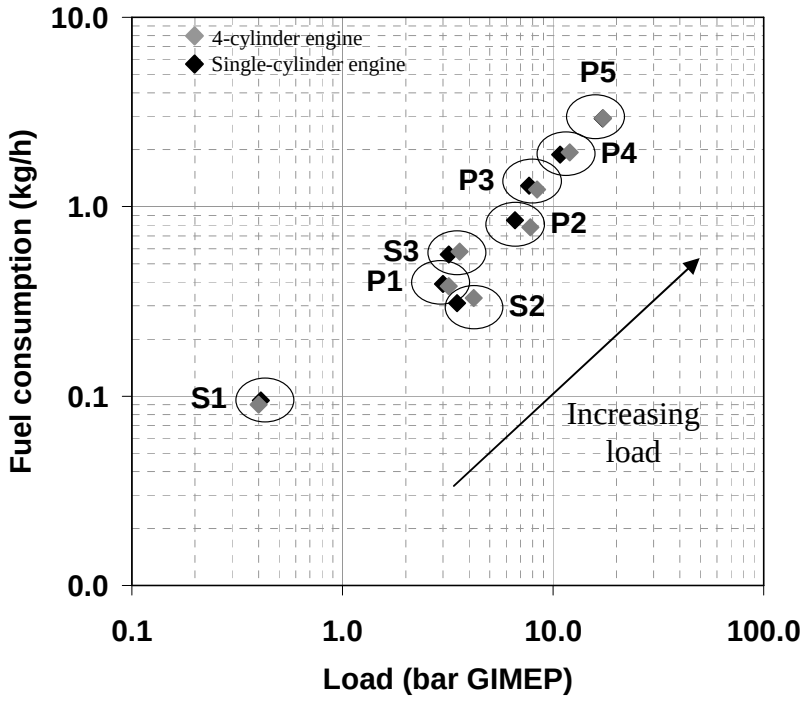

Figure 4-12: Part load fuel consumption and load comparison summary.

4.6 Conclusions

The engine matching exercise focused on the development of a single-cylinder engine to make it behave like its 4-cylinder version over a range of key operating points. The transfer of 4-cylinder engine Euro 5 operating conditions to the single-cylinder engine and its subsequent fine tuning have been described. Despite a few discrepancies observed in terms of smoke emissions, mostly resolved by changing the injector-

nozzle protrusion, transferability between engines has been demonstrated, which confirms the suitability of the single-cylinder engine for the future planned investigations in the research programme. The main conclusions from this chapter are:

- Representative blow-down pressure curves and pumping losses at 4000 rev/min full load and at the other key points could be achieved by the use of an orifice plate of 27 mm in diameter and specific backpressure valves settings. This yielded representative intake and exhaust events in the single-cylinder engine
- Despite representative intake and exhaust events, the gas dynamics were not identical due to the mismatch in charge-air, EGR and exhaust flows. Therefore a re-optimisation of the swirl throttle position was undertaken for the three primary key points using the swirl throttle
- Since the injection-system control was slightly different to that of the 4-cylinder engine, a re-optimisation of the main-injection timings was undertaken
- Reference values for NO_x, soot, smoke, HC, CO emissions, noise, gross load and fuel consumption were established as baselines for the evaluation of potential engine operating conditions on the Build #2 single-cylinder engine
- Links between NO_x emissions and the initial and maximum gradients of the instantaneous heat release have been suggested. At this stage, no links were found between NO_x emissions and the maximum instantaneous heat release
- Increased soot or smoke emissions compared with the 4-cylinder engine led to additional investigations, which highlighted that an increased injector-nozzle protrusion was beneficial in terms of air utilisation and resulted in closer soot or smoke emissions
- Improvements in the experimental set-up and processes were identified and implemented to facilitate the subsequent investigations and to improve data quality.

5 HARDWARE FOR FUTURE ENGINES

5.1 Introduction

Improvements in the design of engine hardware have the potential to be major contributors towards reducing emissions, as has been illustrated in Section 2.2.3. Reducing compression ratio has shown evidence of decreasing NO_x emissions as mentioned by Takeda et al. (1996), Gatellier and Walter (2002) and Araki et al. (2005), as it contributes to reduced combustion temperatures. It is an established fact that reductions in combustion temperature lead to reduced NO_x emissions, as illustrated in Figure 2-3 by Nakayama et al. (2003). The aim of the reduced compression ratio is to bring the in-cylinder temperatures, hence flame temperatures downwards during the combustion in Figure 2-3. This route to reduced NO_x emissions has not been implemented to date due to its associated negative effect on cold-start capability. In view of the developments in cold-start technology and with the appearance of variable compression ratio technology, generated either geometrically or thermodynamically, this route now appears to be a feasible hardware option for future engines. It offers a simple means of reducing NO_x emissions when compared with NO_x after-treatment systems. Furthermore, reducing the compression ratio also offers specific power output benefits at full load, since the maximum in-cylinder pressure reached for a given inlet-manifold pressure is reduced. This gives scope for more advanced injection timings, reducing smoke emissions and exhaust-manifold temperatures, and hence the possibility to inject more fuel before reaching the maximum exhaust-manifold temperature and smoke limits.

In order to exploit these possibilities modifications were made to the piston to reduce the compression ratio from 18.4 to 16.0:1. In addition to the compression ratio change, the inlet ports were modified in order to increase their flow capabilities. This effective increase in volumetric efficiency was accompanied by a need to reduce the minimum level of swirl of the cylinder head as was found necessary at full load. The increased volumetric efficiency of the cylinder head has two potential benefits: an increased air mass flow or a reduced inlet-manifold pressure requirement from the turbocharger for the same air mass flow. These modifications were implemented in the Build #2 engine, described in more detail in Section 3.5.

The main objective for the investigations reported in this chapter was to understand the impact of compression ratio on the fuel-air mixing and combustion characteristics at part load. For this part of the study, three primary key points were selected and injection-timing investigations conducted in Build #1 engine were repeated in Build #2 engine whilst maintaining all other operating conditions fixed. A comparison was made between the emissions and fuel consumption obtained on the two build versions. Analyses were also carried out that correlated the variations in emissions and fuel consumption with in-cylinder and combustion characteristics. Manipulated in-cylinder pressure data have been presented to summarise the impact of compression ratio as well as of injection timing on the combustion characteristics. A schematic summary of their impact on the fuel-air mixing and the combustion temperatures is also given. Although this approach does not offer a direct comparison between optimised operating conditions, it isolated the compression ratio effect and offered a detailed understanding of its impact. A second objective was to compare the effects of both compression ratio and volumetric efficiency on the in-cylinder and combustion characteristics at full load.

5.2 Analysis at part load

5.2.1 Comparison process

The investigations detailed in present chapter were all conducted using the 7 hole, 680 cc/min flow, 154 ° cone angle, 0.76 coefficient of discharge injector nozzle and a 1.6 mm protrusion washer. The compression ratio was reduced from 18.4 to 16.0:1 by increasing the piston-bowl volume from 22.0 to 26.3 cc. This was done by reducing the size of the centre-pip of the piston bowl without modifying the squish effect of the combustion chamber, as shown in Figure 3-7. It was therefore expected that the impact of the centre-pip would be negligible on emissions and fuel consumption at most conditions since it had little influence on the fuel-air interactions even at full load, where the fuel-air and piston-bowl interactions are essential for good air utilisation, as shown in a computational fluid dynamic result at full load in Figure 5-1. In the present investigations, the impact of the centre-pip would not be dissociable from the effects of the compression ratio.

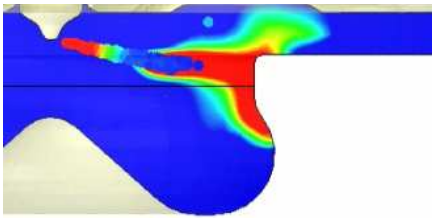

Figure 5-1: Key point F3 fuel spray interactions with piston bowl.

Key points P1, 1500 rev/min 3.0 bar GIMEP, P3, 2000 rev/min 7.7 and P4, 10.8 bar GIMEP were the primary key points chosen for these investigations as they represented key points ranging from light to high load conditions. Two preliminary remarks can be made concerning the approach. The first one concerns the pilot-injection operating conditions used at key points P1 and P3 to reduce noise. In order to make a realistic comparison between the engines, a re-optimisation of the pilot injection was conducted for the lower compression ratio Build #2 test points since Build #1 engine pilot-injection operating conditions were not transferable. It is believed that the reduced in-cylinder pressures and temperatures suppressed the combustion of the pilot injection. This increased the premixed-combustion phase and led to increased noise. Their re-optimisation consisted in reducing the separation and increasing the quantity, thereby preventing the pilot injection from over-leaning and ensuring its combustion before the main injection. Once the pilot injections redefined, their pulse duration and their separation from the main injection were fixed.

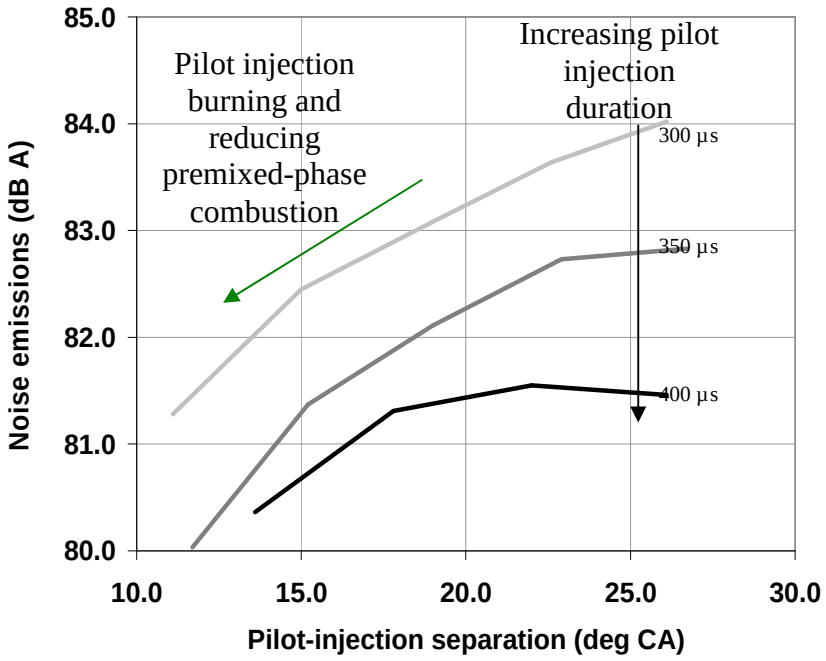

Figure 5-2: Impact of pilot-injection operating conditions on level of noise.

The second remark concerns the level of swirl. The swirl throttle position was kept fixed from one engine build to the other, despite it leading to reduced levels of swirl in Build #2 engine. This approach was chosen in an attempt to highlight the effect of the volumetric efficiency alone at part load, but in fact, little effect of improved volumetric efficiency was seen at these operating conditions where inlet-manifold pressures were not high enough. Volumetric efficiency will therefore not represent part of the analysis. A swirl response was carried out at key points P2 and P4 with all other operating conditions fixed to understand its impact on emissions and fuel consumption. NO_x and soot emissions are shown in Figure 5-3 and HC emissions and fuel consumption in Figure 5-4.

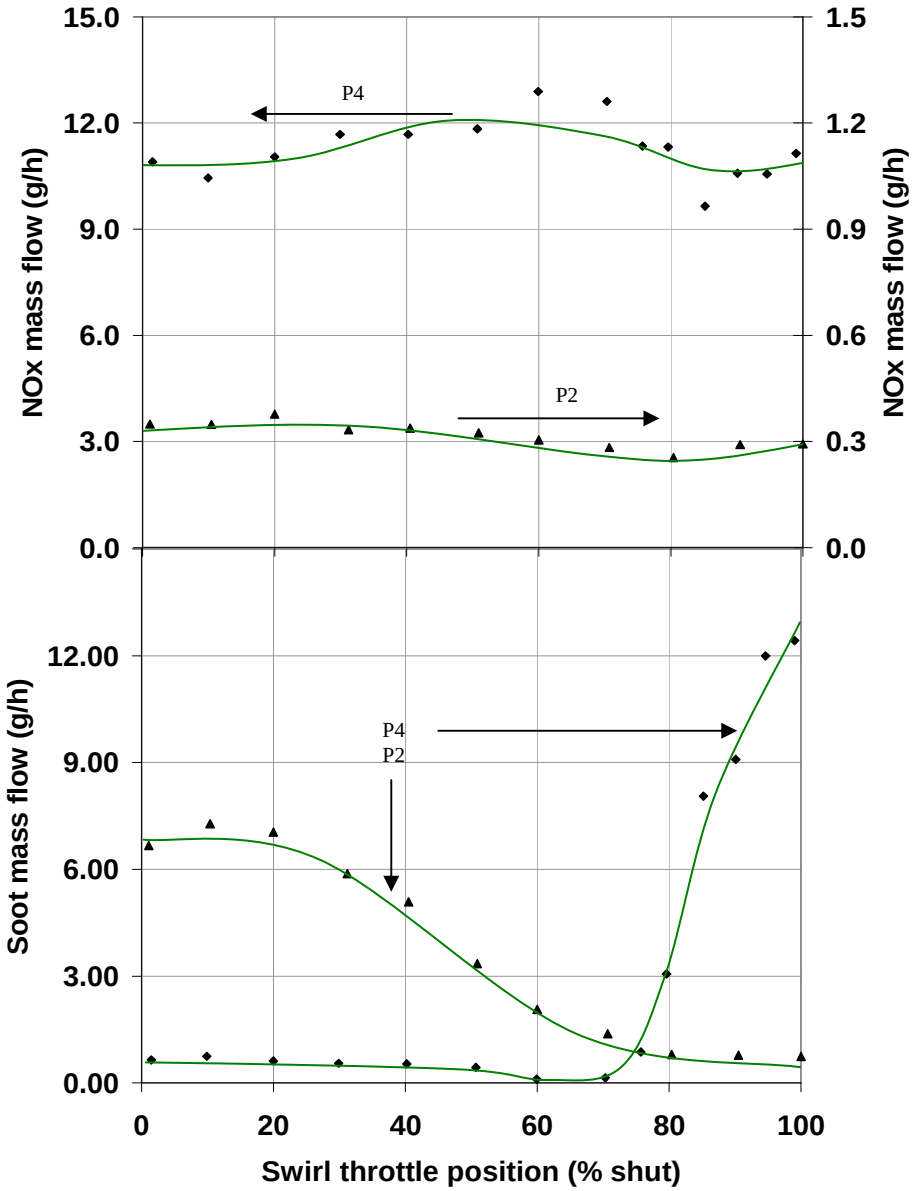

Figure 5-3: Swirl impact on NO_x and soot emissions in Build #2 engine.

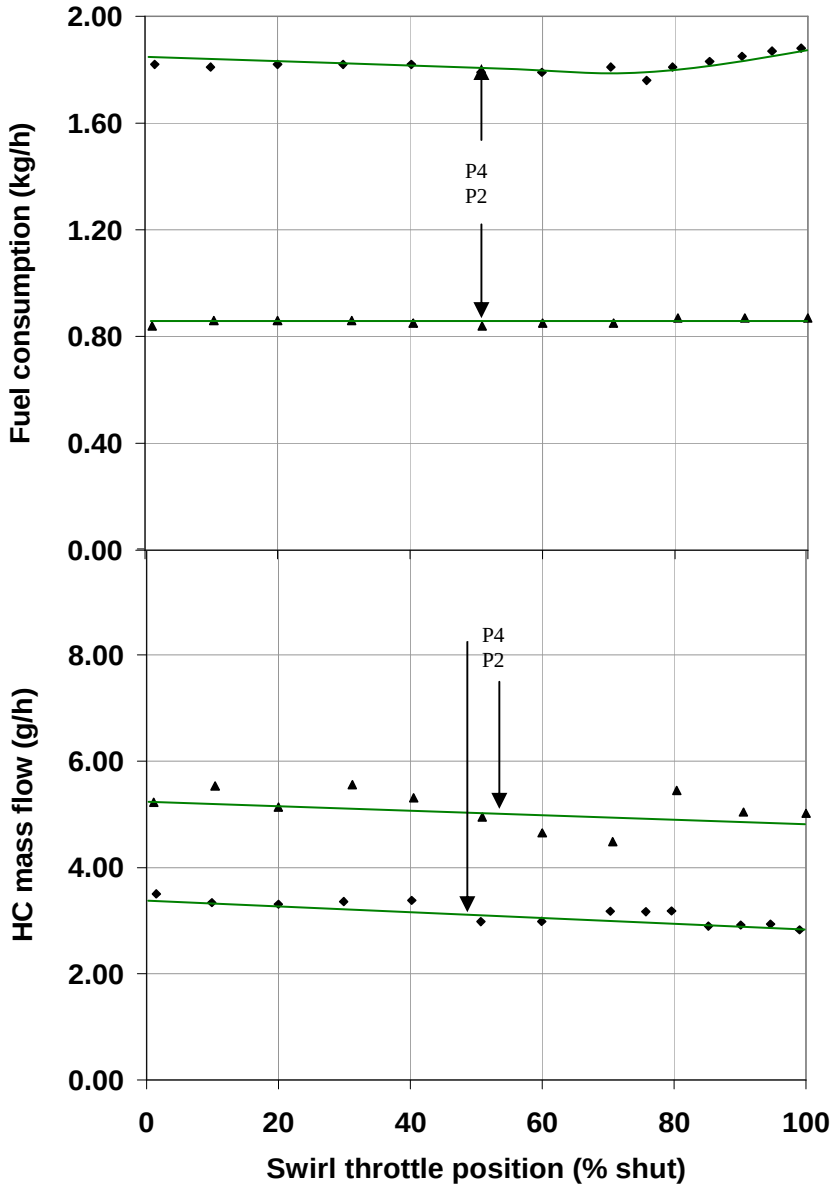

Figure 5-4: Swirl impact on HC emissions & fuel consumption in Build #2 engine.

The varying level of swirl had no significant effect on NO_x emissions nor did it affect fuel consumption, however, its increase did lead to slightly reduced HC emissions. The main consequence of operating with fixed swirl throttle positions was expected to be on soot emissions, as can be seen from the swirl responses in Figure 5-3. For lower and medium loads, represented by the key point P2, the more the swirl increased, the more soot emissions were reduced. This contrasted with the response obtained in Section 4.5.2 and is thought to be linked with the fact that this response was conducted at a higher EGR rate and hence longer auto-ignition delay. This minimised the diffusion combustion whilst the swirl increased the mixing. However, at the higher load, represented by key point P4, the increase in swirl had little effect up to a

certain threshold, after which a further increase led to higher soot emissions. It was believed that at high loads, where there was an important part of diffusion combustion around the fuel spray plumes, an initial increase in swirl had a minimal impact. This may be linked with the fact that swirl does not affect the liquid phase of the spray, as described by Browne et al. (1986). However, a further increase would lead to gaseous fuel plume-to-plume interactions, which result in a poorer mixing and a rapid rise in soot emissions. These results indicate that by fixing the swirl throttle position from Build #1 to Build #2 engines, hence reducing the level of swirl, soot emissions should increase at the same operating condition following the green arrows added in Figure 5-3.

Injection-timing responses conducted during the single to 4-cylinder-engine matching on Build #1 engine were repeated on Build #2 engine. Particular attention was given to match the Build #2 engine operating conditions with those of Build #1 at each key point in terms of AFR, EGR rate, injection pressure, inlet-manifold temperatures, swirl throttle position and backpressure valves settings. The only changes made were in terms of pilot-injection operating conditions redefined and the level of swirl altered as a consequence of the new cylinder head. Once the match was complete, injection-timing responses were conducted maintaining all the conditions fixed and adjusting only the main-injection quantity to achieve the load. These covered the injection-timing range investigated in Build #1 engine. The load used as target was the gross load since it was an accurate measurement on a single-cylinder engine and it enabled the investigations to focus on the compression and expansion strokes and to avoid complications with the pumping and friction losses. This is summarised in Figure 5-5, representing a schematic of the engine, similar to that presented in Chapter 4. The same colour scheme as earlier has been applied to the operating conditions. This was also applied to the hardware, as some of it has been changed for the present investigations. A summary of the values or ranges of the operating conditions and hardware is given in Table 5-1. The parameters investigated and shown in red are the injection timing and the compression ratio, varied by increasing the piston bowl volume.

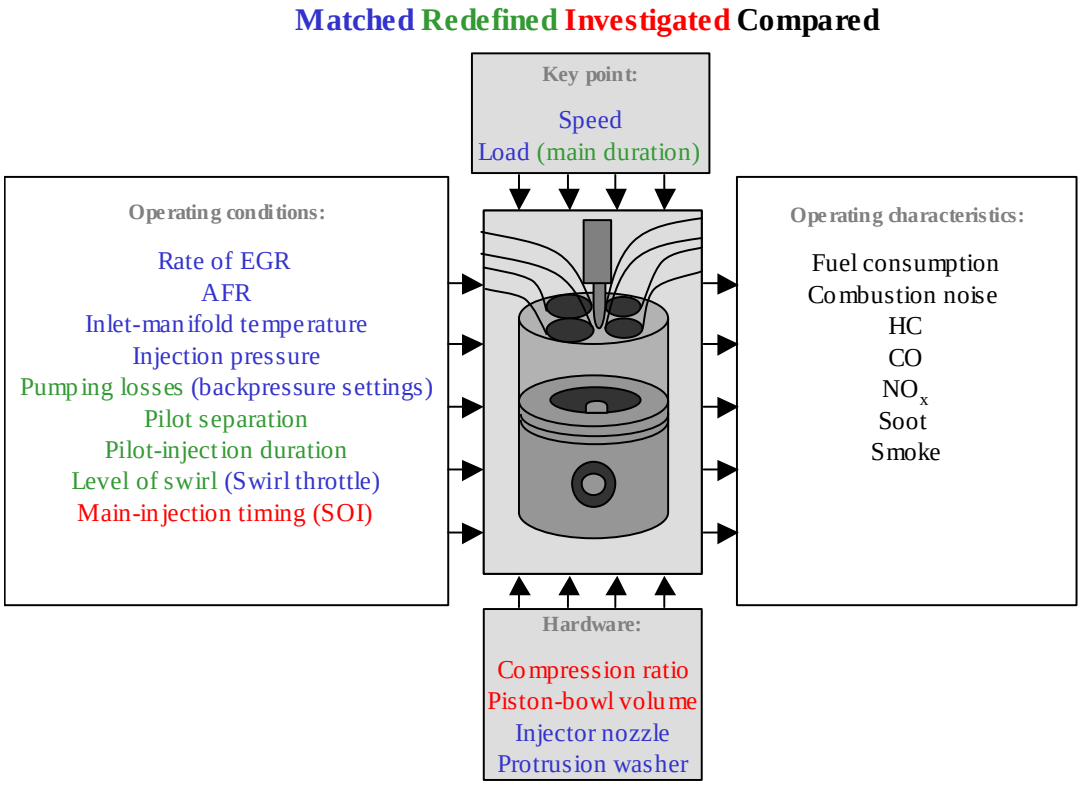

Figure 5-5: Operating conditions and hardware modified during investigations.

	Values or ranges investigated					
Chapter	4	5	4	5	4	5
Key point	P1		P3		P4	
Speed (rev/min)	1500		2000		2000	
Gross load (bar GIMEP)	3.0		7.7		10.8	
Compression ratio (-)	Chapter 4: 18.4:1 / Chapter 5: 16.0:1					
Piston-bowl volume (cc)	Chapter 4: 22.0 / Chapter 5: 26.3					
Injector nozzle	7-hole, 680 cc/min, 154 °, 0.76 coefficient of discharge					
Protrusion washer (mm)	1.6					
Main-injection quantity	Adjusted to maintain load					
Injection pressure (bar)	545		1070		1190	
Pilot-injection duration (µs)	300	350	210	250	N/A	N/A
Pilot separation (°CA)	26.0	19.0	33.0	16.0	N/A	N/A
SOI 2 (°CA ATDC)	-5.0 to 3.0		-4.0 to 2.0		-1.0 to 3.0	
Wet EGR rate (%)	45.4		31.3		21.3	
Dry AFR (-)	29.3:1		21.6:1		21.1:1	
Swirl throttle (% shut)	46		64		0	
Inlet temperature (°C)	88		68		58	
Backpressure valves settings	1: 24.0 half turns & 2:shut		1: 23.5 half turns & 2:shut		1: 23.0 half turns & 2:shut	

Table 5-1: Main operating conditions and hardware values or ranges investigated.

A comparison of the operating characteristics of the two engine builds was then undertaken and explanations for the impact of lower compression ratio were sought by analysing the in-cylinder and combustion characteristics. These analyses were based on the in-cylinder pressure data of the kind shown in the Figure 5-6. It represents a single-cycle in-cylinder pressure trace with its associated rate of pressure change, for identical operating conditions on both engine builds at key point P3. The main operating conditions held constant were the AFR of 21.6:1 and the EGR rate of 31.3 %. The fact that the level of fuelling was identical in both cases meant that the AFR match corresponded to a match in the trapped air mass. As this was achieved for identical inlet-manifold pressures in both engines and leads to the conclusion that the impact of the higher flow head was negligible at that load. An injection timing and pressure of -2 °CA ATDC and 1070 bar were used. The inlet-manifold temperature was controlled to 68 °C and the swirl throttle position was held constant at 64 % shut. The value of compression ratio is thus the only difference between the two cases.

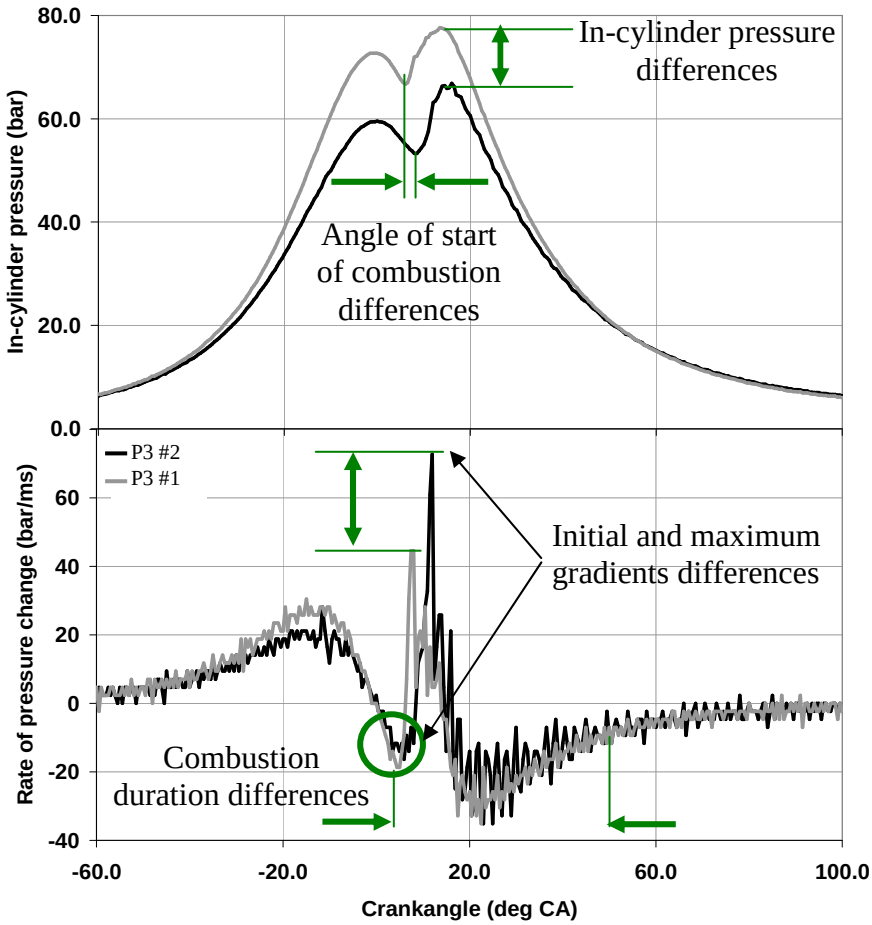

Figure 5-6: In-cylinder and combustion characteristics analysed for key point P3.

The main characteristics analysed were the in-cylinder pressure and temperature during the injection and at start of combustion, the angle of start of combustion and its duration, the rate of pressure change and its maximum value during the combustion.

5.2.2 Impact on NO_x emissions

Figure 5-7 shows the impact of compression ratio on NO_x emissions recorded at the three loads tested. As observed in Chapter 4, NO_x emissions decreased as the injection timing was retarded. NO_x emissions were all lower when the compression ratio was reduced from 18.4:1 to 16.0:1. The reductions were more pronounced at the higher load key points P3 and P4 than at key point P1. It is believed that the limited high-temperature, stoichiometric combustion at the light load key point P1 offered small potential benefit from the lower compression ratio. As the injection timing was retarded, the emissions differences between engine builds became negligibly small. This would suggest that the impact of the different in-cylinder pressure and temperature was reduced, as was already the case at key point P1. This highlights that NO_x emissions were mainly controlled by other parameters, expected to be AFR and EGR rate.

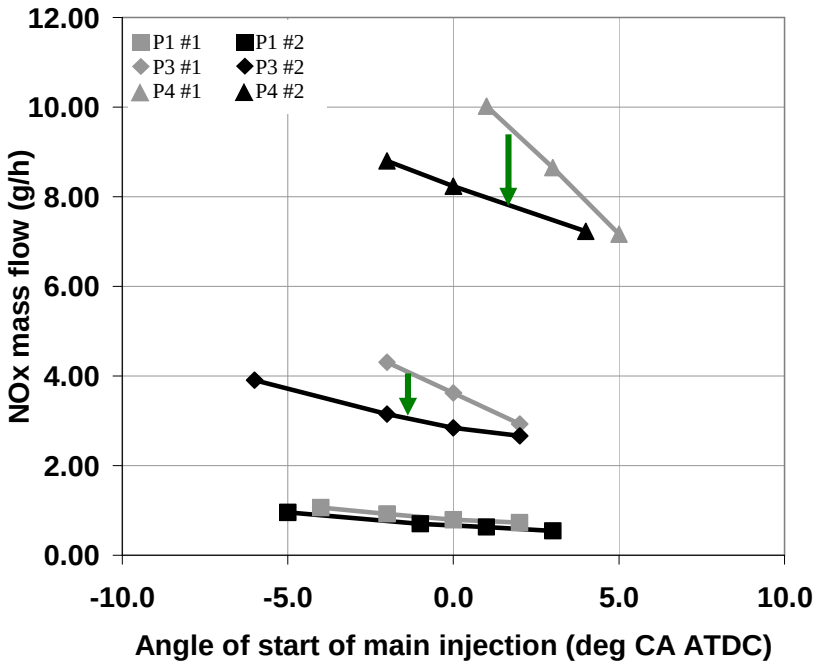

Figure 5-7: Impact of compression ratio on NO_x emissions.

As can be seen in Figure 5-6, the effect of reducing the compression ratio on the maximum rate of pressure change at key point P3 was similar to retarding injection timing as observed during an injection-timing response at key point P2 in Figure 4-7: the rate of pressure change reached a higher value in the case of the lower compression ratio engine, and yet, led to lower NO_x emissions. In this case, it illustrated that these emissions were not linked with the maximum rates of pressure change and indicated that the premixed combustion and its maximum rate of pressure change were not indicative of NO_x emissions. This corroborates conclusions by Heywood (b) (1988) that premixed-combustion represents a far smaller contributor of NO_x emissions compared to diffusion combustion. A closer inspection of the initial gradient in the rate of pressure change in Figure 5-6 revealed a lower gradient, indicative of a slower rate of combustion in the case of the lower compression ratio. However, after the initial phase, it is believed that an increased portion of premixed-fuel burning simultaneously compensated for the slower rate of combustion. This cumulative effect led to both a steeper gradient in the rate of pressure change and a higher maximum rate of pressure change at key point P3. The maximum rates of pressure change for the three key points tested can be seen in Figure 5-8 and confirm these observations for key points P3 and P4. This explanation is consistent with the high noise recorded with HCCI combustion. Usually, high noise or NO_x emissions are associated with high rates of pressure change, since these imply a rapid rate of combustion during premixed-combustion, leading to a high increase in the in-cylinder temperature, and hence a rapid rate of combustion during the diffusion-combustion phase, thereby leading to ideal NO_x forming conditions. However, it is thought that a high rate of pressure change, hence noise, with a highly, but not fully, premixed-charge combustion should be considered as an indication of both how fast a rate and how large the premixed-combustion is rather than a representation of NO_x emissions. At the light load key point P1, where there was fully-premixed-charge combustion, the slower rate of combustion of the same amount of fuel due to the lower compression ratio or retarded injection timing also led to a lower maximum rate of pressure change. The impact of reducing compression ratio on a fully-premixed-charge combustion reduces the rate of combustion, which is not compensated for by an increase in the premixed fuel quantity, and results in a slower combustion.

An additional comment can be made concerning the variations with injection timing at each key point. Key point P1 results are expected to be the most accurate since they were obtained for fully-premixed-charge combustions which were characterised by a smooth rate of pressure change profile. However, obtaining a maximum rate of pressure change during combustions where both premixed and diffusion combustion were present was more difficult. The pressure oscillations captured by the in-cylinder pressure transducer led to large variations in the recorded values. It is why the maximum rates of pressure change were manually derived from the actual pressure curves at key points P3 and P4 in Figure 5-8 and key point P4 results showing high deviations.

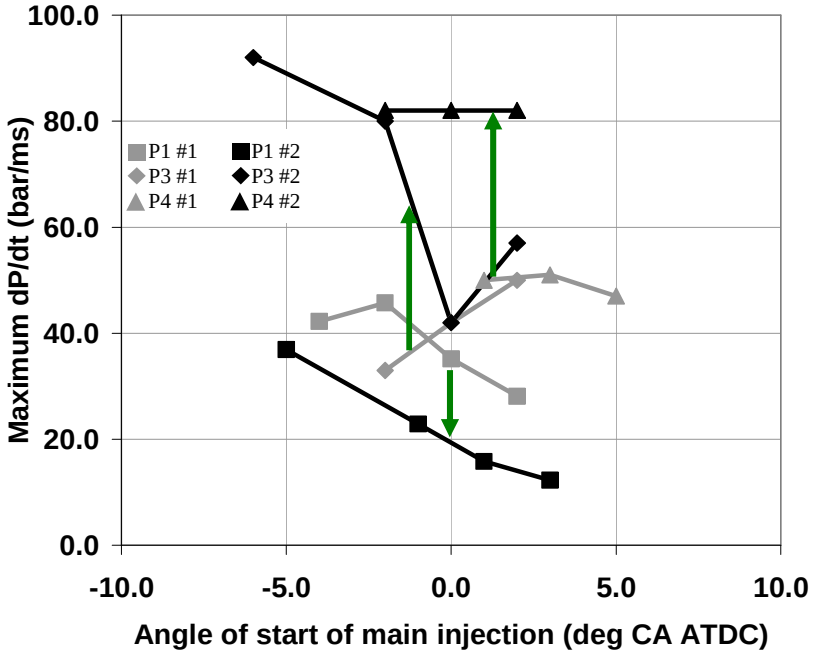

Figure 5-8: Impact of compression ratio on maximum rate of pressure change.

Also visible for key point P3 in Figure 5-6 is the impact of a reduction in the compression ratio on the in-cylinder pressure, reduced by 14 bar at TDC for similar inlet-manifold pressures. This obviously has a direct impact on the maximum temperature reached before combustion and therefore on those reached during the combustion. The temperatures were calculated using the perfect gas law and polytropic coefficients derived from each set of high-speed data. The in-cylinder pressures and temperatures reached at the moment of auto-ignition as a function of the injection timing are shown in Figure 5-9 for the three part load key points and two compression ratios. The temperatures were reduced from 260 to 230 °C at key point

P1 and from 175 to 150 °C at key point P4 in Build #2 engine. This did not represent a large reduction relative to the peak flame temperatures but it would act in two ways. Firstly, it would increase the mixing time by delaying the auto-ignition, which reduces the starting temperature for the combustion and, secondly, would reduce the rate of combustion, as the fuel-air mixing would reduce the portion of stoichiometric fuel-air mixture.

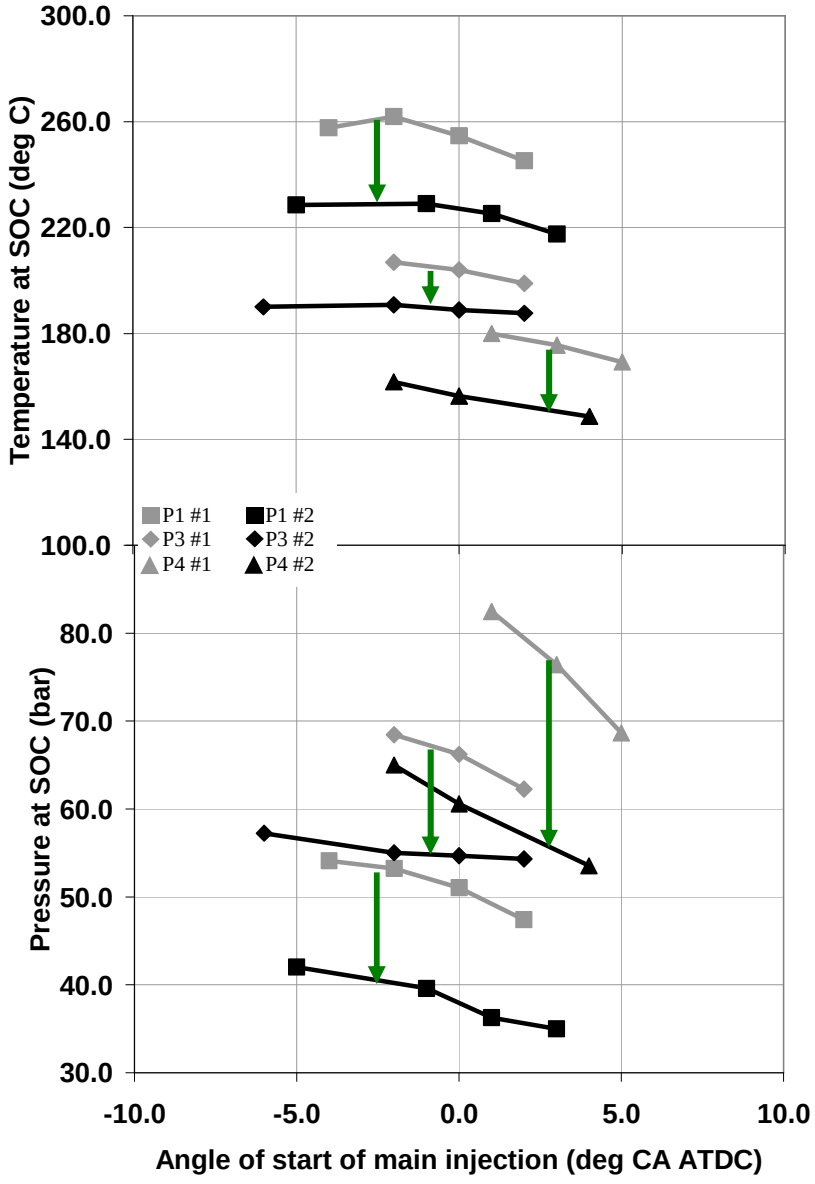

Figure 5-9: Impact of compression ratio on in-cylinder pressure and temperature.

An observation was made earlier on the diminishing impact of the compression ratio on NO_x emissions as the injection timing was retarded at the two higher loads. The fact that NO_x emissions converged at the most retarded injection timings in Figure

5-7, but that the in-cylinder pressures and temperatures did not, indicated that these emissions were not solely dependent on pressure or temperature. This contradicts the generally accepted strong link between temperatures at the start of combustion during the combustion and NO_x emissions. This is believed to be linked with the nature of the combustion. At the light load key point P1, an examination of the rates of pressure change showed that the combustion resembled a fully-premixed-charge combustion for both engine builds and at all injection timings. This led to very similar NO_x emissions in both cases, which were therefore less sensitive to in-cylinder pressure or temperature. On the other hand, an observation of the rates of pressure change at key points P3 and P4 revealed a change in the combustion type during the injection-timing response. It progressed from combined premixed and diffusion combustion at the most advanced injection timings to largely premixed-charge combustions at the more retarded injection timings. The fact that NO_x emissions converged as diffusion combustion reduced consolidated Heywood (b) (1988) conclusions that NO_x emissions formed during diffusion combustion of a close-to-stoichiometric mixture are very sensitive to in-cylinder pressures and temperatures. These results imply that NO_x emissions formed during premixed combustion are less affected by in-cylinder pressure or temperature and highlight the existence of the third factor, the combination of AFR and EGR rate or local oxygen concentration, which seems to become dominant below a certain temperature threshold or during fully-premixed-charge combustions.

The effect of reducing the compression ratio on the rate of pressure change was similar to that of retarding the injection timing. Both these measures retarded the start of combustion for similar injection timings and operating conditions. This led to improved mixing, reduced in-cylinder temperatures, and therefore reduced high-temperature, close-to-stoichiometric diffusion combustion.

5.2.3 Impact on soot emissions

The impact of the compression ratio on soot emissions is displayed in Figure 5-10 in terms of smoke emissions. It shows the variation at the three loads tested with the two compression ratios and was chosen instead of soot emissions to relate the results

directly with the smoke meter measurement accuracy of +/- 0.2 FSN. The impact of the compression ratio was not as pronounced as with NO_x emissions, but its reduction did lead to lower soot emissions within the measurement accuracy of the smoke meter. The Build #2 engine emissions results behave similarly to the emissions in the Build #1 engine at each load. However, since these results were obtained with reduced levels of swirl, which would tend to increase soot emissions (based on Figure 5-3) any reductions gain in significance.

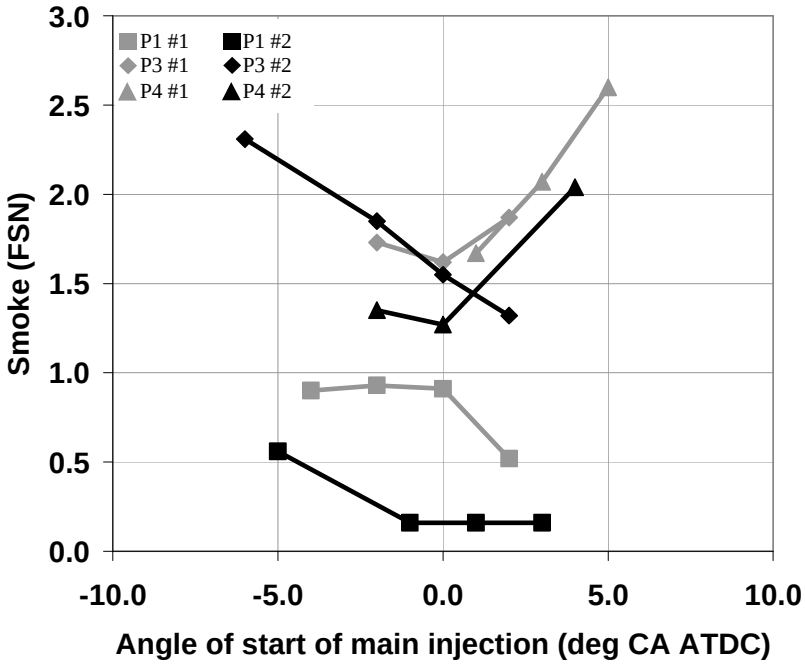

Figure 5-10: Impact of compression ratio on smoke emissions.

The compression ratio showed a small effect at the higher load key points P3 and P4, where the largest difference of 0.5 FSN was recorded at key point P3 when injecting at 2 °CA ATDC. The main effect was seen at the light load key point P1 where smoke emissions were almost halved in Build #2 engine compared with Build #1 engine. It is believed that PM was formed during the combustion in Build #1 engine but that in-cylinder temperatures were too low to promote its post-combustion oxidation. In the case of Build #2 engine, it is believed that the increased mixing associated with the lower compression ratio suppressed PM formation, eliminating the need for high in-cylinder temperatures for the oxidation process.

Despite soot emissions resulting from complex phenomena, such as fuel-air and piston-bowl interactions, in-cylinder and combustion pressures and temperatures, some explanations can be found for these results. The lower in-cylinder pressures at start of injection, as can be seen in Figure 5-11 for the three part load conditions, and the associated lower temperatures at start of injection in Build #2 engine are believed to contribute to the emissions differences.

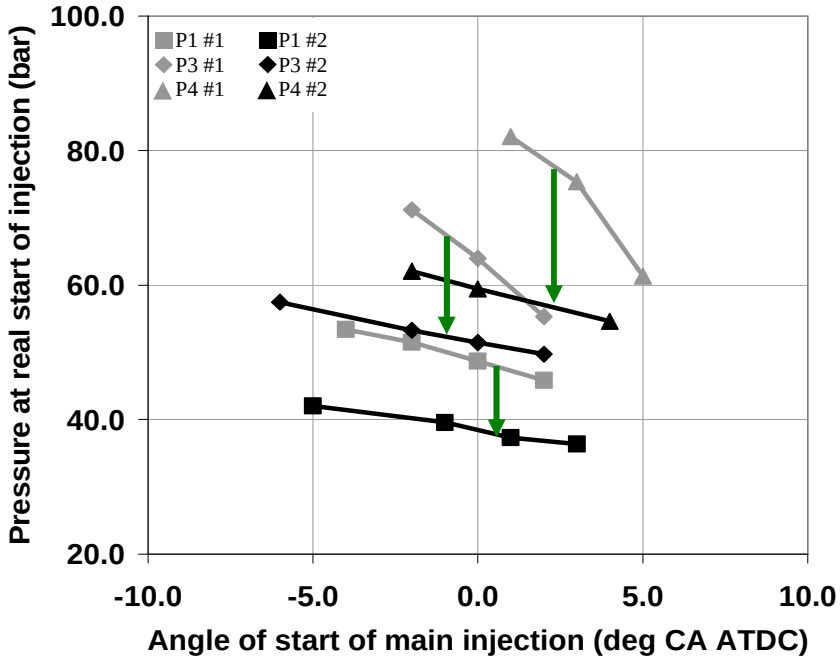

Figure 5-11: Impact of compression ratio on pressure at start of injection.

The lower in-cylinder pressure environment allows the fuel spray to penetrate further into the combustion chamber, which improves the air utilisation. The lower pressures and temperatures also lead to increased auto-ignition delays, as shown by the angles of start of combustion obtained during the injection-timing responses at key points P1, P3 and P4 in Figure 5-12. For comparable injection timings, the combustion started generally from 2 to 4 °CA later. These increased auto-ignition delays were in line with spray-rig observations made by Crua (2002). The increased delay resulted in longer mixing times and hence larger premixed-combustion phases and less diffusion combustion. The impact of the lower pressure and increased auto-ignition delay are cumulative, since the delay also allowed more time for the fuel to penetrate still further. In parallel with these explanations, it seems soot emissions result from a balance between high combustion temperatures during diffusion combustion, which promote soot oxidation, and limited diffusion combustion, avoiding soot formation. It

is useful to note at this stage that soot emissions increased as NO_x emissions decreased when the injection timing was retarded.

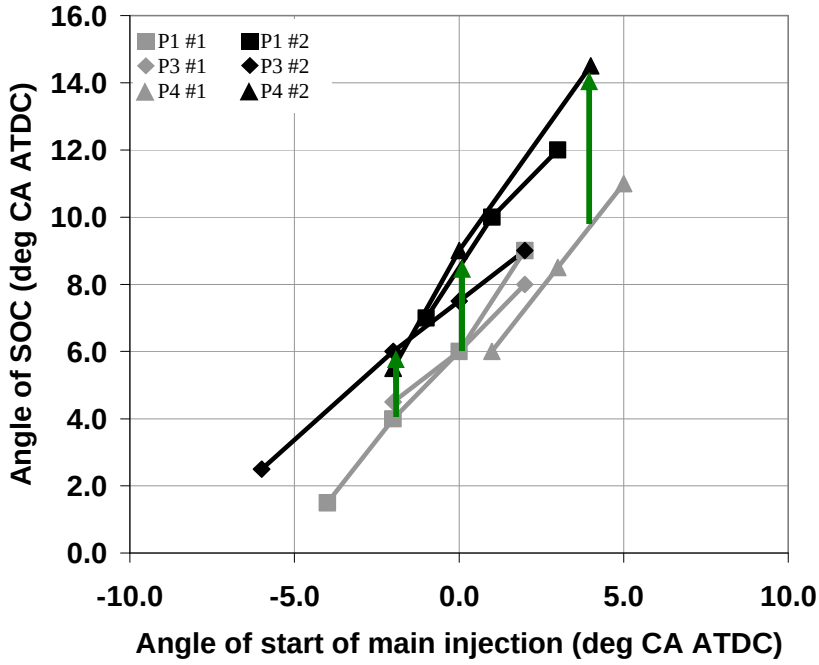

Figure 5-12: Impact of compression ratio on auto-ignition delay.

5.2.4 Impact on fuel consumption

Compression ratio did not seem to affect fuel consumption very much, as seen in Figure 5-13, which shows the fuel consumption during injection-timing responses at the three loads tested in both engine builds. The difference between engine builds was close to the measurement accuracy of +/- 1.0 % and may therefore be considered negligible except at key point P4, where a clear increase in fuel consumption is seen. Since the tests were carried out at fixed gross indicated load, the fuel consumption was a measure of the fuel conversion efficiency and concealed any differences in friction. Fuel consumption increased as expected as the injection timing was retarded to maintain the load constant. One of the justifications for reducing compression ratio was that the combustion efficiency would fall more slowly than the friction, as suggested by Taylor (1984), thereby increasing overall engine efficiency. It suggests the possibility of reducing NO_x emissions whilst maintaining similar fuel consumption or of maintaining similar NO_x emissions for an improved fuel consumption by advancing the injection timing.

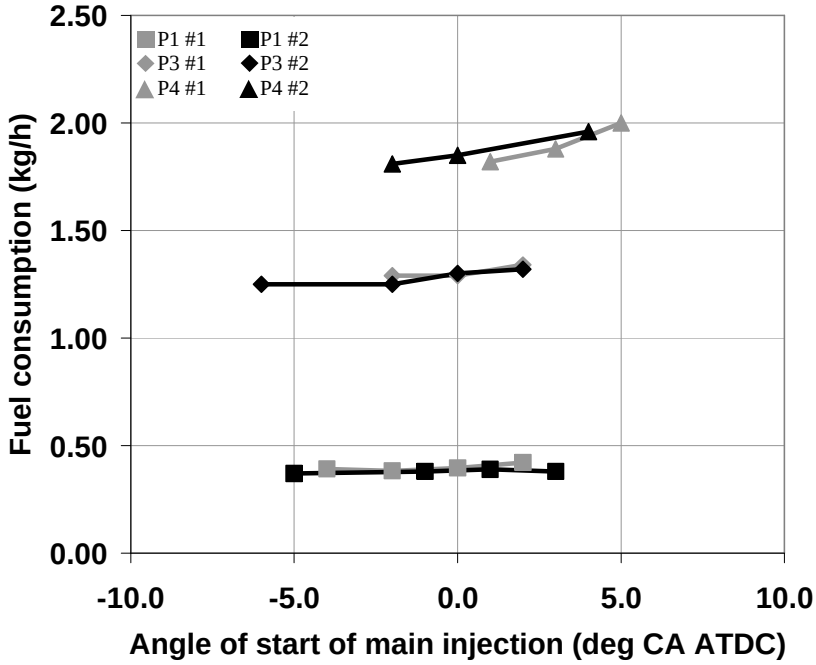

Figure 5-13: Impact of compression ratio on fuel consumption.

As can be deduced from the in-cylinder pressure traces at key point P3 in Figure 5-6, the combustion was later with Build #2 engine for an identical injection timing. However, results in Figure 5-13 indicate that the retarded combustion obtained with Build #2 engine resulted in a similar fuel consumption. It is believed that a faster global burn compensates for the later start of combustion and reduced initial rate of combustion. This can be illustrated for the three part load conditions tested, by examining the angle of 50 % burn, Figure 5-15, and the time to 50 % fuel burn derived from the angle of 50 % burn and the angle of start of combustion, Figure 5-14. The angles of 50 % burn were all more than 1 °CA later in the lower compression ratio case, which was equivalent to retarding the injection timing by the same angle. However, the time required to burn the first 50 % of fuel was systematically shorter in the lower compression ratio engine, which suggests compensation for the retarded angle of 50 % burn. At the higher load key point P4, where the fuel consumption clearly increased with the Build #2 engine, despite the time to 50 % burn being much shorter, this did not translate into a combustion efficiency increase. It is expected that the phasing of the combustion relative to TDC is a greater factor in fuel consumption than the rapidity of the combustion of the first 50 % of the fuel, especially at the higher loads. Statements concerning the combustion duration can not be made because of the lack of precision in determining the angles of end of combustion. However, an examination of the rate of pressure change traces

obtained during the different responses suggested the combustion duration decreased at high loads and increased at light loads.

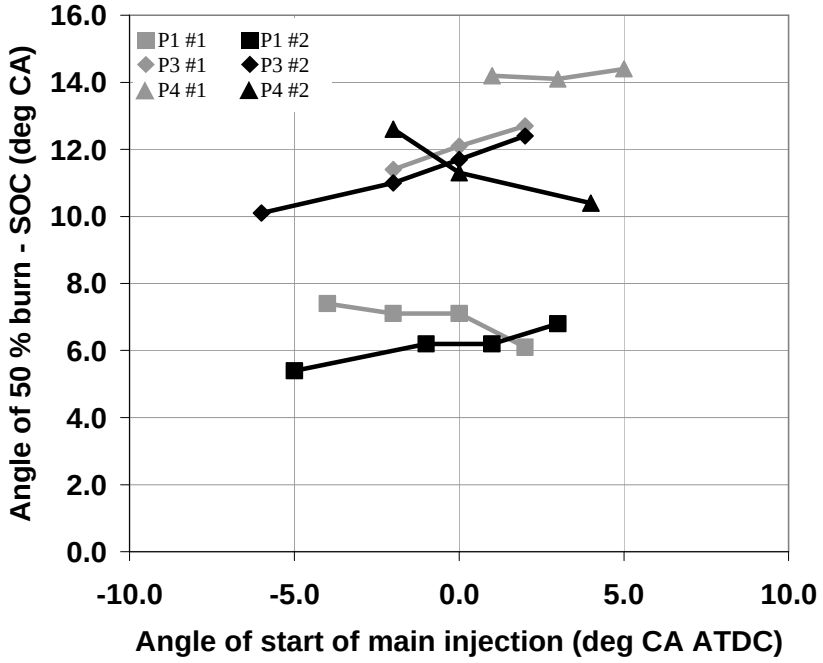

Figure 5-14: Impact of compression ratio on burn duration.

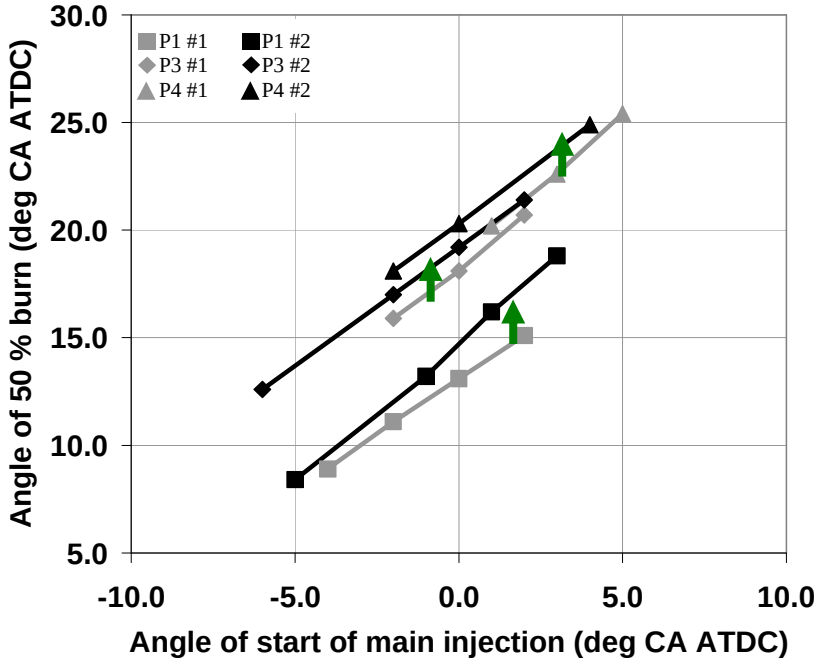

Figure 5-15: Impact of compression ratio on combustion phasing relative to TDC.

5.2.5 Impact on HC and CO emissions

The impact of the change of compression ratio on HC emissions is shown in Figure 5-16, where the results for each of the three loads are presented for both compression ratios. The largest increase was observed at the lowest load condition key point P1 and the effect of compression ratio became less pronounced as load increased.

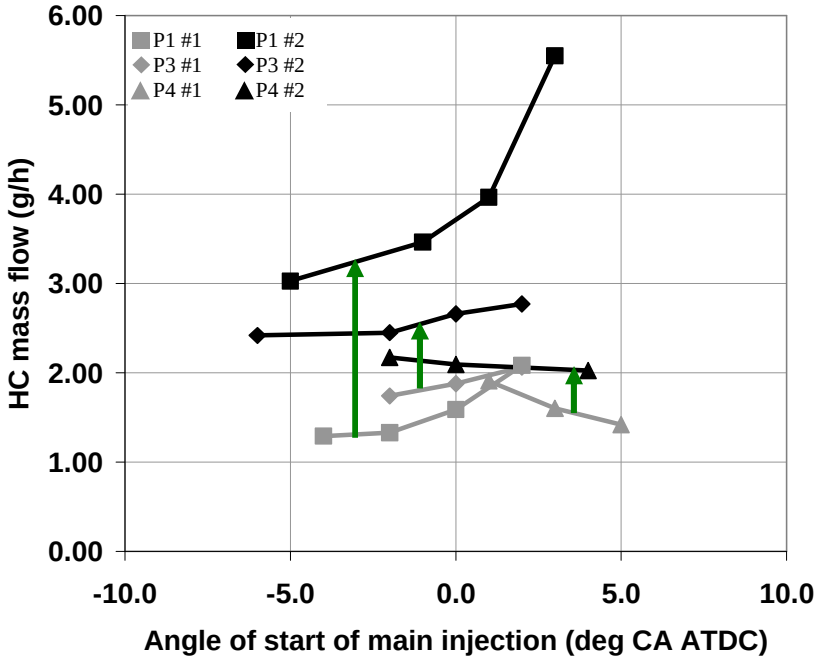

Figure 5-16: Impact of compression ratio on HC emissions.

It is believed that the conditions for HC formation are more prevalent at light loads with lower in-cylinder pressures and temperatures leading to over-leaning and quenching of the flame and thus to HC emissions. The same causes behind low soot emissions with the lower compression ratio engine are behind the increase in HC emissions: the reduced pressure at the start of injection and the longer penetration time allowed by the increased auto-ignition delay increase the penetration of the fuel spray into the chamber. This leads to excessive fuel-air dilution from increased mixing at the boundary of the mixture. In addition, the increased penetration of the fuel spray is more likely to reach the colder cylinder walls, as in gasoline applications, which provides ideal conditions for flame quenching and incomplete combustion. It was found that CO emissions varied similarly to HC emissions. The findings related to HC emissions are therefore also considered valid for CO emissions. The extreme case of fully-premixed-charge combustion could reach HC and CO emissions as high

as those seen in gasoline engines. It is accepted that the oxidation of these emissions could be dealt with by after-treatment. However, the reduced combustion temperatures and hence engine-out temperatures would lead to concern for the after-treatment system efficiency since it is designed to operate at elevated temperatures.

5.3 Summary of impact of compression ratio and injection timing

For any operating condition the pressure-time history over the relevant part of the cycle can be manipulated to yield an indication of the variation of instantaneous heat release with time. This is done by subtracting the element of pressure due to motoring and differentiating the resultant curve. This result is a rate of pressure change comparable with the instantaneous heat release but simpler to obtain. This procedure has been applied to the data from all three key points considered in this chapter and schematics of the results are displayed in Table 5-2. The results shown are valid whether reducing compression ratio or retarding the injection timing as it is suggested that both measures affect the combustion behaviour in the same way.

There are two main types of behaviour identified from the present work, which are dependent on the initial nature of the combustion, whether it is initially a combined premixed and diffusion combustion or a fully-premixed-charge combustion. The first is for the higher loads such as key point P4, where the impact of retarding the injection timing or reducing the compression ratio increases the auto-ignition delay and hence the premixed-combustion phase whilst reducing diffusion combustion. An observation made from the rate of pressure change traces was that the reducing portion of diffusion combustion decreases the combustion duration. The increase in fuel burned during premixed-combustion leads to an apparent higher rate of combustion, visible by the steeper gradient of the variation and a higher peak in the maximum rate of pressure variation. It is suggested that the steeper gradient in the rate of pressure change is an effect of the increased amount of fuel available for the premixed combustion and but that the visibly slower rate of pressure change during the initial phase of the combustion confirms the reduced rate of combustion. The second behaviour identified is for the lower loads such as key point P1, where retarding the injection timing or reducing the compression ratio affects an already

fully-premixed-charge combustion. The rate of combustion decreases as in the case of the higher load, which results in a slower combustion. The gradient of the variation and its peak are both reduced and the end of the combustion occurs later. At key point P3, a combination of both types of behaviour was observed during an injection-timing response as the combustion developed from combined premixed and diffusion combustion to a fully-premixed-charge combustion. The profile of the traces of rate of pressure change during this is depicted at the top of Figure 5-17.

Key point	Impact of reducing compression ratio or retarding injection timing	Summary	Observations
High load P4	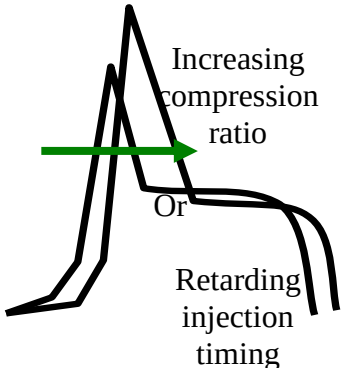	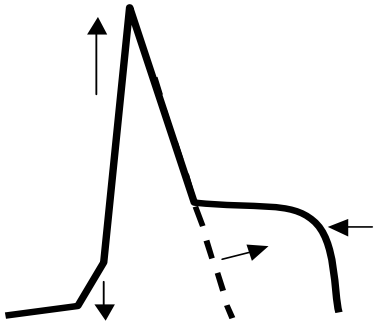	Slower initial rise Steeper gradient Higher peak Later 50 % burn Shorter 50-0 % burn Shorter combustion duration
Light load P1	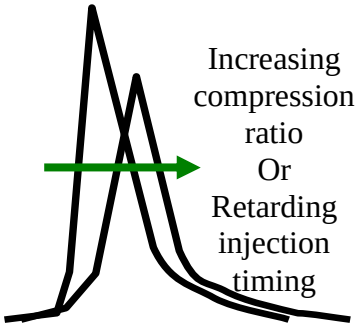	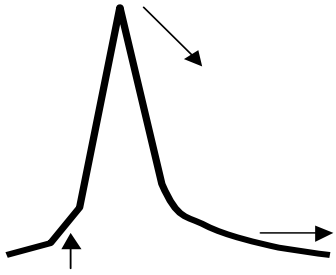	Slower initial rise Lower gradient Lower peak Later 50 % burn Longer 50-0 % burn Longer combustion duration

Table 5-2: Compression ratio & injection timing impact on rate of pressure change.

A schematic summary of the impact on the combustion processes of reducing the in-cylinder pressures and temperatures during the injection, either via compression ratio or injection-timing change is given in Figure 5-17. The auto-ignition is delayed in both cases which increases fuel-spray penetration and gives opportunity for increased fuel-air interactions. The combustion changes from combined premixed and diffusion

combustion to a fully-premixed-charge combustion as compression ratio is reduced or injection timing is retarded. The disappearance of diffusion combustion leads to reductions in the associated NO_x emissions, since it is a close-to-stoichiometric, high-temperature environment favourable to NO_x formation. Once the diffusion combustion fuel has been converted to premixed-combustion fuel, the premixed-combustion will be characterised by higher levels of instantaneous heat release or rates of pressure change. These will increase the in-cylinder temperatures, however, the fact that the mixture has moved further away from stoichiometry avoids high NO_x formation. Further reductions in compression ratio or retarding of the injection timing will result in clear reductions in the rates of pressure change, hence in combustion rates, which will result from the leaning out of the mixture. Further NO_x emissions reductions would be associated with undesirable increases in HC and CO emissions.

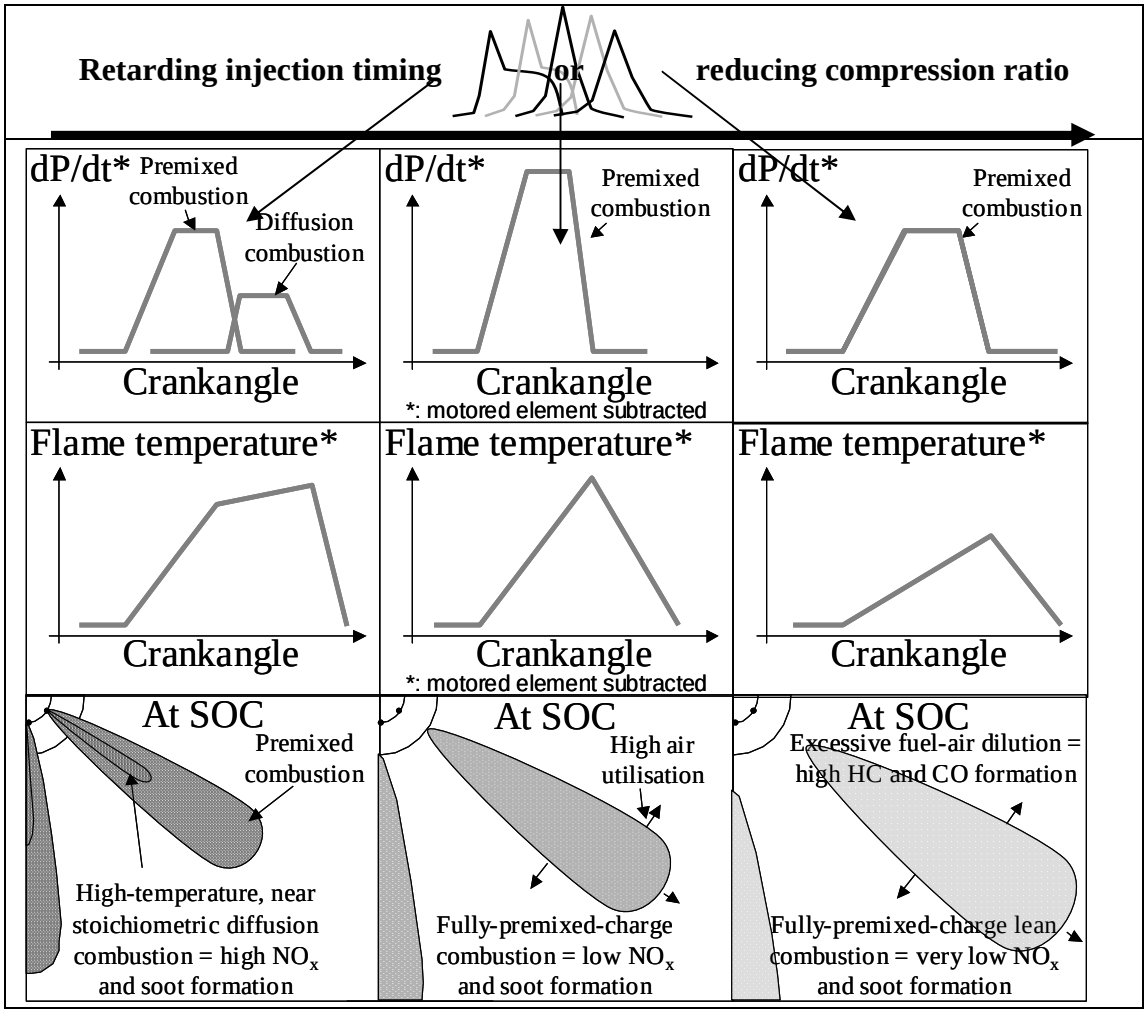

Figure 5-17: Summary of the impact on mixing and combustion characteristics.

5.4 Analysis at full load

5.4.1 Comparison process

As well as the compression ratio reduction for Build #2 engine, the inlet ports were also modified to increase the volumetric efficiency of the cylinder head. This had the effect of limiting the notional turbocharger requirements or increasing the EGR rate or AFR of the engine for the same inlet-manifold pressure. The effect of changing compression ratio was expected to be seen across the speed and load range, whereas the increased volumetric efficiency was expected to have its main influence at higher load where the inlet-manifold pressures required were highest. The 4000 rev/min full load key point F3 was therefore used to investigate the combined impact of lower compression ratio and increased volumetric efficiency, as both measures would have a visible impact. A similar approach as in the previous section was used to obtain Build #2 results for these investigations, therefore the relevant operating conditions and characteristics shown in Figure 5-5 remain valid. Table 5-3 gives a summary of the values or ranges of the operating conditions and hardware used.

Analogous in-cylinder pressures to those obtained during the single to 4-cylinder engine matching on Build #1 engine were targeted on Build #2 engine during the injection-timing response in order to fully exploit the potential of reduced compression ratios at full load as described in Section 2.2.3. Particular attention was given to matching AFR, injection pressure, inlet-manifold temperature, swirl throttle position and backpressure valves settings and maintaining them steady during the response. Both the load and the level of fuelling obtained during the Build #2 engine testing phase were a few percent higher than those from the Build #1 engine testing. However, since both have increased, the specific fuel consumption calculated using the gross load was closely comparable to the Build #1 engine test results, which made the comparison of the results valid. A comparison of the operating characteristics of the two engine builds was then undertaken and explanations for the combined impact of lower compression ratio and higher volumetric efficiency were sought by analysing the in-cylinder and combustion characteristics.

	Values or ranges investigated	
Chapter	4	5
Key point	F3	
Speed (rev/min)	4000	
Gross load (bar GIMEP)	17.1	
Compression ratio (-)	18.4:1	16.0:1
Piston-bowl volume (cc)	22.0	26.3
Injector nozzle	7-hole, 680 cc/min, 154 °, 0.76 coefficient of discharge	
Protrusion washer (mm)	1.6	
Main-injection quantity	Adjusted to maintain load	
Injection pressure (bar)	1567	
Pilot-injection duration (µs)	N/A	
Pilot separation (°CA)	N/A	
SOI 2 (°CA ATDC)	-15.0 to -19.0	-19.0 to -26.0
Wet EGR rate (%)	0.0	
Dry AFR (-)	20.1:1	
Swirl throttle (% shut)	0	
Inlet temperature (°C)	57	
Backpressure valves settings	1: open & 2: 20.0 half turns shut	

Table 5-3: Main operating conditions and hardware values or ranges investigated.

5.4.2 Impact of higher volumetric efficiency

The effect of the increase in volumetric efficiency can be seen in Figure 5-18 where the levels of inlet-manifold pressures required to achieve the same AFR are shown. The figure clearly shows the reduced inlet-manifold pressure requirements with the higher volumetric-efficiency cylinder head. This is all the more persuasive as the tests were carried out at a fixed AFR of 20.1:1 (+/- 0.1) but at a higher load in the case of the lower compression ratio engine. Higher fuelling at constant AFR implied a need for more air, however, as a result of the increased volumetric efficiency of the engine, this could be met without increasing the inlet-manifold pressure. This re-emphasised that the improved flow characteristics of the cylinder head enabled at least equivalent trapped air mass in the cylinder for equivalent or lower levels of inlet-manifold pressure.

The higher volumetric efficiency of the cylinder head offers potential reserves in inlet-manifold pressures, which can be used in several ways. They allow the load to be increased, as in the present case, whilst maintaining a similar AFR, thereby limiting the increase in smoke emissions at the higher loads. Alternatively, the engine can be operated at the same load condition with a higher AFR, hence reducing smoke emissions, which was the reason behind the AFR increase tested in Section 4.5.3. The engine can be operated at the same part load condition at a higher EGR rate whilst maintaining the AFR, hence reducing NO_x emissions. Finally, the turbocharger size can be decreased in order to improve the transient response of the engine due to the smaller inertia of the turbine.

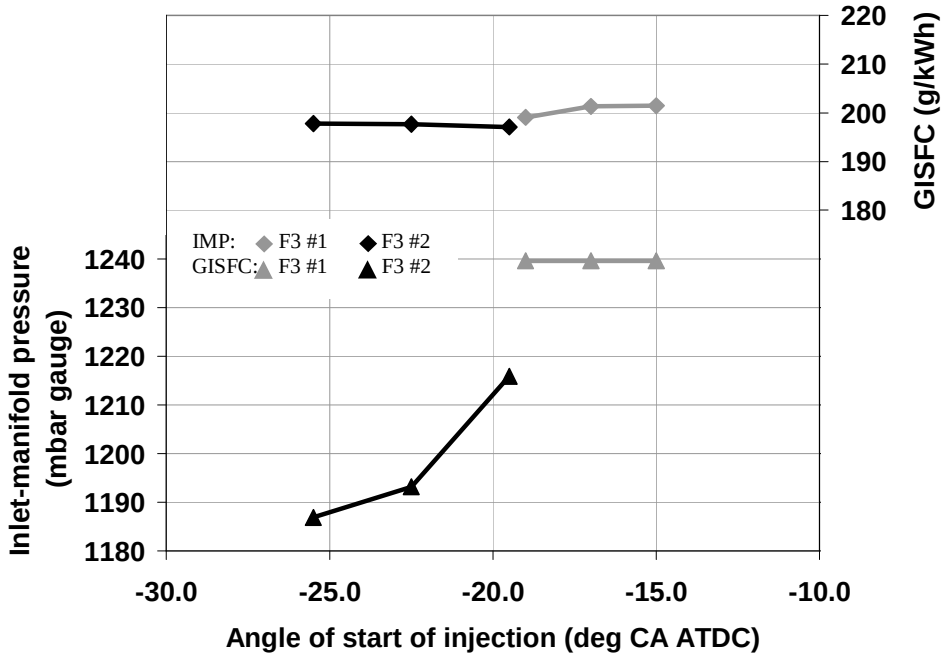

Figure 5-18: Impact of volumetric efficiency on inlet-manifold pressure.

5.4.3 Impact of compression ratio

The analysis of the effect of compression ratio at full load is focused on performance and on smoke emissions. With a lower compression ratio, the performance can be increased since the injection timing can be advanced a few degrees crankangle before reaching the in-cylinder pressure limit, as can be seen in Figure 5-19. It plots the maximum in-cylinder pressures reached as well as the angles of start of combustion obtained during the injection-timing response in each engine build.

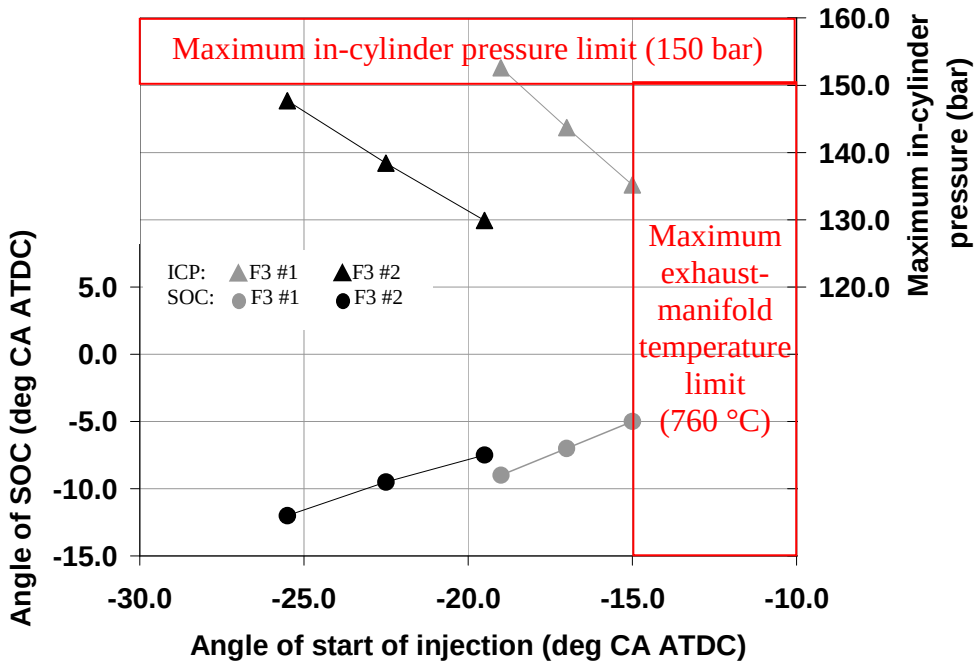

Figure 5-19: Impact of compression ratio on combustion characteristics.

Both engine builds follow the expected trend of combustion, that is, occurring earlier and reaching higher maximum in-cylinder pressures as the injection timing is advanced. The reduced compression pressure of Build #2 engine offered the possibility of an advance of 7 °CA compared to the earliest injection timing in Build #1 engine before reaching the maximum in-cylinder pressure limit. This results in a higher load in itself and also offers scope for increasing the injection duration whilst remaining within the exhaust temperature limit, also represented in the figure. The lower compression ratio offers possibilities to reduce smoke emissions, which are a limiting factor at full load since, although not regulated, smoke visibility must be limited at the exhaust pipe. This is illustrated in Figure 5-20, where lower smoke emissions were obtained with the Build #2 engine, despite it operating at a slightly higher load. Soot emissions are closely linked with the in-cylinder conditions, such as temperature and pressure, as well as the piston position and fuel-air interactions. Lower levels of swirl are likely to assist in the reduction of smoke emissions at full load as they prevent gaseous fuel plume-to-plume interactions, which resulted in a sudden rise in soot emissions as can be seen at key point P3 in Figure 5-3. It is expected that the sudden rise in emissions would occur at lower level of swirl as the load increases. In addition, by virtue of the reduced pressure and temperature, the lower compression ratio engine showed a 2 °CA longer auto-ignition delay for a similar injection timing, as shown in Figure 5-19. This will promote the mixing by

increasing the fuel-spray penetration, as will the longer auto-ignition delays. The diffusion-combustion phase will be reduced, thereby reducing the soot formation. In addition, the more advanced injection timing leads to earlier combustion, which increases the residence time of soot emissions, promoting their oxidation process in the hot in-cylinder environment after the combustion.

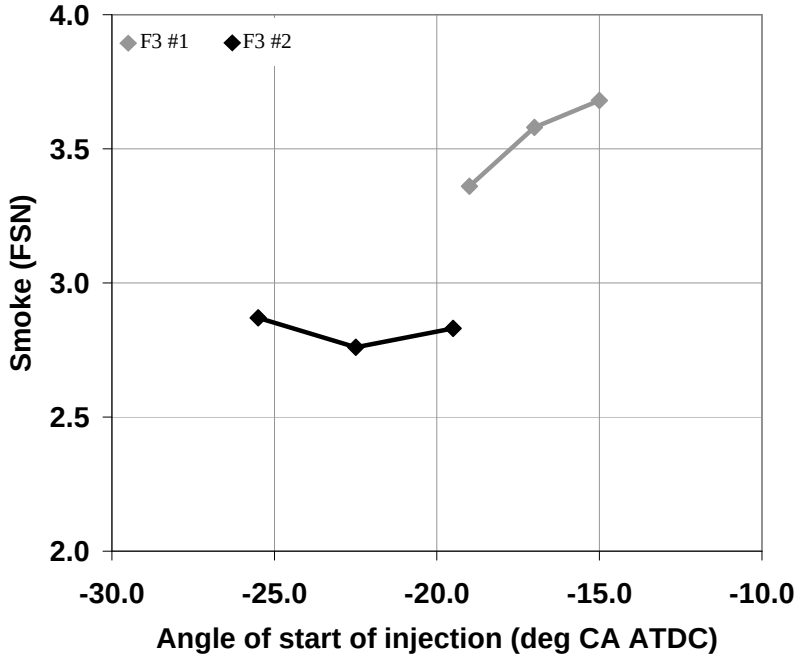

Figure 5-20: Impact of compression ratio on smoke emissions.

5.5 Conclusions

It is a well-known fact that NO_x emissions are reduced when the combustion temperatures are lower. Reducing the compression ratio contributes to a lowering of the combustion temperatures. Modifications were made to the engine hardware to reduce the compression ratio from 18.4 to 16.0:1. Three part load key points were investigated with both compression ratio engine builds by conducting injection-timing responses with all the other operating conditions kept constant. A detailed analysis of the results has yielded an improved understanding of the impact of compression ratio on the combustion characteristics. The results did not represent an optimised engine calibration but enabled the isolation of the impact of compression ratio and injection timing on the emissions and fuel conversion efficiency. Similar emissions and fuel consumption trends to those obtained by Araki et al. (2005) were obtained. The effect

of reduced compression ratio was similar to the effect of late intake valve opening on the maximum rate of pressure change shown by Kawano et al. (2005), which was used as means of reducing compression ratio, however, the authors approach did not isolate the varying compression ratio from the changing AFR. Lower compression ratio effects were interpreted and explained through an analysis of the in-cylinder and combustion characteristics. Its influence was also compared with that of injection timing. The effect of increased flow, hence volumetric efficiency, of the cylinder head was also analysed at full load, where it was most visible. The main conclusions from this chapter are:

- The use of compression ratio to reduce NO_x and soot emissions is appealing, but would lead to a clear increase in HC and CO emissions indicating poorer combustion
- A reduction in fuel conversion efficiency was not visible with the reduction in compression ratio, however, the expected reduction in engine friction is likely to result in improved fuel consumption
- A more rapid combustion of the first 50 % of fuel, for identical operating conditions, compensated for the later start of combustion and angle of 50 % burn in the lower compression ratio engine build at the light load key points P1 and P3. However, this faster burn of the first 50 % of the fuel was not sufficient to offset the later angle of 50 % burn at higher loads, represented by key point P4
- Both reducing the compression ratio and retarding the injection timing greatly reduced NO_x emissions at the loads where both premixed and diffusion combustion were present. Since the effect of lowering the compression ratio was less visible in the case of a fully-premixed-charge combustion, it is possible to conclude that the varying temperature, consequence of the varying pressure with compression ratio or injection timing, is the main factor controlling NO_x emissions during diffusion combustion
- Equally, since varying the in-cylinder temperature had little effect on NO_x emissions during premixed-combustion, it highlight the existence of the third factor, AFR and EGR rate or local oxygen concentration, which seem to become dominant during fully-premixed-charge combustion

- The fully-premixed-charge combustion resulted in some cases with a higher maximum rate of pressure change, which was linked to the larger proportion of the fuel burning simultaneously in the premixed combustion rather than a faster rate of combustion
- Both reducing the compression ratio and retarding the injection timing reduced soot emissions. These measures acted in two ways. Firstly, the fuel spray can penetrate further thereby increasing the mixing. Secondly, the auto-ignition is delayed, increasing the proportion of premixed-combustion through increased mixing time, which limited soot emissions
- At full load, the increased volumetric efficiency enabled the engine to operate at the same AFR and fuel consumption with reduced inlet-manifold pressures. A further advance of the injection timing was possible with the reduced compression ratio, thereby reducing smoke emissions and offering increased load possibilities.

6 COMBUSTION STRATEGIES FOR ULTRA-LOW EMISSIONS

6.1 Introduction

The use of compression ratio as a means to reduce NO_x and soot emissions whilst maintaining acceptable fuel consumption has been demonstrated in Chapter 5 and explanations have been given for these reductions. The increased mixing time due to the longer auto-ignition delays and the associated increased fuel-air interactions, also linked with the lower in-cylinder pressures, have suppressed diffusion combustion at light loads and reduced it at the higher loads. By suppressing or minimising the high-temperature, close-to-stoichiometric characteristics of diffusion combustion, NO_x and soot formation are significantly reduced. The approach envisaged in the present investigations for further reductions in NO_x and soot emissions also aims to reduce diffusion combustion and flame temperatures further and has two components. The first of these is the injection timing, identified in Section 2.3. Takeda et al. (1996) suggested early and Kawashima et al. (1998) suggested late injection timings. The timing has a strong influence on auto-ignition delay, which determines how much mixing occurs before combustion starts. The second component is oxygen concentration, as suggested by Nakayama et al. (2003) (see Figure 2-3), whereby reducing the local concentration in the flame will limit the temperature and hence NO_x formation, as it increases the heat capacity of the charge, Heywood (e) (1988). This is also expected to influence the auto-ignition delay. In practise, this is achieved by lowering AFRs and / or increasing EGR rates. This approach offers the potential for reducing the NO_x after-treatment requirements to meet future US Tier 2 Bin 5 or possible Euro 6 targets, especially in view of the turbocharger developments that allow higher EGR rates for the same AFR, and of injection systems, offering higher injection pressures and therefore allowing control of soot emissions despite low oxygen contents.

The main objective for the investigations reported in this chapter was to understand the requirements in terms of operating conditions to achieve ultra-low NO_x and soot emissions and the influence these have on the fuel-air mixing and combustion in an evolutionary but conventional combustion system (Build #2 engine). The two primary key points at 1500 rev/min were selected for the main part of the investigations as

they were representative of loads where different approaches had been tested and not always successfully, as described by Gatellier and Walter (2002) for a compression ratio of 16.0:1. The approach consisted firstly of an emissions and fuel consumption comparison obtained during injection-timing responses for different AFRs and EGR rates whilst maintaining all the other conditions fixed. These injection-timing responses covered a wide range of crankangles in order to cover both PCCI and HCCI combustion. Secondly, analyses were conducted by correlating the variations in emissions and fuel consumption with in-cylinder and combustion characteristics. A schematic of the combustion types and potential NO_x emissions as a function of load and injection timing is given, as well as a graphical summary of the impact of oxygen concentration or injection timing on the rate of pressure change, the fuel-air mixing and the combustion temperatures. Finally, PCCI combustion was applied to higher speeds and loads to exploit the full potential and results were compared with typical Euro 4 operating conditions and characteristics.

6.2 Experimental approach

The investigations detailed in this chapter were conducted on the Build #2 engine, using a 7 hole, 680 cc/min flow, 154 ° cone angle, 0.76 coefficient of discharge injector nozzle and the protrusion increased by 0.6 mm since this had improved soot emissions as detailed in Section 4.5.4. Key points P1 and P2, respectively 1500 rev/min 3.0 and 6.6 bar GIMEP, were the primary key points chosen for these investigations as they represented a light load at which both PCCI and HCCI combustion have been demonstrated, and a medium load at which HCCI combustion becomes very difficult to achieve and beyond which it is not possible.

As reported in most low NO_x emissions research, the three main influencing factors are the injection timing, the AFR and the EGR rate both locally and globally. The reasoning is that the oxygen concentration decreases as the AFR decreases and the EGR rate increases. Nakayama et al. (2003) derived the following linear relationship:

$$[O_2]_{cylinder} = [O_2]_{air} \cdot \left(1 - \frac{EGR/100}{Lambda}\right) \quad (6\text{-}1)$$

$$Lambda = AFR / AFR_{Stoichio} \quad (6\text{-}2)$$

Where $[O_2]_{cylinder}$ is the dry volumetric concentration of oxygen in the cylinder (%),

$Lambda$ is the relative air fuel ratio (-)

$[O_2]_{air}$ is the dry volumetric concentration of oxygen in air (%),

EGR is the EGR rate (% volume),

AFR, $AFR_{Stoichio}$ are the measured and stoichiometric (14.5:1) AFRs (-).

It expresses the oxygen concentration as a function of EGR rate divided by Lambda. An indication of the in-cylinder oxygen concentration is given by the ratio EGR/Lambda: increasing values of EGR/Lambda indicate decreasing oxygen concentration in the cylinder. In practise, for a fixed inlet-manifold pressure, increasing the EGR rate would result in a lower AFR due to the lost volume of air displaced by exhaust gases. However, by increasing the level of charge-air pressure as well as increasing the EGR rate, a target AFR can be maintained for engine transient response purposes.

Injection-timing responses were conducted for different AFRs and EGR rates, or EGR/Lambda ratios, whilst maintaining all the other operating conditions fixed and adjusting only the main-injection quantity to achieve the gross load. These injection-timing responses covered a wide range of crankangles in an attempt to achieve both PCCI and HCCI combustion. They went from the most retarded injection timings before misfire to the earliest timings the hardware would allow. At the light load key point P1, the early injection-timing limit was reached when evidence of fuel spraying onto the cylinder walls was found, this was a direct consequence of the conventional injector-nozzle cone angle. At the medium load key point P2, the early injection-timing was limited by the maximum allowable in-cylinder pressure. In addition to the injection-timing responses, some injection-pressure investigations were carried out, whereas the swirl throttle position was held constant at 100 % shut since it proved beneficial in terms of soot, HC and CO emissions and had little impact on NO_x emissions and fuel consumption for loads below 1500 rev/min 6.6 bar GIMEP as illustrated in Chapter 5. Single injections were used for these investigations since pilot injections would tend to reduce premixed combustion by increasing the in-cylinder pressure and temperature before the main injection, hence decreasing the auto-ignition delay. Operating conditions such as inlet-manifold temperature and backpressure

settings were known to affect NO_x emissions but were believed to be secondary parameters in comparison with oxygen concentration and injection timing and therefore were kept constant at each key point throughout the investigations. Figure 6-1 and Table 6-1 summarise which operating conditions were fixed, redefined and investigated and gives the main values or ranges for the present investigations.

A comparison of the operating characteristics during each injection-timing response was undertaken and explanations for the impact of lower oxygen concentration and injection timings were sought by analysing the in-cylinder and combustion characteristics as in Chapter 5.

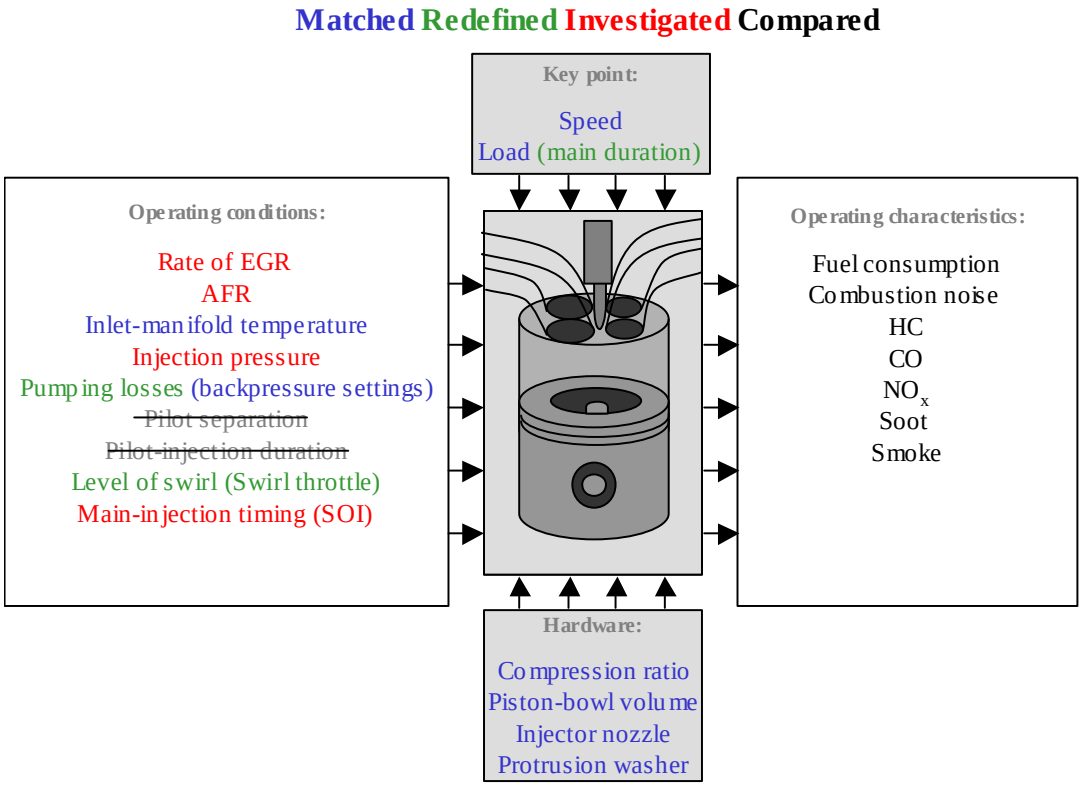

Figure 6-1: Operating conditions and hardware modified during investigations.

	Values or ranges investigated			
Chapter	4	6	4	6
Key point	P1		P2	
Speed (rev/min)	1500		1500	
Gross load (bar GIMEP)	3.0		6.6	
Compression ratio (-)	Chapter 4: 18.4:1 / Chapter 6: 16.0:1			
Piston-bowl volume (cc)	Chapter 4: 22.0 / Chapter 6: 26.3			
Injector nozzle	7-hole, 680 cc/min, 154 °, 0.76 coefficient of discharge			
Protrusion washer (mm)	Chapter 4: 1.6 / Chapter 6: 1.0			
Main-injection quantity	Adjusted to maintain load			
Injection pressure (bar)	545	400 to 800	900	900 to 1100
Pilot-injection duration (μs)	300	N/A	260	N/A
Pilot separation (°CA)	26.0	N/A	26.0	N/A
SOI 2 (°CA ATDC)	-4.0 to 2.0	-36.0 to 0.0	1.0 to 9.0	-27.0 to 7.0
Wet EGR rate (%)	45.4	45.0 to 63.0	28.1	28.0 to 46.0
Dry AFR (-)	29.3:1	17:1 to 24:1	22.0	17:1 to 22:1
EGR/Lambda (-)	22	27 to 54	18	18 to 39
Swirl throttle (% shut)	46	100	65	100
Inlet temperature (°C)	88		70	
Backpressure valves settings	1: 24.0 half turns & 2: shut		1: 23.5 half turns & 2: shut	

Table 6-1: Main operating conditions and hardware values or ranges investigated.

6.3 Analysis of impact of advanced combustion operation

6.3.1 Impact on NO_x emissions at light load

In the case of the light load key point P1, two sets of data were obtained. Initial testing was conducted to investigate different combinations of AFR and EGR rate at light load, using a fixed injection pressure of 550 bar. Subsequent testing was conducted using a fixed injection pressure of 750 bar, since it reduced soot, HC and CO emissions. For values of EGR/Lambda above 45, NO_x emissions were relatively insensitive to injection pressure as can be seen in Figure 6-2, where two injection-pressure responses are shown. The injection pressure was varied by almost 300 bar at two different combinations of AFR and EGR rate, with values of EGR/Lambda above 45, at an injection timing of -26 °CA. However, when the values of EGR/Lambda were below 45, the injection pressure was found to have an impact on NO_x emissions

especially when the angle of start of injection was near -30 °CA ATDC, as can be seen in Figure 6-3. The values of EGR/Lambda are shown in both figures.

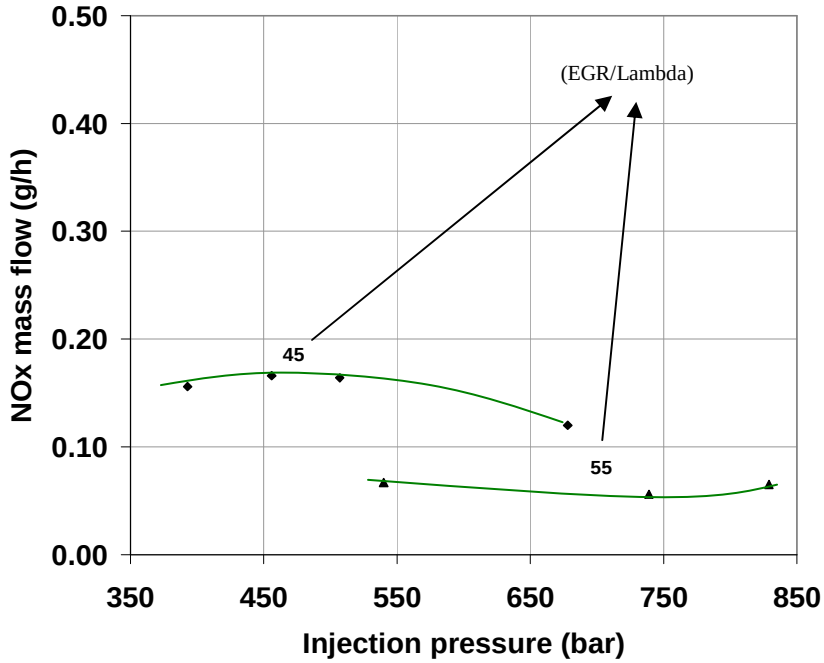

Figure 6-2: Injection pressure impact on NO_x emissions at -26 °CA ATDC.

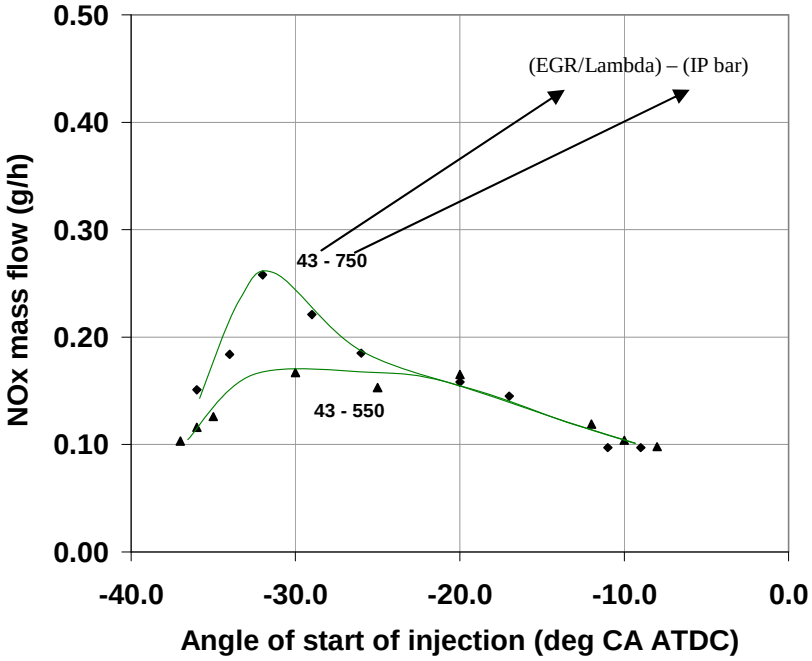

Figure 6-3: Injection pressure impact on NO_x emissions at fixed EGR/Lambda.

For values of EGR/Lambda greater than 45, as the injection pressure increased, NO_x emissions remained unchanged. It is believed that the injection and combustion were decoupled due to a very long auto-ignition delay resulting from the low AFRs and the

high EGR rates. The injection pressure did not impact on the combustion as it does during conventional combustion. It was therefore possible to group NO_x emissions results obtained at different injection pressures, as long as certain conditions were met in terms of AFR, EGR rate and injection timing. For values of EGR/Lambda below 45, an injection-timing region centred near -30 °CA ATDC highlights a zone where this grouping is not valid. This region expands as EGR/Lambda decreases.

The Figure 6-4 displays NO_x emissions over several long injection-timing responses at different combinations of AFR and EGR rate, hence EGR/Lambda values. Again, these values have been indicated on the figure. The ratio values result from combinations of AFR from 17.0:1 to 24.0:1 and EGR rates from 45 % to 63 %. The injection pressure has also been indicated in each case. A line has been added to the figure giving the injection-timing ranges where injection pressure becomes a major influencing parameter on NO_x emissions (as in conventional diesel combustion) if the value of EGR/Lambda decreases below 45, as deduced from Figure 6-2 and Figure 6-3.

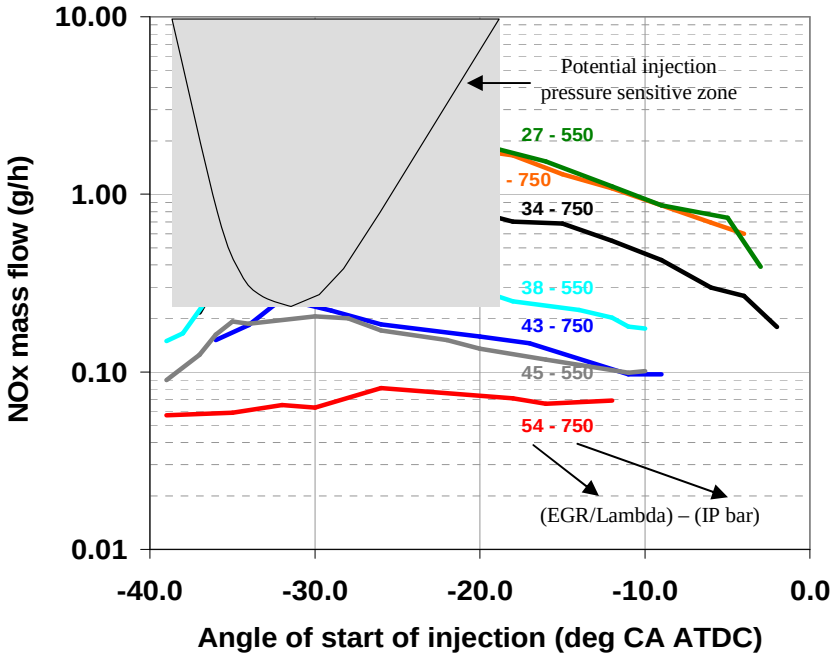

Figure 6-4: Injection timing & EGR/Lambda impact on NO_x emissions (P1).

As EGR/Lambda was increased, or oxygen concentration was reduced, the emissions were greatly reduced. At the most retarded injection timings, NO_x emissions reduced as injection timing retarded as shown during the single to 4-cylinder-engine matching.

However, as the injection timing was advanced beyond -30 °CA ATDC, where the emissions reached a peak, there was a reversal in the response. NO_x emissions decreased rapidly to the initial levels or lower. A further advance, beyond -39 °CA ATDC, was not possible with the current injector-nozzle configuration due to fuel spraying on the cylinder walls. The NO_x emissions response profile was very similar to those obtained by Yanagihara (2001), conducted at fixed fuelling.

The traces of in-cylinder pressure and corresponding instantaneous heat release (as defined in Equation 3-20) obtained during a typical injection-timing response are shown in Figure 6-5. The rate of pressure change traces are also shown as defined in Chapter 5 and before the motored element is subtracted. The figure shows the results for an injection pressure of 550 bar, an AFR of 20.0:1 and an EGR rate of 52 % leading to a ratio value of 38. The peak in the emissions curve in Figure 6-4 corresponds to the curve in Figure 6-5 for which combustion is earliest and very rapid. It is considered that a combination of high in-cylinder pressure and temperature during the injection and the proximity of the injection and combustion led to a high-temperature, near-stoichiometric combustion. A clear reversal in some parameters that help to explain the NO_x emissions reversal can be seen as the injection timing is further advanced. Three possible contributions to the reversal were found. Firstly, as the injection timing was advanced, the auto-ignition delay increased, as can be seen in Figure 6-6 by the gradient of the response being lower than unity. These angles were defined as the crankangles at which the main phase of heat release occurred, rather than start of low temperature oxidation, which occurred in some cases. The angles of start of combustion reached a plateau at the very early injection timings. It is believed that the combination of in-cylinder conditions in terms of local AFR, temperature and pressure required for auto-ignition (Heywood, (g), 1988) were only met later in the compression cycle. Figure 6-7, where the in-cylinder pressure at start of combustion is shown for all key point P1 tests during the present investigations, reveals a minimum in-cylinder pressure and associated temperature required for auto-ignition of approximately 38 bar. Variations from this would be expected with variations in oxygen concentration within the mixture. It is expected that for a further reduction in compression ratio, at least the same in-cylinder pressure for auto-ignition would be required, therefore retarding the start of combustion further. This would affect the angle at which the reversal occurred. Secondly, the lower oxygen concentrations led

to later combustion across the injection-timing response as can be seen in Figure 6-6. Thirdly, the delay linked with the in-cylinder conditions itself led to an additional source of auto-ignition delay: the mixture becomes leaner due to the increased mixing time as indicated by the premix ratio in Figure 6-8.

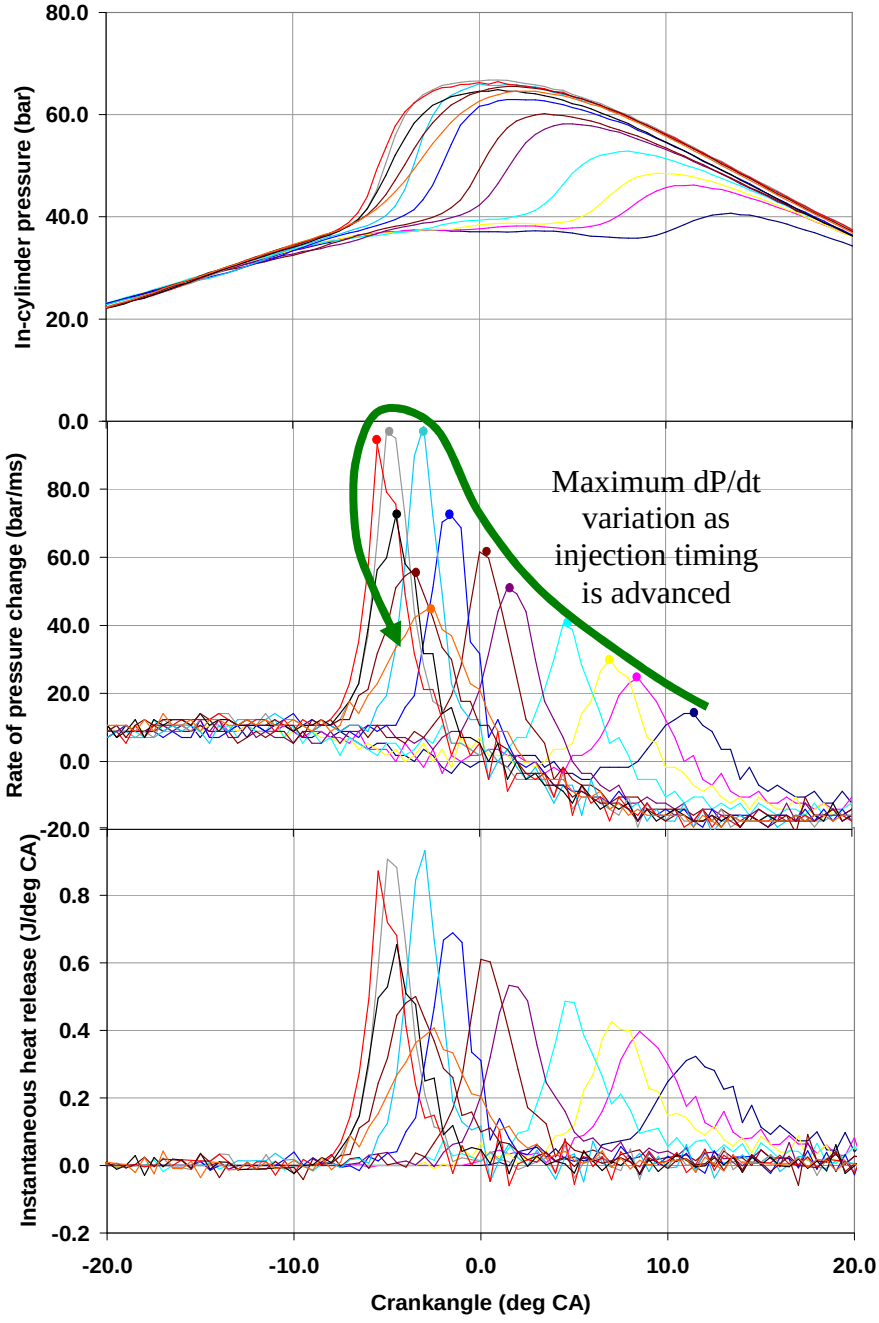

Figure 6-5: Example of combustion characteristics during a response (P1).

The parameter premix ratio was used as an indication of the global level of mixture homogeneity within the charge and is given by:

$$Premix\ ratio = \frac{SOC - Real\ SOI}{Real\ EOI - Real\ SOI} \qquad (6\text{-}2)$$

Where SOC is the angle of start of combustion (°CA ATDC),

$Real\ SOI$ and EOI are angles of real start and end of injection (°CA ATDC).

The angles of real start and end of injection were corrected using an opening and closing offset map derived from fuel injection rate measurements shown in Appendix B. If the premix ratio is below unity, it indicates that the start of combustion occurred before the injection ended. As the ratio increases over unity, it is taken as an indicator that the level of homogeneity increases. This approximation does not take into account the fact that, to avoid diffusion combustion, the fuel injected into the chamber then needs to evaporate and mix with air before it burns. However, it offers an insight into the impact of injection timing and oxygen concentration on the nature of the mixture as it ignites. As the injection timing was advanced, the premix ratio increased due to the plateau in angles of start of combustion and the increasing real start of injection term in Equation 6-2.

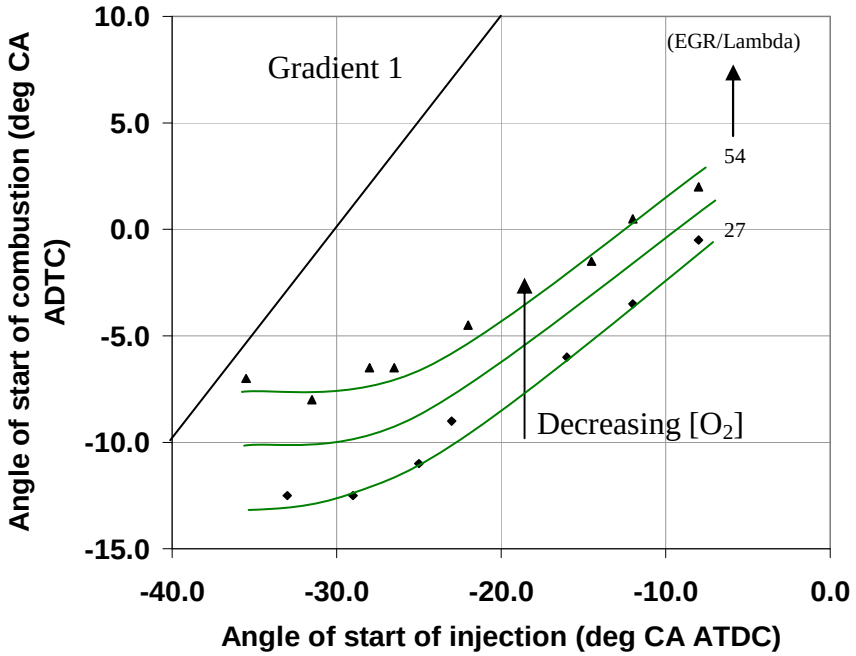

Figure 6-6: Injection timing & EGR/Lambda impact on start of combustion (P1).

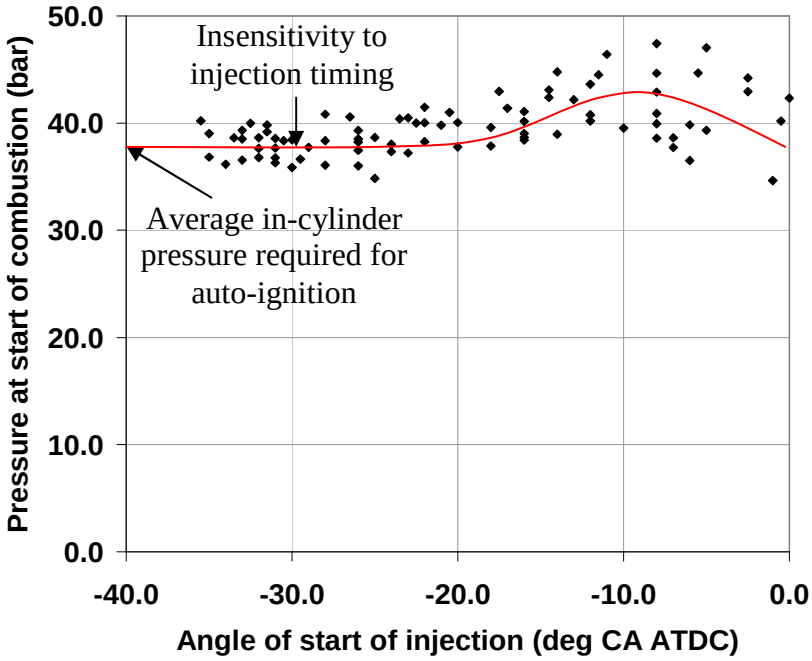

Figure 6-7: In-cylinder pressure at start of combustion (P1).

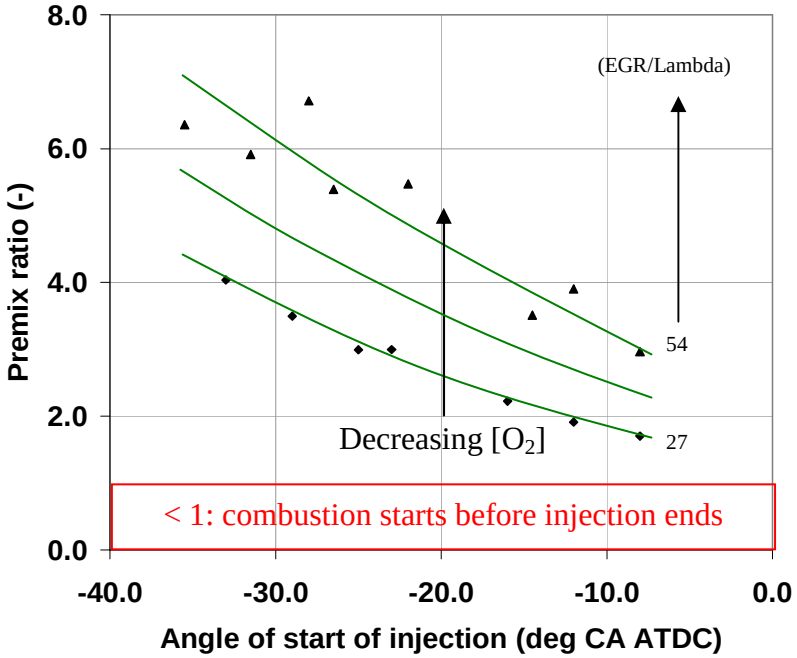

Figure 6-8: Injection timing & EGR/Lambda impact on premix ratio (P1).

The three possible contributions, mentioned earlier, all have as a consequence increased levels of mixing which lead to the reversal in NO_x emissions as the injection timing is advanced. In terms of combustion characteristics, the maximum rate of pressure change decreased when the injection timing was advanced beyond the angle of reversal, reflecting a slower rate of combustion, as can be seen in Figure 6-9. In addition, the increased EGR rate to reduce oxygen concentration, and therefore the

increased heat capacity for a similar level of fuelling, also decreased the rate of combustion. The advanced injection timing beyond the angle of reversal and the increased values of EGR/Lambda led to later combustion with longer duration as shown in Figure 6-10 and Figure 6-11. Therefore, it was possible to obtain extremely low NO_x emissions using both early and late injection timings. The early injection timing led to HCCI combustion, where the combustion was decoupled from the injection. Despite the combustion occurring nearer TDC, low NO_x emissions were achieved. The late injection timing led to PCCI combustion, where low NO_x emissions were also achieved due to the low in-cylinder pressures and temperatures once past TDC. It is interesting to note that the maximum rates of pressure change showed the same pattern as the NO_x emissions variations seen in Figure 6-4. In terms of choice of parameters to correlate with NO_x emissions, it can be seen that maximum rate of pressure change and oxygen concentration are goods choices, as will be discussed later.

Analyses of other in-cylinder characteristics were undertaken. The in-cylinder temperature at the start of injection or combustion offered no correlation with NO_x emissions and is therefore considered as a secondary factor relative to the primary factors injection timing and oxygen concentration.

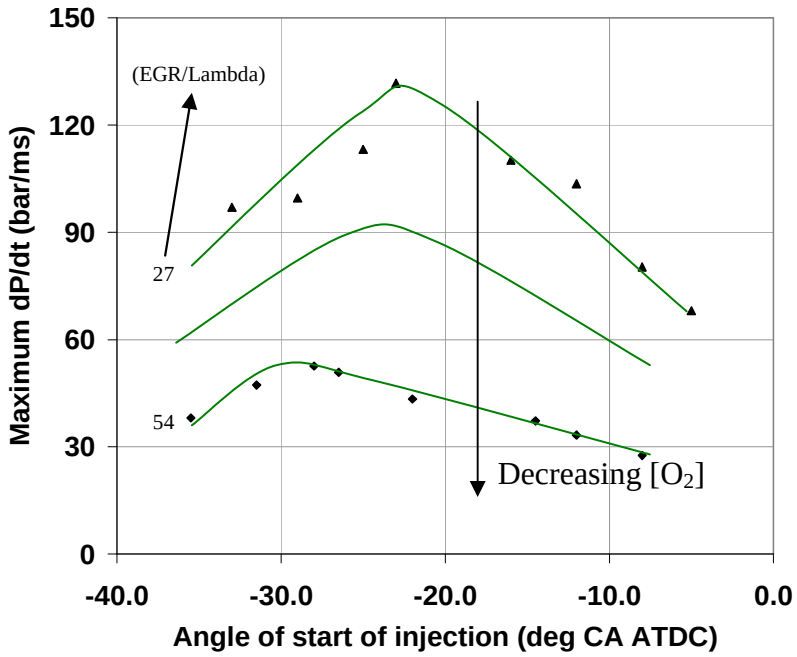

Figure 6-9: Injection timing & EGR/Lambda impact on rate of pressure change (P1).

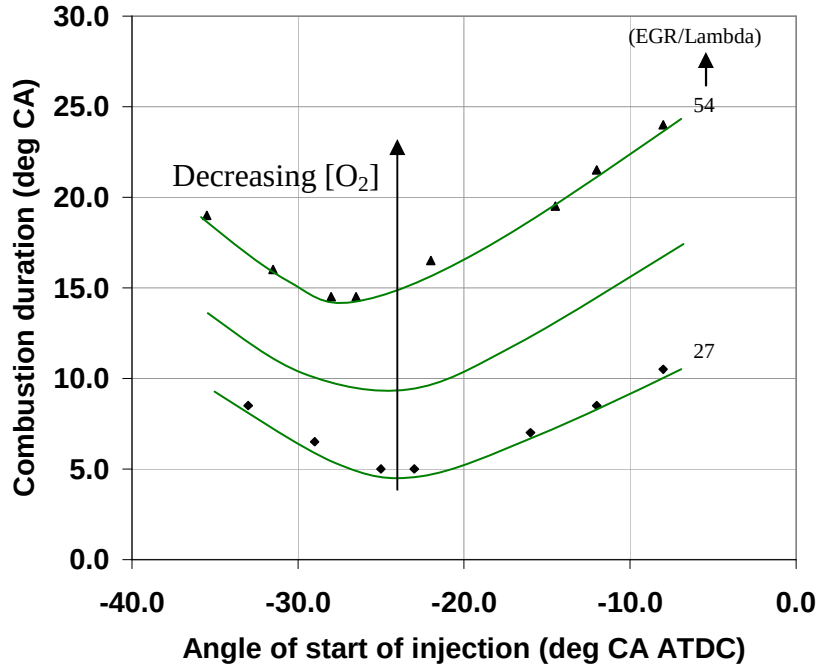

Figure 6-10: Injection timing & EGR/Lambda impact on combustion duration (P1).

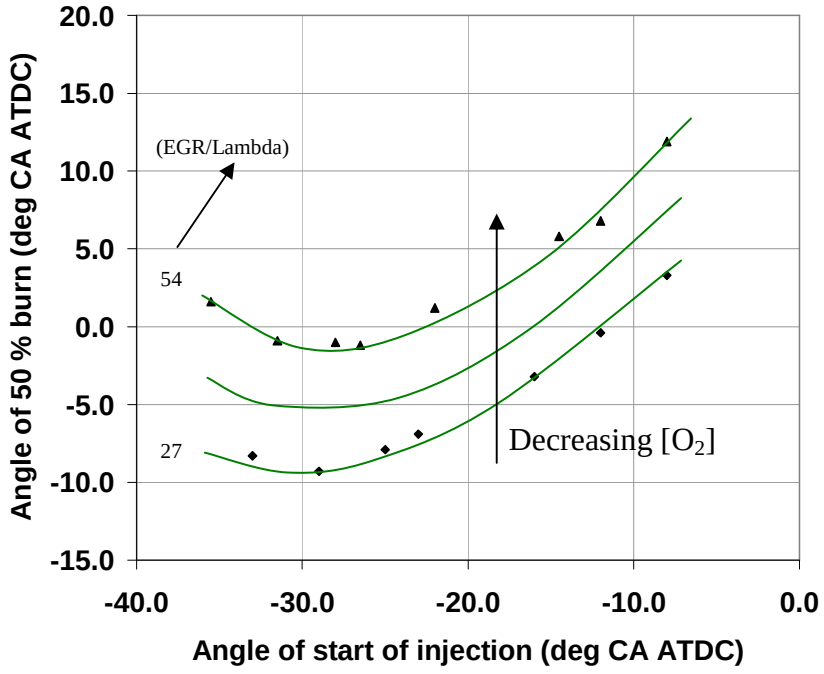

Figure 6-11: Injection timing & EGR/Lambda impact on angle of 50 % burn (P1).

6.3.2 Impact on NO_x emissions at medium load

At medium load, most tests were carried out with an injection pressure of 1000 bar. Figure 6-12 displays NO_x emissions for several long injection-timing responses at

different combinations of AFR and EGR rates. The values of the EGR/Lambda ratio are indicated on the figure. The ratio values result from combinations of AFR from 17.0:1 and 22.0:1 and EGR rates from 28 % to 46 %. The injection pressure has also been indicated for each curve. Again, emissions fell as EGR/Lambda was increased or as the oxygen concentration was reduced. Despite AFRs as low as 17.0:1 and EGR rates as high as 46 %, resulting in a ratio of 39, there was no evidence of a reversal in NO_x emissions as the injection timing was advanced. The responses were not continued beyond approximately -28 °CA ATDC due to high in-cylinder pressures approaching the safe operating limit. It seems that the values of EGR/Lambda were insufficiently high and the injection timing insufficiently advanced to increase the level of mixing and delay the auto-ignition. The influence of injection pressure on NO_x emissions was not totally suppressed as at light load.

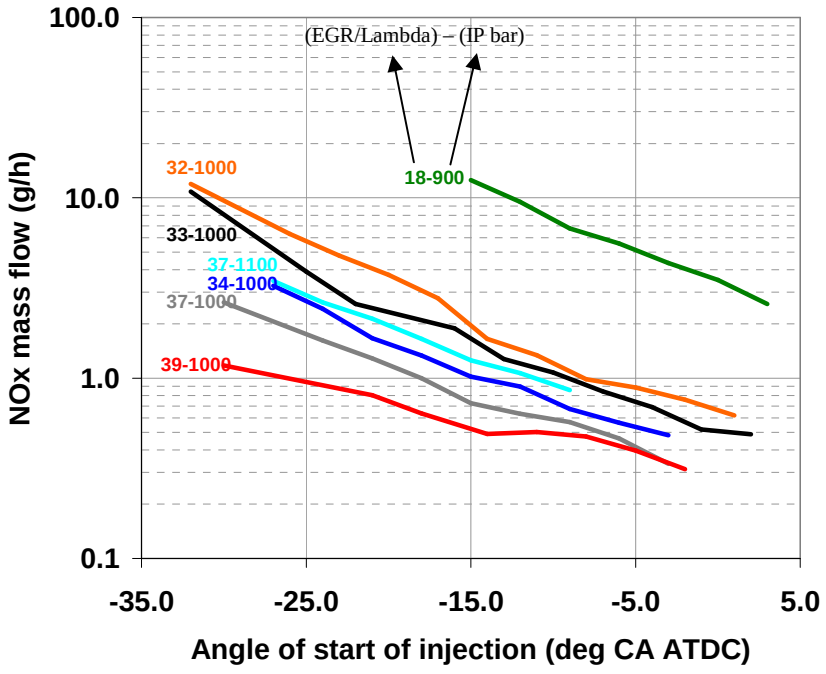

Figure 6-12: Injection timing & EGR/Lambda impact on NO_x emissions (P2).

The in-cylinder pressure traces and corresponding instantaneous heat release and rate of pressure change obtained during a typical test are shown in Figure 6-13. The figure shows the results of an injection-timing response carried out at 1000 bar injection pressure, with an AFR of 17.0:1 and an EGR rate of 40 % leading to an EGR/Lambda value of 34. In order to understand and explain why the reversal in NO_x emissions

seen at light load key point P1 did not occur here, similar analyses as before were undertaken.

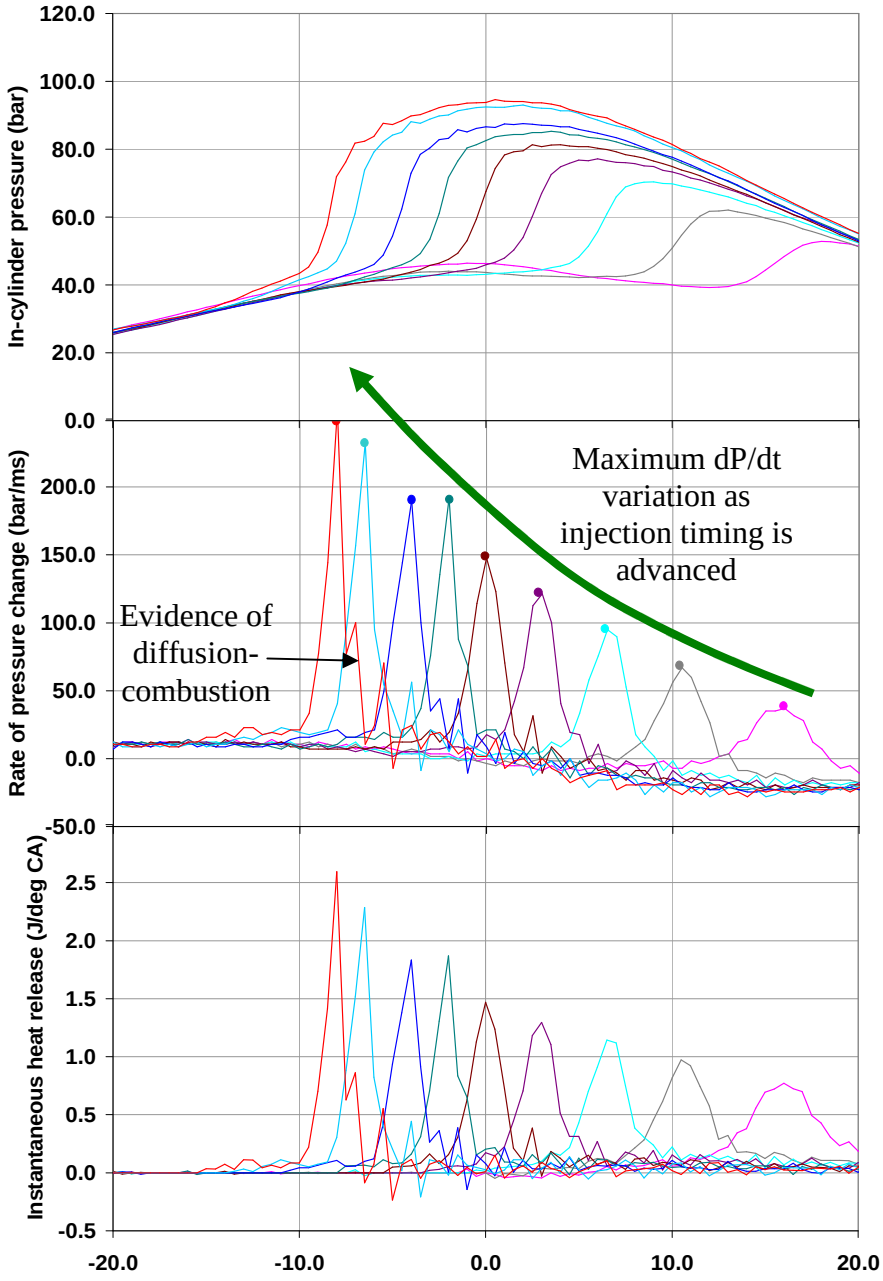

Figure 6-13: Example of combustion characteristics during a response (P2).

Three possible explanations had been found for the reversal in NO_x emissions at light load. Firstly, advancing the injection timing led to increased auto-ignition delays. This impact was not as pronounced at this higher load as can be seen in Figure 6-14, with the gradient of the response closer to unity than at light load in Figure 6-6. This could be associated with the lower values of EGR/Lambda examined from 18 to 39 compared with 27 to 54 at key point P1. Values as high as 54 were not realistic at key

point P2 due to the extremely high levels of inlet-manifold pressures required to increase EGR rate whilst maintaining AFR appropriate for engine transient response purposes. The increased auto-ignition delays leading to the plateau in angles of start of combustion with earlier injections did not occur as distinctly here where the start of combustion can be seen to continue to advance as the injection timing advances. Secondly and thirdly, the oxygen concentration and the leaning out of the mixture led to later start of combustion, which clearly did not occur at the higher load.

The combustion was not decoupled from the injection as observed at the light load as can be seen in Figure 6-15, since pressure at start of combustion changed with injection timing. There are two possible factors to help explain why the auto-ignition still occurred. The first is that in-cylinder pressures and hence temperatures were much higher even at the early crankangles therefore providing conditions favourable to auto-ignition, due to the high inlet-manifold pressure to maintain AFR above 17.0:1 for a fuel consumption approximately doubled from key point P1, as visible in Table 4-3, and to compensate for high EGR rates. The second is that the premix ratios obtained in the present study were much lower than at light load, as can be seen in Figure 6-16, where the envelop of premix ratios obtained at the light load are also depicted. It is expected that the local AFRs will be distributed over a range going from lower levels than at light load to infinitely high levels. These low AFRs, i.e. fuel-rich zones, are likely to trigger auto-ignition even at lower in-cylinder pressures and temperatures, explaining the lack of reversal at this load. These contribute to a shorter auto-ignition delay as well as a more rapid rate of pressure change, indicative of faster rates of combustion, as the injection timing is advanced as can be seen in Figure 6-17. As at light load, it is interesting to point out that the profiles of the maximum rates of pressure change in Figure 6-17 were similar to the NO_x emissions profiles in Figure 6-12. The findings at key point P2, 1500 rev/min 6.6 bar GIMEP, will apply at all speeds and loads above these values and thus highlight the load limitation of early injection timings. The late injection timings corresponded to the PCCI combustion, which offered scope for application at higher speeds and loads. The reduction in NO_x emissions is a function of how well-mixed the charge is at the moment of ignition as well as of how retarded the injection timing is.

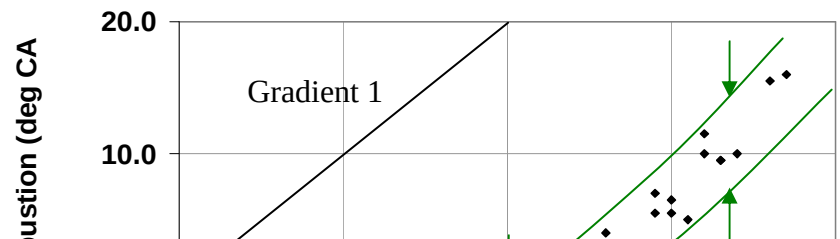

Figure 6-14: Injection timing impact on start of combustion (P2).

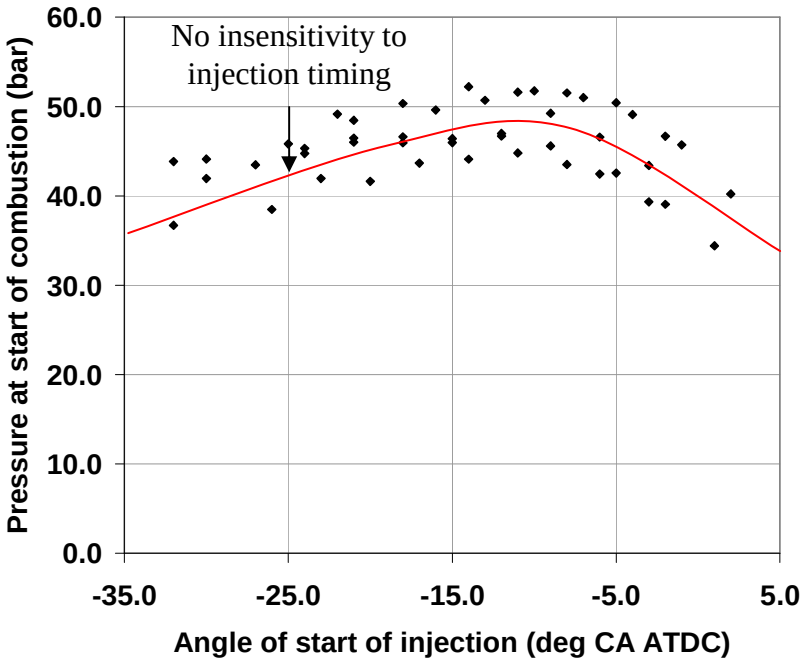

Figure 6-15: In-cylinder pressure at start of combustion (P2).

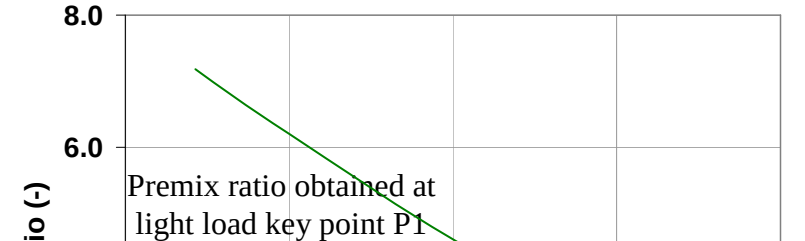

(EGR/Lambda)

Figure 6-16: Injection timing impact on premix ratio (P2).

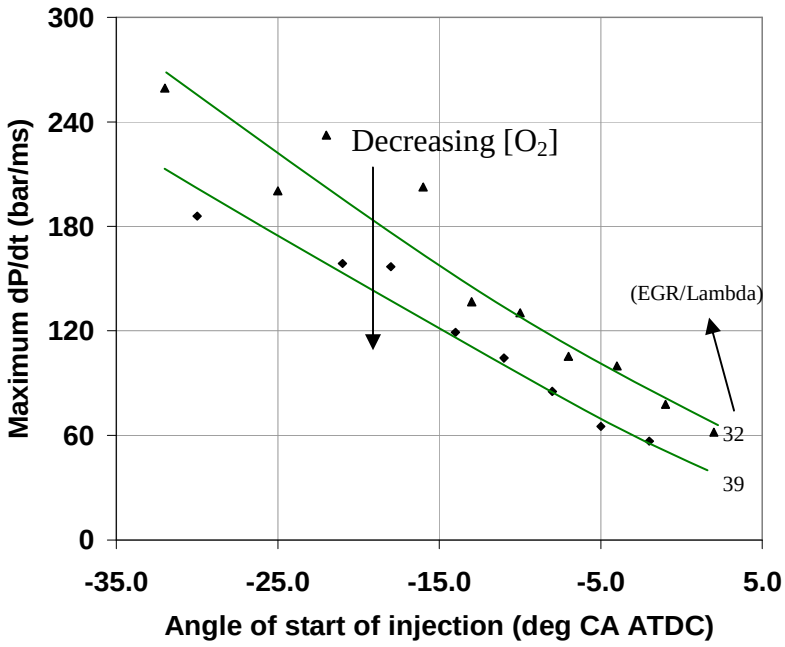

Figure 6-17: Injection timing & EGR/Lambda impact on rate of pressure change (P2).

6.3.3 Impact on soot emissions

Soot emissions measured during the injection-timing responses carried out at key points P1 and P2 are shown in Figure 6-18 and Figure 6-19 respectively.

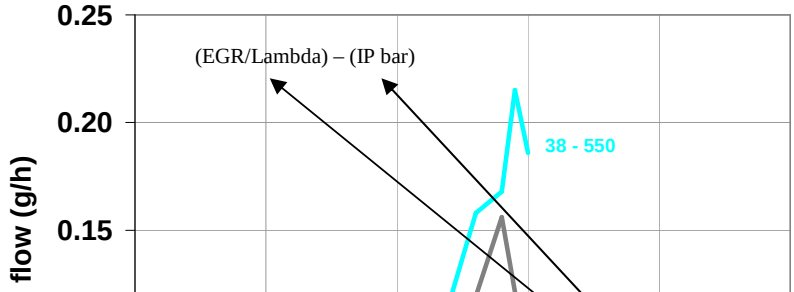

Figure 6-18: EGR/Lambda, injection timing and pressure impact on soot (P1).

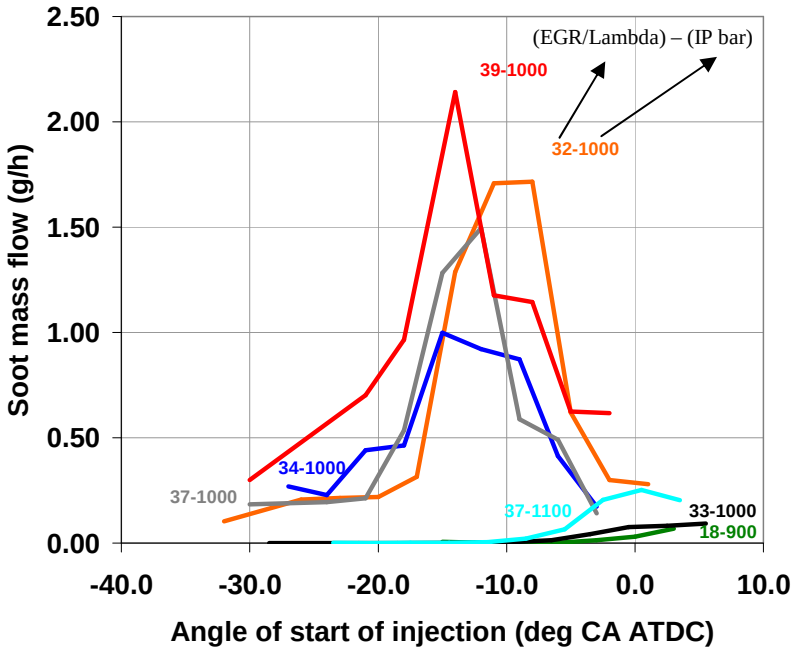

Figure 6-19: EGR/Lambda, injection timing and pressure impact on soot (P2).

A descriptive schematic of the influence of injection timing and pressure on soot emissions is shown in Figure 6-20. In the case of key point P1, four main regions can be identified and a similar pattern is visible at the higher load key point P2 with substantially higher soot emissions. The trends observed were also in agreement with those presented by Yanagihara (2001). The first region for retarded injection timings later than -7 °CA ATDC, denoted A, is the injection timing above which the engine is likely to misfire. This limit occurs later at the higher load, possibly due to the higher

in-cylinder pressures and lower premix ratios, which explained why the reversal in NO_x emissions did not occur, since auto-ignition was more readily achieved.

A second region, denoted B, from -20 to -7 °CA ATDC, is where soot emissions reached their highest levels with a maximum around -12 °CA ATDC. As the injection was advanced, the combustion went from a fully-premixed-charge combustion to combined premixed and diffusion combustion. It is accepted that soot emissions result from a balance between formation and oxidation (Crua, 2002). On one hand, high soot formation is expected from diffusion combustion, whereas lower formation is expected form premixed combustion, on the other hand, high combustion temperatures and hence high levels of soot oxidation are expected with diffusion combustion, whereas lower combustion temperatures and hence low levels of soot oxidation are expected with premixed combustion. Unlike with NO_x emissions, the oxygen concentration and injection timing were no longer the only parameters controlling these emissions. In some cases, lower soot emissions were obtained despite having lower oxygen concentrations. It is believed that this results from a balance between suppressing diffusion combustion with high values of EGR/Lambda thus limiting soot formation and having diffusion combustion with subsequent soot oxidation in the case of low EGR/Lambda values. It is believed that the higher in-cylinder pressures obtained at TDC with lower oxygen concentrations (but same AFR) could also explain higher soot emissions. These higher in-cylinder pressures at the start of and during the injection could modify fuel, air and piston-bowl interactions as a result of different fuel spray penetration, as detailed by Bae et al. (2002). Equally, the different in-cylinder temperatures at the start and during the injection could also affect these interactions. These temperatures were a function of the injection timing since the inlet-manifold temperatures were controlled. This would explain why soot emissions were obtained in the light load case despite a premix ratio greater than 2. In this region, the premix ratio alone was not sufficient to characterise soot emissions. On the other hand, the impact of injection pressure was obvious. Increased injection pressures systematically improved the utilisation of air leading to lower soot emissions. These results highlight the complexity of the mechanisms of soot formation. The utilisation of air, in-cylinder pressure and temperature, piston-bowl interaction, nature of the combustion, injector-nozzle type and position all affect the soot formation and oxidation processes.

A third region, denoted C, ran from injection timings of -30 to -20 °CA ATDC in which soot emissions were not measurable for all injection pressures and oxygen concentrations tested. It is conjectured that it is the high rates of combustion that occurred at these injection timings, which led to the peak in NO_x emissions. However, the resulting low soot emissions indicate that soot formed during the diffusion-combustion phase is totally oxidised before leaving the combustion chamber. This did not occur in the region B due to lower in-cylinder temperatures during the combustion and the reduced residence time of soot, as described by Morgan et al. (2003). Here, it is believed that soot emissions are mainly determined by the premix ratio, as indicated in Figure 6-8 and Figure 6-16, with high ratios leading to low soot emissions.

A fourth region, denoted D, ran from the earliest injection timings (circa -38 °CA ATDC) to around -30 °CA ATDC and was linked with the combustion chamber design. Here soot emissions are apparent as the fuel spray impinges on the cylinder walls. Yanagihara (2001) did not find this increase with injection timing advance, which may be due to the injector-nozzle configuration. Soot emissions obtained with the earliest injection timings could be suppressed using a different injector-nozzle cone angles or even multiple injections, as suggested by Gatellier and Walter (2002).

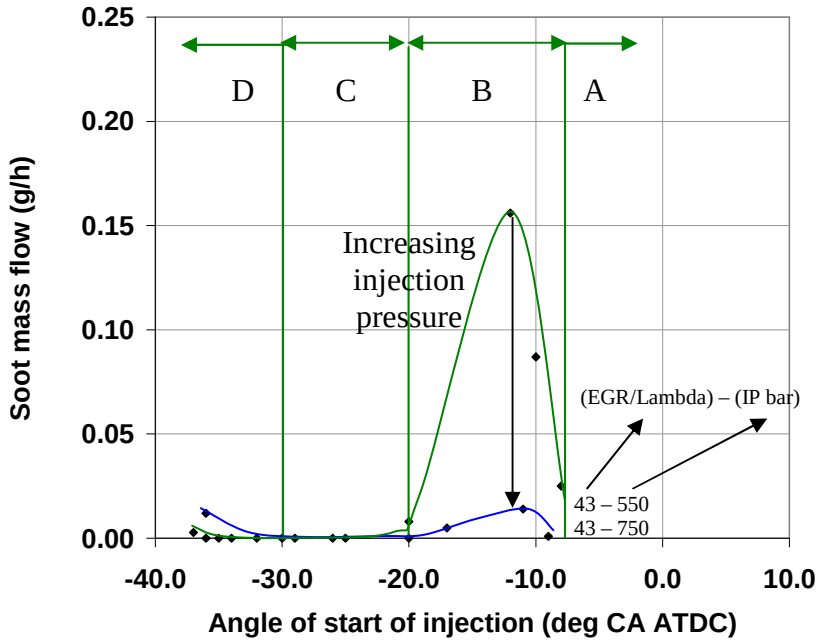

Figure 6-20: Injection timing and pressure impact on soot emissions.

6.3.4 Impact on fuel consumption

The values of the fuel consumption obtained during the injection-timing responses carried out at key points P1 and P2 are summarised in Figure 6-21 and Figure 6-22 respectively. As previously mentioned, since the tests were carried out at fixed gross load, the fuel consumption can be an indicator of the fuel conversion efficiency. The parasitic losses associated with the delivery of higher injection pressures or higher levels of compressor work required for the inlet-manifold pressures are not taken into consideration here. Both 550 and 750 bar injection pressure results are shown at key point P1 whereas only 1000 bar results at key point P2. Overall, the injection timing was the dominant factor controlling fuel consumption. The main impact of oxygen concentration seems to be that its increase allows further retard after TDC of the injection timing before misfire occurs. It is believed that the higher oxygen contents and in-cylinder pressure compensate for the injection later in the expansion cycle in reducing in-cylinder pressures. This effect is also observed with increasing load.

Fuel consumption showed a minimum for injection timings around -13 °CA ATDC at both key points. Retarding the injection timing resulted in sharply rising fuel consumption whereas advancing it showed only a gradual increase. Eventually, with further advance, fuel consumption rose sharply again when the fuel started impinging on the cylinder walls, visible for soot emissions increase at the early injection timings at key point P1. The same conclusion could not be confirmed for key point P2. At key point P1, injection pressure had no impact on fuel consumption for early injection. However, higher injection pressures reduced fuel consumption at injection timings after -20 °CA ATDC. The decoupling of the injection from the combustion is thought to be the reason for the insensitivity at early injection timings. At the more retarded injection timings, the injection pressure acted as in more conventional diesel combustion. The higher injection pressure resulted in a more rapid combustion by limiting the diffusion-combustion phase duration. By reducing the combustion duration, the centre of the combustion occurred earlier, which had a similar impact on fuel consumption as advancing the injection timing.

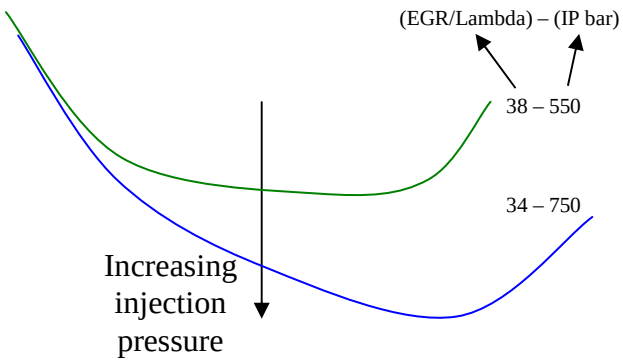

Figure 6-21: Injection timing and pressure impact on fuel consumption (P1).

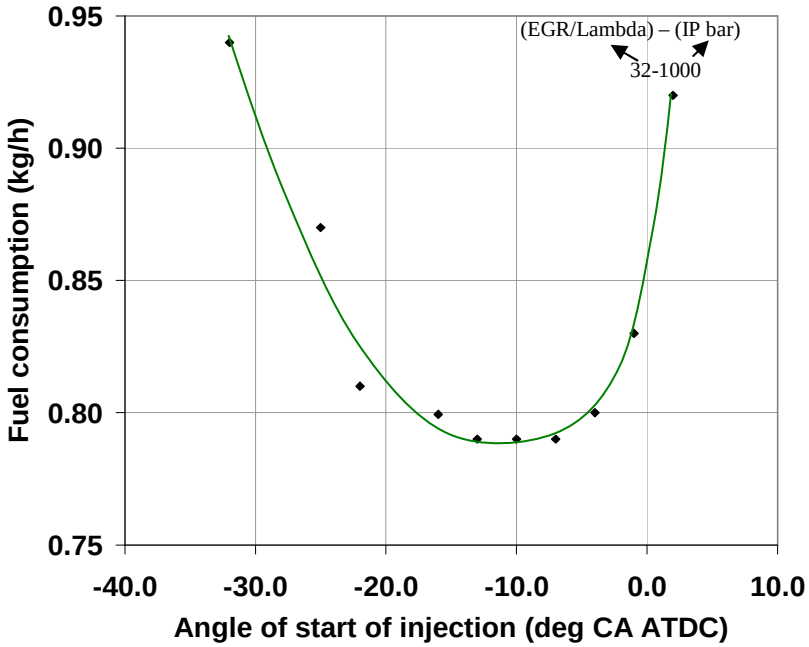

Figure 6-22: Injection timing impact on fuel consumption (P2).

Explanations for the increase in fuel consumption for more retarded or advanced injection timings from -13 °CA ATDC can be found by analysing the combustion characteristics at key point P2. Figure 6-23 represents the fuel consumption for all test data collected at key point P2, plotted against combustion phasing relative to TDC, represented by the angle of 50 % burn, and combustion duration. The spread of test data is included in the figure.

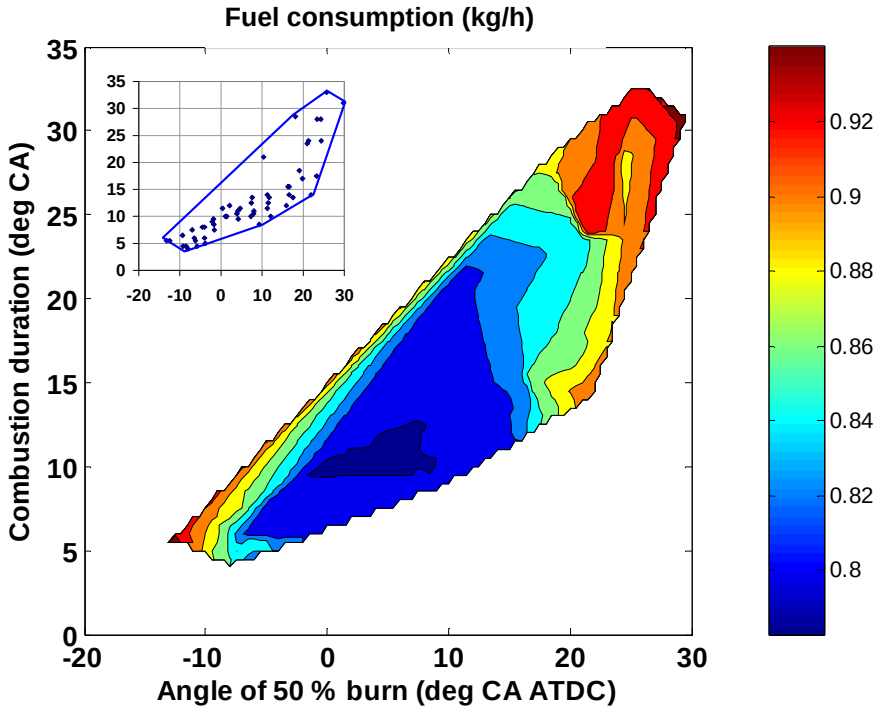

Figure 6-23: Combustion phasing and duration impact on fuel consumption (P2).

It is well-known that a rapid combustion, well-phased relative to TDC, traditionally 0 to 10 °CA ATDC, is the key to optimum fuel consumption. A clear optimum was visible for a combustion centred somewhere between 0 and 10 °CA ATDC and having a duration of 10 °CA. The extremely short duration was the result of very early combustion. This results in high levels of negative work, hence high fuel consumption values. A long combustion duration was the result of late combustion. This led to higher fuel consumption due to the work lost when the exhaust valves opened and also due to the reduced combustion efficiency linked with lower in-cylinder pressures. It highlights clear limitations on how retarded the injection timing can be before leading to high increases in fuel consumption. The injection timing, the level of inlet-manifold pressure and the compression ratio are the main determinants of the mean in-cylinder pressure during the combustion, which in turn is the determinant of the combustion duration. This had little impact on fuel consumption when the combustion was centred between 0 and 10 °CA ATDC. Injection pressure sensitivity was not specifically investigated at key point P2 but is expected to have the same impact on fuel consumption as observed at retarded injection timings at light load but across most of the injection-timing range investigated. This would be due to the more closely-coupled nature of the injection and combustion. A similar representation of fuel consumption results for key point P1 showed that the angle of 50 % burn was the

dominant factor, but that operating conditions had a minimal impact on the combustion duration and was therefore not shown here as it added little to Figure 6-21. From these results, it can be seen that compression ratio and combustion timing relative to TDC are the key to achieving low NO_x emissions and fuel consumption.

6.3.5 Impact on HC and CO emissions

HC emissions measured during the injection-timing responses carried out at key point P1 and P2 are summarised in Figure 6-24 and Figure 6-25 respectively. As in Chapter 5, findings related to HC emissions were considered valid for CO emissions. 550 and 750 bar injection pressure results are shown at key point P1, whereas only 1000 bar results at key point P2. As for fuel consumption, the injection timing had the greatest effect on HC emissions. The lowest levels achieved at key point P1 in the present investigations were at least twice the highest level recorded in Build #1 engine in Chapter 4. HC emissions behaved in an opposite manner to NO_x emissions. At injection timings where NO_x emissions were highest, HC emissions were at their lowest. Equally, as the oxygen concentration decreased, these emissions increased. This leads to the conclusion that the high temperature NO_x forming conditions prevented the survival of HC emissions formed during the injection and combustion.

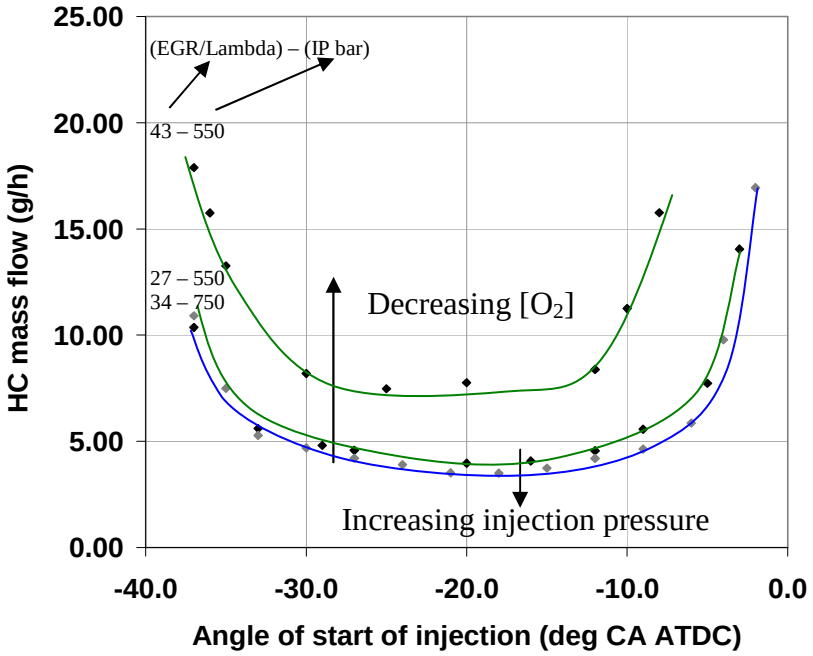

Figure 6-24: EGR/Lambda, injection timing and pressure impact on HC (P1).

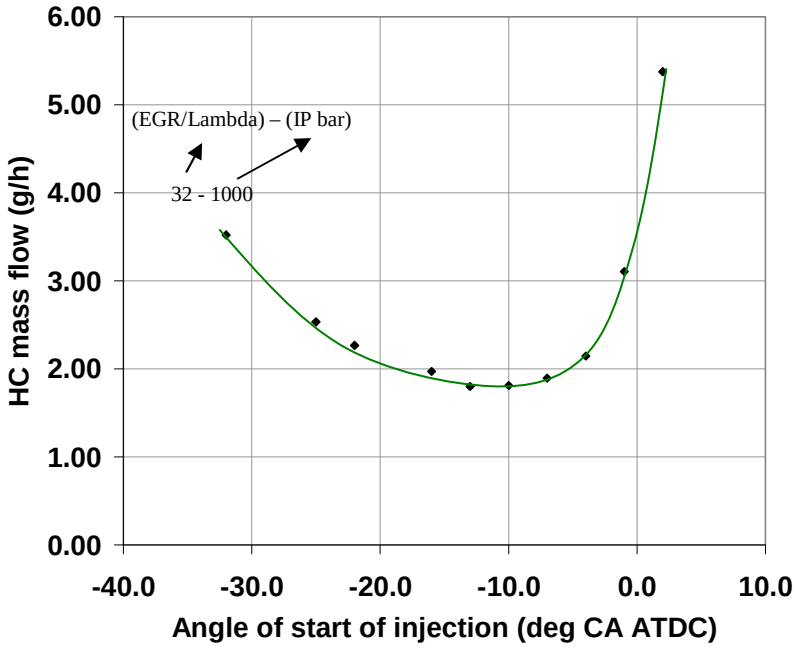

Figure 6-25: Injection timing impact on HC (P2).

The high levels obtained were in line with other data for operating conditions based on low oxygen concentrations, late or early injection timings and low compression ratios, such as Takeda et al. (1996) or Yanagihara et al. (1997). The in-cylinder conditions during the injection and combustion affected the fuel spray penetration and the flame temperature, which increased the size of the quenching zone of the charge. The increase in HC emissions observed as the injection timing was advanced was associated with the fuel and air mixture approaching the cylinder walls, where further quenching occurs due to the low wall temperatures. The rapid increase for the most advanced injection timings corresponded to the fuel impinging on the cylinder walls. At the most retarded injection timings, the increase in HC emissions could be explained by the increased levels of fuelling due to the poorer combustion efficiency as well as the reduced residence time in the hot cylinder environment. Higher injection pressures reduced HC emissions, which is thought to be associated with a more concentrated core of mixture, associated with the shorter injection duration, rather than a highly-diluted envelope of mixture. Despite higher injection pressures leading to faster penetration, a trade-off between air entrainment and pulse duration may limit the flame quenching effect.

6.4 Summary of impact of advanced combustion strategies

The effect of reducing the oxygen concentration or increasing the value of EGR/Lambda and retarding or advancing the injection timing at light load and retarding at medium load was to suppress diffusion combustion as well as to slow the rates of combustion, as described in Table 5-2. Both approaches led to ultra-low NO_x and soot emissions. Lower oxygen concentration or appropriately chosen injection timing resulted in longer auto-ignition delay and combustion duration, indicative of a reduced rate of combustion. The auto-ignition delay resulted in the leaning out of the fuel-air mixture and hence a highly-diluted premixed combustion. The reduced oxygen present in the flame reduced the probability of high-temperature combustion. The delayed and slower combustion with early injection timings helped reduce negative work, which was beneficial for fuel consumption, whereas with late injections had the same effect as retarding the injection timing on fuel consumption.

In the work just described, the early end of the injection timing range corresponded to HCCI combustion, as described by Takeda et al. (1996) or Yanagihara et al. (1997). The level of homogeneity within the charge remains open to debate, but it is generally accepted as being homogeneous. The late end of the injection timing range corresponded to PCCI combustion, as described by Kawashima et al. (1998). The fuel was expected to be well mixed with air at auto-ignition as unmixed fuel would lead to diffusion combustion and thus higher NO_x and soot emissions than measured. A schematic of the impact of advanced combustion operation in terms of NO_x emissions as a function of load and injection timing is presented in Figure 6-26. The lowest and highest curves of constant load are based on the light and medium load key points investigated, highlighting the reversal behaviour, or not, observed in the NO_x emissions responses in Figure 6-4 and Figure 6-12 or in the rates of pressure change in Figure 6-9 and Figure 6-17. The early injection timing curve for key point P2 is conjectured based on data from Takeda et al. (1996) (see Figure 2-7).

The schematic highlights the region of PCCI combustion limited by increased fuel consumption or risk of misfire as the injection timing is retarded. It also shows the region of HCCI combustion needing to be as advanced as possible beyond the reversal angle to obtain low NO_x emissions. As load increases, the angle of reversal advances

as a consequence of the need for the mixture to be leaner to avoid premature combustion and hence high NO_x emissions. However, as found in the present investigations, as the injection timing was advanced at key point P2, the in-cylinder pressure reached the maximum limit. This schematic highlights the fact that HCCI combustion rapidly becomes impossible at higher loads unless very early injection timings combined with low oxygen concentrations are used. To overcome this limit, a much more advanced injection timing must be used but the present injector-nozzle configuration did not allow this without a great fuel consumption penalty and an impact on the engine durability due to oil dilution. However, even with appropriate injector nozzles it presents a serious challenge, as described by Gatellier and Walter (2002), who were unable to operate above 6 bar IMEP, due to difficulties in delaying the combustion. Another difficulty of HCCI combustion concerns the transition from HCCI to conventional operation, which needs to pass through injection timings, which present risks of excessively high in-cylinder pressures. The angle of reversal for NO_x emissions was a function of the oxygen concentration, and it is expected that further compression ratio reductions or increased injection pressures will also retard the angle of reversal.

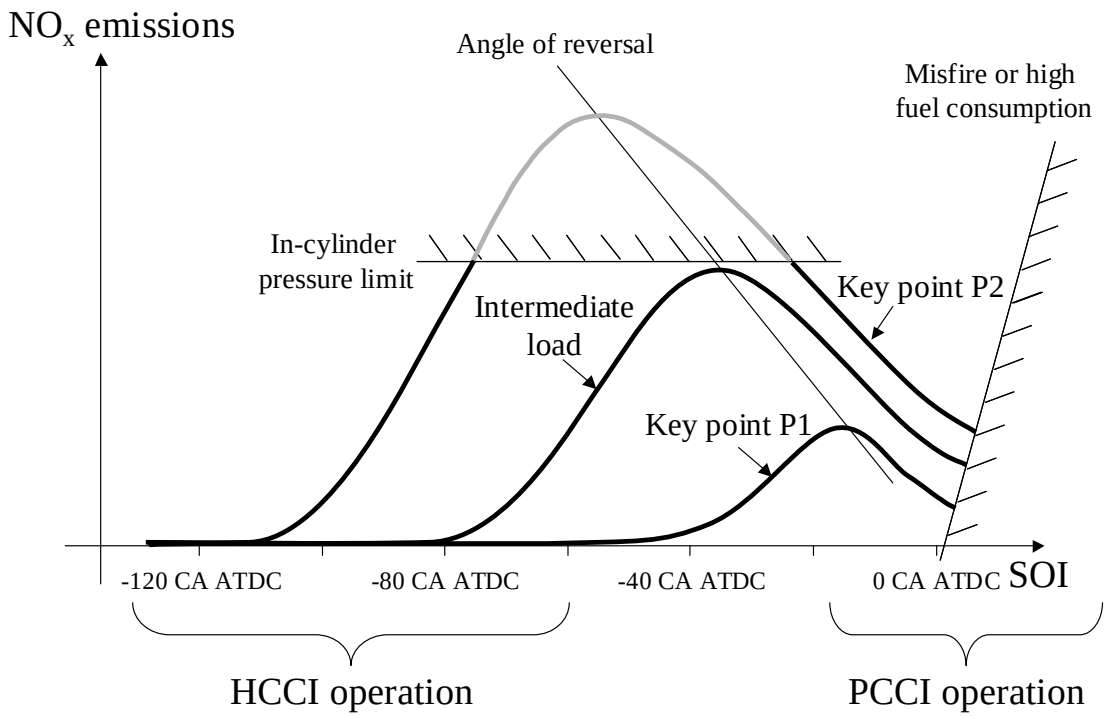

Figure 6-26: Injection timing & load impact on advanced combustion operation.

A graphical summary of the impact of reducing the oxygen concentration on the combustion by means of lower AFR or raised EGR rate is given in Figure 6-27. At the lighter loads, a reduction of the oxygen concentration as well as early or late injection extends the auto-ignition delay, increasing the fuel-spray penetration and fuel-air interactions. A more diluted charge results and the heat capacity is increased, limiting flame temperature. At the higher loads, the impact of lower oxygen concentration on auto-ignition is not seen, however, the heat capacity in the flame increases as a result of the global increase in heat capacity. The highly-premixed, low-temperature combustion leads to large reductions in NO_x and soot emissions but is accompanied by increased HC and CO emissions, as observed in Chapter 5.

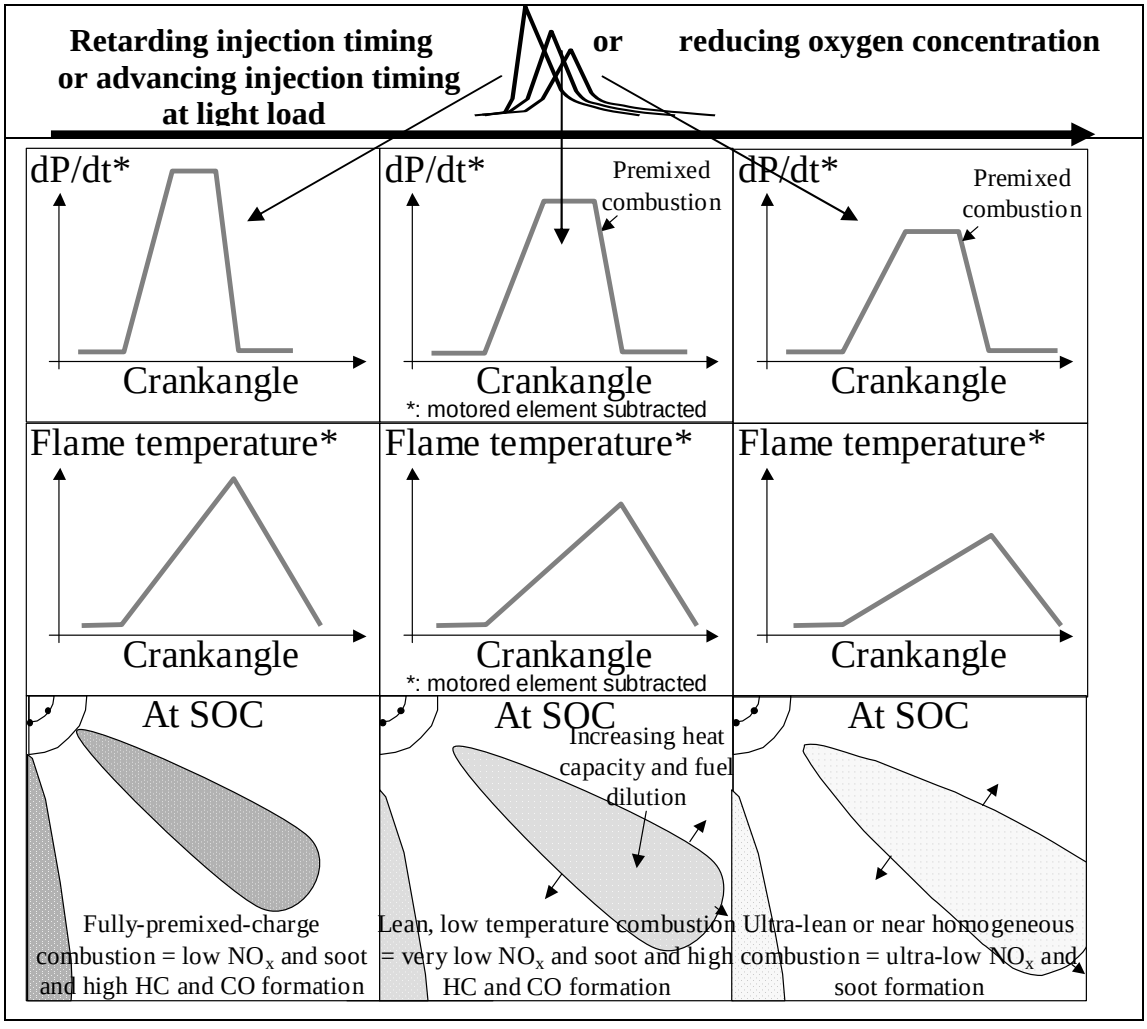

Figure 6-27: Summary of the impact on mixing and combustion characteristics.

6.5 Application of PCCI combustion to higher speeds and loads

HCCI combustion has a limited yet extendable operating range. These limits can be further extended, through yet lower compression ratios, injection systems adapted for early injection timings and advanced turbo-charging systems. However, there will remain a speed and load boundary beyond which HCCI operation will not be possible. This is particularly unacceptable in passenger-car engines where a wide range of operating conditions is required. HCCI combustion will require complex control strategies to be developed and implemented in order to allow the passage from HCCI to conventional or PCCI combustion. On the other hand, there are fewer boundaries to the PCCI combustion in terms of speed and load. The approach can be generalised to the higher speeds and loads, and in the cases where a fully-premixed-charge, i.e. PCCI combustion, is not achieved, the only consequence will be the reappearance of diffusion combustion and hence more NO_x and soot emissions. This gives it a substantial advantage over HCCI combustion.

The PCCI combustion has been applied to the primary key points in an aim to exploit its low NO_x and soot emissions benefits. High EGR rates with low AFRs were used to reduce the oxygen concentration. Late single injections were used in combination with high injection pressures in order to minimise HC, CO and soot emissions. The high injection pressures also assisted in terms of fuel conversion efficiency. An 8-hole injector nozzle was used for the PCCI study instead of the 7 hole injector nozzle used in the previous experiments. The hole size was the same but the additional hole increased the flow of the injector. It is believed that this measure contributes to shorter injection durations whilst providing similar fuel-air interactions. AFR, EGR rate, injection timing and pressure were varied on the single-cylinder Build #2 engine, optimised operating conditions were defined using tested or interpolated points and these are summarised in Table 6-2. For comparison, typical Euro 4 results from the 4-cylinder version of the engine as well as the Euro 5 results from the Build #1 engine are included. The 4-cylinder engine fuel consumption values are factored for the difference between the single and 4-cylinder engines observed during the single to 4-cylinder engine matching phase. This enabled the results to be compared as if they had all been obtained on the single-cylinder engine.

The optimum PCCI points were selected as they reduced NO_x emissions from Euro 4 to PCCI by approximately 90 %, representative of requirements to meet future US Tier 2 Bin 5 or possible Euro 6 targets defined by simulation on a 1600 kg inertia vehicle without NO_x after-treatment. Compared with PCCI operation results from Kimura et al. (2001), the present NO_x emissions are lower by a factor of 5, from 50 to 10 ppm at 1500 rev/min 5 bar BMEP, whereas HC emissions are increased form 200 to 450 ppm. Compared with HCCI operation results from Gatellier and Walter (2002), at 1500 rev/min 5 bar BMEP, the present NO_x emissions are higher by a factor of 8, from 0.014 to 0.119 whereas HC emissions are reduced by a factor of 10, from 8.1 to 0.8 g/kWh. Despite not reducing NOx emissions as much as HCCI operation, the results being achieved in a in an evolutionary but conventional combustion system. The comparisons with the HCCI results were made using the friction and pumping losses recorded during the experiments in Chapter 4, which is a similar assumption to the one made by Gatellier and Walter as they used losses of 2.0 bar MEP and the losses were of 1.6 bar MEP, from 5 bar BMEP to 6.6 bar GIMEP.

The start of injection from Euro 4 to PCCI operation was not necessarily retarded. It was advanced in some cases to compensate for the increased auto-ignition delay. However, the start of combustion was systematically retarded relative to the start of injection (detailed in Figure 6-29). Soot emissions were not necessarily lower, however, diesel particulate filters assumed necessary for Euro 5 would trap these emissions. This is due to the fact that HC emissions decrease as the injection timing is retarded in PCCI combustion, as can be seen in Figure 6-20, however, the timing retard was limited to cap the fuel consumption increase at 5 %. Soot emissions were particularly high at key point P3, which could be dealt with by increasing the oxygen concentration and hence NO_x emissions. Exhaust temperatures increased from Euro 4 to Euro 5 operation and decreased from Euro 5 to PCCI operation. It is believed that for the Euro 5 results the later combustion increased the exhaust temperatures despite lower peak and average temperatures in the cylinder. However, the PCCI results were for combustion that did not take place much later in the expansion cycle but with a further reduction in peak and average temperatures, thus lowering the exhaust-manifold temperatures.

	P1: 1500 rev/min 3.0 bar GIMEP (1.3 kW) (1)			P2: 1500 rev/min 6.6 bar GIMEP (3.1 kW) (1)		
Operating conditions	Euro 4	Euro 5	PCCI	Euro 4	Euro 5	PCCI
Fuel consumption (kg/h)	0.43	0.39	0.41	0.84	0.85	0.88
Wet EGR rate (%)	34.0	45.4	58.0	16.0	28.1	59.0
Dry AFR (-)	31.0	29.3	21.0	26.0	22.0	20.0
EGR/Lambda	15.9	22.5	40	8.9	18.5	42.8
Injection pressure (bar)	559	545	750	925	900	1500
Swirl throttle (% shut)	N/A	46	100	N/A	65	100
Pilot separation (°CA)	24.0	26.0	N/A	24.5	26.0	N/A
SOI (°CA ATDC)	3.1	0.0	-6.0	2.2	5.0	0.0
Pilot duration (µs)	375	300	N/A	310	260	N/A
Combustion noise (dB A)	83.6	84.3	73.6	83.5	88.2	91.0
HC (g/h)	1.09	1.57	7.12	0.79	N/A	2.49
CO (g/h)	14.49	16.81	38.43	7.98	10.33	24.95
NO_x (g/h)	1.18	0.78	0.13	7.05	2.61	0.37
Soot (g/h)	0.19	0.16	0.00	0.18	0.17	0.12
Smoke (FSN)	0.94	0.91	0.00	0.65	0.64	0.50
Max dP/dt (bar/ms)	N/A	N/A	40	N/A	N/A	102
Exhaust temperature (°C)	234	245	238	331	429	315

	P3: 2000 rev/min 7.7 bar GIMEP (5.0 kW)(1)			P4: 2000 rev/min 10.8 bar GIMEP (8.3 kW) (1)			P5: 2000 rev/min 17.2 bar GIMEP (13.3 kW) (1)		
Operating conditions	Euro 4	Euro 5	PCCI	Euro 4	Euro 5	PCCI	Euro 4	Euro 5	PCCI
Fuel consumption (kg/h)	1.20	1.29	1.25	1.78	1.88	1.85	2.86	2.92	2.90
Wet EGR rate (%)	11.0	31.3	56.0	11.0	21.3	45.0	1.0	14.0	27.0
Dry AFR (-)	23.0	21.6	20.0	23.0	21.1	20.0	22.0	18.3	20.0
EGR/Lambda	6.9	21.0	40.6	6.9	14.6	32.6	0.7	11.1	19.7
Injection pressure (bar)	1065	1070	1600	1119	1190	1600	1129	1197	1600
Swirl throttle (% shut)	N/A	64	73	N/A	0	66	N/A	0	0
Pilot separation (°CA)	32.5	33.0	N/A	N/A	N/A	N/A	N/A	N/A	N/A
SOI (°CA ATDC)	0.6	0.0	-2.5	-1.3	3.0	3.0	-4.4	-2.0	0.5
Pilot duration (µs)	280	210	N/A	N/A	N/A	N/A	N/A	N/A	N/A
Combustion noise (dB A)	85.2	87.9	92.5	85.2	88.4	90.5	85.1	83.8	88.0
HC (g/h)	1.06	1.88	0.96	1.49	1.60	1.99	1.70	1.79	1.70
CO (g/h)	6.60	14.46	16.64	9.29	15.99	14.98	7.60	26.86	9.90
NO_x (g/h)	10.68	3.62	0.96	30.33	8.65	2.16	127.12	27.32	14.15
Soot (g/h)	0.20	0.92	2.56	0.28	1.98	1.35	0.13	7.60	0.37
Smoke (FSN)	0.51	1.62	3.00	0.51	2.07	2.00	0.18	3.46	0.48
Max dP/dt (bar/ms)	N/A	N/A	101	N/A	N/A	89	N/A	N/A	98
Exhaust temperature (°C)	392	450	377	470	508	478	517	588	544

(1): Brake power calculated using losses in Chapter 4.

Table 6-2: Results of PCCI operation applied at primary key points.

As appealing as these results may be, two remarks must be added. The first relates to the increase in fuel consumption limited to 5 %. This would enable the diesel engine to remain competitive with the gasoline engine in terms of fuel economy. However, as described earlier, the tests were conducted at constant gross load. It is therefore expected that fuel consumption should increase in a stand-alone 4-cylinder engine for the same brake output, as the extra pumping losses from the turbocharger will need compensation. It is expected that this could represent an extra 10 % increase in fuel consumption. Equally, the swirl throttling system and the increased fuel injection

pressure would also represent additional parasitic losses, affecting the pumping and friction losses, but their impact is not expected to be as significant. The second point of concern relates to noise, traditionally reduced using pilot injection. This would conflict with PCCI combustion by attempting to limit the premixed-combustion phase. It is expected that lower compression ratios or higher levels of dilution will reduce the rate of combustion and assist in reducing noise.

The reduction in oxygen concentration and the corresponding impact on NO_x emissions from Euro 4 to PCCI operation can be seen in Figure 6-28. The increased mixing time typical of PCCI operation is also compared with those for typical Euro 4 operation in Figure 6-29. Durations used in the figure are from actual PCCI operating conditions test data shown in the table or from the nearest test data when interpolated results are given. The decrease in pulse duration due to increased injection pressures and higher injector-nozzle flow from Euro 5 to PCCI is clear. The increase in mixing time trend is also clear, however, the actual premix ratios are below unity at the higher load key points P3 and P4 and far from below unity for key point P5, due to the long injection duration and short auto-ignition delay.

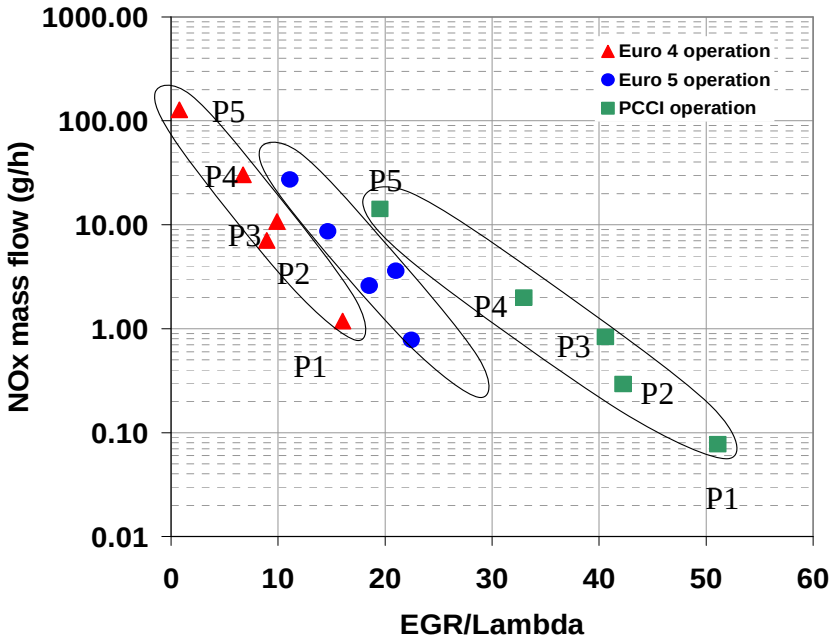

Figure 6-28: NO_x versus EGR/Lambda from Euro 4 to PCCI operation.

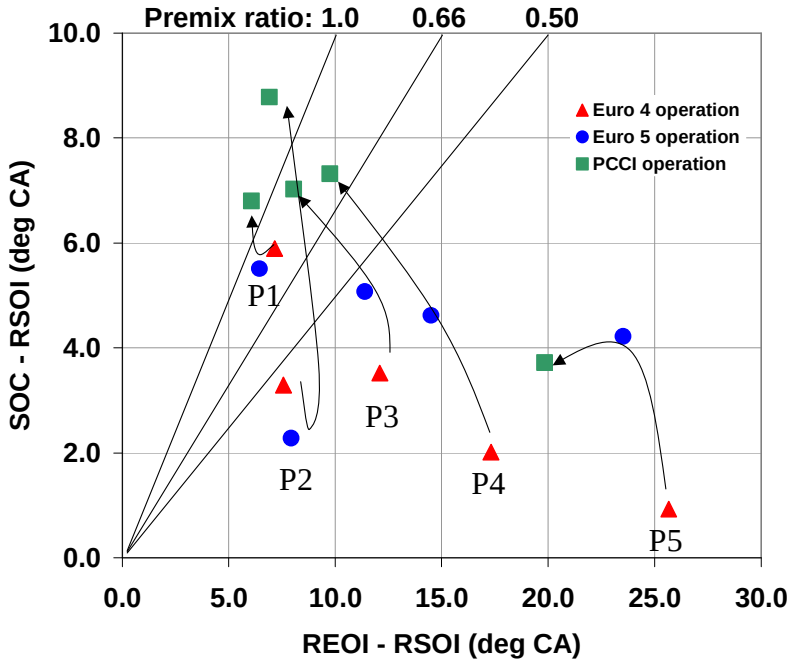

Figure 6-29: Mixing time evolution from Euro 4 to PCCI operation.

Plots of the oxygen concentration across the speed and load range of the engine are shown in Figure 6-30 for the calibrations necessary to meet the three different levels Euro 4, Euro 5 and Tier 2 Bin 5 or possible Euro 6. The associated reduction in oxygen concentration is clear. This does not mean that the oxygen mass in the cylinder is reduced but that the EGR rates are increased. This points up the need for high inlet-manifold pressure capability to balance the EGR pressure and meet oxygen requirements for the combustion. Large regions are at 21 % oxygen concentration at higher speeds and loads where emissions are not regulated. In the PCCI combustion map, the low oxygen concentration zone is stretched towards higher loads since the regulated speed and load zone is larger for the Tier 2 Bin 5 regulations.

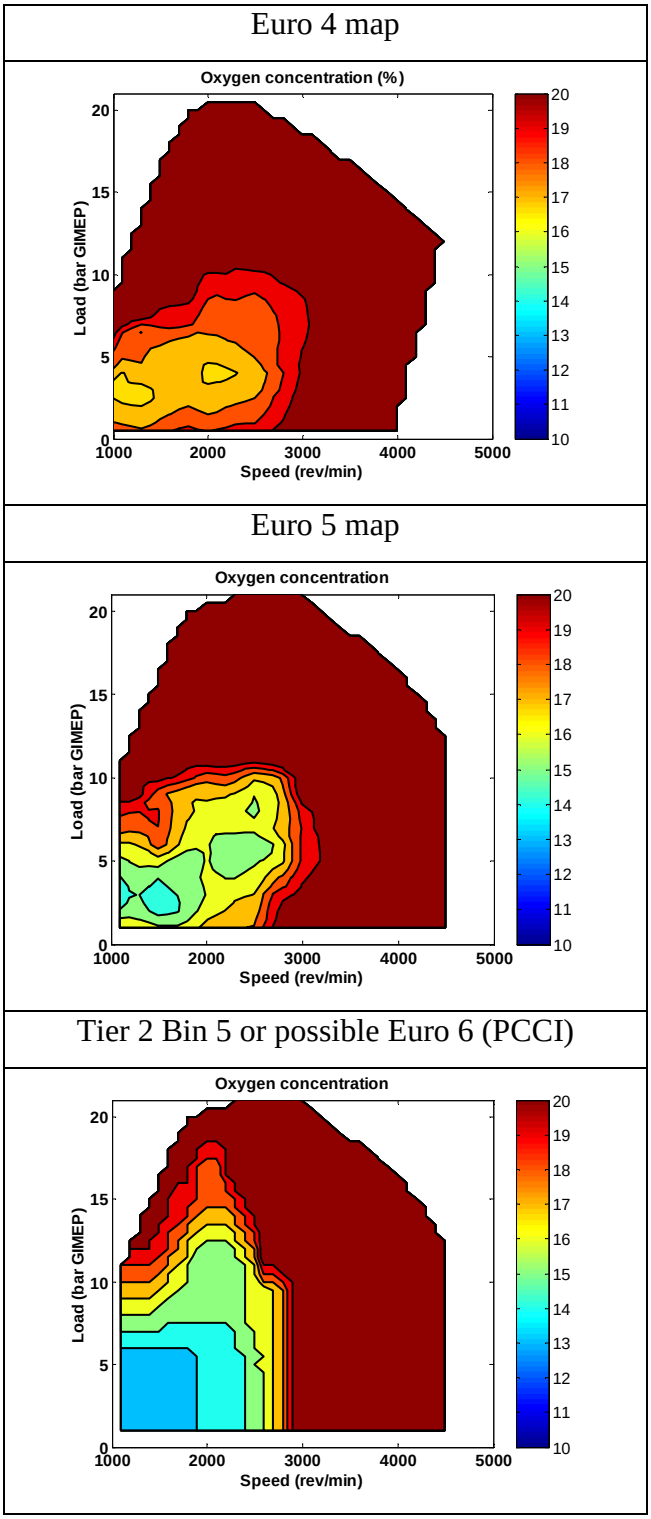

Figure 6-30: Oxygen concentration from Euro 4 to PCCI operation.

6.6 Conclusions

This chapter has offered an understanding of the requirements for advanced combustion operating conditions for ultra-low NO_x and soot emissions as well as their

impact on the subsequent combustion. This was achieved by conducting injection-timing responses with different oxygen concentrations and injection pressures at two different loads whilst maintaining all the other operating conditions constant. The impact on emissions and fuel consumption was explained through an analysis of the in-cylinder and combustion characteristics. Some of the results obtained here can be compared with those from Kawano et al. (2005), as closing the intake valve later leads to reduced oxygen concentration, however, the present study has also dissociated that effect from reduced compression ratio. The main conclusions from this chapter are:

- Two timing regions were identified where NO_x and soot emissions were reduced. The early region yielded HCCI combustion and the late region resulted in PCCI combustion
- At light load, reduced AFRs and increased EGR rates to lower oxygen concentration combined with early or late injection timing resulted in ultra-low NO_x and soot emissions. The impact on combustion was similar to that of reducing compression ratio or retarding injection timing in terms of reducing the rate of combustion as seen in the reduced maximum rate of pressure change
- At light load, for values of EGR/Lambda above 45, the combustion was decoupled from the injection, which made it insensitive to injection pressure
- At light load, injection timings before -28 °CA ATDC in low in-cylinder pressures and temperatures led to increased premix ratios. These cumulative effects delayed start of combustion and reduced its rate, leading to a reversal in the NO_x emissions profile and HCCI combustion. At medium load, injecting early enough to increase premix ratios was not possible due to the combustion chamber design. The earliest injection timings tested were always in conditions suitable for auto-ignition, which did not give time for the mixture to lean out and led to rapid rates of combustion
- At light and medium load, lower oxygen concentration with late injection timings, leading to PCCI combustion, also reduced NO_x and soot emissions. Reductions in NO_x emissions of 90 % across the primary key points extended the benefits of PCCI combustion. Fuel consumption, HC and CO emissions and noise remain the main concerns

- The lower oxygen concentration, or higher heat capacity if AFR is fixed, and the increased mixing time given for an appropriate choice of injection timing contribute to the leaning out of the fuel-air mixture and to the limitation of the flame temperature
- In terms of choice of parameters to correlate with NO_x emissions, it can be seen that maximum rate of pressure change and oxygen concentration are good choices
- The main factor for good fuel consumption was a phasing of the combustion just after TDC. Retarding the injection timing too much inevitably increases fuel consumption. Early injection timings associated with sufficiently low oxygen concentrations can lead to good fuel consumption, thanks to the resultant slow but well-phased combustion
- For future applications, still lower compression ratios would achieve similar NO_x emissions with more advanced injection timings. This would lower soot emissions and may be beneficial in the NO_x emissions versus fuel consumption trade-off, as shown in the Chapter 5. However, noise, HC and CO emissions as well as cold-start behaviours will need to be addressed, but any solution may be simpler than implementing NO_x after-treatment systems
- Inlet-manifold temperature, level of swirl, multiple injections are expected to have some impact on the combustion, but these are expected to be secondary.

7 SIMPLIFIED NO_X FORMATION CONCEPT

7.1 Introduction

Observations and findings presented in Chapters 5 and 6 showed that NO_x emissions were very closely linked to injection timing, compression ratio and to the combination of AFR and EGR rate, that determine the oxygen concentration in the mixture. The injection timing and compression ratio determine the initial pressure and temperature conditions at the start of combustion and their development during the combustion process. The oxygen concentration in the cylinder determines the maximum flame temperature during the combustion, as illustrated by the modelling results of Nakayama et al. (2003) using the extended Zeldovich mechanism. In light of future emissions legislation, where it is accepted that targeted levels of NO_x emissions will be smaller than the present variability in emissions, improvements are required, not only in terms of meeting the targets, but equally in terms of achieving them over a prolonged period. Potential advanced combustion operations have been assessed and have shown capabilities of achieving ultra-low NO_x and soot emissions. However, their knife-edge aspect means that any small variation in operating conditions can have a huge effect on emissions. In terms of soot emissions, it is likely these can be trapped by a particulate filter. However, in terms of NO_x emissions, where the wish is to avoid after-treatment by using HCCI or PCCI operation, small variations in operating conditions will have large effects on tailpipe emissions. This will be one of the main challenges for advanced combustion operation that aims to avoid the use of NO_x after-treatment systems.

The main objective of this chapter is to propose a new simplified concept for NO_x formation based on findings from previous experiments and to present the justification for this hypothesis. It is suggested that this concept is used as foundation for closed-loop systems aiming to control NO_x emissions accurately. This concept is based on the close relationship demonstrated between NO_x emissions and both the oxygen concentration and the maximum rate of pressure change. It has also some potential to be used independently of load in operating regions of the engine where diffusion combustion is suppressed. Some hypotheses have been made to justify this possibility. Other objectives of the chapter are to present the potential applications of the concept

to development and operation of advanced combustion systems together with an indication of its limitations.

7.2 Background

Accurate control of the engine operating conditions is essential for the implementation of robust advanced combustion systems. Currently, the majority of injection control systems in diesel engines are model-based open-loop control systems, using the measurement of the air mass flow sensor, the engine speed and the pedal position to determine the level of fuelling. Some closed-loop control systems are in place to define when the regeneration of the particulate trap should occur, and which are based the monitoring of pressure drop across the trap. The next step in diesel engine injection control is likely to replace this open-loop by closed-loop control modes. This will offer not only accurate control but also reliable control during the engine lifetime since the system is based on feedback and can therefore self-compensate for ageing or drift effects of the hardware. The impact of a 10 % variation in the EGR rate can be seen in Figure 7-1, which demonstrates how sensitive the new combustion processes are compared with a more conventional Euro 5 operation, especially in the case of HCCI combustion, where early injection timings are used. This highlights the fact that control strategies need to be developed to compensate for eventual issues such as EGR system fouling and general wear of the engine. The controllers would also need to run periodical self-diagnostics to ensure good operations.

Some closed-loop control approaches have been discussed in Section 2.2.3, such as that of Nakayama et al. (2003), Olsson et al. (2001) or Neunteufl et al. (2004). The present concept is a development of the control concept of Gartner et al. (2002), which used the angle of 50 % burn and an indication of oxygen content in the cylinder, based on the air mass flow, as feedback. The angle of 50 % burn can remain a secondary control parameter for the control of fuel consumption, whereby setting a target value in between TDC and 10 °CA ATDC will ensure minimum fuel consumption, as demonstrated by results in Figure 6-23. For the present purposes where NO_x emissions are targeted, there is an opportunity to use rate of pressure change and oxygen concentration as feedback parameters in closed-loop control, as

they offered a good correlation with NO_x emissions for PCCI combustion, as well as for HCCI operation where combustion is decoupled from injection.

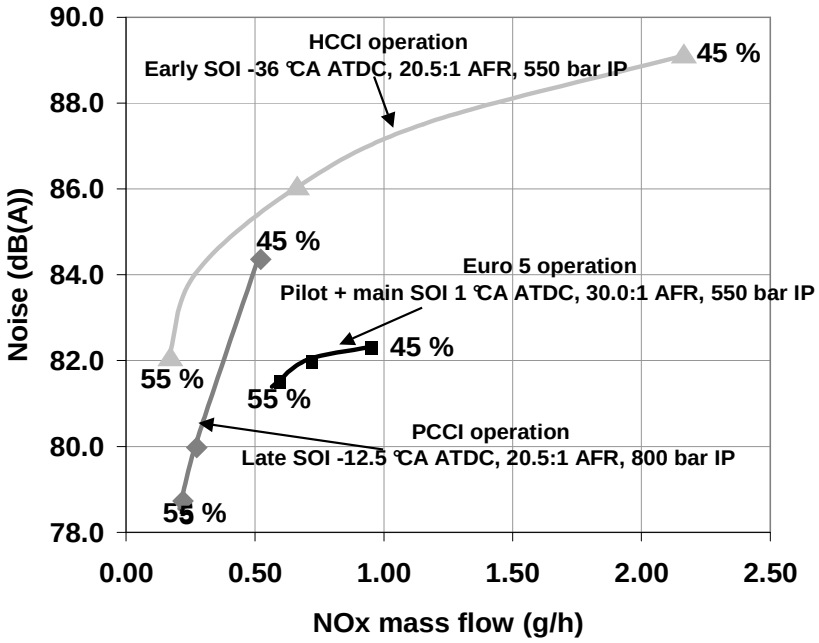

Figure 7-1: Sensitivity to EGR rate of advanced combustion.

7.3 Presentation of concept

The illustration of the potential for a simplified NO_x formation concept is shown in Figure 7-2 and Figure 7-3 where all the NO_x emissions data obtained at key point P1, 1500 rev/min 3.0 bar GIMEP, and key point P2, 6.6 bar GIMEP, respectively and described in Chapter 6 were included. The NO_x emissions data was plotted on a graph of oxygen concentration against maximum rate of pressure change. A representation of the spread of data is included in an insert in each figure.

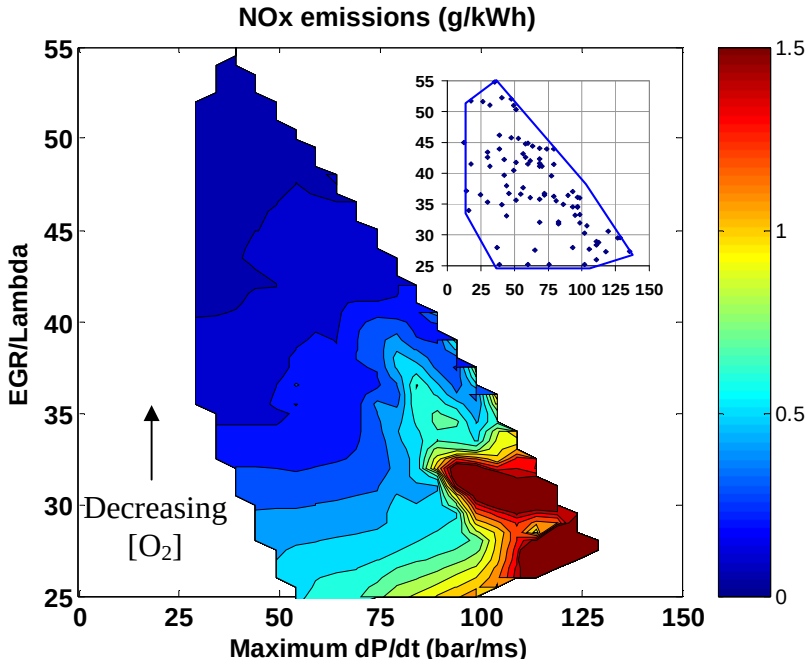

Figure 7-2: NO_x emissions versus EGR/Lambda & rate of pressure change (P1).

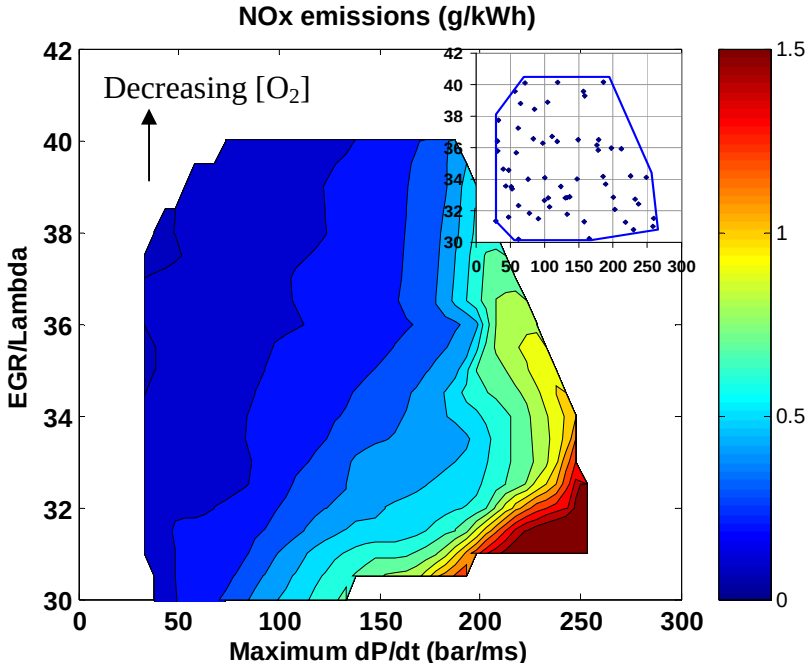

Figure 7-3: NO_x emissions versus EGR/Lambda & rate of pressure change (P2).

At the lower load, when the injection timing was advanced or retarded from -30 °CA ATDC, the rate of pressure change decreased, whereas at the higher load, the rate of pressure change decreased only when the injection timing was retarded. In both cases, bands of identical levels of NO_x emissions were visible, suggesting a direct relationship between the emissions and oxygen concentration and rate of pressure change. As the EGR rate over Lambda increased, the emissions decreased. Equally, as

the rate of pressure change decreased, the emissions decreased. The regularity of the bands disappeared when both higher oxygen concentrations and higher rates of pressure change were present, resulting in higher NO_x emissions regions. At key point P1, two separate high NO_x emissions regions are visible, which correspond to data from the two different injection pressures tested, where pressure is influential (EGR/Lambda lower than 45). These high NO_x emissions regions correspond to the appearance of diffusion combustion, which invalidates the concept as the emissions become function of local mixture parameters such as temperature and pressure and can no longer be associated with just two global variables. This represents one limitation of the concept which is valid only for fully-premixed-charge combustion, and does not have the complexity of the more complete Zeldovich mechanism.

Another aspect of the NO_x formation concept is illustrated in Figure 7-4 by associating the results at key point P1 and P2. As described earlier, the bands of identical NO_x emissions could also be seen despite the results coming from two different loads. The profiles of the bands were very close but some differences in the levels were visible. These remained small and in the order of 0.1 g/kWh, which corresponds to a difference of approximately 10 ppm by volume of emissions recorded at either load. This difference is small but becomes significant as emissions targets shrink. It is thought that three main contributors explained these differences. First, the inlet-manifold temperature was different at the two loads, which could affect NO_x formation and not be incorporated in the rate of pressure change. Second, the premix ratio could also contribute to the difference in emissions as higher NO_x emissions are expected with the lower premix ratios obtained at key point P2, as they indicate a lower homogeneity of the charge, and hence higher fuel-rich regions. The premix ratio could be compensated for by higher injection pressure at key point P2, which itself forms the third potential contributor to the difference between data sets. Injection pressure was 550 or 750 bar at key point P1 and 1000 bar at key point P2.

Figure 7-5 is an alternative representation of the results and offers a better understanding of where the concept is valid and where it reaches its limitations, as diffusion combustion appears. As the injection timing was varied, it led in some cases to high rates of pressure change. Having reached a maximum rate of pressure change, corresponding to the highest level of premixed-combustion at the highest rate of

combustion, the remaining fuel was burned during the diffusion-combustion phase. This no longer affected the maximum rate of pressure change but led to a large increase in NO_x emissions. This translates into the near vertical increases in NO_x emissions once the rate of pressure change has reached approximately 125 bar/ms at key point P1 and 230 bar/ms at key point P2.

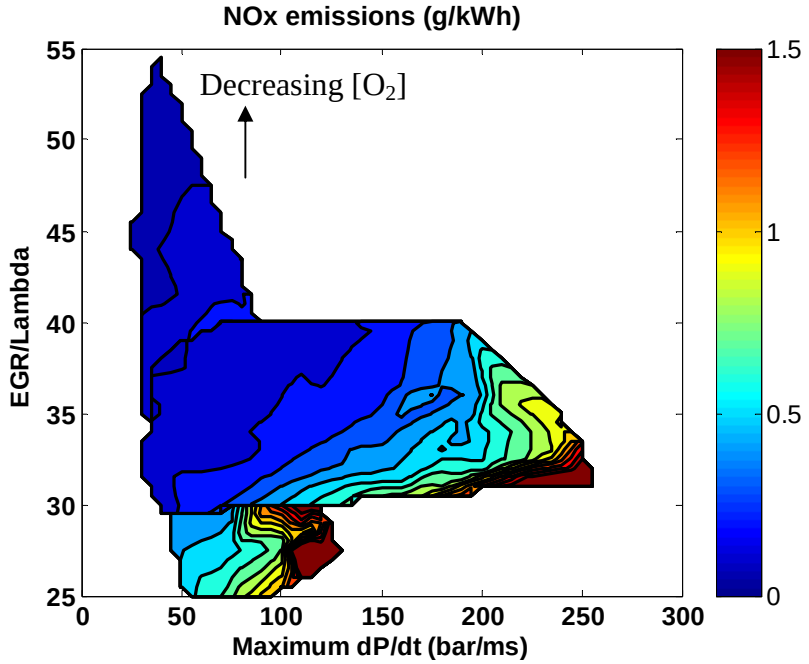

Figure 7-4: NO_x emissions versus EGR/Lambda and rate of pressure change (P1 & P2).

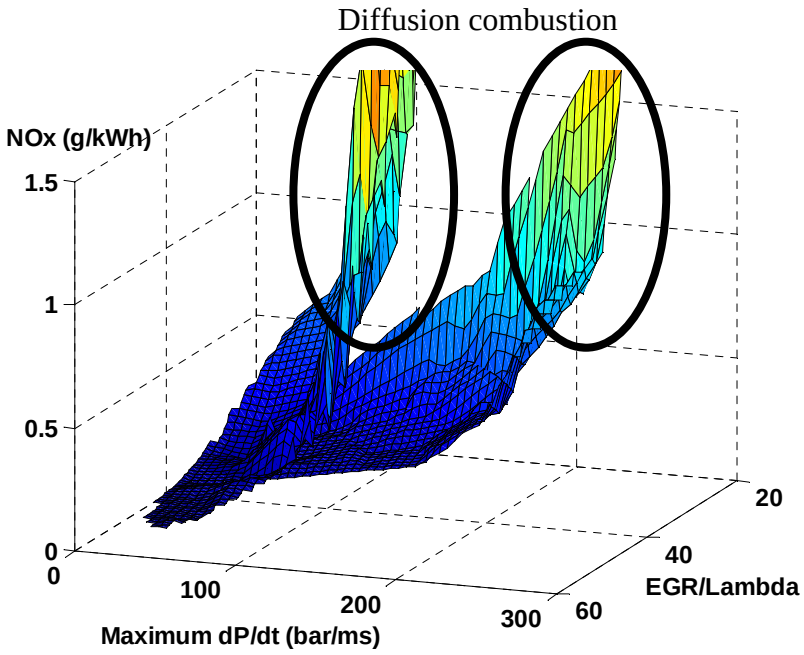

Figure 7-5: Surface plot of NO_x emissions versus EGR/Lambda and rate of pressure change at key points P1 and P2.

An equation was derived to characterise NO_x emissions as a function of the global parameters maximum rate of pressure change and EGR/Lambda. A correlation was obtained with the product of the contributing parameters at key points P1 and P2 for NO_x emissions below 1.0 g/kWh as follows:

$$NOx = 250 \cdot \left(\frac{EGR}{Lambda} \right)^{-3.07} \cdot \left(\frac{dP}{dt} \right)^{1.11} \qquad (7\text{-}1)$$

Where NOx is the specific NO_x emissions (g/kWh),

EGR is the EGR rate (% volume),

$Lambda$ is the relative air fuel ratio (-)

$\frac{dP}{dt}$ is the maximum rate of pressure change (bar/ms).

The equation reveals that EGR/Lambda is the dominant parameter contributing to NO_x formation. The predicted and measured results were cross-plotted giving confidence in this concept to predict or indicate NO_x formation, as can be seen by the coefficient of determination of 0.82 in Figure 7-6. When using Equation 7-1 with data from Table 6-2 at the higher speed and load (key points P3, P4 and P5), the predicted NO_x formation was higher than measured values in all cases. It is thought that varying degrees of diffusion combustion invalidate the concept under these conditions.

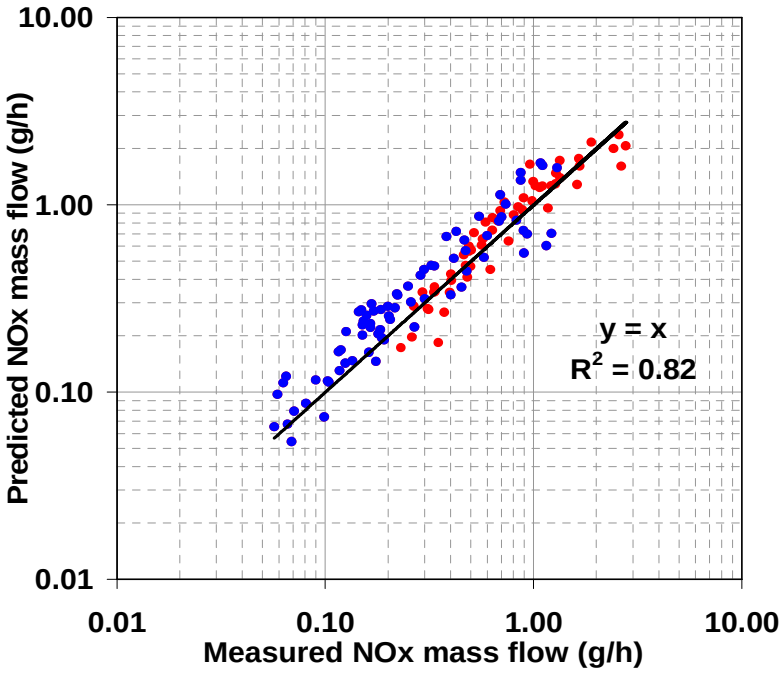

Figure 7-6: Measured versus predicted NO_x emissions (P1 & P2).

7.4 Justification of concept

The advanced combustion engine data assessed in Chapter 6 all indicated the need for increased levels of mixing of the charge prior to combustion in order to limit the flame temperature. In light of the increased homogeneity, it is assumed that the local in-cylinder characteristics, such as temperature, pressure, oxygen concentration, as well as combustion characteristics, such as flame temperature, effectively become global parameters. Measured values become representative of local values across the entire charge rather than an indication of their average, as depicted in Figure 7-7, where the inhomogeneity of a conventional combustion operation reveals a wide range of local excess air values, whereas the more homogeneous advanced operation is characterised by a single value. It is also believed that this explains the high sensitivity of advanced combustion operation seen in Figure 7-1. The microscopic aspects of the in-cylinder and combustion characteristics therefore take on more macroscopic aspects. This forms the foundation of the concept and explains why the rate of pressure change as well as oxygen concentration can be used as a simple NO_x formation indicator or predictor. The concept is made possible by the relative insensitivity of NO_x emissions to injection pressure and fuel and air interactions (piston-bowl geometry, protrusion, injector-nozzle configuration). An equivalent indicator of soot emissions would also be valuable but sensitivity to in-cylinder geometrical, physical and chemical factors make non-feasible.

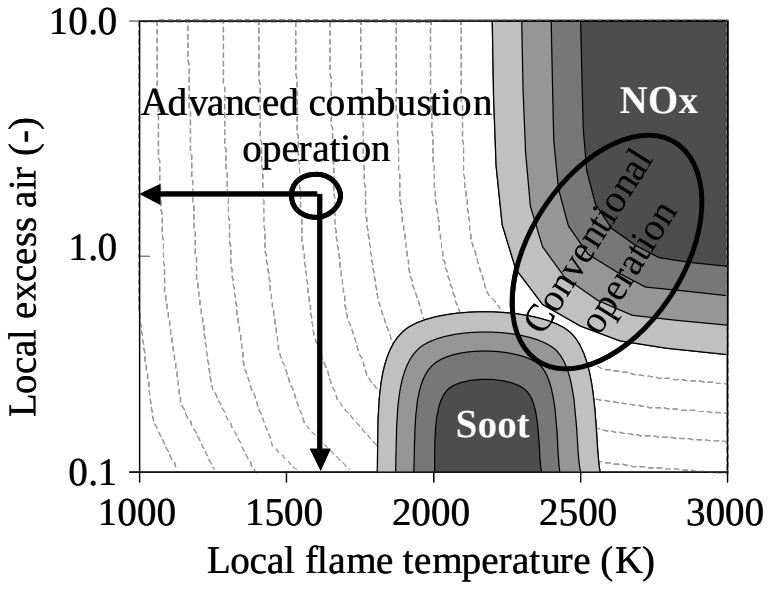

Figure 7-7: Summary from conventional to advanced combustion operation.

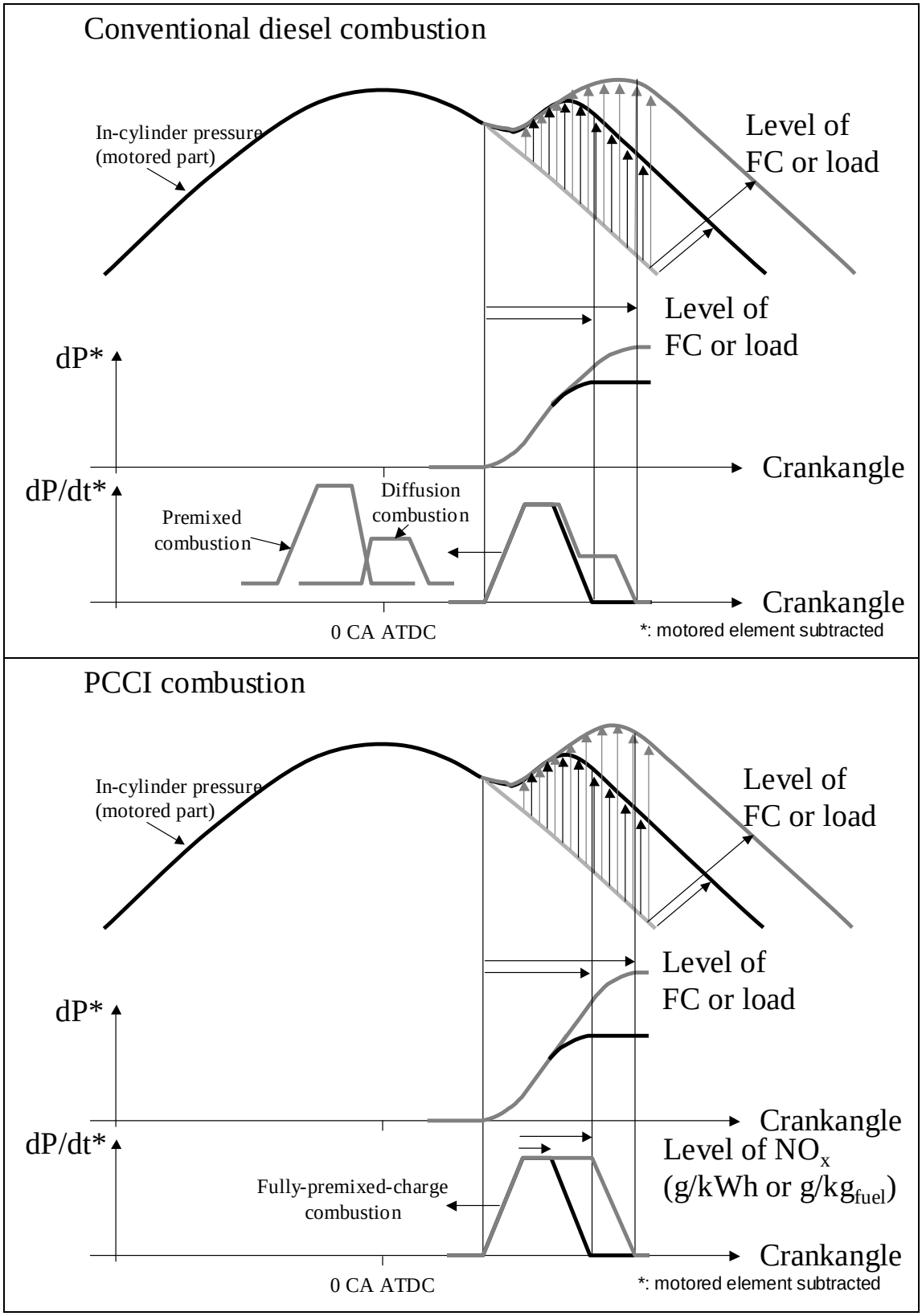

Figure 7-8: Summary of conventional and PCCI combustions.

Figure 7-8 describes how the in-cylinder and combustion characteristics are used to indicate NO_x emissions in advanced combustion. It also illustrates why this is not

possible with conventional diesel combustion, since the premixed combustion characteristics do not represent the NOx formation process during the diffusion-combustion phase. As displayed in the figure, the in-cylinder rates of pressure change in conventional diesel combustion exhibits two phases. An initial premixed-combustion phase with a high rate of pressure change was followed by a diffusion-combustion phase with a relatively lower rate of pressure change. Despite the lower rate, a high level of NO_x formation was expected from the diffusion-combustion phase since the burning mixture was closer to stoichiometric and at elevated temperatures due to the increased in-cylinder pressure and temperature resulting from the initial premixed-combustion phase. However, advanced combustion operation was characterised by fully-premixed-charge combustion, visible from the rates of in-cylinder pressure change. This formed the foundation of the concept, since the results of Chapter 6 showed that NO_x formation is directly proportional to two elements in fully-premixed-charge combustion. The first is the maximum rate of pressure change, which incorporates operating conditions such as in-cylinder pressure and temperature, as well as oxygen concentration and the second is oxygen concentration itself. The second part of the concept illustrated in Figure 7-4 was that NO_x formation could be made load independent by using indicated specific emissions relative either to fuelling or to gross load. The result is a particular level of NO_x formation for a given oxygen concentration and rate of pressure change, which could be transformed into total emissions when multiplied by load or fuelling. An interesting aspect of this result is that inlet-manifold temperature, injection pressure and combustion duration are very different at both key points, and yet NO_x formation is expressed by a very similar map. From Figure 7-8, the main assumption underpinning this is that the duration of the combustion, which could be associated with the rates of propagation and combustion, at the highest stable rate of pressure change reflects the total amount of NO_x emissions.

Additional remarks can be made concerning the initial and final stages of the combustion. An initiation combustion phase occurred which led to limited rates of pressure change due to the limited amount of fuel burning. The cause of this behaviour was believed to be linked with the chemical properties of the fuel (aromatics) not reaching auto-ignition conditions simultaneously and to some variability in the level of physical homogeneity. A termination phase of the

combustion which resembled the initiation phase also occurred. It is likely to be associated with isolated combustion of the charge remaining after the bulk of the combustion. Both these components of the combustion are neglected in the concept as they represent only a small portion of the emissions.

The following assumptions have been made in developing the concept:

- Air utilisation must be optimised for there to be negligible impact on the NO_x formation. As long as this is achieved, the injector-nozzle configuration and protrusion, combustion chamber design and fuel path in the combustion chamber can be ignored
- Combustion is of a fully-premixed-charge type. Small traces of diffusion combustion may not be tolerated since they are likely to invalidate the concept as they would contribute to NO_x formation, without it showing in the maximum rates of pressure change
- Injection pressure affects the premix ratio rather than increases the level of premixed combustion since diffusion combustion is already negligible. Its effect is expected to be incorporated in the rate of pressure change
- The effect of in-cylinder temperature is also expected to be included in the rate of pressure change
- A certain premix ratio must be achieved to guarantee the mixture homogeneity is sufficient to consider local parameters as representative of global ones, i.e. requiring low oxygen concentrations and late or early injection timings depending on the load
- The combustion of one zone of fuel has minimal impact on the in-cylinder conditions of surrounding zones due to the rapid and global nature of the combustion. The global parameters such as the in-cylinder rate of pressure change and oxygen concentration are representative of each zone of fuel burning rather than an average of different rates of pressure change in the cylinder
- All the fuel does not burn instantly and simultaneously. The maximum rate of pressure change is a function of in-cylinder pressure and temperature and the

oxygen concentration. The time spent at the maximum rate is a function of the rates of propagation and combustion.

7.5 Benefits and limitations

There are two main benefits of the proposed NO_x formation concept. The first is the fact that NO_x formation can be predicted or indicated using two global variables and that local variables, impossible to measure in the present engine were not necessary. The second is that they can be expressed independently of load, injection pressure and inlet-manifold temperature, making it generic. The latter has been proven in the present research programme at light and medium loads where advanced combustion operating conditions were used at very different operating conditions. It is believed that this is allowed by the maximum rate of pressure change, which incorporates the impact of the in-cylinder and mixture conditions on the rate of combustion, such as in-cylinder pressure and temperature, therefore taking into account both the injection timing and the compression ratio. The expression of the emissions in g/kWh or g/kg_{fuel} and of the rate of pressure change in bar/ms rather than bar/°CA also assisted in its generic nature.

There are several fields where such a concept would be beneficial. A first would be in the field of simulation, where both computational fluid dynamics and 0 and 1 dimensional models are used. The concept offers a predictive tool for NO_x emissions based on the oxygen concentration and rate of pressure change when advanced combustion operation is envisaged. This would also allow some form of prediction to be made in computational fluid dynamics, without the need for complex calculations based on the chemical models and the Zeldovich mechanism. A second would be in the field of engine calibration, where design of experiments is often used to optimise the engine parameters such as air mass flow, injection timing, AFR and EGR rate at several key points. Rather than aiming for a low NO_x emissions target using a model-based open-loop control mode, it would be more advantageous to aim for actual target rates of pressure change and oxygen concentration at the several key points, as these would represent feedback conditions directly controlling NO_x emissions. In a related engine control field, advanced combustion operation will

require model-based closed-loop control systems, thus using the results of the current operating condition to define the following operating condition. The rate of pressure change forms a target and is assessed at each engine cycle and in each cylinder. Any difference with the target triggers a screening of the operating conditions. Should the rate of pressure change be too high, a reduction of the oxygen concentration or a retardation of the injection timing would be implemented. An increase of the injection pressure could also be envisaged to increase the premix ratio. This would help the controller to identify the fault and to compensate for it. A potential benefit of using the rate of pressure change also resides in the type of sensor required: a sensor such as an accelerometer could provide valuable information to the controller, which could reflect the rate of pressure change achieved during the fully-premixed-charge combustion, without the need to be intrusive. Other expensive in-cylinder pressure transducers could be used and would provide additional quantitative information such as the maximum level of pressure and its angular location as well as combustion characteristics such as the angle of 50 % burn, useful in terms of fuel economy monitoring.

The main limitation of the concept is that it is no longer valid as soon as there is diffusion combustion. With the current single-cylinder engine, this translated into a load limitation of 1500 rev/min 6.6 bar GIMEP. This poses a problem for emissions legislation such as future US Tier 2 Bin 5 since these also target higher load conditions. Currently, the moderately reduced compression ratio, the available injection system and EGR rate capabilities present load limitations as illustrated by the premix ratios. However, these may be extended by future developments in advanced combustion operation and the associated hardware. Another uncertainty concerning the validity of the concept is the limited understanding of the impact of the inlet-manifold temperature and injection pressure. At this stage it is unclear whether these operating conditions would increase the rate of the pressure change, therefore increase NO_x emissions whilst remaining on the surface in Figure 7-5 or whether the response will require further superimposed surfaces.

7.6 Conclusions

The simplified NO_x formation concept offers an approach to the control of advanced combustion operation. It has been achieved through a better understanding of the impact of advanced combustion on combustion characteristics and on NO_x emissions. The main conclusions from this chapter are:

- High sensitivity to operating conditions leads to high variation in noise and NO_x emissions. This is a concern for the application of advanced combustion strategies where ultra-low emissions are targeted
- The concept is based on the existence of a single combustion phase, i.e. a fully-premixed-charge combustion and associates NO_x emissions with the oxygen concentration and the rate of pressure change. It is justified by the fact that high levels of mixing give local variables a more global meaning, therefore allowing global measurements to represent the combustion and the NO_x formation
- The duration at the maximum rate of pressure change is a function of the level of fuelling or load, and determines the total NO_x emissions
- Clear bands of NO_x emissions versus oxygen concentration and rate of pressure change were seen at key points P1 and P2. The profile of these bands were very similar and an equation was derived which fit reasonably well the data and demonstrates that the concept can be applicable across load conditions, despite different inlet-manifold temperatures, injection pressures and loads
- High NO_x emissions regions were found with high oxygen concentration and rates of pressure change, highlighting the presence of diffusion combustion and invalidating the concept in those regions
- There are several applications in which the concept may be of value, such as in simulation, engine calibration and engine control.

8 CONCLUSIONS AND RECOMMENDATIONS FOR FUTURE WORK

8.1 Conclusions

Many research programmes have focused on reducing engine-out emissions by applying advanced combustion operation. Results have highlighted the potential for achieving ultra-low NO_x and soot emissions by using early injection timings associated with low AFR, highly cooled EGR rates and high injection pressures, yielding HCCI combustion. However, it has been shown that this approach leads to extremely high HC and CO emissions and is limited to lower load ranges. The load constraint also implies issues regarding transient control when passing through operation modes. Late injection timings have been shown to yield PCCI combustion. It is clear that PCCI operation does not present the same low NO_x emissions nor does it present the same increase in HC and CO emissions, however, its ease of implementation and its less complicated control requirements make it a very appealing short-to-medium term solution. The work described here has extended the limits for PCCI operation to result in a further decrease in NO_x and soot emissions over a broader operating region. This approach has aimed to achieve HCCI operation NO_x and soot emissions results whilst minimising HC and CO emissions. The exploration of the fundamentals of diesel combustion to achieve low engine-out emissions has resulted in an improved understanding of the in-cylinder phenomena and the relationship with emissions.

In order to allow an extensive exploration, a single-cylinder diesel engine was employed and the test cell was developed such that operating conditions could be set independently precluding the limitation imposed by multi-cylinder production hardware characteristics. A single to 4-cylinder engine matching was accomplished to ensure realistic operation of the research engine and to demonstrate the validity of conducting subsequent research on such a facility. This consisted of correlating Euro 5 style 4-cylinder engine operating conditions with the single-cylinder engine at eight part load and three full load conditions. Firstly the single-cylinder engine gas exchange processes were equated to the 4-cylinder engine for each load condition, by establishing exhaust valves settings and an orifice plate that offered and appropriate representation of the engine after-treatment and turbocharger. Secondly, injection-

timing and swirl responses were conducted. Operating conditions were selected which provided a good match in terms of NO_x and soot emissions, fuel consumption and load. This also formed a solid baseline for future investigations. Ultimately, the transferability has been verified since a reverse correlation (single-cylinder to 4-cylinder engine) has been successfully demonstrated subsequent to this programme. The results have not been presented for reasons of confidentiality.

Once a series of reference points was acquired, investigations were carried out to analyse the impact of reducing compression ratio and of modifying the inlet ports to increase their flow capabilities. These changes represented an evolution of the conventional combustion system and are likely in the near future. The effect of these hardware changes was assessed across three part load conditions and one full load condition, whilst maintaining fixed all operating conditions. At part load, soot and NO_x emissions were reduced with the latter effect diminishing as injection timing was retarded. Fuel consumption was generally unchanged but HC and CO emissions increased. It was concluded that lower pressure and temperature during the injection and combustion promoted fuel-air mixing, which reduced both the rate of combustion and proportion of diffusion combustion. When diffusion combustion was suppressed, the results showed NO_x emissions to be less sensitive to in-cylinder pressure and temperature. It was found that when the starting point was a fully-premixed-charge combustion, reducing the compression ratio decreased the maximum rate of pressure change, whereas when diffusion combustion was present, its reduction fuelled the premixed combustion thereby increasing the maximum rate of pressure change. At full load, increased load capabilities were possible by advancing the injection timing further and reduced smoke emissions were possible for the same inlet-manifold pressure due to the increased volumetric efficiency. These investigations illustrated that reducing compression ratio offered similar benefits as retarding injection timing, but that noise emissions were increased with combined premixed and diffusion combustion. They also illustrated the potential to increase full load capabilities making compression ratio reduction a favoured option for future diesel engines.

Having observed the impact of compression ratio on reducing the rate of combustion and suppressing diffusion combustion, further means were investigated to pursue this approach. Oxygen concentration and injection timing have been identified as key

enablers and were assessed in an aim to extend the limits for PCCI and HCCI operation, whilst developing understanding of the relationship between emissions and in-cylinder and combustion characteristics. The main effects of lowering oxygen concentration were to increase the heat capacity and to delay auto-ignition. Injection timing also contributed to increasing auto-ignition delay. The increased mixing time resulted in a leaner mixture prior to auto-ignition and, combined with the increased heat capacity, limited the rate of combustion and maximum flame temperature. This was observed at 1500 rev/min 3.0 bar GIMEP where ultra-low NO_x and soot emissions were obtained. The rates of pressure change reduced as oxygen concentration decreased and at the most advanced or retarded injection timing tested, yielding HCCI or PCCI operation respectively. At the higher load of 1500 rev/min 6.6 bar GIMEP, ultra-low NO_x emissions were achieved only at the most retarded injection timing. It was shown that the early injection timings tested at light load were not sufficient early to obtain a level of mixing, which could delay auto-ignition at the higher load. Only much earlier injection timings (with adapted nozzle and combustion chamber designs) would provide sufficient mixing to retarding the auto-ignition. In addition to these findings, for extreme cases of oxygen concentration, evidence of the decoupling of combustion from the injection was given, which was confirmed by the insensitivity of NO_x emissions to injection pressure. In terms of other operating characteristics, soot emissions were not as predictable as NO_x emissions, and resulted from a compromise between mixing time, fuel-air-piston interactions, oxygen contents in the flame and in-cylinder temperature. HC and CO emissions were increased when reductions in NO_x emissions were made, highlighting one of the new trade-off curves for advanced diesel combustion. The other trade-off curve was with NO_x emissions and fuel consumption, where retarding injection timing increases fuel consumption but reduces NO_x emissions. The PCCI operation was then extended to higher loads to result in ultra-low NO_x emissions and reduced soot emissions without the uncontrolled increase in HC and CO emissions associated with HCCI operation. This was achieved by lowering global oxygen concentration, retarding injection timing and increasing injection pressure to promote PCCI combustion. This highlighted the high levels of inlet-manifold pressure and several other sources for increased fuel consumption, which further outlines the requirement for lower compression ratio rather than for more retarded injection timing or ultra high EGR rates to achieve ultra-low NO_x emissions.

Finally, the stringent limits on emissions for diesel engines in passenger-car applications require the emissions from future passenger-car engines to be controlled to levels which are within the limits of variation of today's engines. This calls for more complex control strategies, such as closed-loop control to facilitate the required combustion operation. A NO_x formation concept has been proposed for combustion characterisation, which associates NO_x emissions with the global oxygen concentration and the rate of pressure change. It has been proposed that it could offer a foundation for these control modes. When all the experimental data from two load conditions is collected together, it is shown that NO_x emissions come together in bands when plotting against oxygen concentration and maximum rate of pressure change. The potential for using macroscopic parameters to represent microscopic events is made possible by the increased homogeneity of the charge and the single-phase nature of the combustion. This NO_x formation concept uses only two variables to monitor NO_x emissions and could be beneficial in several fields, such as in simulation, engine calibration and engine control. It is thought that with the types of sensors required for monitoring rate of pressure change, i.e. accelerometers, currently available, cheap and easy to implement, this concept could prove to be a relatively simple solution in production engines.

8.2 Recommendations for future work

In the present research programme, a conservative evolution of the compression ratio has been adopted. This was made for cold-start and production-feasibility requirements. Sufficiently low NO_x emissions have been achieved to meet future emissions legislation, however, these were achieved with an increase in fuel consumption and extremely high levels of inlet-manifold pressures to compensate for the high EGR rates. The increased inlet-manifold pressures would result in extra parasitic losses, and hence fuelling to compensate for the turbine work and would therefore represent an additional fuel consumption increase. To minimise these drawbacks, a lower compression ratio could be implemented, allowing less retarded injection timings to be used and possibly lower levels of inlet-manifold pressures, which would both benefit fuel consumption. The expected increase in HC and CO emissions as well as cold-start issues will need to be addressed, however, these may

be easier to handle than implementing either a NO_x after-treatment system or an advanced air system. The lower compression ratio could also extend the PCCI operating region where diffusion combustion does not occur, offering confirmation of the simple NO_x formation concept applicability over a greater proportion of the drive cycle.

Other detailed investigations which could benefit the present work concern the effect of injection pressure, inlet-manifold temperature. Higher injection pressures could be beneficial to NO_x emissions since they would increase the premix ratio and enable the injection timing to be retarded whilst maintaining an appropriate combustion phasing for fuel economy reasons. A more detailed analysis of the impact of inlet-manifold temperature on the combustion and its rate of pressure change would provide a more complete NO_x formation concept. One of the main assumptions to justify load independency of the NO_x formation concept was based on a stable rate of pressure change during the combustion, limited by the rate of propagation and combustion. The evidence for this is lacking at this stage and would benefit from investigations in computational fluid dynamics and ultimately in an optical engine to observe the combustion process under fully-premixed-charge combustion. The optical engine would also provide evidence of the level of mixing and potentially of the regions of NO or HC formation.

REFERENCES

Akagawa, H., Miyamoto, T., Harada, A., Sasaki, S., Shimazaki, N., Hashizume, T., Tsujimura, K. (1999) "*Approaches to Solve Problems of the Premixed Lean Diesel Combustion*", SAE Paper 1999-01-0183

Aoyama, T., Hattori, Y., Mizuta, J., Sato, Y. (1996) "*An Experimental Study on Premixed-Charge Compression Ignition Gasoline Engine*", SAE Paper 960081

Araki, M., Umino, T., Obokata, T., Ishima, T., Shiga, S., Nakamura, H., Long, W.-Q., Murakami, A. (2005) "*Effects of Compression Ratio on Characteristics of PCCI Diesel Combustion with Hollow Cone Spray*", SAE Paper 2005-01-2130

Badami, M., Mallamo, F., Millo, F., Rossi, E., E. (2002) "*Influence of Multiple Injection Strategies on Emissions, Combustion Noise and BSFC of a DI Common Rail Diesel Engine*", SAE Paper 2002-01-0503

Bae, C. H., Kang, J. (2000) "*Diesel Spray Characteristics of Common-Rail VCO Nozzle Injector*", Proceedings of Thiesel 2000, Thermofluidynamic Processes in Diesel Engines, pp 57-66

Bae, C., Yu, J., Kang, J., Kong, J., Cuenca, R., Lee, K., O. (2002) "*The Influence of Injector Parameters on Diesel Spray*", Proceedings of Thiesel 2002, Thermo- and Fluid Dynamic Processes in Diesel Engines, pp. 55-66

Beatrice, C., Belardini, P., Bertoli, C., Lisbona, M., G., Rossi Sebastiano, G., M. (2002) "*Diesel Combustion Control in Common Rail Engines by New Injection Strategies*", International Journal of Engine Research, 2002, Volume 3, Number 1, pp. 23-36

Beatrice, C., Bertoli, C., Migliaccio, M. (2002) "*Basic Concepts of the homogeneous Charge Compression Ignition Engines*", ATA, Volume 55, Issue 7/8, pp. 226-234

Bjerregaard, R. (1999) "*Commission Recommendation of 5 February 1999 on the reduction of CO_2 emissions from passenger cars*", Official Journal of the European Communities, reference 1999/125/EC

Blessing, M., Köenig, G., Krüger, C., Michels, U., Schwarz, V. (2002) "*Analysis of Flow and Cavitation Phenomena in Diesel Injection Nozzles and its Effects on Spray and Mixture Formation*", Proceedings of Fuel Injection Systems Conference, 2002, number 3

Brooks, T., D., Pugh, G., J., Gambrill, R., Shayler, P., J. (2004) "*Investigating the Effects of Split Main Fuel Injection Parameters on NOx, Soot, HC and CO Emissions from a Light Duty Diesel Engine*", Proceedings of Internal Combustion Engine Performance and Emissions Conference, 2004, pp. 1-12

Browne, K., R., Partridge, I., M., Greeves, G. (1986) "*Fuel Property Effects on Fuel/Air Mixing in an Experimental Diesel Engine*", SAE Paper 860223

Chi, Y., Cheong, J., Kim, C., Choi, K. (2002) "*Effects of VGT and Injection Parameters on Performance of HSDI Diesel Engine with Common Rail FIE System*", SAE Paper 2002-01-0504

Chmela, F., Riediger, H. (2000) "*Analysis Methods for the Effects of Injection Rate Control in Direct Injection Diesel Engines*", Proceedings of Thiesel 2000, Thermofluidynamic Processes in Diesel Engines, pp. 333-344

Christensen, M., Johansson, B. (2002) "*The Effect of In-Cylinder Flow and Turbulence on HCCI Operation*", SAE Paper 2002-01-2864

Crua, C. (2002) "*Combustion Processes in a Diesel Engine*", Thesis (PhD), University of Brighton, United Kingdom

Department for Transport web page, visited on 24th January 2003, www.roads.dft.gov.uk/cv/power/carbon

Flynn, P., Hunter, G., Durrett, R, Farrell, L., Akinyemi, W. (2000) "*Chemistry Limits on Minimum In-cylinder NOx Production for Internal Combustion Engines*", Proceedings of 21st Century Emissions Technology Conference, 2000, C588/027/2000

Gartner, U., Hohenberg, G., Daudel, H., Oelschlegel, H. (2002) "*Development and Application of a Semi-Empirical NOx Model to Various HD Diesel Engines*",

Proceedings of Thiesel 2002, Thermo- and Fluid Dynamic Processes in Diesel Engines, pp. 487-506

Garvine, A. (2002) "*One Giant Leap*", Interview of Armstrong, Engine Technology International, Issue 3/2002, pp. 20-23

Gatellier, B., Walter, B. (2002) "*Development of the High Power NADI^{TM} Concept Using Dual Mode Diesel Combustion to Achieve Zero NOx and Particulate Emissions*", Proceedings of Thiesel 2002, Thermo- and Fluid Dynamic Processes in Diesel Engines, pp. 131-143 and SAE Paper 2002-01-1744

Gill, D., Chmela, F., Jager, P. (2002) "*The Emissions and Performance Potential of a Pressure Modulated Common Rail Injection System on a Heavy Duty Diesel Engine*", Proceedings of Fuel Injection Systems Conference, 2002, number 10

Groenendijk, A., Müller, E. (2002) "*Mixture Formation and Combustion Control for Low Emission DI Diesel Combustion with HCCI-Characteristics*", Proceedings of Thiesel 2002, Thermo- and Fluid Dynamic Processes in Diesel Engines, pp. 145-157

Hasegawa, R., Yanagihara, H. (2003) "*HCCI Combustion in DI Diesel Engine*", SAE Paper 2003-01-0745

Henein, N., A., Lai, M.-C., Singh, I., Wang, D., Liu, L. (2001) "*Emissions Trade-Off and Combustion Characteristics of a High-Speed Direct Injection Diesel Engine*", SAE Paper 2001-01-0197

Henein, N., A., Singh, I., P., Zhong, L., Lai, M.-C., Bryzik, W. (2003) "*New Integrated "O.P.E.R.A.S." Strategies for Low Emissions in HSDI Diesel Engines*", SAE Paper 2003-01-0261

Heywood, J., B. (1988) "*Internal Combustion Engine Fundamentals*", McGraw-Hill series in mechanical engineering (a) pp. 505-506, (b) pp. 567-648, (c) pp. 170-172, (d) pp. 725-726, (e) pp. 836-839, (f) pp. 470-472, (g) pp. 539-552

Hultqvist, A. – Engdar, U., Johansson, B., Klingmann, J. (2001) "*Reacting Boundary Layers in a Homogeneous Charge Compression Ignition (HCCI) Engine*", SAE Paper 2001-01-1032

Iwabuchi, Y., Kawai, K., Shoji, T., Takeda, Y. (1999) "*Trial of New Concept Diesel Combustion System – Premixed Compression-Ignited Combustion*", SAE Paper 1999-01-0185

Jackson, N., S. (2000) "*The High Speed Direct Injection Diesel Engine – Future Potential*", Proceedings of Thiesel 2000, Thermofluidynamic Processes in Diesel Engines, pp. 33-42

Kaneko, M., Morikawa, K., Itoh, J., Saishu, Y. (2001) "*Study on Homogeneous Charge Compression Ignition Gasoline Engine*", Proceedings of COMODIA 2001, Fifth International Symposium on Diagnostics and Modeling of Combustion in Internal Combustion Engines, pp. 457-462

Kawamoto, K., Araki, T., Shinzawa, M., Kimura, S., Koide, S., Shibuya, M. (2004) "*Combination of Combustion Concept and Fuel Property for Ultra-Clean DI Diesel*", SAE Paper 2004-01-1868

Kawano, D., Suzuki, H., Ishii, H., Goto, Y., Odaka, M., Murata, Y., Kusaka, J., Daisho, Y. (2005) "*Ignition and Combustion Control of Diesel HCCI*", SAE Paper 2005-01-2132

Kawashima, J.-I., Ogawa, H., Tsuru, Y. (1998) "*Research on a Variable Swirl Intake Port for 4-Valve High-Speed DI Diesel Engines*", SAE Paper 982680

Kennaird, D., Crua, C., Lacoste, J., Heikal, M., Gold, M., Jackson, N. (2002) "*In-cylinder Penetration and Break-up of Diesel Sprays Using a Common-rail Injection System*", SAE Paper 2002-01-1626

Kidoguchi, Y., Miwa, K., Goda, E. (2002) "*Effect of Stratified Rich and High Turbulence Combustion on the Reduction of NOx and Particulate Emissions from a DI Diesel Engine*", Proceedings of Thiesel 2002, Thermo- and Fluid Dynamic Processes in Diesel Engines, pp. 227-235

Kimura, S., Aoki, O., Kitahara, Y., Aiyoshizawa, E. (2001) "*Ultra-clean Combustion Technology Combining a Low-Temperature and Premixed Combustion Concept for Meeting Future Emission Standards*", SAE Paper 2001-01-0200

Kimura, S., Aoki, O., Ogawa, H., Muranaka, S., Enomoto, Y. (1999) "*New Combustion Concept for Ultra-Clean and High-Efficiency Small DI Diesel Engines*", SAE Paper 1999-01-3681

Knecht, W. (2000) "*European Emission Legislation of Heavy Duty Diesel Engines and Strategies for Compliance*", Proceedings of Thiesel 2000, Thermofluidynamic Processes in Diesel Engines, pp. 289-302

Kong, S.-C., Marriott, C., D., Reitz, R., D. - Christensen, M. (2001) "*Modeling and Experiments of HCCI Engine Combustion Using Detailed Chemical Kinetics with Multidimensional CFD*", SAE Paper 2001-01-1026

Laguitton, O., Gold, M., Kennaird, D., Crua, C., Lacoste, J., Heikal, M. (2002) "*Spray Development and Combustion Characteristics for Common Rail Diesel Injection Systems*", Proceedings of Fuel Injection Systems Conference, 2002, number 6

Laguitton, O., Streater, S., R., Gordon, R., L. (2002) "*Realising the Benefits of Supervisory Control – An Essential Approach for Hybrid Drivetrains*", Proceedings of Total Vehicle Technology – How do we get the innovation back into vehicle design?, I.Mech.E. Paper T002/003/2002, pp. 29-45

Lejeune, M., Lortet, D., Michon, S. (2002) "*Combustion Development for Euro 4*", Proceedings of Thiesel 2002, Thermo- and Fluid Dynamic Processes in Diesel Engines, pp. 277-292

Lejeune, M., Michon, S., Hedna, M. (2000) "*Combustion Process Optimisation for Euro 3*", Proceedings of Thiesel 2000, Thermofluidynamic Processes in Diesel Engines, pp. 347-367

Mahr, B. (2002) "*Future and Potential of Diesel Injection Systems*", Proceedings of Thiesel 2002, Thermo- and Fluid Dynamic Processes in Diesel Engines, pp. 5-17

Mira web page, visited on 8th January 2003, www.mira.co.uk/vept/powertrain/Emissions/E_world_wide%20legislation.htm

Monaghan, M., L. (1995) "*The Design and Development of the High Speed Direct Injection Diesel*", Proceedings of Koex 95, Seoul Motor Show Seminar, Korea SAE, Paper 5

Morgan, R., E., Gold, M., R., Laguitton, O., Crua, C., Heikal, M., R. (2003) "*Characterisation of the Soot Formation Processes in a High Pressure Combusting Diesel Fuel Spray*", SAE Paper 2003-01-3086

Morimoto, S., S., Kawabata, Y., Sakurai, T., Amano, T. (2001) "*Operating Characteristics of a Natural Gas-Fired Homogeneous Charge Compression Ignition Engine (Performance Improvement Using EGR)*", SAE Paper 2001-01-1034

Morita, A., Iwashiro, Y., Aoyagi, Y., Hashizume, T. (2000) "*Observation of the Diesel Combustion Process in Multiple Stage Injection*", Proceedings of Thiesel 2000 Thermofluidynamic Processes in Diesel Engines, pp. 447-452

Najt, P., Foster, D., E. (1983) "*Compression-Ignited Homogeneous Charge Combustion*", SAE Paper 830264

Nakayama, S., Fukuma, T., Matsunaga, A., Miyake, T., Wakimoto, T. (2003) "*A New Dynamic Combustion Control Method Based on Charge Oxygen Concentration for Diesel Engines*", SAE Paper 2003-01-3181

Neunteufl, K., Unger, E., M., Burgler, L., Herzog, P., L. (2004) "*Closed Loop Combustion Control – a Prerequisite for Alternative Diesel Combustion*", Proceedings of SIA 2004 Le Diesel: aujourd'hui et demain

Nishijima, Y., Asaumi, Y., Aoyagi, Y. (2002) "*Impingement Spray System with Direct water Injection for Premixed Lean Diesel Combustion Control*", SAE Paper 2002-01-0109

Noda, T., Foster, D. E. (2001) "*A Numerical Study to Control Combustion Duration of Hydrogen-fueled HCCI by Using Multi-zone Chemical Kinetics Simulation*", SAE Paper 2001-01-0250

Oakley, A., Zhao, H., Ladommatos, N. - Ma, T. (2001) "*Experimental Studies on Controlled Auto-ignition (CAI) Combustion of Gasoline in a 4-Stroke Engine*", SAE Paper 2001-01-1030

Olsson, J.-O., Tunestal, P., Johansson, B. (2001) "*Closed-Loop Control of an HCCI Engine*", SAE Paper 2001-01-1031

Onishi, S., Jo, S., H., Shoda, K., Jo, P., D., Kato, S. (1979) "*Active Thermo-Atmosphere Combustion (ATAC) – A New Combustion Process for Internal Combustion Engines*", SAE Paper 790501

Payri, F., Benajes, J., Molina, S., Manuel Rieso, J. (2003) "*Reduction of Pollutant Emissions in a HD Diesel Engine by Adjustment of Injection Parameters, Boost Pressure and EGR*", SAE Paper 2003-01-0343

Peng, Z., Zhao, H., Ladommatos, N. (2003) "*Effects of Air/Fuel Ratios and EGR Rates on HCCI Combustion of n-heptane, a Diesel Type Fuel*", SAE Paper 2003-01-0747

Ranini, A., Potteau, S., Gatellier, B. (2004) "New *Developments of the NADI^{TM} Concept to Improve Operating Range, Exhaust Emissions and Noise*", Proceedings of Thiesel 2004, Thermo- and Fluid Dynamic Processes in Diesel Engines, pp. 469-482

Ricardo web page, visited on 8th January 2003, www.ricardo.com/free_emleg/trialhome.htm

Ricaud, J.-C., Lavoisier, F. (2002) "*Optimizing the Multiple Injection Settings on an HSDI Diesel Engine*", Proceedings of Thiesel 2002, Thermo- and Fluid Dynamic Processes in Diesel Engines, pp. 251-276

Ryan III, T., W. (2000) "*Fuels for Compression Ignition Engines*", Proceedings of Thiesel 2000, Thermofluidynamic Processes in Diesel Engines, pp. 233-248

Ryan III, T., W., Matheaus, A. (2002) "*Fuel Requirements for HCCI Engine Operation*", Proceedings of Thiesel 2002, Thermo- and Fluid Dynamic Processes in Diesel Engines, pp. 362-375

Shenghua, L., Ou, C., J., Won, H., J. (1999) "*Development of New Swirl System and its Effect on DI Diesel Engine Economy*", SAE Paper 1999-01-2889

Shimazaki, N., Akagawa, H., Tsujimura, K. (1999) "*An Experimental Study of Premixed Lean Diesel Combustion*", SAE Paper 1999-01-0181

Shimazaki, N., Tsurushima, T., Nishimura, T. (2003) "*Dual Mode Combustion Concept with Premixed Diesel Combustion by Direct Injection near Top Dead Center*", SAE Paper 2003-01-0742

Shudo, T., Ono, Y. (2002) "*HCCI Combustion of Hydrogen, Carbon Monoxide and Dimethyl Ether*", SAE Paper 2002-01-0112

Simescu, S., Fiveland, S., B., Dodge, L., G. (2003) "*An Experimental Investigation of PCCI-DI Combustion and Emissions in a Heavy-Duty Diesel Engine*", SAE Paper 2003-01-0345

Society of Motor Manufacturers and Traders web page, visited on 26th July 2005, www.SMMT.co.uk

Su, W., Lin, T., Pei, Y. (2003) "*A Compound Technology for HCCI Combustion in a DI Diesel Engine Based on the Multi-Pulse Injection and the BUMP Combustion Chamber*", SAE Paper 2003-01-0741

Suzuki, H., Koike, N., Ishii, H., Odaka, M. (1997) "*Exhaust Purification of Diesel Engines by Homogeneous Charge with Compression Ignition Part 1: Experimental Investigation of Combustion and Exhaust Emission Behavior Under Pre-Mixed Homogeneous Charge Compression Ignition Method*", SAE Paper 970313

Takasaki, K., Takaishi, T., Ishida, H., Iwamoto, K. (2002) "*Timely Control of Diesel Combustion Using Water Injection*", Proceedings of Fuel Injection Systems Conference, 2002, number 17

Takeda, Y., Keiichi, Na., Keiichi, Ni. (1996) "*Emission Characteristics of Premixed Lean Diesel Combustion with Extremely Early Staged Fuel Injection*", SAE Paper 961163

Takeuchi, K., Toyao, T. (2002) "*Development of 2nd Generation Common Rail System*", Proceedings of Fuel Injection Systems Conference, 2002, number 1

Tanaka, K., Endo, H., Imamichi, A., Oda, Y. – Takeda, Y., Shimada, T. (2001) "*Study of Homogeneous Charge Compression Ignition Using a Rapid Compression Machine*", SAE Paper 2001-01-1033

Taylor, C., F. (1984) "*The Internal Combustion Engine in Theory and in Practise – Combustion, Fuels, Materials, Design*", Volume 2, Revised Edition, pp. 103-104

Thring, R., H. (1989) "*Homogeneous-Charge Compression-Ignition (HCCI) Engines*", SAE Paper 892068

Trueba, A., Barbeau, B., Pajot, O., Mokaddem, K. (2002) "*Pilot Injection Timing Effect on the Main Injection Development and Combustion in a DI Diesel Engine*", SAE Paper 2002-01-0501

Weissback, M., Csato, J., Glensvig, M., Sams, T., Herzog, P. (2003) "*Alternative Combustion – An approach for Future HSDI Diesel Engines*", MTZ Worldwide, Volume 64, Issue 9/2003, pp. 17-20

Whelan, S. (2001) "*Down-Sizing Diesel Powertrain for Use in Fuel Efficient Mild Hybrid Vehicles*", JSAE Paper 20015343

Wuensche, P., Moser, F., X., Dreisbach, R., Sams, T. (2003) "*Can the Technology for Heavy Duty Diesel Engines be Common for Future Emission Regulations in USA, Japan and Europe?*", SAE Paper 2003-01-0344

Yanagihara, H. (2001) "*Ignition Timing Control at Toyota "UNIBUS" Combustion System*", Proceedings of the IFP International Congress, A New Generation of Engine Combustion Processes for the Future?, pp. 35-42

Yanagihara, H. (2002) "*A Study on Combustion Structure of Premixed Compression Ignition Diesel Engines*", Proceedings of Thiesel 2002, Thermo- and Fluid Dynamic Processes in Diesel Engines, pp. 111-129

Yanagihara, H., Sato, Y., Mizuta, J. (1997) "*A Study of DI Diesel Combustion Under Uniform Higher-Dispersed Mixture Formation*", JSAE Review, July 1997, pp.247-254

Yokota, H., Kudo, Y., Nakajima, H., Kakegawa, T., Suzuki, T. (1997) "*A New Concept for Low Emission Diesel Combustion*", SAE Paper 970891.

APPENDIX A

Fuel characteristics:

The table below summarises the main specifications of the diesel BP Ford reference fuel used for the investigations. Two different batches were used, with slightly different properties (second batch values shown in brackets). The impact of the change on the combustion behaviour was not noticeable.

Property	Value	Unit	Analysis protocol
Density at 15 °C	833 (837)	kg/m^3	ASTM D 4052
Sulphur	0.004	% (concentration)	IP 336
Aromatics	20.8	% (volume)	ASTM D 1319
Olefins	2.00	% (volume)	ASTM D 1319
Saturates	77.2	% (volume)	ASTM D 1319
Gross calorific value	45.9 (46.1)	MJ/kg	IP 12
Viscosity at 40 °C	2.887	cSt	IP 71
Hydrogen content	13.15	% (concentration)	ASTM D 5291
Carbon content	85.3	% (concentration)	ASTM D 5291
H/C ratio	1.87 (1.84)	(-)	
Cetane number	53.5	CN	ASTM D 613
Flash point	67	°C	ASTM D 93
Initial boiling point	177.5	°C	
Final boiling point	352.5	°C	
Recovery	98.5	% (volume)	
Residue	1.0	% (volume)	
Loss	0.5	% (volume)	

APPENDIX B

Opening and closing delays:

Injector opening delays is the time between the start of drive current and the first trace of fuel injected, detected by the pressure transducer. Injector closing delay is the time between the end of current drive and the last trace of fuel injected, detected by the pressure transducer. The phenomena are illustrated in the sample of injection rate data and the related traces shown below:

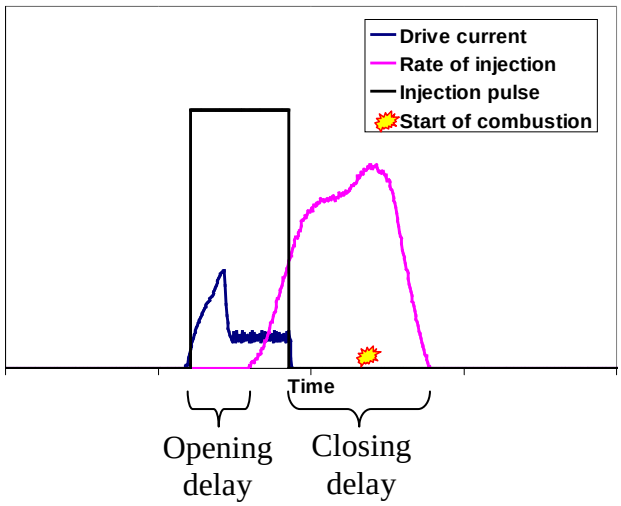

The opening delay decreased as the injection pressure increased, which is due to the positive effect injection pressure has on the lifting of the needle. The fit to the measured data is displayed in the figure below.

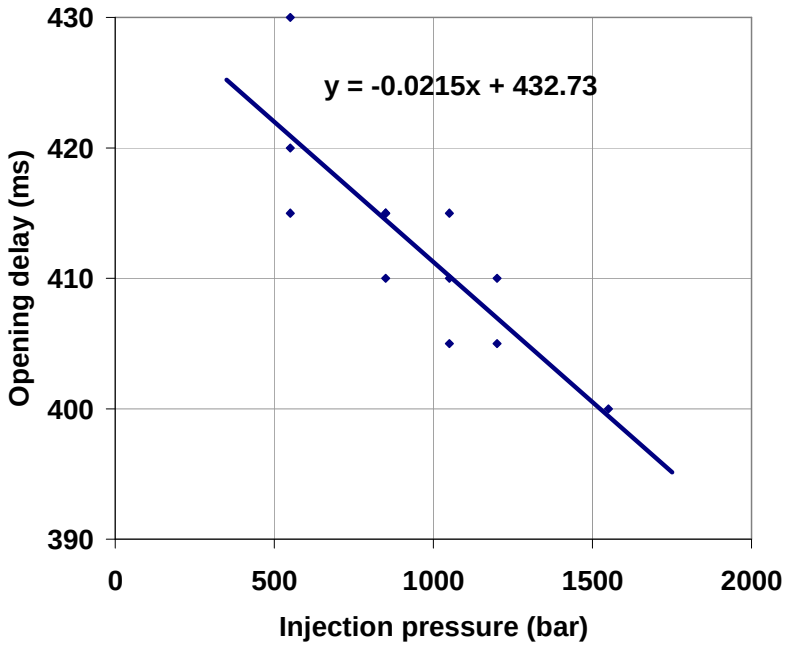

The closing delay is mainly a function of the injection duration but evidence of the injection pressure affecting the closing delay was also visible. The measured results for the closing delay are shown in the figure below.

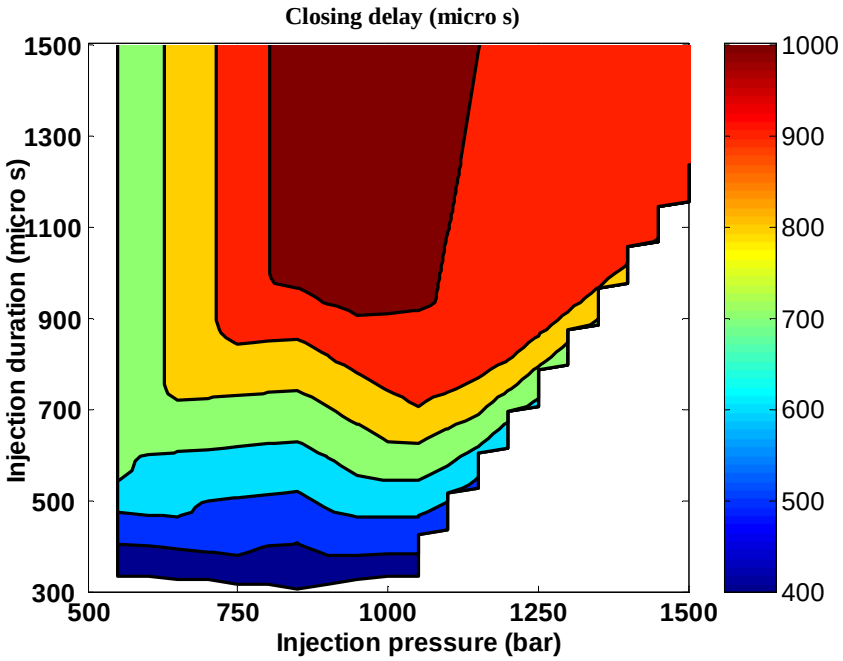

Both these sets of delays were determined from injection rate data for the 7 hole injector nozzle and were assumed identical for the 8 hole nozzle.